AD_____

Award Number: W81XWH-10-1-0026

TITLE: P53 Suppression of Homologous Recombination and Tumorigenesis

PRINCIPAL INVESTIGATOR: Bijal Karia, Ph.D.

CONTRACTING ORGANIZATION: Texas, University of, Health Science Center at San
                           Antonio
                           San Antonio, TX 78229

REPORT DATE: July 2013

TYPE OF REPORT: Annual Summary

PREPARED FOR: U.S. Army Medical Research and Materiel Command
               Fort Detrick, Maryland 21702-5012

DISTRIBUTION STATEMENT: Approved for Public Release;
                        Distribution Unlimited

The views, opinions and/or findings contained in this report are those of the author(s) and
should not be construed as an official Department of the Army position, policy or decision
unless so designated by other documentation.

REPORT DOCUMENTATION PAGE

Form Approved
OMB No. 0704-0188

Public reporting burden for this collection of information is estimated to average 1 hour per response, including the time for reviewing instructions, searching existing data sources, gathering and maintaining the data needed, and completing and reviewing this collection of information. Send comments regarding this burden estimate or any other aspect of this collection of information, including suggestions for reducing this burden to Department of Defense, Washington Headquarters Services, Directorate for Information Operations and Reports (0704-0188), 1215 Jefferson Davis Highway, Suite 1204, Arlington, VA 22202-4302. Respondents should be aware that notwithstanding any other provision of law, no person shall be subject to any penalty for failing to comply with a collection of information if it does not display a currently valid OMB control number. **PLEASE DO NOT RETURN YOUR FORM TO THE ABOVE ADDRESS.**

1. REPORT DATE	2. REPORT TYPE	3. DATES COVERED
July 2013	Annual Summary	1 January 2010 - 30 June 2013

4. TITLE AND SUBTITLE

P53 Suppression of Homologous Recombination and Tumorigenesis

5a. CONTRACT NUMBER

5b. GRANT NUMBER
W81XWH-10-1-0026

5c. PROGRAM ELEMENT NUMBER

6. AUTHOR(S)

Bijal Karia

E-Mail: BIJALKARIA79@GMAIL.COM

5d. PROJECT NUMBER

5e. TASK NUMBER

5f. WORK UNIT NUMBER

7. PERFORMING ORGANIZATION NAME(S) AND ADDRESS(ES)

Texas, University of, Health Science Center at San Antonio
San Antonio, TX 78229

8. PERFORMING ORGANIZATION REPORT NUMBER

9. SPONSORING / MONITORING AGENCY NAME(S) AND ADDRESS(ES)

U.S. Army Medical Research and Materiel Command
Fort Detrick, Maryland 21702-5012

10. SPONSOR/MONITOR'S ACRONYM(S)

11. SPONSOR/MONITOR'S REPORT NUMBER(S)

12. DISTRIBUTION / AVAILABILITY STATEMENT

Approved for Public Release; Distribution Unlimited

13. SUPPLEMENTARY NOTES

14. ABSTRACT

Please see next page.

15. SUBJECT TERMS

HOMOLOGOUS RECOMBINATION, P53 HOTSPOT MUTATIONS, BREAST CANCER, GENOMIC INSTABILITY, TUMORIGENESIS

16. SECURITY CLASSIFICATION OF:			17. LIMITATION OF ABSTRACT	18. NUMBER OF PAGES	19a. NAME OF RESPONSIBLE PERSON USAMRMC
a. REPORT	b. ABSTRACT	c. THIS PAGE			
U	U	U	UU	212	19b. TELEPHONE NUMBER *(include area code)*

14. ABSTRACT

p53 is the most studied protein in cancer; however, the complex multifunctional nature of p53 has made understanding it's mechanism(s) of tumor suppression difficult. The p53 protein is not essential for life as p53 nullizygous mice are viable. Nonetheless, p53 is important for responding to cellular stresses that disrupt the normal cellular homeostasis and threaten genomic integrity. To date many *in vitro*, tissue culture and mouse models have been created to study functions of p53. Mouse models that retain certain aspects of p53 function (cell cycle arrest and/or apoptosis) still succumb to spontaneous tumors, suggesting that multiple facets of p53 function that remain poorly defined are involved. Here, we evaluate whether two separation-of-function p53 mutants can affect homologous recombination and ask how this impacts genomic stability.

The role of p53 in homologous recombination has been somewhat controversial and its relevance to general genome stability and tumor suppression poorly evaluated. We use a mouse model, pink-eyed unstable, to assess homologous recombination *in vivo* during somatic development for two p53 point mutation models. The p53 R172P homozygous mutant retains the ability to arrest the cell cycle, but is incapable of eliciting apoptosis. This mutant suppressed homologous recombination similar to wildtype p53. The more aggressive p53 R172H dominant negative mutant has a dysregulated DNA binding domain and is incapable of either transactivating known p53 target genes or binding proteins whose interaction is mediated by this domain. This mutant has lost the capability to suppress homologous recombination similar to the p53 nullizygous mouse.

The pink-eyed unstable assay is based on the deletion of one copy of a 70 kb tandem duplication, essentially a copy number variant. We examined the status of copy number variations in the genome by performing array comparative genomic hybridization on cells derived from the two-p53 mutant mice. We examined mouse embryonic fibroblasts derived from the p53 mutants, as well as, genotype-matched tumors and observed that p53 suppresses the acquisition of somatic changes in these structures during normal and tumor development. These results recapitulate the finding that Li-Fraumeni patients, who inherit a dominant negative p53 mutation, and show increased copy number variation compared with the general population. Further, it provides an interesting potential mechanistic basis for the genetic anticipation phenotype observed with Li- Fraumeni families, as we observe many of these somatic variants have become fixed in our populations. Finally, this study provides evidence that p53 can directly suppress genomic instability which may otherwise facilitate tumorigenesis.

In addition to our work on p53, we also set out to determine whether a variety of developmental exposures can induce somatic genomic rearrangements by increasing the frequency of homologous recombination. We exposed pregnant dams to various differently acting DNA-damaging agents at a specific time in embryo development. We observed an increased frequency of recombination events following exposure to cisplatin, methyl methanesulfonate, ethyl methanesulfonate, 3-aminobenzamide, bleomycin, and etoposide but a decreased frequency following camptothecin and hydroxyurea exposure. This study demonstrates that even an acute *in utero* exposure to an exogenous damage can have long-term consequences on somatic genomic variation.

Taken together, the goal of this work was to examine the effects of p53 mutation on homologous recombination as a measure of genomic instability. Our results suggest that the control of homologous recombination by p53 may participate in its tumor suppressive functions by protecting genome stability from daily insults. Somatic genetic rearrangements occurring early in development induced in response to endogenous and exogenous factors may threaten genomic integrity while the p53 pathway serves to mitigate these changes. p53 is often a targeted therapy and further insight into the function of p53 in DNA repair pathways can be vital to finding novel points of targeted therapy. Our data will add insight to the important paradigm of genomic instability and its relation to breast cancer etiology.

Table of Contents

Introduction

The purpose of this project is to determine the mechanism for how the tumor suppressor, p53, suppresses homologous recombination. P53 is implicated in 50% of all human cancers and inactivated in some form in 100% of human cancers. Homologous recombination (HR) is an error proof repair mechanism that is able to repair any type of DNA lesion with high fidelity. However, when the HR machinery uses an incorrect template for repair large deletions in the genome can occur leading to a predisposition for cancer. P53 has been implicated in suppressing homologous recombination in order to maintain genomic stability, however the mechanism is still unknown. In the first year of this grant huge strides have been made in the numbers of mice breed and relevant cells collected for the purposes of experiments outlined in the aims below. The PI has optimized the pun assay and mouse husbandry in the first year of this grant and has collected data during the second year of the grant period. The second and third year accomplishments included four middle author publications (Appendix 1-4) due to the PI's knowledge, and expertise in various areas including p53 mutation, DNA repair and cell cycle function. The PI also attended two conferences in the preceding year where she presented a poster and had several committee meetings to evaluate the work progress. In the last report period, the PI completed work for specific aims listed in the initial proposal and revised SOW (Appendix 6) and was in the process of completing two first author manuscripts and writing her dissertation. In the extension period (final report) the PI has completed all necessary experiments and final committee meetings and has successfully defended her PhD dissertation on May 9, 2013. One first author manuscript is under revision for the journal titled *DNA Repair* (Appendix 5) and the other manuscript is currently being prepared for submission. A review article encompassing the introduction to the approved dissertation is being prepared currently for publication. The PI is also preparing a second review in collaboration with other graduate students and post-doctoral fellows in the lab detailing homologous recombination involved in cancer, environmental and genetic factors.

Body

P53 is a potent tumor suppressor that shields the genome from daily interrogations of endogenous and exogenous damage, most importantly through its ability to arrest the cell cycle. In response to damage, p53 up regulates transcription of p21 leading to G1 arrest, which allows adequate time for repair of lesions before entering S phase (1, 2). Furthermore, p53 has been linked to G2/M arrest through multiple overlapping p53-dependent and p53-independent pathways that inhibit cdc2 (3). As a final resort if the damage is severe enough p53 has been shown to induce apoptosis in certain situations (2, 4).

P53 has also been linked to various DNA repair pathways such as non-homologous end joining (NHEJ) and homologous recombination (HR). Homologous recombination is a high fidelity DNA repair mechanism that can repair almost any type of DNA lesion when in correct equilibrium. When this delicate balance is disrupted as seen in *Blm* null cells resulting in hyperrecombination or hyporecombination in *Brca1* null cells the ensuing result is genomic instability (5).

It has been reported previously that p53 down regulates spontaneous homologous recombination in chromosomally integrating plasmid substrate models. Bertrand *et al*. using a plasmid-based system with PJS3-10 (mouse L cell lines) overexpressed the mutant $p53^{175\ (Arg>His)}$, which showed a 5-20 fold increase in spontaneous recombination compared to wild type control cells. Further analysis showed that the effect of the p53 mutation acted on both rad51 dependent gene conversion events and deletion events (6).

Willers *et al*. also showed an increase in recombination frequency in a temperature sensitive p53 mutant (Ala135 to Val) using a plasmid substrate that stably integrated into p53 null mouse embryonic fibroblasts (MEFs). This study further established the uncoupling of p53's function in suppressing HR and its role as a cell cycle checkpoint protein (7).

The Wiesmuller lab has explored the role of p53 in HR using a rare cutting endonuclease ISCE-1 in breast cancer cells with varying p53 mutations. This study used a DSB repair assay to show that some p53 mutants retain partial ability to repair double strand breaks by repressing aberrant HR and less infrequently through NHEJ and SSA(8).

P53 is mutated in 50% of all human cancers and most likely inactivated by some other mechanism in the other 50%. Patients with Li Fraumeni syndrome suffer from a germ line mutation in p53 and subsequently endure an early onset of cancer. Mouse models have been created to recapitulate this phenomenon and are surprisingly viable. 80% of P53 null mice come down with lymphomas within 6 months and the rest suffer from sarcomas. MEFs from these mice show aneuploidy, allelic loss and gene amplification. Most of these germline mutations are missense mutations occurring in the DNA binding domain of p53. One such mutant is the p53-R172P and p53-

R172H mouse model (9). The p53-R172P mouse is able to induce partial cell cycle arrest in response to DNA damage but is defective in promoting apoptosis. Mice homozygous for this mutation escape the early onset of lymphomas that is typical for p53 null mice, however these mice eventually do succumb to tumors that have a normal diploid number of chromosomes in contrast to p53 null tumors. The p53-R172H mouse shows an inability to transactivate p53 target genes as well as a defect in apoptosis induction (10). A majority of mice homozygous for p53-R172H developed lymphomas similar to p53 null mice with a smaller percent developing sarcomas. P53-R172H heterozygous mice developed sarcomas and a surprising number of osteosarcomas and carcinomas that metastasized, which were not seen in p53 heterozygous mice (9). Interestingly, the p53-R172H tumors showed a high level of aneuploidy similar to p53 null mice but unlike p53-R172P mice. Given this we sought to look at the HR frequency of these two mutants to determine if there is a difference in in the ability to suppress HR similar to WT given the different functionalities of these to mutants. HR is measure of genomic instability, even though it can fix any type of genotoxic lesion, when used incorrectly it can cause large deletions and lesions in the genome. Using the in vivo pun assay we have seen an increase in HR frequency in many mouse models of the DNA damage repair pathway. HR frequency is increased in BLM null, p53 null and parp null mice and decreased in Brca1 and Brca2 null animals (5, and unpublished work).

Given the power of this assay here we used the *in vivo p^{un}* assay to determine the consequence of HR suppression in two breast cancer hotspot p53 mutant mouse models with differing loss of function. The p53-R172P mice, which are defective in their ability to induce apoptosis but are able to induce cell cycle genes, retained the ability to suppress HR similar to wild type p53 animals. The more aggressive p53-R172H mouse showed increase HR similar to p53 null mice, which do not produce any p53 protein at all.

Specific Aim 1: Determine whether DNA-damaging agents with varying modes of action can induce somatic change in an in vivo mouse model of homologous recombination

Much of our understanding of homologous recombination, as well as the development of the working models for these processes, has been derived from extensive work in model organisms, such as yeast and fruit flies, and mammalian systems by studying the repair of induced double strand breaks or repair following exposure to genotoxic agents *in vitro.* We therefore set out to expand this *in vitro* work to ask whether DNA-damaging agents with varying modes of action could induce somatic change in an *in vivo* mouse model of homologous recombination. We exposed pregnant dams to DNA-damaging agents, conferring a variety of lesions at a specific time in embryo development. To monitor homologous recombination frequency, we used the well-established retinal pigment epithelium pink-eyed unstable assay. Homologous recombination resulting in the deletion of a duplicated 70 kb fragment in the coding region of the Oca2 gene renders this gene functional and can be visualized as a pigmented eyespot in the retinal pigment epithelium. We observed an increased frequency of pigmented eyespots in resultant litters following exposure to cisplatin, methyl methanesulfonate, ethyl methanesulfonate, 3-aminobenzamide, bleomycin, and etoposide with a contrasting decrease in the frequency of detectable reversion events following camptothecin and hydroxyurea exposure. The somatic genomic rearrangements that result from such a wide variety of differently acting damaging agents implies long-term potential effects from even short-term *in utero* exposures.

Mouse cohort and breeding

C57BL/6J p$^{un/un}$ mice were obtained from the Jackson Laboratory (Bar Harbor, ME). Experimental cohorts were maintained by breeding homozygous p$^{un/un}$ mice to generate sufficient numbers of animals for exposure experiments. All animal studies were conducted in accordance with University and Institute IACUC policies, as outlined in protocol 07005-34-02-A,B1,C.

Timing of pregnancy and exposure to agents

Mice homozygous for p$^{un/un}$ were bred with successful copulation, which was indicated by a vaginal plug and timed as 0.5 days post coitum. Pregnant dams were then exposed to various DNA-damaging agents (Table A.1) on embryonic day 12.5.

10

Table A.1: Summary of different classes of reagents purchased from Sigma (St. Louis, MO) and administered intraperitoneally on embryo day 12.5 to pregnant dams

Agent	Mode of action	CAS no.
Control (0.9% normal saline)		7647−14−5
Cis-diamineplatinum(II) dichloride	Cross-linking agent	15663−27
Methyl methanesulfonate Ethyl methanesulfonate	Alkylating agents	66−27−3
3-aminobenzamide	PARP inhibitor	62−50−0
Bleomycin sulfate	Radiomimetic agent	3544−24−9
Etoposide	Topoisomerase II inhibitor	9041−93−4
Camptothecin	Topoisomerase I inhibitor	33419−42−0
Hydroxyurea	Ribonucleotide reductase inhibitor	7689−03−4

The DNA-damaging agents were prepared in 0.9% normal saline (also used as a control) and injected intraperitoneally to pregnant dams. The dose of each agent was calculated based on the weight of the pregnant dam (per 30 g) and prepared in a 0.2 mL solution.

Eye dissection and p^{un} reversion (homologous recombination) assay

Eyes from 30-day-old pups derived from exposed pregnant dams were harvested and dissected as previously described [8]. RPE whole mounts were prepared and imaged using a Zeiss Lumar version 12 stereomicroscope, Zeiss AxioVision MRm camera, and Zeiss AxioVision 4.6 software (Thornwood, NY). For each RPE, the total number of pigmented eyespots was scored along with the number of cells that comprised each eyespot as detailed in Claybon et al. [18]. The position of each pigmented eyespot was also recorded to confirm the correlation between the time of exposure and the location of any induced reversion events, as previously described [9]. The criterion for scoring a p^{un} reversion event as well as the analysis of its position on the RPE was also previously outlined in Bishop et al. [8]. Briefly, an eyespot was scored as one or more reverted cell (indicated by black pigmentation in an otherwise transparent cell layer), separated by no more than one unpigmented cell.

Statistics

Statistical analysis was performed using GraphPad Prism 6.0 (La Jolla, CA) software. We first performed a normality test and determined that our data did not follow a normal Gaussian distribution. We therefore chose nonparametric tests that compare distributions of 2 unpaired groups. A Mann-Whitney test was used to analyze p^{un} reversion frequency between DNA-damaging agents and control. We used a Kolmogorov-Smirnov test to analyze distribution differences in eyespot position data between control and differing DNA-damaging agents.

Results

Survival analysis of pregnant dams' post exposure to varying doses of DNA-damaging agents

Dosing for each agent was empirically derived based on a combination of reported LD_{50} (lethal dose 50%) levels, published fetotoxicity data, and previous work done with the p^{un} fur-spot assay [10]. We performed a survival analysis study to determine which doses maximized dam survival, litter size, and p^{un} fur-spot induction (Table 1). The fur-spot assay was used merely as an indicator to confirm that the chosen dose for each agent was capable of inducing HR by our assay, but it generally requires many more mice to establish statistical significance compared to the eyespot assay. For cisplatin and MMS, a dose of 2.5 mg/kg and 0.2 mg/kg, respectively, resulted in robust litter sizes and p^{un} fur-spot induction. The 100 mg/kg dose for EMS did not result in spotted pups; however, given that the eyespot assay is more sensitive (one-cell resolution) compared with the clonal expansion of revertant cells needed to visualize a fur-spot, we went forward with this dose for our study. Bleomycin proved to be quite toxic to the pregnant dams; therefore, we selected a dose of 5 mg/kg, which gave larger litter sizes and an 18% fur-spot frequency. In contrast, we selected the highest dose tested for 3AB because it did not appear to harm the dams. The topoisomerase inhibitors, etoposide and camptothecin, resulted in very few litters at high doses; however, lower doses of these agents still elicited a robust 36% fur-spot frequency. A midrange dose of the replication inhibitor, HU, resulted in a 27% fur-spot frequency and 100% survival (Table 1).

Table 1: p^{un} Fur-spot assay results following exposure to varying DNA-damaging agents and a saline control

agent	dose (mg/k)	number of dams injected	litters	number of pups								total pups	spotted pups	% spotted
Control	0.9% normal saline	8	8	8	8	8	6	6	5	5	4	50	9	18
Cisplatin	2.5	7	4	9	8	5	3					25	8	32
MMS	100.0	6	4	7	6	6	4					23	23	100
	0.2	6	6	9	8	8	8	7	5			45	10	22
EMS	100.0	4	3	7	6	5						18	0	0
Bleomycin	10.0	5	2	3	1							4	3	75
	5.0	4	3	11	8	3						22	4	18
	2.5	8	5	8	7	6	6	5				32	5	16
	1.0	3	1	3								3	0	0
3AB	400.0	4	3	8	6	6						20	0	0
	300.0	4	3	9	8	7						24	0	0
	200.0	4	3	7	6	4						17	0	0
	100.0	4	3	11	10	6						27	0	0
Etoposide	60.0	3	0											
	40.0	3	0											
	20.0	7	2	6	8							14	3	21
	10.0	7	0											
	5.0	6	1	4								4	3	75
	2.5	3	3	7	5	2						14	5	36
	1.0	3	3	7	5	4						16	3	19
Camptothecin	40.0	4	0											
	20.0	4	0											
	10.0	4	0											
	5.0	3	0											
	2.0	9	2	2	4							6	1	17
	1.0	5	5	8	5	6	5	4				28	10	36
Hydroxyurea	5000.0	4	0											
	3000.0	4	1	8								8	2	
	1000.0	4	0											
	300.0	3	3	8	6	8						22	6	27
	200.0	2	1	3								3	1	33
	100.0	2	2	6	2							8	0	0

Exposure to DNA-damaging agents with different modes of action induces homologous recombination

Either naturally or by design, chemotherapeutic agents with differing modes of action lead to a variety of lesions, such as strand breaks, DNA adducts, and DNA cross-links, among others. These lesions are detected by surveillance machinery that operates by triggering a robust DNA-damage signal cascade, thereby prompting appropriate DNA-repair pathways. HR is one such pathway; however, much of our understanding of this pathway stems from either lower organisms or tissue-culture studies on the repair of induced double-strand breaks. Therefore, we set out to ask whether differing types of DNA lesions could induce somatic HR in vivo. We exposed pregnant dams at a specific time in embryo development (12.5 dpc) to DNA-damaging agents that have differing modes of action. The simplest assessment of these agents is to determine the frequency of reversion events in each RPE for each agent exposure compared to the saline control. Upon examining the frequency of eyespots (p^{un} reversions) per RPE, we found that all agents, except camptothecin and HU, significantly induced HR compared to the control (Fig. 1a and Table 2). The cross-linking agent, cisplatin, and both alkylating agents, MMS and EMS, showed a twofold induction of eyespots per RPE ($P < 0.0001$; Mann-Whitney test). Though not as robust, PARP inhibition ($P < .001$; Mann-Whitney test), bleomycin, and the Top2 poison, etoposide ($P < .01$; Mann-Whitney test), also significantly induced HR in comparison to the control agent (Fig. 1a and Table 2). Whereas most of the agents resulted in a concomitant increase in the number of revertant cells (Table 2), camptothecin and HU showed a highly statistically significant decrease in the number of eyespots ($P < .0001$; Mann-Whitney test) and an overall fewer number of cells per RPE, possibly due to the dose selected for this study (Fig. 1a and Table 2). It is interesting that these latter data contrast with the clear induction observed using the fur-spot assay, which indicated that the selected doses should induce p^{un} reversion, albeit with possible cytotoxic effects in the RPE (Table 1). The resultant litters from pregnant dams exposed to EMS, showed a clear induction of p^{un} reversion in the RPE (compared with no induction in the fur), which indicates an increased sensitivity of the eyespot assay to detect damage-induced HR events. These results suggest that many forms of damage—not just strand breaks—are capable of inducing recombinogenic lesions.

Table 2: Summary of p^{un} reversion events and RPE examined following a saline control and various DNA-damaging agents

Agent	Dose (mg/kg)	Total			Average		
		RPE	Eyespots	Cells	Eyespots per RPE	Cells per RPE	Cells per eyespot
Control	Saline	26	104	203	4.0 ± 1.1	7.8 ± 4.0	2.0 ± 1.3
Cisplatin	2.5	16	140	404	8.8 ± 3.2	25.3 ± 22.5	2.9 ± 4.4
MMS	0.2	15	123	290	8.2 ± 3.6	19.3 ± 14.2	2.4 ± 2.9
EMS	100.0	17	133	281	7.8 ± 2.6	16.5 ± 9.6	2.1 ± 2.2
3AB	400.0	17	104	215	6.1 ± 2.6	12.6 ± 9.6	2.1 ± 2.0
Bleomycin	5.0	17	106	274	6.2 ± 3.0	16.1 ± 15.7	2.6 ± 3.4
Etoposide	2.5	16	97	255	6.1 ± 2.4	15.9 ± 10.5	2.6 ± 3.5
Camptothecin	1.0	17	31	45	1.8 ± 1.9	2.6 ± 3.3	1.5 ± 1.7
Hydroxyurea	300.0	17	29	78	1.7 ± 2.4	6.5 ± 14.4	3.0 ± 3.5

Induction of single-cell and multicell reversion events differ depending on the mode of action of DNA-damaging agents

In addition to directly providing HR frequency information in a developing mouse RPE, the p^{un} RPE-based reversion assay allows for the further subdivision of eyespot frequency into those eyespots consisting of one cell (single-cell eyespots) and those with more than one cell (multicell eyespots). The idea is that events resulting in multicell eyespots are more likely to have been tied to replication, such that reversion in one cell that is actively replicating its DNA clonally expands into a group of daughter cells. Thus, according to our criteria, we would score a clonally expanded multicell eyespot as a single reversion event. In contrast, a single-cell eyespot might have been derived from an event that was not necessarily tied to replication or in a cell that was in its terminal division and did not continue to divide once the revertant p gene segregated into one daughter cell. However, the p^{un} reversions that result in single-cell eyespots may result from cells that are in G1 through a single strand annealing type event. Since we observe that the induced events occur in specific regions of the RPE (and not in regions that are post mitotic at the time of exposure) suggests that whether single-cell or multicell, p^{un} reversions arise in cells that are actively dividing at the time of exposure. Our data showed a significant increase in frequency of single-cell reversion events for cisplatin, EMS, and MMS ($P < .0001$; Mann-Whitney) with only a small increase in multicell events for MMS ($P < .05$;

Mann-Whitney; Figs. 1b and 1c). 3AB and bleomycin also showed an increase in single-cell events (P < .05 and P < .01, respectively; Mann-Whitney) with no induction of multicell events (Figs. 1b and 1c).

In contrast, HU exposure resulted in a significant decrease in single-cell events (P < .01; Mann-Whitney); in addition, both HU and camptothecin appeared to have a significant decrease in the frequency of multicell eyespots compared with the control agent (P < .001 and P < .0001, respectively; Mann-Whitney; Figs. 1b and 1c). An interesting finding was that, of the 17 RPE analyzed following camptothecin exposure, only 5 of 31 eyespots were scored as multicell reversion events, compared with 50% in the control group. Further, we observed an induction of reversion events following camptothecin exposure using the p^{un} fur-spot assay (similar to that reported by others; eg, [19]), but a decrease in the p^{un} eyespot assay for the same animals. This suggests a tissue-specific difference in response, perhaps with RPE cells being more sensitive to camptothecin, resulting in greater cell death, permanent cell cycle arrest, or repair by other pathways without induction of HR events.

Figure 1
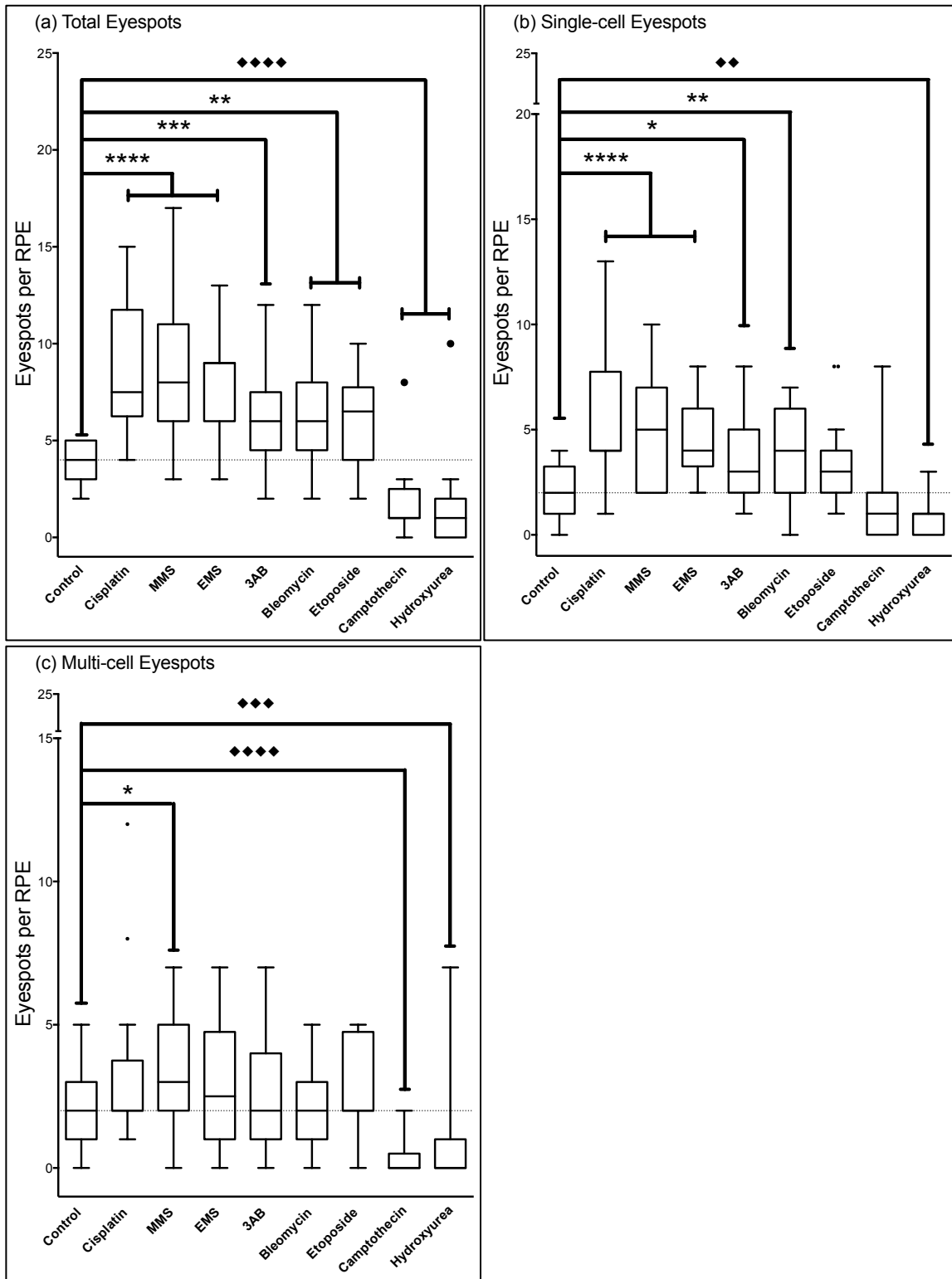
Figure 1: Tukey box and whiskers plot of the frequency of p^{un} reversion events for (a) total (b) single-cell and (c) multicell eyespots per RPE following saline control and DNA-damaging agents. The dashed line indicates the control frequency for comparison. A nonparametric Mann-Whitney test was used to analyze the frequency data; increased significance is denoted by asterisks (*P < .05, **P < .01, ***P < .001, ****P < .0001) and a significant decrease is denoted by diamonds (uu$P$ < .01, uuu$P$ <

17

.001, [uuuu]$P < .0001$).

Position frequency of reversion events following exposure to DNA-damaging agents

In addition to examining the frequency of events, another aspect of the p[un] eyespot assay is that the position of events found in the adult RPE can be related to the specific time during development when they occurred [8]. The RPE development results from an edge-biased pattern of proliferating cells that orient outward radially [20]. Previously, Bishop et al. demonstrated that the time of exposure to a DNA-damaging agent during development correlates strongly with the location of induced revertant events in the adult RPE [8]. Therefore, those eyespots that are near to the centrally located optic nerve occurred early in development, whereas those positioned toward the edge of the RPE (distal to the optic nerve head) most likely occurred later in embryo development. Considering that all of the exposures were conducted at embryo day 12.5, we expect this to correlate to an induction of p[un] reversion events at approximately one third of the distance from the optic nerve head to the edge of the RPE (ie, "position 0.3").

To determine whether there was a positional effect of the observed increase in eyespots following exposure to DNA-damaging agents, we analyzed the distribution of p[un] reversion events using a nonparametric Kolmogorov-Smirnov test to evaluate pattern shifts of eyespots between the control RPE and those exposed to DNA-damaging agents (Fig. 2a). Cisplatin ($P < .01$; Kolmogorov-Smirnov), MMS and EMS ($P < .05$; Kolmogorov-Smirnov) showed a significant shift in distribution of total reversion events compared to control (Fig. 2a). We further compared and contrasted the pattern of eyespot distribution for single- and multicell events separately. An examination of RPE for single-cell eyespots (Fig. 2b) revealed an induction pattern similar to that observed for total eyespots but positioned more toward the proximal region of the RPE for these agents ($P < .01$, $P < .05$, $P < .01$, respectively; Kolmogorov-Smirnov), with no significant distribution difference in multicell reversion events compared to the control agent (Fig. 2c).

Bleomycin did not have a significant pattern change in total eyespots but there was a significance in single-cell eyespots ($P < .05$; Kolmogorov-Smirnov) with an apparent spike of reversion events in regions following induction suggesting a quick mode of action for this agent compared to the control agent (Figs. 2a and 2b). PARP inhibition and etoposide exposure also resulted in a robust distribution change in total eyespots ($P < .01$; Kolmogorov-Smirnov) and a shift to more proximal regions for single-cell eyespots ($P < .05$, $P < .01$, respectively; Kolmogorov-Smirnov), which was more substantial following 3AB induction compared to the control agent (Fig. 2b). Again no significance was indicated in multicell reversion events (Fig. 2c). The differences in position and

pattern shifting between single and multicell events have been reported for various genetic backgrounds [21] and following DNA-damage exposure [8, 9].

It is interesting that the significant decrease seen in the total frequency of eyespots ($P < .05$, $P < .01$, respectively; Kolmogorov-Smirnov) was also recapitulated in the distribution pattern of these eyespots following camptothecin and HU exposure (Fig. 2a). For HU, the distribution difference is significant amongst single-cell reversion events ($P < .05$; Kolmogorov-Smirnov), with an apparent lack of eyespots directly following exposure, possibly due to cell death (Fig. 2b). Although not significant, the patterning of eyespots following camptothecin exposure indicates a loss in multicell eyespots in the more distal regions of the RPE, suggesting cytotoxicity in proliferating cells or an alternative pathway to repair the damage (Fig. 2c).

Previous work by Bishop et al. correlated an induction of damage-induced HR (using benzo[a]pyrene) to a particular time in fetal development [8]. Based on these calculations, we performed our inductions at embryo day 12.5 to maximize exposure to proliferating cells. However, the lack of significance in multicell reversion events following most of the DNA-damaging agents suggests that we might have missed the optimal "signal-to-noise" ratio for the agents used. Still, the results reported here suggest a significant difference in the repair of different types of lesions resulting from exposure to different types of agents.
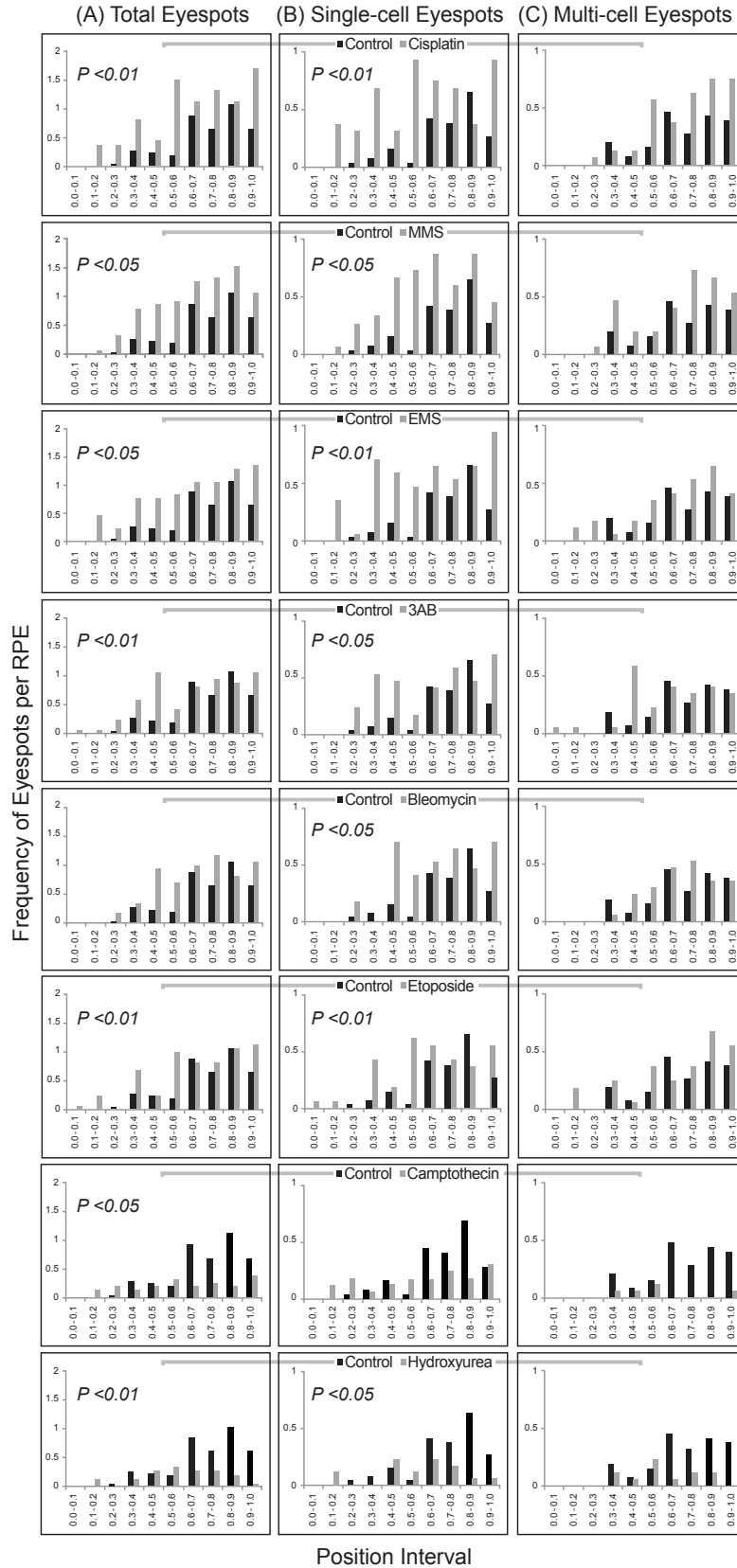
Figure 2: Position analysis of reversion events per RPE. Position intervals are indicated on the x-axis, where the 0.0 position interval corresponds to the central region of the RPE near the optic nerve and the position interval 1.0 represents the edge of the RPE. A Kolmogorov-Smirnov test was used to analyze position distributions with individual significance denoted in each figure.

Discussion

Exposure to environmental genotoxins or endogenous byproducts of normal cellular processes represents a peril to genomic integrity. Given this, many species have adapted a robust set of DNA-repair processes that can remove DNA lesions and hopefully maintain the integrity of the genetic material. Each repair process has a preferred substrate, although the significant redundancy that exists between these processes creates overlap in the substrates. For example, it has been shown that base excision repair, nucleotide excision repair, and recombination can all repair the alkylation damage associated with MMS exposure [22]. Actually, HR is a process that should be capable of repairing any genotoxic DNA lesion given the appropriate homologous template. However, the fact that HR must be kept in delicate balance to maintain genomic integrity and curb tumorigenesis is evidenced by mouse models deficient in key HR proteins. For instance, previous work using the p^{un} eyespot assay with mice deficient in BRCA1 (breast cancer, 1 early onset) resulted in a decreased frequency of HR compared to wild-type mice, In contrast, a hyperrecombination HR phenotype was seen in mice lacking RecQ helicase, BLM, the gene associated with Bloom syndrome [23]. BRCA1 and BLM deficiency yield a polarized HR phenotype, yet both lead to a higher incidence of cancer, most likely because of increased chromosomal instability due to an imbalance of HR repair. In this study, we sought to determine whether previously established DNA-damaging agents, either naturally occurring or manufactured, were able to elicit deletion events at a particular locus by using the *in vivo* p^{un} mouse model. By determining the frequency of pigmented cell spots in the RPE, we demonstrated that *in utero* exposure to these agents at an established time in embryo development resulted in an increased frequency of reversion events in our system compared to a saline control. This increased frequency of HR in the RPE following exposure to DNA-damaging agents is likely to be representative of the somatic mutation and genetic alterations that may be induced in other highly proliferative cells during embryo development. Any such somatic change in development has the potential to be clonally expanded, altering the genetic makeup of subsets of cells in the adult body with long-term consequences on the genetic integrity of cells.

The cytoplasm of a wild-type RPE cell is packed with melanosomes (specialized organelles filled with melanin granules), which give these light-sensitive cells their dark guise. The murine pink-eyed dilution gene, *p* (also called the *Oca2* gene) encodes for the P protein, which is involved in maintaining the pH balance necessary for melanin production [24]. When the *p* gene is nonfunctional (as in the $p^{un/un}$ genotype), melanin production is compromised, resulting in a dilute color compared to the normal, robust, black-brown pigmentation in the RPE and other pigmented tissues, such as the

fur. In the event of an HR reversion of the disrupting 70 kb duplication segment in the p^{un} mutation, a pigmented eyespot can be visualized among a clear background. This readout allows us to determine baseline frequencies of HR, which we suggest is normal maintenance to ensure genomic integrity as well as any deviations—either hypo- or hyperrecombination—as evidenced by the aforementioned work done with mouse models deficient in HR proteins [23], as well as others [18, 25].

Studies that offer information about the developmental timing in which drugs might act can provide insight into consequences of clonal expansion of these somatic mutations. Due to its modes of action (adduction and cross-linking of DNA), cisplatin results in DNA damage. Once this damage is detected, DNA-repair machinery (such as HR) is initiated, or else the damage elicits an apoptotic response. Exposure to cisplatin has been shown to increase sister chromatid exchanges (SCEs) [26], a crossover event between 2 sister chromatids that is most likely a result of HR [27]. In agreement with the findings of this *in vitro* study, cisplatin was also a strong inducer of HR in our assay for the dose that was used. We saw a robust increase in total and single-cell eyespots and a nonsignificant increase in multicell eyespots in the RPE of embryos harvested from pregnant dams exposed to a single dose of 2.5 mg/kg of cisplatin. This dose would be considered relatively low by clinic standards, which are often higher and given in multiple regimens; nonetheless, the dose was able to elicit a response in our system, suggesting that HR is instigated in response to lesions involving DNA adducts and cross-linking damage.

Alkylating chemotherapy drugs, such as temozolomide, ifosfamide, and cyclophosphamide, have their effect in every phase of the cell cycle and are thus desirable for use on a wide range of cancers. They have been shown to be very effective in the treatment of slow-growing cancers, solid tumors, and leukemia but are also used to treat lung cancer, ovarian cancer, breast cancer, and others. Both MMS and EMS are S(N)2 agents involved in base N-methylation that can lead to the formation of apurinic sites that block replication [28]. Point mutations are a common and typical consequence of alkylation damage due to guanine alkylation, as are DNA strand breaks and DNA fragmentation. That these agents induce HR has been indicated by an increase in SCEs in various murine tissues (including bone marrow, liver, and kidney tissues) following intraperitoneal injection of MMS [29]. The frequency of HR was also examined using recombination between 2 tandemly arranged neomycin gene fragments in the ovary cells of Chinese hamsters (CHO:5) and was found to be increased by MMS treatment [30]. Using the *in vivo* p^{un} fur-spot assay, other studies have demonstrated that HR is induced by either EMS or MMS [10], which we now recapitulate in this paper using the more sensitive RPE-based p^{un} mouse model. We observed a significant increase in total and single-cell eyespots and a less robust increase in eyespots consisting of more than one cell later in development (distal regions of RPE) following MMS exposure. The latter results contrast our initial

finding with the p^{un} fur-spot assay, which is reliant on clonal expansion of p^{un} reversion events to produce observable fur spots, indicating that we were able to detect multicell events in this tissue. We interpret this result to mean that the induction of multicell events was too weak for the dose used to observe an increase above the background frequency of spontaneous events in the RPE. Alternatively, if we had performed our exposures at an earlier time in fetal development (for example at E10.5 similar to previous studies with other agents [9]), then perhaps we could have observed a clearer induction as the background spontaneous frequency of multicell events is considerably less in the proximal region of the RPE. This may explain the general lack of significant induction of multicell events for all our exposures in this study.

Seminal work showing that PARP1 is involved in DNA repair [31] and activated by ionizing radiation and alkylation damage paved the way for PARP inhibitors to be used in a "synthetic lethality" approach with chemotherapeutic agents [32]. Much work has been done in the form of mouse models of PARP and in *in vitro* work that reveals its role as an early responder to DNA damage and facilitator of HR [33, 34]. PARP inhibition by 3AB is a potent inducer of SCEs in CHO cells [35, 36]. A hyperrecombination phenotype was also observed in work done by Claybon *et al*. using Parp1 nullizygous mice [18]. In the present study, we also show that pharmacological inhibition of PARP1 activity can induce HR in the *in vivo* p^{un} eyespot assay. We saw a significant increase in total and single-cell eyespots, and although not significant, a spike in multicell events closely following 3AB exposure. In the Parp1 nullizygous study, the greatest increase was in multicell events, which is to be expected considering that PARP1 preferentially binds to single-strand breaks, which is a critical step in base-excision repair. In the absence or inhibition of PARP1, a situation occurs where single-strand breaks are not repaired correctly, resulting in a collapsed replication fork due to recombinogenic-associated double-strand break lesions in replicating cells [37, 38]. The weaker response in multicell events observed in the present study might reflect either the transient nature of the inhibitor exposure or the aforementioned issue with high background in spontaneous multicell events for our selected time of exposure.

Several studies involving radiation influence have reported an increased occurrence of cancer following *in utero* exposure [39, 40]. Bleomycin is generally considered to be radiomimetic and a potent source of oxidative stress [41]. Bleomycin and the other enediyne antibiotics achieve site-specific free radical attacks on sugar moieties in both strands of DNA that can result in double-strand breaks [41]. These breaks have been shown to induce HR following bleomycin exposure, as measured by SCEs in CHO cells [42]. A similar phenomenon of robust induction of HR reversion events in more central regions of the RPE, and specifically in single-cell eyespots as seen in this study, was also reported in a paper by Bishop *et al*. using the p^{un} eyespot assay with X-ray damage

[9]. Further, the single-cell reversion events appear to have occurred quickly and for a limited duration, following bleomycin exposure, similar to the inductions observed with ionizing radiation reported previously [43].

Etoposide belongs to one of 2 classes of agents involved in enzyme-mediated anticancer properties through the stabilization of TOP2-DNA complexes and halting processes, such as transcription or replication. Although effective in clinical therapy, etoposide often results in secondary malignancies; indeed, it is thought that chemotherapy drugs targeting the TOP2β isoform may be the source. Etoposide has been shown to induce recombination in several studies. For instance, etoposide induces SCEs in both CHO cells [44] and cultured human lymphocytes [45]. Furthermore, this potent TOP2 inhibitor has been shown to induce somatic intrachromosomal recombination in a whole mouse transgenic (pKZI) mutagenesis model in which a lacZ transgene is only expressed after a DNA inversion [46, 47]. In our study we were able to directly demonstrate that etoposide is capable of strongly inducing HR, specifically resulting in an increase of single-cell eyespots.

Camptothecin binds the TOP1-DNA complex selectively and efficiently, making it a potent chemotherapeutic. This agent has been shown to be involved in recombination in many tissue culture studies involving the induction of SCEs in CHO and human lymphoid cell lines [45, 48, 49, 50, 51, 52]. Enhanced frequency of reversion was seen in an *Hprt*-gene-based reversion-mutation assay in a CHO V79 plasmid system measuring intrachromosomal recombination following camptothecin exposure [53]. Surprisingly, we did not have a robust induction of HR in our p^{un} eyespot assay, although our preliminary fur-spot results indicated an induction recapitulating an earlier report with the p^{un} fur-spot assay using this agent [19]. Again, we observed a clear difference between our RPE and the fur-spot assay, suggesting tissue-specific differences. A developmental requirement for functional TOPI has also been evidenced by the death of *Top1* knockout mice early in embryogenesis [54]. Nucleotide pool disequilibrium is now a strong possibility in explaining many phenomena, such as replication stress associated with aberrant activation of the RB-E2F pathway in early stages of cancer [55] and slowed replication speed in Bloom syndrome [56]. HU inhibits ribonucleotide reductase, an enzyme crucial in the conversion of ribonucleotides into deoxyribonucleotides essential for DNA synthesis. A tight balance of intracellular deoxyribonucleoside triphosphate (dNTP) pools must be kept to maintain genomic integrity in yeast and at sites of damage in mammalian cells. In fact, many studies have shown that alterations in dNTP pools are coupled with genomic instability, mutagenesis, and tumorigenesis [57]. Insufficient nucleotides will cause DNA replication stress and perhaps replication fork collapse, situations known to induce HR. In this respect HU treatment has been shown to be a positive inducer of SCEs in CHO cells [58, 59]. However, we did not observe an

induction of HR in the eyespot assay following HU exposure, but did observe a significant decrease, similar to camptothecin.

Both camptothecin and HU exposure produced a surprising result in that, for the doses chosen, there was an apparent induction of fur-spots but a very significant decrease in eyespots. It is possible that, at the time during development that we performed our exposures, E12.5—melanocyte precursors (dormant migrating melanoblasts) that pigment the fur—are more robust or refractory to DNA damage, while the rapidly dividing RPE cells are either more sensitive or utilize an alternative pathway to repair the DNA lesions produced by camptothecin and HU. Cultured human RPE cells appear to be very sensitive to camptothecin [60], and camptothecin cytotoxicity has been shown to be dependent on DNA synthesis, as the DNA polymerase inhibitor aphidicolin completely blocks camptothecin cytotoxicity [61]. Although a tissue specific cytotoxicity in the developing RPE is a plausible explanation, it does not explain why we observed a decrease in HR events in the RPE below that of spontaneous levels. We have only ever observed a decreased frequency of eyespots when there was a genetic deficiency impairing the homologous recombination process, such as BRCA1 or BRCA2 deficiency ([23] and unpublished data). An alternative explanation is that the camptothecin-induced damage in the p^{un} gene is repaired differently in RPE cells compared to melanoblasts. It is interesting to not that the *Oca2* gene within the RPE is expressed at this time of development but not in melanoblasts [62]. Camptothecin will interrupt both RNA and DNA polymerase progression; thus; it is possible that any damage within the p^{un} gene could be repaired by another mechanism, possibly a transcription-coupled repair mechanism, obviating the need for HR repair. Similarly, the lack of recombination following HU exposure might be due to a higher order response that results in a replication restart (thus avoiding frequent double-strand breaks caused by fork collapse) rather than recombination-mediated gene conversions that would be visualized by the p^{un} assay (see model in [23]). For instance, DNA fiber analysis revealed a defect in replication-fork recovery following HU-mediated imbalance of dNTP pools and a subsequent replication block in BLM-deficient cells [63]. This suggests that BLM may be involved in recovering a stalled fork before a collapse can occur (presumably induced by HU). If a low level of exposure to HU stimulates BLM activity, then converse to the hyperrecombination phenotype in the p^{un} eyespot assay we reported in the absence of BLM [23], activated BLM would be expected to reduce the frequency of p^{un} reversion events and may provide a reasonable explanation for the decreased frequency of eyespots we observed. It is interesting that both camptothecin and HU are known to result in BLM phosphorylation and presumably its activation [64].

According to the American Cancer Society, in 2013 about 580,350 Americans are expected to die of cancer. Cancer is the second most common cause of death in the United States, and cancer in

children has an annual incidence of about 150 new cases per 1 million U.S. children. All cancers involve the malfunction of genes and the other contributions may be additive over a lifetime of internal and external risk factors. Given the number of cell divisions during *in utero* development, it is likely that there is a higher sensitivity during this time to carcinogen exposure [66, 67, 68, 69]. In addition, this might be due to less efficient DNA repair or defective apoptotic mechanisms that facilitate DNA damage into subsequent cell divisions [70]. Further, in mice, about one third of mutations arise before birth [71]. Animal and human epidemiologic studies show a causal relationship for *in utero* exposures (*ie*, diagnostic radiographs [72]) and cancer incidence in children [73, 74, 75]. Given this, *in utero* exposure during critical times in development to DNA-damaging agents or other sources of damage may cause a clonal expansion of somatic mutations. The present study showed that a relatively low single exposure to a wide variety of differently acting agents resulted in an increase of genomic rearrangement (a DNA deletion) at one site in the genome. Notably, this one genomic site can be considered to be representative of up to 12% of the genome with similar structures. This would seem to suggest that a significant amount of somatic genomic rearrangements might be occurring as a consequence of environmental fetal exposures, which likely has a significant impact on the genetic diversity present in somatic tissues. This may explain some of the higher incidences of cancer associated with prenatal exposures.

Specific Aim 2 and 3: Determine whether p53 mutants R172P and R172H suppress spontaneous levels of homologous recombination the same as wild-type p53.

In 1992, p53 was coined as the "guardian of the genome" due to its ability to mitigate cellular stresses and uphold genetic integrity. Yet, 21 years later, we are still unsure which functionality or functionalities of p53 are truly responsible for tumor suppression. Upon sensing stress, p53 is quickly stabilized and then efficiently triggers cell cycle arrest, senescence, or apoptosis in a tissue-specific and damage-dependent manner. Substantial *in vitro* and tissue culture work has led to the creation of sophisticated p53 mouse models such as the surprisingly viable p53 nullizygous mouse. Better mouse models have since been created that compromise one or more aspects of p53 function in order to dissect out the mechanisms of p53 function that are important for maintaining genomic integrity. Interestingly, many of these models still result in spontaneous tumors, despite retaining cell cycle arrest capability and/or the ability to induce apoptosis. Therefore, there is more to this story. p53 must be acting additionally in some other way to protect the genome, which is eventually lost upon p53 mutation or inactivation during tumorigenesis. The role of p53 in homologous recombination has been widely studied, and thus we reconsider the possibility that suppression of genomic variation, by homologous recombination in particular, is another layer of protection provided by p53 during tumor suppression. Here we use the established *in vivo p^{un}* assay to demonstrate a difference in homologous recombination suppression between two p53 mutant mouse models that differ in their ability to arrest the cell-cycle or elicit apoptosis. The p53 R172P mutant retains the ability to arrest the cell cycle but is incapable of eliciting an apoptotic response; nonetheless, we observed a retention of HR suppression for this mutant similar to wildtype. The more aggressive p53 R172H mutant is determined to be globally unfolded and incapable of transactivating p53 target genes and has lost many protein interaction capabilities. This mutant has lost the capability to suppress homologous recombination similar to a p53 nullizygous state, which we propose leads to aberrant rearrangement in the genome. Given that the p^{un} assay is based on the deletion of one copy of a 70 kb duplication, a copy number variation, and should be representative of other such genomic structures, we examined the status of copy number variations by performing array comparative genomic hybridization. We examined mouse embryonic fibroblasts derived from the p53 mutants as well as genotype-matched tumors and observed that p53 is capable of suppressing newly acquired somatic changes in these structures during normal and tumor development. These results support previous findings that Li Fraumeni patients, inheriting a defective copy in p53, show increased copy number variation compared with the normal population. Further, it provides an interesting potential mechanistic basis

for the genetic anticipation phenotype observed with Li Fraumeni families and highlights the impact that certain p53 mutations are likely to directly impact genomic integrity of tumors.

Introduction

TRP53 (herein p53) is a potent tumor suppressor that shields the genome from daily endogenous and exogenous damage. In response to damage, p53 accumulates and acts as a sequence-specific transcription factor to alter the expression of a variety of genes or through protein interactions leading to cell cycle arrest, senescence or apoptosis [253,389-393]. The ability to govern the G1/S cell cycle phase checkpoint and clear damaged cells through programmatic apoptosis are functions of p53 thought to preserve organismal fitness by preventing the conversion of DNA damage into cancer-permitting mutations and chromosomal rearrangements.

Given the key role that p53 plays in preventing cancer occurrence, it is not surprising that p53 is mutated in 50% of all human cancers [119]. Furthermore, people who inherit an autosomal dominant mutation of p53 suffer from Li Fraumeni Syndrome (LFS) and are predisposed to early-onset cancers [394]. Mouse models were created to better understand the functions of p53 that are pivotal for its tumor-suppressor capability. Initial models were simple gene knockouts [262,395,396], and it was somewhat surprising to find that these mice were viable. However, a majority of the p53 nullizygous mice developed lymphomas and sarcomas within 2 to 9 months after birth [262,395,396]. Notably, mouse embryonic fibroblasts (MEFs) from these mice displayed aneuploidy, allelic loss, and gene amplification. In this respect, much of the early work on p53 focused on genome instability and gene mutations (point mutations in particular), as such changes are known to facilitate carcinogenesis; however, much of the evidence for p53 suppression of mutagenesis has been weak [397-399]. Recently, an extensive study of LFS families performed by the Malkin group [171] reported an increased frequency of altered copy number variants (CNVs) in p53 mutation carriers compared to the normal population, which would have been missed with standard mutation-analysis studies. The mechanism(s) and consequences of such changes in LFS is not currently understood.

To better recapitulate both LFS and the p53 mutations found in general cancers, mouse models with specific p53 mutations in the DNA-binding domain have been generated. In particular, a known hotspot locus for p53 mutation, which has been observed with LFS, is the arginine in position 175 of human p53, or 172 in mouse (p53R175, or p53R172, respectively) [400] in which a common missense mutation codes for a histidine (p53 R175H). A rare mutation at this same locus found in a sporadic breast cancer tumors substitutes a proline for the arginine (p53 R175P) and displays only a partially impaired p53 functionality, discussed below. Mouse models were created for the p53 R172P and p53 R172H mutations and showed a differential tumor phenotype that was reflective of the degree of loss in p53 function [194,198,401]. These mutations are of particular interest because the

p53 R172P is a recessive mutation that can induce partial cell cycle arrest in response to DNA damage but is unable to cause apoptosis. Mice homozygous for this mutation escape the early onset of lymphomas but eventually succumb to lymphomas and sarcomas around 7–13 months of age [401]. Further, these tumors do not have the chromosomal aneuploidy that is often observed in p53 nullizygous tumors [401]. In contrast, the p53 R172H mutation is autosomal dominant with no apparent ability to transactivate p53 target genes (neither cell cycle genes nor apoptotic genes) [193]. Furthermore, it has been argued that p53 R172H mice have gain-of-function phenotypes, suggesting that the p53 R172H mutation is more detrimental than the p53 R172P mutation in that the former mice have an earlier onset of tumors and a higher incidence of metastasis [198]. The fact that the R172 p53 mutations result in some level of separation of function and a difference in cancer onset provides an exciting opportunity to further dissect the mechanisms involved in p53 tumor suppression.

Despite the lack of evidence for p53 directly suppressing gene mutation, p53 has been linked to various DNA repair pathways, namely nucleotide excision repair, base excision repair, and double-strand break (DSB) repair, including homologous recombination (HR) (for reviews see [402-405]). HR is a DNA repair mechanism recently associated with proliferating cells capable of repairing a variety of lesions that utilizes sequence homology for repair; either through a deletion-mediated event (single-strand annealing, SSA) or a high fidelity strand exchange process (canonical HR) [312,406]. However, presumably because of the high level of repetitive DNA present in mammalian genomes, either hyperrecombination or hyporecombination can be detrimental. This is exemplified by the genomic instability resulting from the hyperrecombination phenotype observed in cancer predisposed Bloom patients [407] or hyporecombination upon loss of *BRCA1* and *BRCA2* [408] leading to a "BRCAness" phenotype that predisposes to breast and ovarian cancer. Numerous studies have examined the effect of p53 on HR. For example, it has been reported that p53 down regulates spontaneous HR in a chromosomally integrated plasmid substrate [282]. The authors overexpressed $p53^{175\ (Arg>His)}$, causing a 5- to 20-fold increase in spontaneous recombination compared to wildtype (WT) control cells; these recombination events appeared to be resultant from both gene conversions and deletion events. Using a similar substrate that only measures gene conversion events and a temperature sensitive p53 mutant (Alanine 135 to Valine) that misfolds at 37ºC, Willers *et al.* also showed that p53 suppresses recombination [285]. The Wiesmüller laboratory has also extensively explored the role of p53 in HR using a rare cutting endonuclease (I*Sce*-I) in breast cancer cells and human lymphoid/leukemia cells with varying p53 mutations. Their studies used a DSB repair assay to show that some p53 mutants retain partial ability to repair DSBs by repressing aberrant HR [270,293].

Another approach to examining HR *in vivo* is the use of the pink-eyed unstable (p^{un}) mouse model. The p^{un} mutation consists of a 70 kb–duplicated region of DNA—effectively a segmental duplication or a CNV—that disrupts the function of the *p* gene (*Oca2*) [323]. The *p* gene encodes for an integral membrane protein that is important for pH regulation in melanosomes to ensure efficient melanin synthesis. The p^{un} mutation causes a dilution of this color in pigmented cells of the mouse, namely melanocytes that confer coat color to fur and in the retinal pigment epithelium (RPE) of the eye. A functional *P* gene is rendered when the 70 kb duplication is reverted (via deletion of one copy of the duplicate), thus allowing for proper melanin packing in cells. These reversion events are scored as black spots on the dilute fur of a mouse or pigmented cells in the RPE of the mouse eye [324]. Because RPE proliferation occurs mainly during embryonic development, we were able to determine the impact on somatic HR using this simple pigment-based assay system [242]. This system was previously used to demonstrate that p53 suppresses HR during normal somatic development in the RPE using p53 knockout mice [247].

In this study, we used the *in vivo* p^{un} assay to explore whether the R172 separation of function p53 mutants differentially affected genome stability. We observed that the R172H mutation was incapable of suppressing recombination either early or late in development, whereas the R172P mutation was incapable of suppressing late developmental events. The early events were associated with clonal expansion and are reminiscent of replication-tied recombination events observed in the absence of BLM or PARP1 [248,250]. The late events appeared to occur without extensive clonal expansion, similar to the types of events observed in the absence of BRCA1 or BRCA2 ([248] and unpublished data) that suggests they may be the result of SSA events. To extend these studies we also used array comparative genomic hybridization (aCGH) to compare MEFs and tumors from respective p53 mutant genotypes for changes in CNVs. Similar to the study by the Malkin laboratory [171], we observed increased acquired changes in CNV frequency in primary MEFs derived from the more aggressively cancer-prone R172H mice compared with R172P mice. This study supports the idea that p53 has a significant role in suppressing HR and maintaining genomic stability through normal somatic development in addition to cell cycle arrest, senescence, and apoptosis in its tumor-suppressing role.

Mouse strains and breeding cohorts

Mice heterozygous for the point mutations $p53^{R172P}$ and $p53^{R172H}$, both on a C57BL/6 genetic background, were kindly provided by Dr. G. Lozano (M.D. Anderson). In addition, 2 crosses were made to C57BL/6J $p^{un/un}$ mice obtained from the Jackson Laboratory (Bar Harbor, ME) to establish

the homozygous $p^{un/un}$ genotype. Mice heterozygous for a targeted nullizygous allele of $p53$ were previously crossed into a C57BL/6J $p^{un/un}$ genetic background as described in Aubrecht *et al*. [264].

All mice were homozygous $p^{un/un}$; otherwise, 3 independent colonies were maintained by intercrossing mice heterozygous for each allele; $p53^{R172P/+}$, $p53^{R172H/+}$, or $p53^{neo/+}$. Each intercross produced homozygous mutant mice (used for the experimental group) or littermate wildtype mice (used for the control group). All animal studies were carried out in accordance with UTHSCSA and IACUC policies as outlined in protocols 05054-34-01-A and 07005-34-02-A,B1,C.

The $p53^{R172P}$, $p53^{R172H}$, and $p53^{neo}$ genotypes were determined by PCR, as previously described [198] and [264], respectively. The $p^{un/un}$ genotype was identified by the phenotypic dilute (grey) coat color.

Eye dissection and p^{un} reversion (homologous recombination) assay

Mice were sacrificed at weaning age and their eyes harvested and dissected to expose the RPE, as previously described [252]. Briefly, each RPE whole mount was digitally photographed and analyzed for eyespots using a Zeiss Lumar version 12 stereomicroscope, Zeiss AxioVision MRm camera, and Zeiss AxioVision 4.6 software (Thornwood, NY), as described in Claybon *et al.* [250]. The criteria for what constitutes an eyespot, was previously defined as one or more reverted cell (indicated by black pigmentation in an otherwise transparent cell layer) separated by no more than one unpigmented cell [252]. To determine the time in development when the eyespots were produced, we followed the criteria set-forth by Bishop *et al.* by measuring (a) the frequency of eyespots (reversion events) per RPE and (b) distribution of the eyespots within the RPE (eyespot position) [245].

Primary mouse embryonic fibroblast culture, tumor harvest and DNA extraction

Primary MEFs were obtained by intercrossing heterozygous mice in each respective cohort to produce p53 mutant homozygous mice ($p53^{R172P/R172P}$ $p^{un/un}$, $p53^{R172H/R172H}$ $p^{un/un}$) along with select littermate controls ($p53^{R172H/+}$ $p^{un/un}$, $p53^{+/+}$ $p^{un/un}$). Pregnancies were timed by confirmation of a vaginal copulation plug and assigned as embryo day E0.5. Embryos were harvested on day E14.5 and mechanically and chemically (0.05% Trypsin-EDTA) homogenized for 20 minutes. Cells were cultured in Dulbecco's Modified Eagle's Medium (DMEM) supplemented with 10,000 U/mL penicillin, 10,000 µg/mL streptomycin, and 25 µg/mL Amphotericin B (Cellgro, VA). Cells were grown at 37°C in the presence of 5% CO_2 in a humidified incubator and allowed to propagate for 2 passages to obtain enough genetic material for experiments.

Tumors arising in each respective p53 mutant cohort were immediately harvested and processed for DNA extraction. From our p53 R172H colony we harvested 2 mice (testicular sarcoma and fibrohistiocytic tumors) and obtained two p53 R172H heterozygous mice tumor samples (fibrosarcoma, sarcoma NOS (not otherwise specified)) from Dr. G. Lozano (MD Anderson) as well as 4 tumor samples from *p53$^{R172P/R172P}$* mice (hemangiosarcoma, sarcoma NOS, neurofibrosarcoma and a liver histiocytic sarcoma).

DNA was extracted from MEFs, tissues and tumors using the Qiagen DNeasy blood and tissue kit following the manufacturer's instructions. DNA was quantified using a NanoDrop spectrophotometer, and quality was assessed by agarose gel electrophoresis.

RNA Microarray analysis

Gene expression microarray analysis was performed using Agilent Whole Mouse Genome 4x44k microarrays with E14.5 MEFs from p53 R172H homozygous (HH) and heterozygous (HWT), p53 R172P homozygous (PP), and wildtype (WT) mice. Quality plots were obtained for all the microarrays using the "arrayQuality" package from Bioconductor. The Loess method was used to normalize the intensities within each array [410]. The data were then grouped according to the different comparisons (HWT vs. WT, PP vs. WT, HH vs. WT, HH vs. HWT, and HH vs. PP) and quantile normalization was performed to adjust for bias between microarrays.

53BP1 co-immunoprecipitation experiment

Plasmids: pCMH6K53BP1-FL are HIS and HA tagged (from Kuniyoshi Iwabuchi [411]). pTHFN-p53WT, pTHFN-p53R175P and pTHFN-p53R175H are HIS and FLAG tagged.

Cell culture: HCT116 (p53$^{-/-}$) cells were maintained at 5% CO_2 in DMEM supplemented with 10% fetal calf serum and penicillin. HCT116 (p53$^{-/-}$) cells were transfected using the TransIT-LTI transfection reagent (Mirus) according to the manufacturer's recommendations. Cells were lysed 48 hours after transfection with cell lysis buffer (50mM Tris-HCl, 150mM NaCl, 1mM EDTA and 1% Triton X-100).

Co-immunoprecipitation: pCMH6K53BP1-FL was overexpressed with either pTHFN-p53WT, pTHFN-p53R175P, pTHFN-p53R175H or pTHFN (empty vector). Prior to performing the immunoprecipitation an aliquot of the cell lysate was removed to serve as the loading control. Rabbit α-FLAG or rabbit α-MYC was then added to the lysate. Rabbit α-FLAG was used to immunoprecipitate p53 and rabbit α-MYC served as the negative control. Additionally, protein G agarose beads previously blocked with 10% BSA were added to the lysate. The lysates were incubated at 4°C for 16 hours. Protein complexes were isolated by centrifugation and the pellets were washed four times with cell lysis buffer. The final wash was then removed and the pellet was resuspended in 2X SDS-PAGE loading buffer. The samples were denatured by heating at 95°C for 5 minutes, resolved by SDS-PAGE and transferred to nitrocellulose for Western blotting. Rabbit α-53BP1FL (Bethyl, TX) and mouse α-p53 (Cell Signaling, MA) were used to detect complex formation and immunoprecipitation efficiency, respectively.

Statistics

Statistical analysis for the p^{un} assay was performed using GraphPad Prism 6.0 (La Jolla, CA) software. We first performed a normality test (D'Agostino & Pearson omnibus normality test and Shapiro-Wilk normality test) and determined that our data did not follow a normal Gaussian distribution. We therefore chose nonparametric tests that compare distributions of 2 unpaired groups. A Mann-Whitney test was used to analyze the frequency of p^{un} reversion events per RPE between wildtype and mice differing in p53 genotype. We used a Kolmogorov-Smirnov test to analyze distribution differences in the position of the p^{un} eyespots on the RPE between wildtype and all p53 genotypes.

Statistical analysis for filtered CNV regions was performed using GraphPad Prism 6.0 (La Jolla, CA) using a nonparametric Mann-Whitney test to compare experimental samples with wildtype. All statistical analyses for microarray experiments were done using the Bioconductor project

implemented in R statistical software. For each of the 5 comparisons; a moderated t test from the limma package was used to identify differentially expressed genes. The P values obtained from the t test were controlled for false discovery rate (0.05) using the Benjamini and Hochberg method.

Results

p53 nullizygosity results in an altered homologous recombination frequency compared with wildtype and p53 heterozygosity

As a potent tumor suppressor, p53 plays an important role in protecting the integrity of the genome from various sources of damage, either endogenous or exogenous. HR is able to repair a variety of DNA lesions with high fidelity during DNA replication when the appropriate homologous sequences are available. However, either too much or too little HR can have deleterious effects on genome integrity. In a previous study the RPE-based p^{un} reversion assay was used to show that absence of p53 resulted in a hyperrecombination phenotype compared to wildtype mice during normal somatic development [247]. In this study, breeding cohorts were established and maintained by intercrossing $p53^{neo/+}$ $p^{un/un}$ mice, resulting in p53 wildtype, p53 heterozygous, and p53 nullizygous animals. We sought to recapitulate the p53 HR phenotype previously reported and also ask whether p53 heterozygosity impacted HR frequency, which would suggest a haploinsufficiency phenotype. Upon examining the frequency of eyespots (p^{un} reversions) per RPE using the *in vivo* p^{un} assay we saw no difference between wildtype mice and mice heterozygous for p53, leading us to believe that one copy of p53 is sufficient to suppress aberrant HR and maintain genomic stability (Tables 3.1 and 3.2(a) and Figure 3.1(a)). In contrast, p53 nullizygous mice showed a two-fold increase in eyespots compared with wildtype and heterozygous mice ($P < .0001$; Mann-Whitney test), similar to what was reported before [247]. The loss of p53 is detrimental in the suppression of aberrant HR events, as evidenced by our model.

TABLE 3.1   SUMMARY OF *p^{un}* REVERSION EVENTS AND RPE EXAMINED IN VARIOUS p53
GENOTYPES

	TOTAL				AVERAGE		
Genotype	RPE	Eyespots	Cells		Eyespots per RPE	Cells per RPE	Cells per Eyespot
Wildtype	34	137	304		4.0 ± 2.1	8.9 ± 6.4	2.0 ± 1.2
p53 heterozygous	29	123	235		4.2 ± 2.7	8.2 ± 7.5	2.0 ± 2.9
p53 nullizygous	22	193	507		8.8 ± 4.3	23.0 ± 19.5	2.6 ± 3.3
p53 R172P homozygous	30	131	347		4.4 ± 2.4	11.6 ± 14.8	2.6 ± 5.0
p53 R172H heterozygous	8	68	149		8.5 ± 2.9	18.6 ± 10.2	2.2 ± 2.6
p53 R172H homozygous	37	319	737		8.6 ± 4.3	20.0 ± 13.8	2.3 ± 2.5

Loss of function mutations in p53 result in differing homologous recombination phenotypes

The $p53^{R172P}$ point mutation is a recessive mutation resulting in p53 protein with a partially misfolded DNA-binding domain that is postulated to be deficient in eliciting an apoptotic response but is able to partially arrest the cell cycle [401]. The more aggressive $p53^{R172H}$ point mutation is a dominant allele that results in a p53 protein product with a substantially misfolded DNA-binding domain. As such, this mutant p53 protein is unable to bind and transcribe many of the putative p53 target genes [198], [194]. In addition, many of the normal protein interactions of p53, particularly those mediated through this domain, are disrupted [194,198]. Given this separation in function between the mutant alleles, we sought to determine whether mutant p53 is capable of suppressing HR in our RPE-based p^{un} assay. Upon examining RPE harvested from the $p53^{R172P/R172P}$ (herein p53 R172P) mice, we did not observe a significant increase in the number of total eyespots compared to wildtype or p53 heterozygous mice (Tables 3.1 and 3.2(a) and Figure 3.1(a)). We examined a limited number of p53 R172P heterozygous RPE and saw no difference from wildtype RPE. Given this observation and the known recessive phenotype of the R172P allele, we did not include this genotype in this study. However, similar to wildtype mice, there was a significant difference in the number of reversion events for p53 R172P homozygous mutant mice compared with p53 nullizygous mice (*P < .001*; Mann-Whitney test). In contrast to the p53 R172P homozygous mice, the total eyespot frequency of p^{un} reversion events in the $p53^{R172H/R172H}$ $p^{un/un}$ (p53 R172H homozygous) mouse was significantly higher than in the wildtype control genotypes and the p53 R172P mutant mouse (*P < .0001*; Mann-Whitney test; Tables 3.1 and 3.2(a) and Figure 3.1(a)). Interestingly, the p^{un} reversion frequencies of the p53 R172H heterozygous and homozygous mice were not significantly different from p53 nullizygous animals (~9 eyespots per RPE). These results suggest that the loss function in p53 R172H mutation results in a lack of suppression of HR similar to that in a mouse that produces no p53 protein whatsoever, and that the R172H allele acts in a dominant negative fashion with regard to this p53 function. In contrast, our initial analysis suggests that p53 R172P mutant mice retain the ability to suppress HR similar to the control genotypes.
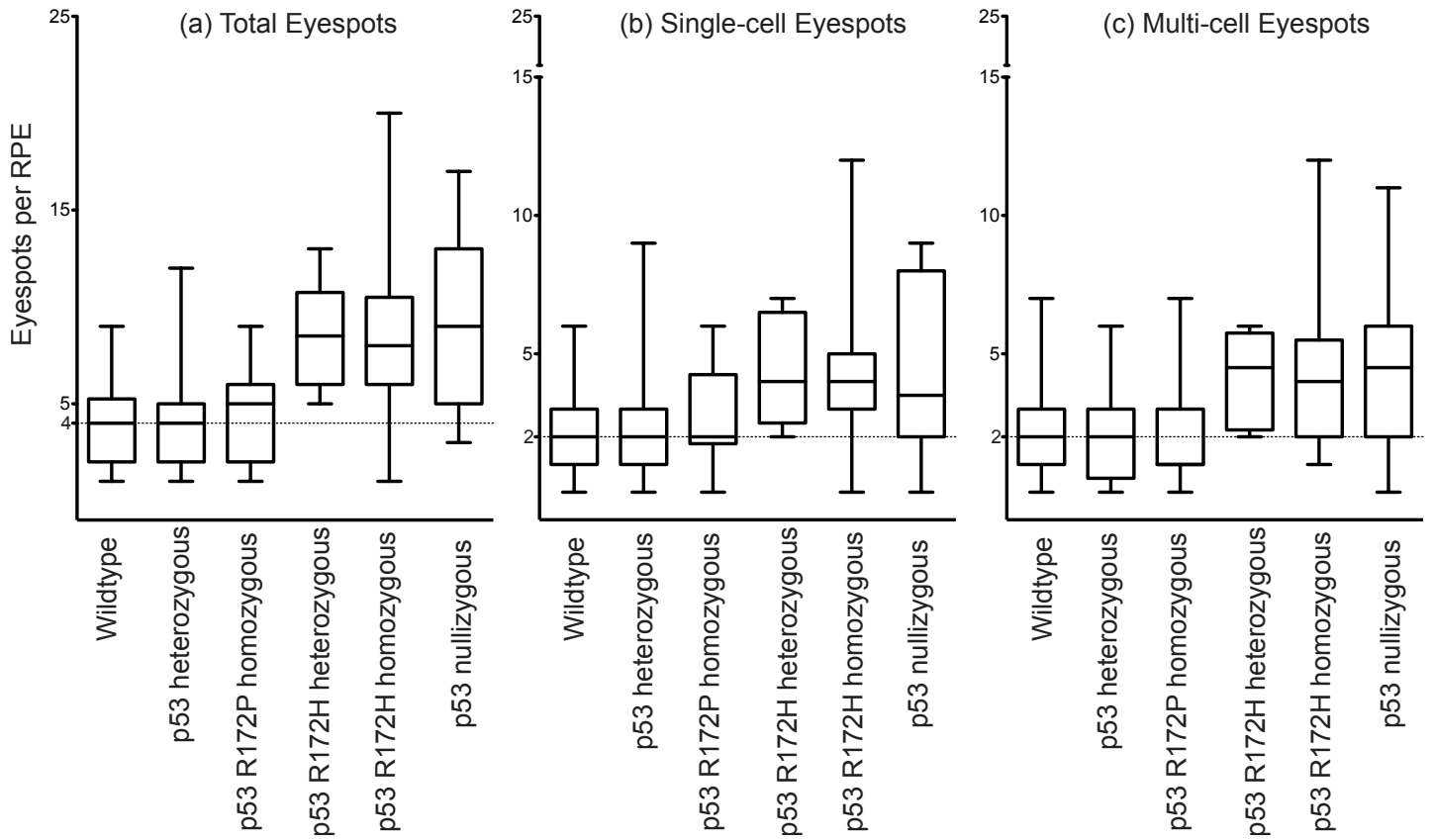
Figure 3.1 **Tukey Box and Whiskers Plot of the Frequency of p^{un} Reversion Events**. Figures are denoted for (a) Total (b) Single-cell, and (c) Multi-cell eyespots per RPE for the various p53 experimental genotypes. The dashed line indicates the average frequency on p^{un} reversion in control WT RPE for comparison.

TABLE 3.2   STATISTICAL SIGNIFICANCE FOR (A) TOTAL, (B) SINGLE-CELL, AND (C) MULTI-CELL EYESPOTS PER RPE FOR THE VARIOUS P53 EXPERIMENTAL GENOTYPES

(a) Total Eyespots	Wildtype	p53 heterozygous	p53 R172P homozygous	p53 R172H heterozygous	p53 R172H homozygous	p53 nullizygous
Wildtype						
p53 heterozygous	ns					
p53 R172P homozygous	ns	ns				
p53 R172H heterozygous	*P <0.001*	*P <0.001*	*P <0.001*			
p53 R172H homozygous	*P <0.0001*	*P <0.0001*	*P <0.0001*	ns		
p53 nullizygous	*P <0.0001*	*P <0.0001*	*P <0.001*	ns	ns	

(b) Single-Cell Eyespots	Wildtype	p53 heterozygous	p53 R172P homozygous	p53 R172H heterozygous	p53 R172H homozygous	p53 nullizygous
Wildtype						
p53 heterozygous	ns					
p53 R172P homozygous	ns	ns				
p53 R172H heterozygous	*P <0.01*	*P <0.05*	ns			
p53 R172H homozygous	*P <0.0001*	*P <0.001*	*P <0.01*	ns		
p53 nullizygous	*P <0.001*	*P <0.01*	*P <0.05*	ns	ns	

(c) Multi-cell Eyespots	Wildtype	p53 heterozygous	p53 R172P homozygous	p53 R172H heterozygous	p53 R172H homozygous	p53 nullizygous
Wildtype						
p53 heterozygous	ns					
p53 R172P homozygous	ns	ns				
p53 R172H heterozygous	*P <0.01*	*P <0.01*	*P <0.01*			
p53 R172H homozygous	*P <0.0001*	*P <0.0001*	*P <0.0001*	ns		
p53 nullizygous	*P <0.01*	*P <0.001*	*P <0.001*	ns	ns	

Note. A nonparametric Mann-Whitney test was used to analyze eyespot frequency data; significance is denoted for all genotypes compared (*ns* = not significant).

Frequency of single-cell and multi-cell reversion events differ depending on p53 status

In addition to generating information regarding the frequency of reversion events, the p^{un} RPE-based reversion assay can be further categorized into those eyespots consisting of one cell (single-cell eyespots) and those with more than one cell (multi-cell eyespots). From work with BLM-, PARP1-, BRCA1-, and BRCA2-deficient mice, the single-cell and multi-cell populations appear to represent different types of events: RAD51-dependent replication-tied HR events and replication independent SSA events ([248,250] and unpublished data). Multi-cell (clonally expanded) eyespots most likely arose from replication-tied events. In contrast, the single-cell eyespots could result from a reversion event that was not necessarily tied to DNA replication or could have occurred in a cell that was in its terminal cell division.

No significant difference in the frequency of single-cell events between wildtype, p53 heterozygous, or p53 R172P homozygous mice was observed (Figure 3.1(b) and Table 3.2(b)). Of note, the overall frequency of p53 R172P single-cell events appeared to be slightly higher than wildtype, although not significantly, and yet the frequency of these events is not significantly different from p53 R172H heterozygous mice. In comparison to p53 R172H and p53 nullizygous animals, the frequency of single cell events in p53 R172P homozygous, though significantly less ($P < .05$; Mann-Whitney), is not as significant as the difference of these genotypes to wildtype or p53 heterozygous mice ($P < .0001$ to .01; Mann-Whitney). Clearly, there was a significant increase in single-cell reversion events in the p53 nullizygous ($P < .01$; Mann-Whitney), p53 R172H mutant heterozygous ($P < .01$; Mann-Whitney) and homozygous ($P < .0001$; Mann-Whitney) mice compared to wildtype mice (Figure 3.1(b) and Table 3.2(b)). Considering the slight, albeit not significant increase in single cell spots in the p53 R172P homozygous animals we decided that these events warranted a little further investigation.

Examination of the multi-cell eyespots revealed no significant difference between the wildtype and p53 R172P genotypes (Figure 3.1(c) and Table 3.2(c)). In contrast, the p53 R172H heterozygous and homozygous mice were similar to the p53 nullizygous mice in that they showed an increased frequency of multi-cell reversion events compared to wildtype and p53 heterozygous mice ($P < .0001$ and $P < .01$, respectively; Mann-Whitney test; Figure 3.1(c) and Table 3.2(c)). p53 nullizygous mice also showed significantly more multi-cell eyespots than did the p53 R172P mutant mice ($P < .01$; Mann-Whitney) but did not show more than the p53 R172H heterozygous or homozygous mutants (Figure 3.1(c) and Table 3.2(c)). Interestingly, unlike the frequency of single cell events, the p53 R172P homozygous mice had as strong of a significant difference from p53 nullizygous and p53

R172H as the wildtype and p53 heterozygous mice. Because p53 R172H heterozygosity seemed to behave similar to the homozygous state (and given its known dominant negative phenotype), we combined these groups for all subsequent analyses (hereinafter p53 R172H). Similarly, the wildtype and p53 heterozygous mice behaved the same and were also combined for subsequent analysis where noted (hereinafter combined control).

The fact that we see an increased frequency of single- and multi-cell reversion events in the p53 R172H mutant suggests that both SSA and RAD51-dependent replication-tied events may be occurring; additionally, a subset of those replication-tied events might be suppressed, with the retention of some wildtype function in the p53 R172P mutant mice.

Position frequency of p^{un} eyespots reveals reversion events later in development for p53 mutants

Another aspect of the p^{un} assay that can provide insight into the type of events that are occurring is to determine the position of each reversion event on the RPE (eyespot position) as that information can be correlated with a time during embryonic development when the event occurred. The RPE develops according to an edge-biased pattern of proliferating cells that orient outward radially [242]. It was demonstrated by Bishop *et al.* that the location of revertant events (in this case induced at a specific time by the DNA-damaging agent benzo(a)pyrene) in the adult RPE) correlated strongly with a specific time in embryonic development (from 8.5 dpc to 17.5 dpc [252]). Therefore, eyespots that are positioned near the centrally located optic nerve occur early in development, whereas those located toward the edge of the RPE (distal to the optic nerve head) most likely occur later in embryo development.

To determine if there was a positional effect between mice with differing p53 protein status, we used a nonparametric Kolmogorov-Smirnov test to evaluate the distribution of the frequency of eyespots in various position intervals (hereinafter position distribution; Figure 3.2). The combined control distribution (shown as dark bars in all position figures) of total eyespots showed that most of the reversion events are in the latter third of the RPE, where 60% of eyespots are in the region from 0.6 to 1.0 (Figures 3.2(a), 3.2(b), and 3.2(c)), similar to what was previously reported [252]. Eyespot position distribution of total combined control eyespots differed significantly from p53 R172P mice (*P* < 8.8e-13; Kolmogorov-Smirnov test), which showed reversion events more distally located on the RPE (Figure 3.2(a)). The position distributions of p53 nullizygous (*P < 0.05*; Kolmogorov-Smirnov test) and p53 R172H (*P < 1.8e-12*; Kolmogorov-Smirnov test) were also significantly different from the combined control in that there was a similar edge effect (Figure 3.2(a)). In addition, p53 nullizygous

41

and p53 R172H mice showed reversion events in the more proximal region of 0.0 to 0.6 when compared to the combined control. This same pattern of earlier events in p53 nullizygous mice has been previously reported by Bishop *et al.* [247].

We extended this analysis by evaluating the pattern of position distribution for single- and multi-cell events independently. Examination of RPE for single-cell eyespots revealed a pattern similar to that of total eyespots (Figure 3.2(b)). All experimental genotypes—p53 R172P, p53 R172H, and p53 nullizygous—were significantly different from the combined control ($P < 2.0e-08$, $P < 4.2e-10$, $P < 2.1e-14$, $P < 0.02$, respectively; Kolmogorov-Smirnov test). These results indicated a preference for single-cell events later in development compared with earlier events, which was also seen in p53 nullizygous and p53 R172H mice. Analysis of the eyespots consisting of more than one reverted cell (multi-cell eyespot) also showed a significant difference in patterning in the distal region of the RPE between the combined control and p53 R172P mice ($P < 4.2e-05$; Kolmogorov-Smirnov test) and p53 R172H mice ($P < 2.8e-04$; Kolmogorov-Smirnov test) (Figure 3.2(c)). No significant difference in position distribution was found between the combined control and p53 nullizygous mice for multi-cell reversion events (greater than 1 pigmented cell); however, a clear pattern of increased early events was observed, suggesting more clonal expansion in proliferating cells in the absence of p53. An increase in these events in the same region was demonstrated with statistical significance in the earlier report with p53 nullizygous mice [247]. Again, the patterning of early and late multi-cell eyespots was similar to what was seen with total and single-cell eyespots in these mice.
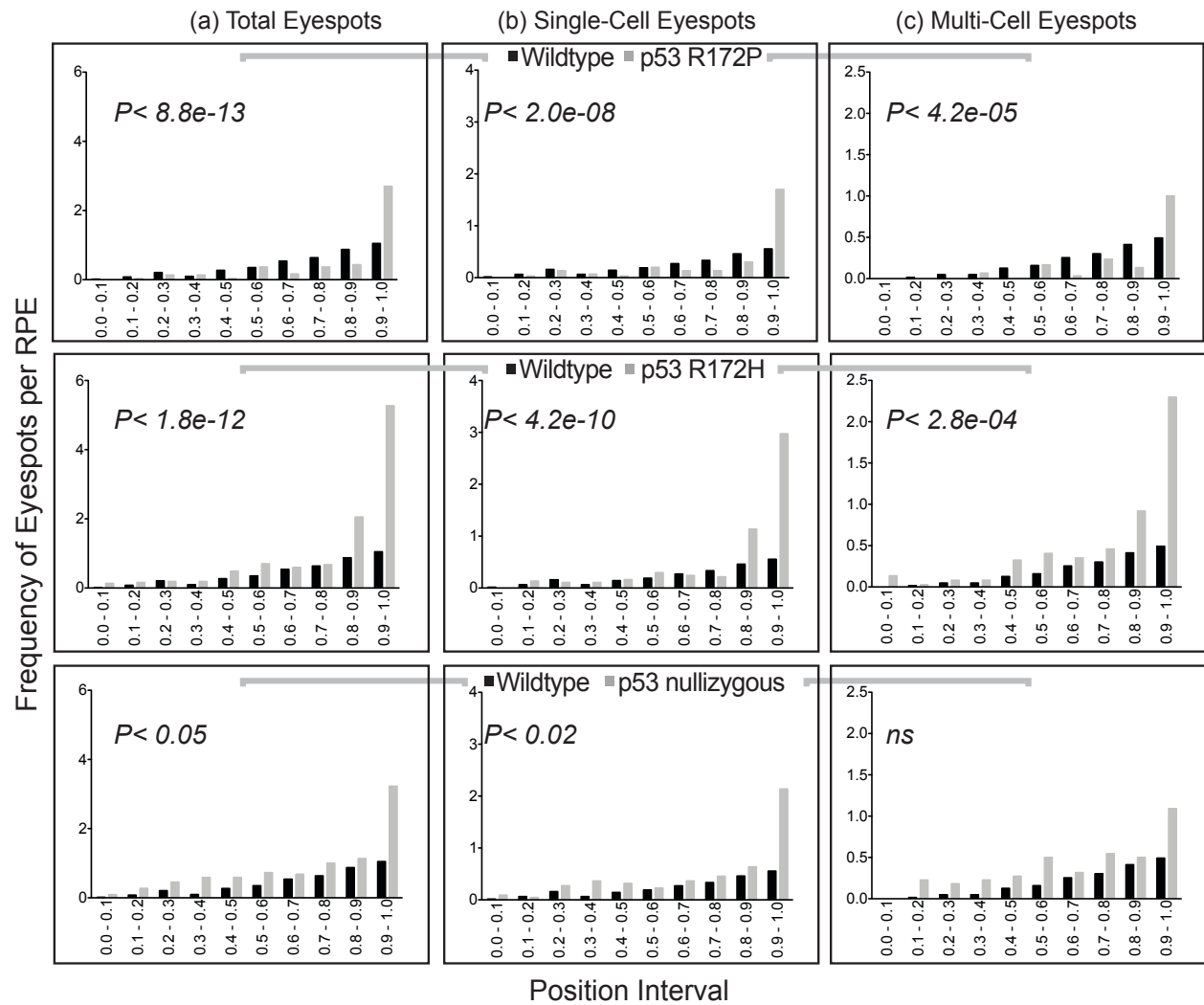
Figure 3.2   **Position Distribution Analysis of p^{un} Reversion Events per RPE**. Denoted for (a) Total, (b) Single-cell, and (c) Multi-cell eyespots. Position intervals are indicated on the x-axis, where 0.0 corresponds to the region near the optic nerve and 1.0 represents the edge of the RPE. A Kolmogorov-Smirnov test was used to analyze distribution differences in position intervals of the RPE for experimental genotypes compared to the combined control (denoted as wildtype in the figure).

Assessment of p53 dependent gene expression in HR suppression

It has been well established that p53 responds to cellular stress signals primarily through its transcriptional regulation of a number of target genes involved in processes such as cell cycle arrest (*e.g.*, *p21, GADD45a, CDC25c, 14-3-3σ*) and apoptosis (*eg*, *PUMA, NOXA, BAX*) [412-414]. Given the differential suppression of HR observed in the p53 mutants in the p^{un} assay, we examined whether there was a change in expression of HR-related genes that might provide a mechanism for this difference in suppressing HR between the 2 mutants. We performed an RNA gene-expression analysis using Agilent Whole Mouse Genome 4x44K microarrays on wildtype, p53 R172H heterozygous and homozygous, as well as p53 R172P homozygous E14.5 MEFs. We saw no obvious gene induction or repression of HR-related proteins (*eg*, *Rpa, Rad51, Brca1, Brca2, Blm, Wrn, etc.*; Figures 3.3 and 3.4 and Table 3.3). We observed a significant increase in the number of genes expressed in p53 R172H heterozygous and homozygous MEFs compared with p53 R172P homozygous MEFs; however, no DNA repair–related genes were observed (Figure 3.4 and Table 3.3). This is in contrast to a study observing transcriptional repression of *Rad51* by p53 [278]. This discrepancy can possibly be explained by the limited number of samples and the sensitivity of the microarray used in this study. However, many tissue culture studies have reported the uncoupling of p53's transcription capability and G1/S arrest function and its role in recombination repair [212,269,285,289].

Implications of dysfunctional protein interaction in the mechanism of p53 suppression of HR

p53 has been shown to interact with HR proteins such as RPA [289] and RAD51 [415], in the transactivation domain and overlapping regions of the DNA binding domain (amino acids 94-160 and 264-315), respectively. Disruption of such interactions has been shown to affect gene conversions, a RAD51 dependent type of HR. To this regard, we sought to determine if the misfolded DBD, conferred by p53 mutation, could cause a disruption in interactions with HR proteins involved in SSA type events. Recently, the association between 53BP1 and HR has been a hot topic given the rescue of embryonic lethality of BRCA1 Δ11 mutation by concomitant loss of 53BP1 [314]. It was reported by Bunting *et al.* that 53BP1 inhibits HR by blocking DNA end resection in BRCA1-deficient cells [313]. We have also observed an increased HR frequency in the *in vivo* RPE-based p^{un} assay in 53BP1-deficient mice (unpublished data). 53BP1 interacts through its BRCT repeats, similar to BRCA1, to

the DNA-binding domain of p53 [416], the same region that is disrupted by R172 mutations. Of note, the embryonic lethality of BRCA1 Δ11 homozygous mutation can also be rescued by p53 deficiency (either heterozygosity or nullizygosity [417,418]). Based on those studies, the known interaction between 53BP1 and p53 and the known role of 53BP1 in modulating HR, we set out to determine if the p53 R172P mutants retained or lost the ability to bind to 53BP1. The p53 R172H, with its complete loss of protein folding in the DNA binding domain has already been shown not to bind to 53BP1 [419]. To test this interaction, we performed a co-immunoprecipitation experiment with full-length-53BP1 (Figure 3.5). The p53 mutants showed equivalent weak binding to 53BP1 compared to wildtype p53. This provides a reasonable explanation as to the mechanism by which neither p53 mutant is able to suppress 53BP1 mediated SSA events. However, this does not explain the difference in overall HR frequency, multi-cell events in particular, seen with the two p53 mutants that we observed in this study. The most likely explanation is that p53 is using some alternative mechanism to suppress RAD51 dependent HR events that remains to be determined.
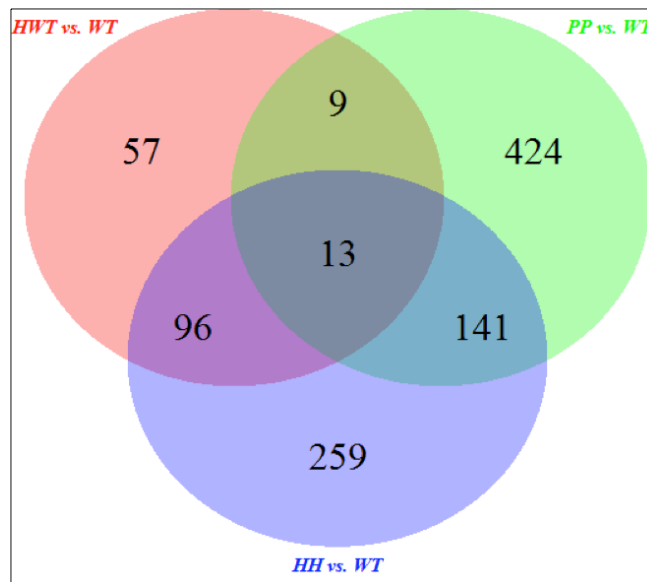
Figure 3.3   **Venn Diagram of Shared and Unique Genes from Microarray Analysis with p53 Mutant Mouse Embryonic Fibroblasts.** p53 mutants are denoted as follows: p53 R172H heterozygous (HWT), p53 R172P homozygous (PP) and p53 R172H homozygous (HH) compared with wildtype (WT).
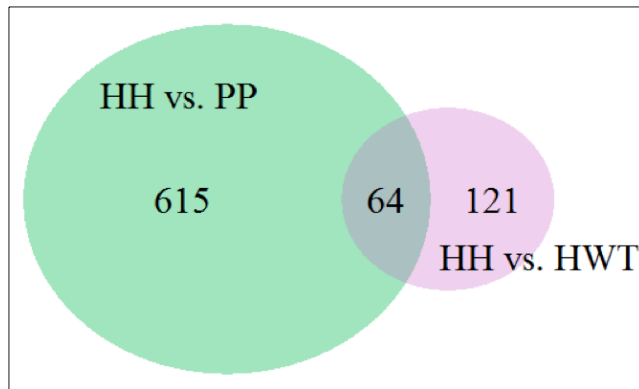
Figure 3.4   **Venn Diagram Showing Shared and Unique Genes between p53 Mutants.** Microarray analysis performed with MEFs from p53 R172H heterozygous (HWT), p53 R172P homozygous (PP), and p53 R172H homozygous (HH) mice.

53BP1FL	+	+	+	+	+
p53 WT	-	-	+	-	-
p53R175P	-	+	-	+	-
p53R175H	-	-	-	-	+
empty vector	+	-	-	-	-
Lane	1	2	3	4	5

Immunoprecipitation — α-53BP1

α-p53

Whole Cell lysate — α-53BP1
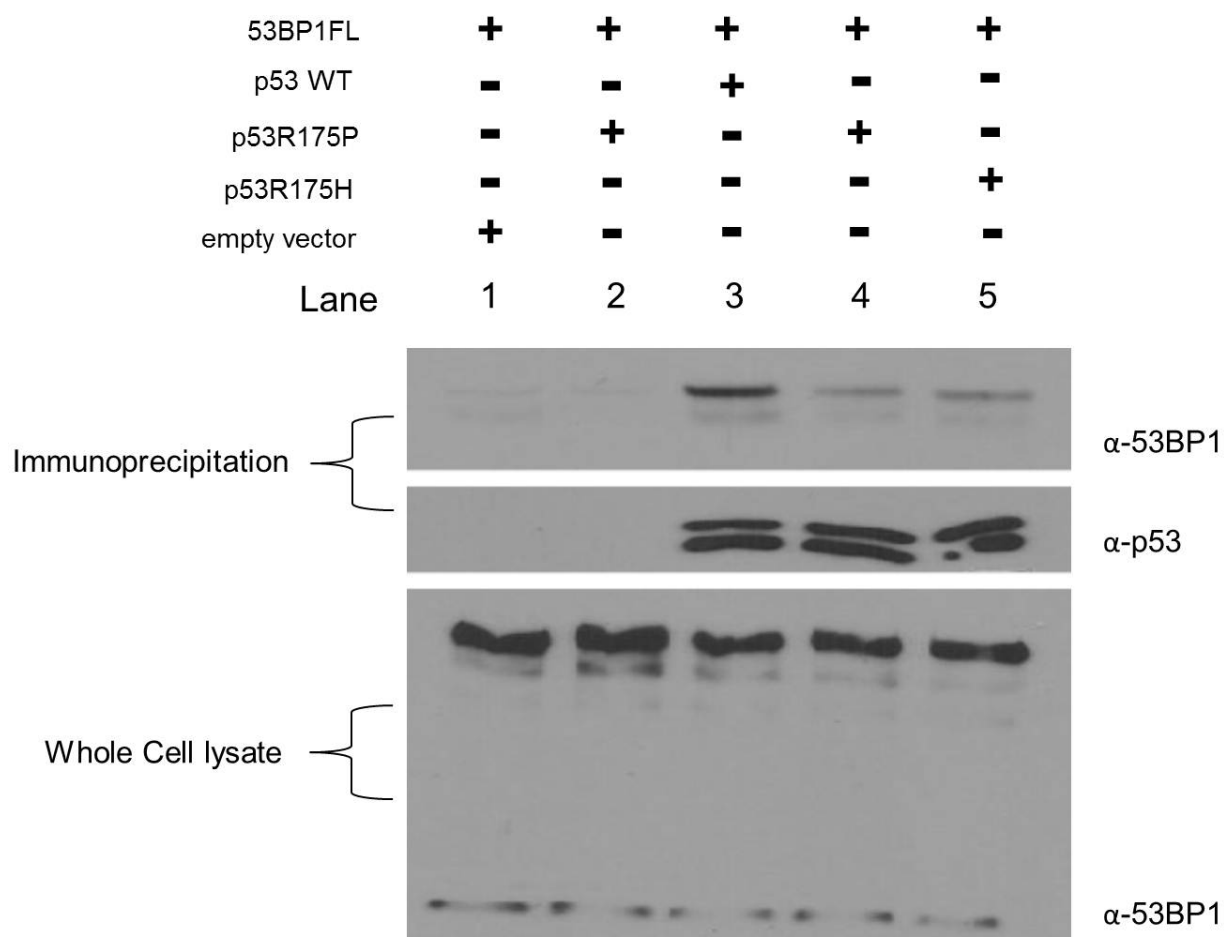
Figure 3.5   **Co-immunoprecipitation Experiment of p53 Mutant and Wildtype Protein with 53BP1**. 53BP1 was co-expressed with either [FLAG]p53WT, [FLAG]p53R175P or [FLAG]p53R175H. In lanes 3,4 and 5 [FLAG]p53 containing complexes were then isolated from the lysates by immunoprecipitation with rabbit α-DDDYK (FLAG) antibody. Lanes 1 and 2 served as negative controls to assess nonspecific binding. Lane 1 did not contain p53 and lane 2 was immunoprecipitated with rabbit α-MYC that was not expected to bind p53 or 53BP1. Protein complexes were resolved by SDS-PAGE prior to western blotting with rabbit α-53BP1 and mouse α-p53.

Specific Aim 3: Determine the global impact of p53 by measuring copy number variation in p53 mutant mouse models.

Array comparative genomic hybridization (aCGH) and analysis

An aCGH experiment was performed using the Agilent mouse genome CGH 105K microarray. Genomic DNA from MEFs (6 different embryonic cell lines each for $p53^{R172P/R172P}$ and $p53^{R172H/R172H}$ and 5 for wildtype) and tumor samples were enzymatically labeled with Cy5 using the Agilent Genomic DNA Enzymatic labeling kit as per manufacturers protocol. For comparison, JAX® sex-matched reference DNA was labeled with Cy3. Experimental and reference DNA was hybridized onto microarrays according to the manufacturer's protocol. Log2 ratios were normalized to minimize differences in labeling affinity between the 2 fluorophores. For individual arrays the Nexus FASST2 segmentation algorithm (threshold 0.3 and −0.3; minimum 3 contiguous probes) was applied. Given the modest resolution of the array used and therefore the possibility that Nexus segmentation may have overlooked smaller CNVs, we looked for differences in copy number variation (CNV) by overlaying the normalized log2 data with CNV coordinates from a recent comprehensive study using a 2.1 million probe aCGH study. The authors compared and validating CNV regions from 7 inbred mouse strains and compared this to a C57BL6/J reference genome [409]. They utilized CNV genomic regions from build NCBI37/mm9, likewise the UCSC Genome Browser Database lift annotation tool was used to convert genome coordinates to build NCBI36/mm8 used in our aCGH study (http://genome.ucsc.edu/). The results were filtered using Microsoft Excel (Mac 2011) for a minimum probe density of 3 and a stringency associated with one half-copy change (log2 threshold 0.32 and −0.4) in CNV compared to the reference genome. An additional post-processing step was performed to remove or group overlapping CNV regions using Excel (Mac 2011).

Evaluation of genomic instability in p53 mutants

The basis of the p^{un} assay is the deletion of one copy of a 70 kb repeated segment of DNA, which essentially equates to the deletion of one copy of a segmental duplication. This is only one locus of the genome, and there are many other segmental duplications and copy number variants in the genome [321]; consequently, the p^{un} reversion assay can be considered representative of these other sites in the genome, and the increased frequency of p^{un} reversion should reflect an increase in the frequency of changes that might be occurring at the CNVs in a population of cells. Given the increased frequency of HR observed in the p53 R172H mutant in our p^{un} assay, we might expect an increased frequency of CNVs in somatic cells from these mice and perhaps in the tumors that arise

as well. In contrast, we might expect a more reduced increase in CNVs in the p53 R172P cells given that our p^{un} data indicates that this protein retains the ability to suppress multi-cell HR events, if not single cell events, and that the tumor latency in p53 R172P mutant mice is much greater. Indeed, a study by the Malkin laboratory showed an increased frequency of CNVs in Li-Fraumeni patients, who harbor germline mutation in p53 [171]. They observed a median of 2 CNVs in a large cohort of healthy ("normal") individuals, compared with a mean frequency of over 12 CNVs in p53 mutation carriers. To assess whether our p53 mutants impact CNVs, we performed aCGH experiments comparing MEFs of differing genotypes. We hypothesized that any embryos harvested on E14.5 results in a fibroblast tissue culture that were derived from somatic mesenchymal cells that display a reasonable level of clonality. Yet, given the highly proliferative nature during this early time in development, these cells would have already undergone sufficient somatic divisions to allow the acquisition of *de novo* changes, if they exist (analogous to the p^{un} assay system). Any polyclonal divergence within the culture would be underrepresented and undetectable by aCGH, thereby minimizing the detection of genomic variation from the tissue culture process itself.

DNA was harvested from cells of differing genotypes in their second passage and used for aCGH comparison to reference DNA purchased from Jackson Laboratories. Normalized log2 values from the aCGH array were imported into Nexus software version 6.1 (BioDiscovery, California, USA) and segmented using the FASST2 segmentation algorithm with a minimum of 3 contiguous probes per segment. To examine changes in known CNVs we mapped our aCGH data to validated CNV coordinates obtained from a recent study comparing various inbred mouse strains to a C57BL6/J reference genome [409]. Indeed, we observed a significantly greater number of CNVs in the MEFs derived from the p53 R172H mutant mice (*Mean* = 5.25; *P < .01*; Mann-Whitney) and the p53 R172P homozygous (*Mean*=5.8; *P < .02*; Mann-Whitney) compared with their respective wildtype controls (*Mean* = 1.4; Figure 3.6(a)). This finding paralleled the increase in CNVs in p53 mutation carriers (peripheral blood leukocytes) observed in the Malkin study, though they reported an even greater increase in CNVs. The subtle mean differences between our studies might be due to differences in species, the cell origin of the samples, or that the MEFs isolated for our study had less opportunity to acquire CNV changes in comparison to the adult samples used in the Malkin study.

Given that we are able to observe an increased frequency of CNV changes in MEFs derived from the p53 mutants, we wanted to ask, at least in a limited fashion, whether this frequency was further increased in tumors. We compared the DNA of tumors to MEFs of equivalent genotype, and observed a nonsignificant increase in CNVs in p53 R172H tumors (*n* = 4, *Mean* = 19.25, *ns*; Mann-Whitney) as well as in p53 R172P tumors (*n* = 4, *Mean* = 12.25, *ns*; Mann-Whitney) (Figure 3.6(b)).

Overall, it would appear that in this limited study neither p53 mutant can suppress CNV changes, though considering that tumors arise much earlier in the p53 R172H mutant animals than in the p53 R172P mutants, we had expected that the rate of genomic change would be much greater for the p53 R172H genetic background if they were facilitating tumor development.
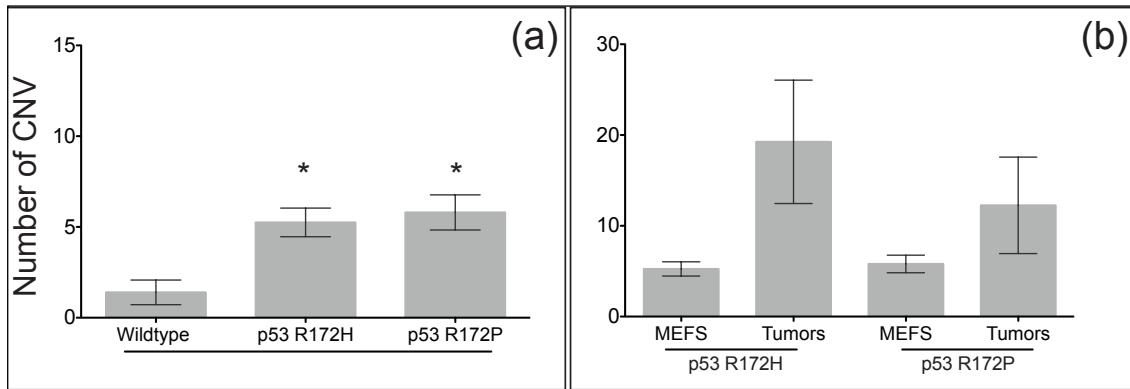
Figure 3.6   **Average Number of Copy Number Variations in Mouse Embryonic Fibroblasts and Tumors from p53 Mutant Mice**. Figure denotes (a) Mean of CNVs in MEFs from differing p53 genotypes. Error bars represent standard error of the mean. A nonparametric Mann-Whitney test was used to analyze aCGH data for WT ($n = 5$), p53 R172H ($n = 12$, $P < .01$), and p53 R172P homozygous ($n = 5$, $P < .02$) MEFs compared with established CNVs in the mouse genome (UCSC Genome Browser Database NCBI36/mm8). (b) Variation was also compared between p53 mutant MEFs and their respective genotype-matched tumors (p53 R172H $n = 4$ and p53 R172P $n = 4$).

p53 R172P suppresses somatic variation until tumorigenesis

Given that we observed a difference in HR suppression between the two p53 mutants in the *p^un^* assay, but the frequency of CNVs in the MEFs and tumors of the two p53 mutants seemed to be basically equivalent, we asked if there was another explanation for the results we obtained with the CNVs. One possibility is that our mutant mouse colonies might be acquiring somatic CNV changes that impact the germline and are then subsequently inherited. This would then affect the frequency of newly acquired somatic CNVs and tumor specific CNVs. To test this possibility we assigned each observed CNV region a number and compared them between MEFs of different genotypes; denoted as follows: wildtype (black squares in Figure 3.7), p53 R172P homozygous (orange squares in Figure 3.7) p53 R172H heterozygous (blue squares in Figure 3.7) and homozygous MEFs (green squares in Figure 3.7; see the inherited CNV regions 1 to 24 in Figure 3.7). Several features of these data become quite obvious and are described as follows (Figure 3.7 panel (a)). Many of the CNVs are shared between independent MEFs, suggesting that they are stably inherited rather than newly acquired. For example regions 2, 6, and 9 appear to be common across multiple samples and cohorts and these alleles are likely segregating within our colonies. Regions 3 and 4 appear to be mainly prevalent in the p53 R172H colony, while region 22 is mainly in the R172P colony, these regions were most likely inherited in relatively early cohort specific generations as they are present in the respective wildtype mice. Four regions occur more often in samples of the R172H colony but occur in at least one sample in the R172P colony (region 1, 10, 14 and 17), these can be considered to be somatically acquired changes. There are apparently more exclusive *de novo* CNV changes present in the p53 R172H colony than the p53 R172P colony (regions 5, 7, 8, 11, 12, 13, 15, 16, 18, 19 and 20, compared to regions 21, 23 and 24). This would seem to be an underestimate for the number of changes occurring in the p53 R172H colony since there are also those events that seem to have occurred in the previous generation. Furthermore, when examining the type of CNV change in terms of gains or losses (denoted as + and –, respectively, in Figure 3.7 panel (a)), it seems that R172H has more variation among samples in the same regions. For example, regions 3, 4, and 13 are indicated as losses in a subset of samples and gains in another subset of samples (Figure 3.7 panel (a)). It is interesting to note that there appears to be much more variation in the p53 R172H colony and that many of the CNV changes have impacted the germline and are now stably inherited in the colony (Figures 3.7 (panel (a) and Figure 3.9).

To determine the impact of CNV changes in our p53 mutants over generations would require a much more rigorous and in depth study than what was conducted here. That said, we were able to examine whether inherited CNV regions 1 to 24 (Figure 3.7 panels (b) and (c)) were present in the

genotype-matched tumors. As expected, the p53 R172H and R172P mutant tumors had on average 4.25 and 3.5 "inherited" CNVs, respectively. Of note, 3 inherited CNV regions in the p53 R172H tumors were exacerbated in the tumor, showing a greater loss or gain of DNA compared to the respective CNV region in the MEFs (region 8- 73kb gain to 276kb loss, region 9- 103kb to1476kb gain, region 20- 469kb loss to equivalent size gain) (highlighted yellow boxes in Figure 3.7 panel (b)). Of the four p53 R172P tumors examined two in particular showed greater change in 6 inherited CNV regions in tumors compared with their genotype-matched MEFs likely due to increased tumor specific genomic instability (discussed below) (region 3- 263kb to 1166kb gain, region 4- 294kb loss to equivalent size gain, region 9- 699kb to 2531kb gain, region 10- 55kb gain to equivalent size loss, region 21- 66kb to 593kb gain, region 24- 1280kb to 2115kb gain) (highlighted black boxes in Figure 3.7 panel (c)). We extended this study in a very limited fashion, comparing tumors with normal tissue from the same animal. Here we expect that any differences in CNVs would correspond to tumor-specific changes, since the comparison was made with tissues from the same animal and thus any inherited or somatically acquired CNV regions would be considered baseline and only those specific to the tumors would pass the stringent thresholds set in the analysis. To validate this concept we compared two normal tissues of a p53 R172H heterozygous mouse and observed no differences in the "inherited" CNVs. Interestingly, when we compared two different p53 R172H tumors with their respective normal somatic tissue we only observed one CNV change within the "inherited" regions, though this result suggests that the tumor either gained or lost this allele indicating its instability. In contrast, for the single p53 R172P tumor we were able to test, we observed three of the "inherited" CNVs displaying *de novo* changes; not only displaying a difference in DNA copy number compared to the somatic tissue, but also an expanded CNV region (highlighted black boxes in Figure 3.7 panel (d)).

Given the difference we see in the inherited CNV regions 1-24, we hypothesized that all other remaining CNV regions in these tumors would have been somatically acquired either in the normal development of the mouse or within the tumor. To test this possibility, we determined which CNV changes were present in tumors but were not found in MEFs (Figure 3.8 regions 25 to 70 panels (a) and (b)). Remarkably, the tumors derived from the p53 R172H colony showed many more newly acquired CNV regions (CNV=34 regions) compared to the tumors derived from the p53 R172P colony (CNV=11 regions) (Figure 3.9). As before, the limited number of samples comparing CNV regions between normal tissue with tumors from the same animal were used to examine tumor specific CNVs (regions 25-114 Figure 3.8 panel (c)); these regions would reflect tumor-specific CNV regions that were not inherited or somatically acquired during early development and are therefore divergent

between the internal control tissue and the tumor. Surprisingly the p53 R172H mutant (n = 2) tissue-tumor comparisons, we only observed 6 and 5 tumor-specific CNVs. In contrast, for the single p53 R172P homozygous tumor we were able to examine (n = 1) we observed 16 tumor-specific CNVs (Figure 3.8 regions 25-114 panel (c) and Figure 3.9).

Although, our sample sizes were limited, our interpretation of these findings is that the p53 R172H protein is incapable of suppressing CNV changes during normal somatic development, while the p53 R172P has retained some, if reduced, capacity to suppress these changes. However, when a p53 R172P tumor arises, further genomic instability ensues, hence the increased frequency of CNV changes in the tumors. Tumors arising in the p53 R172H mice have already acquired substantial somatic variation and do not display a great increase in frequency of additional changes.
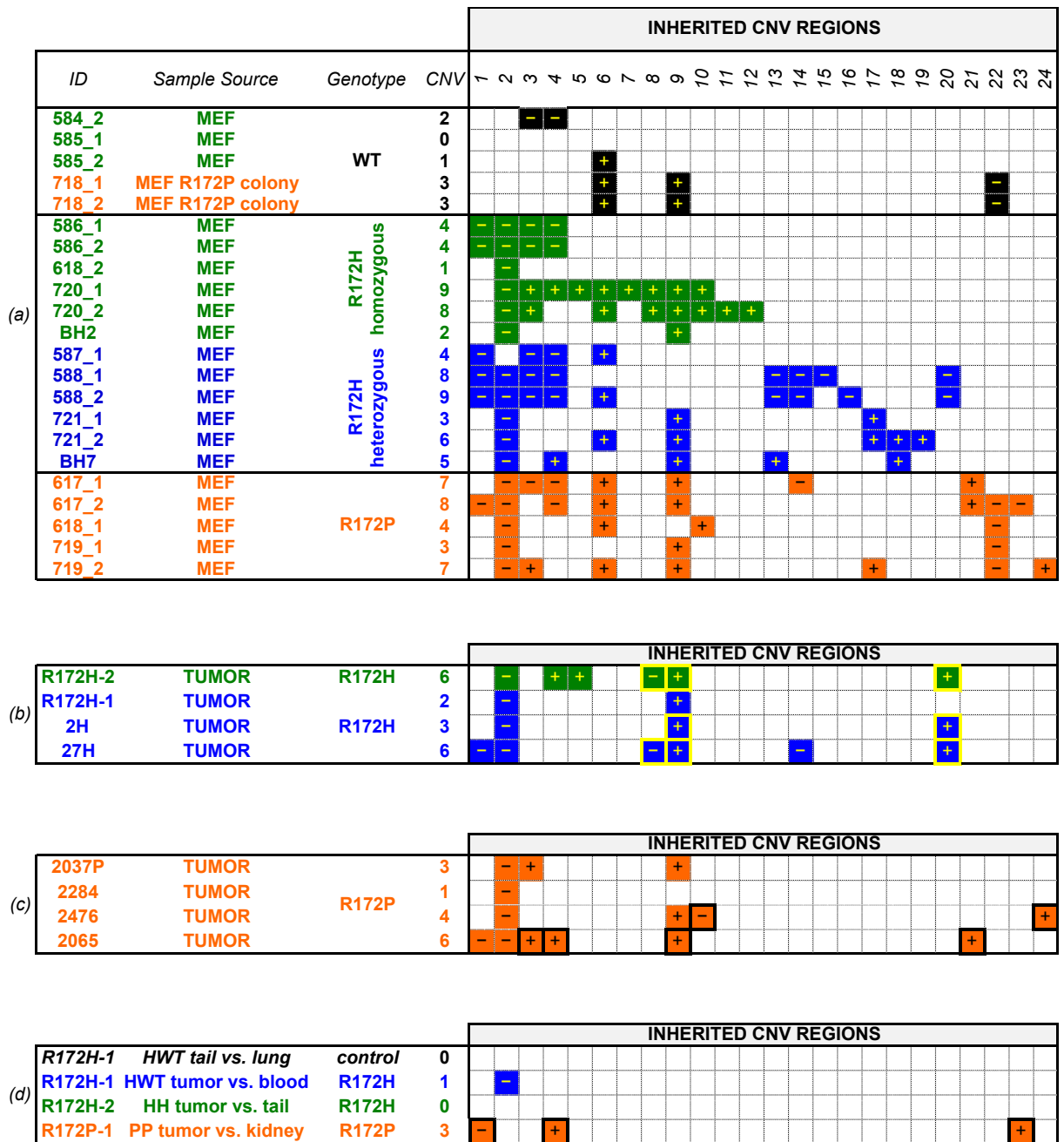
Figure 3.7   **Comparison of Inherited Copy Number Variation Regions in p53 Mutant Mouse Embryonic Fibroblasts**. Regions 1-24 are represented and shaded as follows: black = WT genotype, blue = p53 R172H heterozygous, green = p53 R172H homozygous, and orange = p53 R172P homozygous. A loss in CNV is denoted by a minus sign and a gain in CNV is denoted by a plus sign. Highlighted boxes indicate a change in gain or loss for that CNV region in tumors compared to MEFs of the respective genotype.
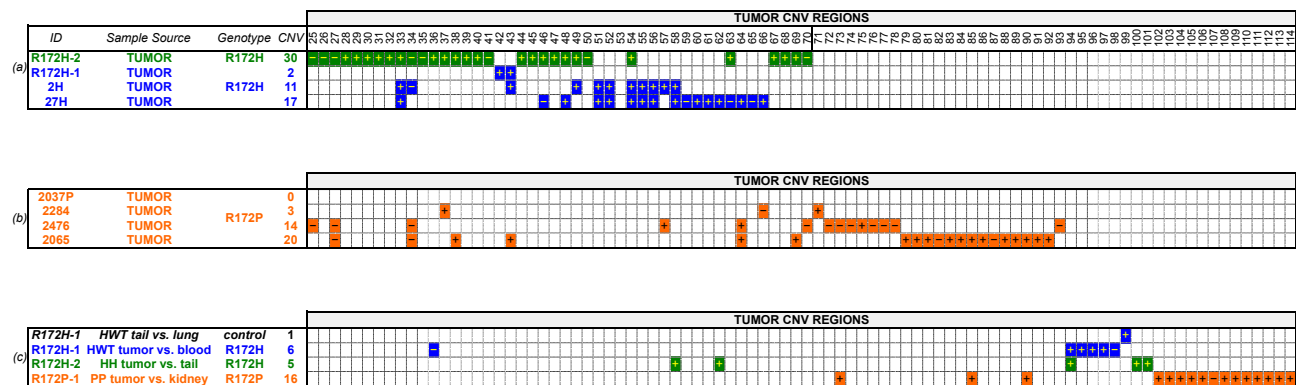
Figure 3.8   **Comparison of Tumor Copy Number Variation Regions in p53 Mutant and Tissue–Tumor Comparisons**. Regions 25-112 are represented and shaded as follows: black = WT genotype, blue = p53 R172H heterozygous, green = p53 R172H homozygous, and orange = p53 R172P homozygous. A loss in CNV is denoted by a minus sign and a gain in CNV is denoted by a plus sign. Highlighted boxes indicate a change in gain or loss for that CNV region in tumor-tissue comparisons with the same region in independent tumors of the respective genotype.
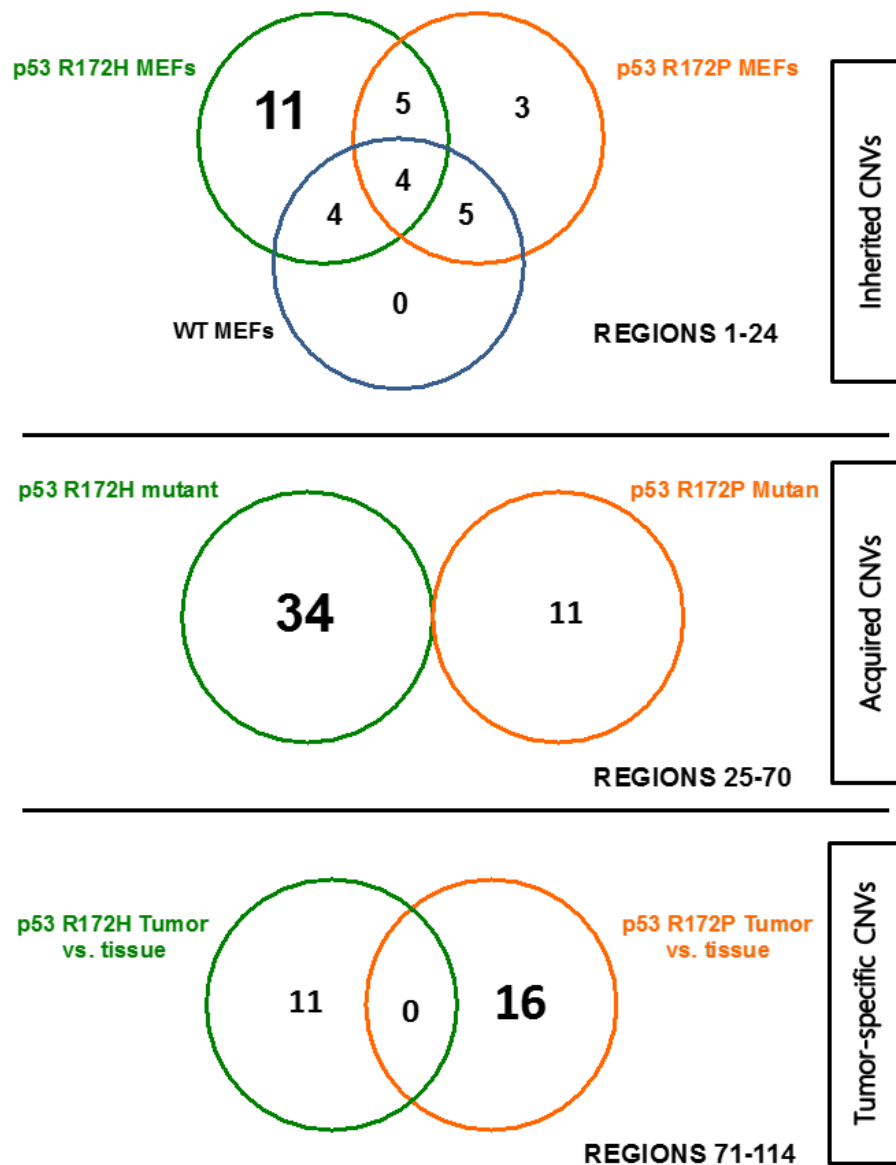
Figure 3.9   **Venn Diagram Comparing Inherited, Acquired, and Tumor-specific Copy Number Variation Regions in p53 Mutant Mouse Embryonic Fibroblasts and Tissue–Tumor Comparisons.** Shading is represented as follows: black = WT genotype, blue = p53 R172H heterozygous, green = p53 R172H homozygous, and orange = p53 R172P homozygous.

Discussion Specific Aim 2 and 3

The *in vivo* p^{un} assay provides a retrospective analysis of HR events that occur during a highly proliferative time of embryo development, in the RPE in particular. The p^{un} assay is able to detect both RAD51-dependent, replication-tied HR events (canonical HR events) as well as RAD52-dependent SSA events. This is based on our observation that the p^{un} assay detected a hyperrecombination phenotype resulting from the loss of the RECQ helicase, *Blm*, and more robustly in *Parp1* nullizygous mice producing mainly an increase in multi-cell events, suggesting that they were tied to replication ([248,250], respectively). The interpretation of the results fits with our current understanding of how BLM acts in Holliday junction dissolution, thus blocking recombination, or PARP1 repairs single stand breaks prior to becoming a recombinogenic substrate during replication. In contrast, *Brca1* and *Brca2* mutants show a decreased frequency of HR, losing the multi-cell p^{un} events while the remaining eyespots are mostly single cell events ([248] and unpublished data, respectively). These studies again suggest that the multi-cell reversion events are the outcome of HR tied to replication, and most of the single-cell events are a result of SSA reversion (RAD52 mediated deletion event) [248,250,268,293]. In this study, we observed a loss of HR suppression in p53 nullizygous mice, as was previously reported by Bishop *et al*. [247]. Further we did not observe any overall haploinsufficient HR phenotype in p53 heterozygous mice. Moreover, retention of overall HR-suppression capability was observed for the p53 R172P mutant that was completely abolished in the p53 R172H mutant (similar to p53 nullizygous). The majority of increased p^{un} reversion events observed in the p53 R172H and p53 nullizygous mice were single-cell eyespots, which suggests that p53 is involved in protecting the genome from SSA-mediated recombination events; however, we also observed a smaller increase in multi-cell events, apparently arising at a different time in development (earlier) in these same animals, similar to the earlier report by Bishop *et al.* [247]. Though the R172P mutant did not display an overall increase in HR events, a more detailed analysis revealed an interesting observation. It appears that the p53 R172P protein is capable of completely suppressing the small increase in multi-cell events that we observed in the p53 R172H mutant and nullizygous animals, but not the increased single cell events that occurred later in RPE development. This is particularly interesting since the p53 binding protein 53BP1, which is known to act in SSA and inhibits BRCA1 mediated HR events, binds the p53 core domain. We observe that neither p53 mutant is capable of co-immunoprecipitating 53BP1 and suggest that this may result in deregulated 53BP1-dependent SSA usage.

Many sophisticated mouse models based on early tissue culture work have begun to elucidate the functions of p53 that are important in suppressing tumorigenesis. p53 knockout mice revealed that p53 was dispensable during development, but its absence led to highly penetrant tumors, mostly T-cell lymphomas and sarcomas. Cells from p53 nullizygous mice exemplified such anomalies as aneuploidy, UV-induced sister chromatid exchange, and allelic loss, providing evidence for a role in protecting genome integrity and not just in stress response [186-188]. Similar to what was previously reported with the same system, here we observed that p53 nullizygous mice have a significant increase in HR events [247]. In particular, we observed a significant increase in single-cell eyespots, suggesting that p53 suppresses SSA in particular. To a lesser extent, p53 suppressed early multi-cell events, as was previously reported [247]. In contrast, p53 heterozygous mice display no defect in HR suppression and were comparable to wildtype mice. The increased genomic variation that arises in the absence of p53, along with the absence of apoptotic function to clear damaged cells, may contribute to tumor initiation and thereby lead to the genomic instability seen in p53 nullizygous tumors.

The need for mouse models that better recapitulated the mutations found in LFS and in spontaneous tumors led to the creation of conditional, knock-in, and more humanized mutant mouse models. One example is the creation of the p53 R172H mutant mouse model, recapitulating a dominant negative mutation found commonly in patients suffering from LFS and has been observed in spontaneous breast cancers [193,194,420]. This mutant succumbs to an early onset of mostly thymic lymphomas and some sarcomas around 6 months of age, similar to p53 nullizygous mice [193,194]. MEFs with the p53 R172H mutation show increased replication and transformation potential [193]. Another p53 mutation in the same locus (R172P), although extremely rare in human cancer, was used to create another mouse model. This mutant is defective in inducing an apoptotic response but is still able to partially arrest the cell cycle. Despite escaping the early lymphomas and sarcomas common in the p53 nullizygous mutation, these mice still succumb to tumors, albeit with a delayed onset and a general retention of a diploid genome, similar to that found in p53 heterozygous mice [401]. We observed that the p53 R172P mutant suppressed HR, similar to WT and p53 heterozygous mice. In contrast, the p53 R172H mutant was incapable of suppressing HR and closely resembled the phenotype observed with p53 nullizygous mice. The increased frequency of HR in both genotypes was most significant in single-cell reversion events, suggesting a loss of suppression of SSA events in particular. Considering that SSA events are, by definition, an error-prone type of repair pathway, it can be expected that their suppression would also be tumor-suppressive.

The mechanism for how p53 suppresses HR has been studied by many groups, both spontaneously, following induction of DSBs [146,247,280,283,285] and at sites of replication forks [421]. WT p53 has been reported to interact with a number of proteins associated with HR: RAD51 and RAD54 [268,281,415], RPA [289], BLM [268], WRN [267], BRCA1 [265], BRCA2 [266], and MSH2 [422]. Given the uncoupling of transcription factor control of HR seen in this study and reported by others [269,285,289], we performed a co-immunoprecipitation experiment with a candidate protein likely to effect SSA repair; the p53 binding protein 53BP1. 53BP1 was first shown to bind to p53 in a yeast two-hybrid study [419]. Similar to BRCA1, 53BP1 contains BRCT repeats (located in the carboxy terminus) that bind to p53's DNA binding domain in the same domain as the R172 locus. In unpublished data, we have seen an increase in HR with 53BP1 deficient mice using the *in vivo p*^{un} assay. Further, the R172 locus would most likely disrupt this interaction given the location of the binding site. We saw a marked decrease in the ability of both mutants to bind 53BP1; however, this does not explain the differential suppression of overall HR seen with these mutants. Although a likely candidate, 53BP1 may not be the mechanism by which p53 suppresses HR, perhaps an exploration of another p53 interacting HR proteins, in the context of these two mutants may better elucidate the mechanism.

The RPE-based *p*^{un} assay provides an *in vivo* model to study spontaneous HR on an actively proliferating front of cells not elicited by a DSB. The resolution of eyespot size allowed us to link the HR mechanism to replication. Given that multiple stressors in the cell—including replication fork arrest—trigger p53, we expected to see very few multi-cell events in wildtype cells. The fact that we see a significant increase in multi-cell events in addition to SSA events in the absence of p53 and p53 R172H mutation suggests suppression of recombination in proliferating cells mediated by some other mechanism. For instance, p53 has been implicated in the replication checkpoint with BLM, whose activity involves facilitating regression of a stalled replication fork. BLM recruits p53 [276] and members of the MRE11-RAD50-NBS1 complex [275], in addition to binding directly to RAD51 [423,424]. p53 induction following the replication inhibitor hydroxyurea was compromised in *Blm* nullizygous and *Nbs1* nullizygous cells; however, the response was still functional in *Brca1* and *Brca2* cells [425]. It is interesting that the p53 induction was weaker (weak induction of p21, stability of p53 protein not as robust) in comparison to p53 levels following the normal DNA-damage response. This suggests a possible p53-mediated intermediate response in a proliferating cell to low levels of endogenous lesions at replication forks that do not trigger a robust DNA-damage response [292].

In an extensive study of Li Fraumeni families by the Malkin group in Toronto, Canada, where the researchers observed an increased CNV frequency in p53 mutation carriers was observed, prompting

us to examine genomic integrity in our p53 mutants. Furthermore, genetic anticipation has been suggested to occur in Li Fraumeni families through the observation of an increased penetrance of the syndrome in each subsequent generation [171,426]. The Malkin group demonstrated an increased frequency of circulating CNVs in offspring from LFS parents, proposing the idea that inherited CNVs and acquired somatic CNVs lead to a worsening outcome for subsequent LFS generations [171]. In parallel with the human study, we also observed a high level of CNVs in both p53 mutants as early as E14.5, as shown in our aCGH comparisons with MEFs. A closer look at the origin of this variation revealed that the p53 R172H tumor had significantly more unique acquired CNVs compared to the p53 R172P tumor and their respective MEFs, suggesting that the suppression of deleterious HR might be an additional tumor-suppressive capability necessary to maintain p53-mediated genomic integrity. The fact that we saw more inherited CNVs from the p53 R172H colony suggests a genetic drift with this mutation in comparison to the p53 R172P mutation. The idea being that the p53 R172H mutation, through the lack of HR suppression and/or some other mechanism confers more genomic instability that can be passed on to subsequent generations in the breeding cohort. This idea perhaps explains the worsening generational effect seen in LFS families.

In conclusion, we propose a working model that provides support for another layer of tumor suppressive capability, specifically HR suppression, to aid p53's ability to play a guardian and caretaker role in the fight for genomic integrity (Figure 3.10). Using the *in vivo p^{un}* assay and an aCGH analysis, we confirmed p53's ability to suppress HR, most likely through SSA. The effector response of cell-cycle arrest and apoptosis are not enough to explain the delay in tumorigenesis, as seen in mouse models of Li Fraumeni and the worsening generational effect detected in the human condition. The ability of p53 to suppress SSA recombination events in combination with a cell-cycle arrest response helps to maintain genomic integrity by minimizing newly acquired somatic mutation; still, the eventual loss of p53 functionality by other upstream or downstream means initiates tumorigenesis. Resistance to DNA-damaging agents is a common therapeutic problem in the treatment of cancer and is typically caused by a loss of WT p53 function [427,428]. The elucidation of p53's functions in apoptosis, cell-cycle arrest, and DNA recombination has clinical promise for improved treatment of malignant tumors.
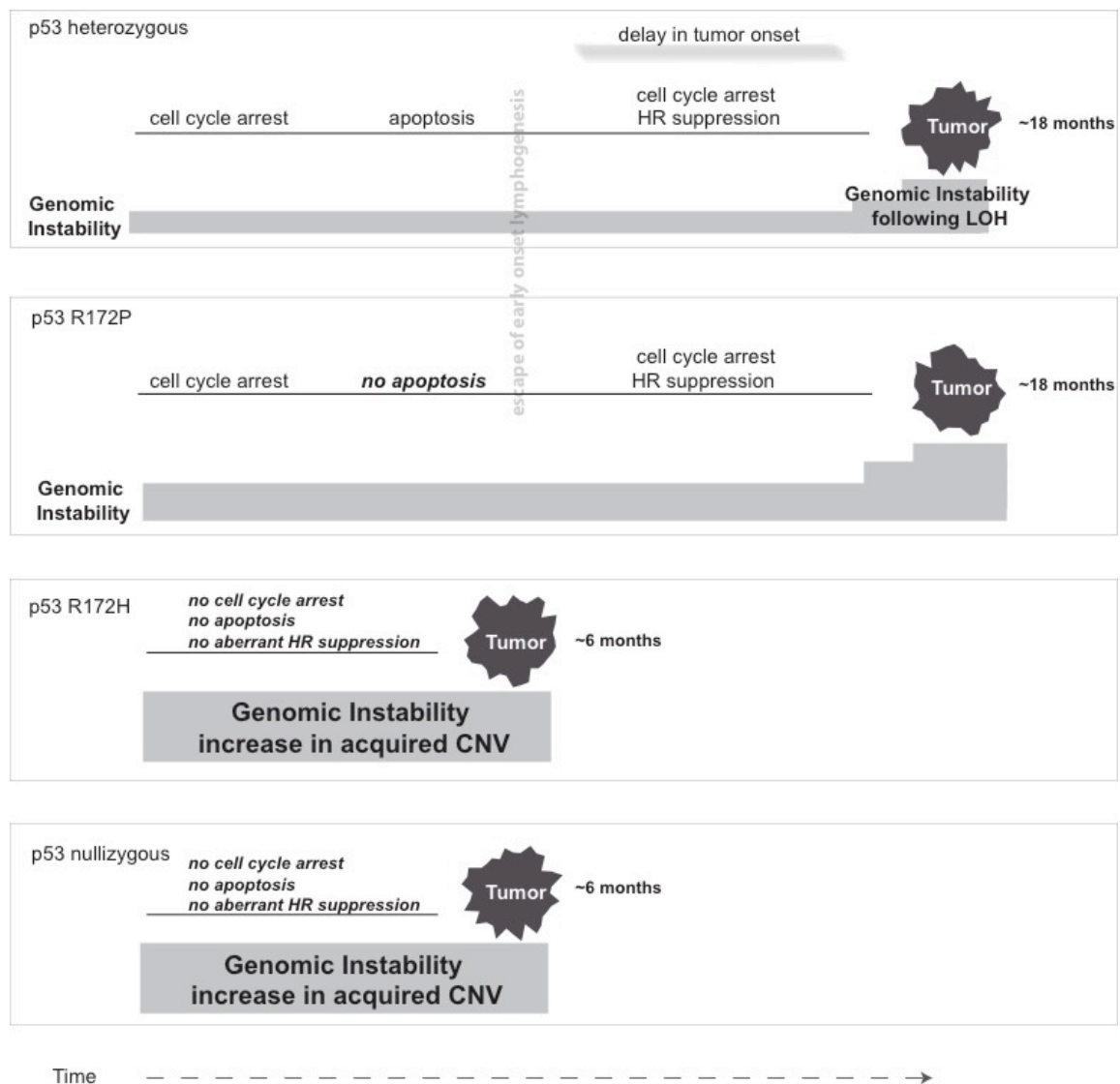
Figure 3.10   **Working Model to Illustrate Suppression of Homologous Recombination as an Additional Tumor-suppressive Functionality of p53**. p53 mutant mice and functionalities are denoted. Arrow represents time to tumors.

Key Research Accomplishments

- R172P mutant mice are able to suppress HR similar to wild type suggesting the mechanism is not due to the transactivation of apoptotic genes but through cell cycle or protein: protein interactions.

- R172H mutant mice have a decrease in HR similar to p53 null mice, which do not produce p53 protein. This suggests a protein: protein interaction defect and a possible indirect regulatory role for p53 in the regulation of HR.

- Exposure to irradiation in R172P mutant mice leads to a robust induction of HR similar to WT. In contrast the R172H mutant has lost some functionality necessary for eliciting a proper p53 response to IR damage.

- Many DNA damaging agents with differing modes of actions and resultant lesions can elicit an HR response.

Reportable outcomes:

PUBLICATIONS (PEER REVIEWED)

Zimmer SN, Lemieux ME, **Karia BP**, Day C, Zhou T, Zhou Q, Kung AL, Suresh U, Chen Y, Kinney MC, Bishop AJ, Rebel VI. Mice heterozygous for CREB binding protein are hypersensitive to γ-radiation and invariably develop myelodysplastic/myeloproliferative neoplasm. Exp Hematol. 2012 Apr;40(4):295-306.e5.
PMID: 22198154 **(APPENDIX 3)**

Lin S, Yu L, Yang J, Liu Z, **Karia B**, Bishop AJ, Jackson J, Lozano G, Copland JA, Mu X, Sun B, Sun LZ. Mutant p53 disrupts role of ShcA protein in balancing Smad protein-dependent and -independent signaling activity of transforming growth factor-β (TGF-β). J Biol Chem. 2011 Dec 23;286(51):44023-34. PMID: 22039050 **(APPENDIX 2)**

Ravi D, Chen Y, **Karia B**, Brown A, Gu TT, Li J, Carey MS, Hennessy BT, Bishop AJ. 14-3-3 σ expression effects G2/M response to oxygen and correlates with ovarian cancer metastasis. PLoS One. 2011 Jan 10;6(1):e15864.
PMID: 21249227 **(APPENDIX 4)**

Claybon A, **Karia B**, Bruce C, Bishop AJ. PARP1 suppresses homologous recombination events in mice in vivo. Nucleic Acids Res. 2010 Nov;38(21):7538-45.
PMID: 20660013 **(APPENDIX 1)**

PUBLICATIONS (SUBMITTED)

Manuscript submitted to DNA Repair March 28, 2013-Under review
Bijal Karia, Jo Ann Martinez, and Alexander J. R. Bishop. Induction of Homologous Recombination Following *in utero* Exposure to DNA-Damaging Agents. *DNAR 13-0059.* **(APPENDIX 5)**

PUBLICATIONS (IN PREPARATION)

Bijal Karia, Hung-I Harry Chen, Lyndsey Myers, Aparna Gorthi, Carolina Cantu, Uthra Suresh, Donald McEwen, Guillermina Lozano, Yidong Chen and Alexander J. R. Bishop. P53 Suppression of Homologous Recombination reconsidered as an additional mechanism for the maintenance of genomic integrity.

Successfully defended PhD-Bijal Karia
May 9, 2013   Ph.D. Cellular and Structural Biology
                          University of Texas Health Science Center San Antonio
                          Greehey Children's Cancer Research Institute

PERSONEEL RECEIVING PAY FOR WORK:

Bijal Karia PhD

Conclusions

The main focus of this grant was to train me for future as an independent breast cancer investigator. Using the funds from this grant this year I have attended 2 meetings related to genomic instability (Keystone Symposia), as well as the Era of Hope Meeting where I interacted with fellow DoD awardees. My attendance at these meetings allowed me to make contacts with breast cancer investigators all over the world. I was exposed to cutting-edge research that was being done in the field of breast cancer research. My poster presentation allowed for good discussion and feedback from other investigators that will help shape future experiments and thinking about breast cancer. I have had 1 dissertation committee meeting this year (2-21-2011) in which the discussion of my progress was key. My committee gave me invaluable advice on analysis of experiments, interpretations, statistical help and time management for progression of my PHD. We have had our final meeting and I have been given the go-ahead to complete my manuscripts and begin writing my dissertation.

I continue to attend seminars twice a week to better keep up with ongoing research in many fields. This has been a great lesson in critically thinking about the work of others and how they answered questions and solved problems.

I continually meet with my mentors on a weekly basis to discuss experiment results, future experiment planning and troubleshooting strategies.

In the first year I have made significant progress. Animal models are very difficult but I have managed to learn and master mouse husbandry and now have a thriving healthy breeding colony. The cohorts mentioned in the statement of work have all been established and experiments are underway. Assays for measuring RAD51 foci, NER, BER have been learned by the PI and are currently being used in the lab.

The most significant finding that has come from the second and third year of this grant is that there is a difference between the two p53 mutants in terms of homologous recombination frequency. Given the separation of function of these two mutants we can now tease out the mechanism for how p53 suppresses homologous recombination both in a spontaneous situation and following damage. The microarray analysis showed no differential expression of HR relevant genes between the mutants as and thus our focus will be on determine what protein-protein interaction has been disrupted between the mutants that might explain the difference in HR frequency. We are currently optimizing these experiments and hope to submit a manuscript on these findings in 2013. We will also continue

to gather enough RPE to complete IR induction experiments in hopes of a their first author publication.

"So what"

the significance of these initial findings is that we are closer to determining what p53 mutations are exactly doing and not doing in cells. If we can determine what main "normal" functions of p53 are altered or lost or broken in cancer cells we can develop better targets and therapies that address these issue particularly. For example if it is determined that the more aggressive R172H mutation has a broken protein: protein interaction that causes it to have hyper recombination leading to genomic instability leading to cancer than there is a chance for targeted therapy to repair this interaction in order to restore normal DNA repair function. The research that has been done in this field by previous investigators has been on in vitro plasmid based models with questionable results. Here we use an in vivo assay in a clean genetic system that provides an excellent model for determining genomic instability by way of measuring HR.

Introduction and Body References

1. Lane DP. Cancer. p53, guardian of the genome. Nature. 1992 Jul 2;358(6381):15-6.
2. Sherr CJ. Cancer Cell Cycles. Science. 1996 Dec 6;274(5293):1672-7.
3. Taylor WR, Stark GR. Regulation of the G2/M transition by p53. Oncogene. 2001 Apr 5;20(15):1803-15.
4. Ko LJ, Prives C. p53: Puzzle and Paradigm. Genes Dev. 1996 May 1;10(9):1054-72.
5. Brown AD, Claybon AB, Bishop AJ. A conditional mouse model for measuring the frequency of homologous recombination events in vivo in the absence of essential genes. Mol Cell Biol. 2011 Sep;31(17):3593-602. Epub 2011 Jun 27.
6. Bertrand P, Rouillard D, Boulet A, Levalois C, Soussi T, Lopez BS. Increase of spontaneous intrachromosomal homologous recombination in mammalian cells expressing a mutant p53 protein. Oncogene. 1997 Mar 6;14(9):1117-22.
7. Willers H, McCarthy EE, Wu B, Wunsch H, Tang W, Taghian DG, Xia F, Powell SN. Dissociation of p53-mediated suppression of homologous recombination from G1/S cell cycle checkpoint control. Oncogene. 2000 Feb 3;19(5):632-9.

8. Akyüz N, Boehden GS, Süsse S, Rimek A, Preuss U, Scheidtmann KH, Wiesmüller L. DNA substrate dependence of p53-mediated regulation of double-strand break repair. Mol Cell Biol. 2002 Sep;22(17):6306-17.

9. Lang GA, Iwakuma T, Suh YA, Liu G, Rao VA, Parant JM, Valentin-Vega YA, Terzian T, Caldwell LC, Strong LC, El-Naggar AK, Lozano G. Gain of function of a p53 hot spot mutation in a mouse model of Li-Fraumeni syndrome. Cell. 2004 Dec 17;119(6):861-72.

10. Olive KP, Tuveson DA, Ruhe ZC, Yin B, Willis NA, Bronson RT, Crowley D, Jacks T. Mutant p53 gain of function in two mouse models of Li-Fraumeni syndrome. Cell. 2004 Dec 17;119(6):847-60.

11. Aubrecht J, Secretan MB, Bishop AJ, Schiestl RH. Involvement of p53 in X-ray induced intrachromosomal recombination in mice. Carcinogenesis. 1999 Dec;20(12):2229-36.

12. Bishop AJ, Kosaras B, Carls N, Sidman RL, Schiestl RH. Susceptibility of proliferating cells to benzo[a]pyrene-induced homologous recombination in mice. Carcinogenesis. 2001 Apr;22(4):641-9.

13. Claybon A, Karia B, Bruce C, Bishop AJ. PARP1 suppresses homologous recombination events in mice in vivo. Nucleic Acids Res. 2010 Nov;38(21):7538-45. Epub 2010 Jul 21.

14. Bishop AJ, Hollander MC, Kosaras B, Sidman RL, Fornace AJ Jr, Schiestl RH. Atm-, p53-, and Gadd45a-deficient mice show an increased frequency of homologous recombination at different stages during development. Cancer Res. 2003 Sep 1;63(17):5335-43.

Specific Aim 1 References

[1] D.J. Kirkland, M. Aardema, N. Banduhn, P. Carmichael, R. Fautz, J.-R. Meunier, et al., In vitro approaches to develop weight of evidence (WoE) and mode of action (MoA) discussions with positive in vitro genotoxicity results, Mutagenesis. 22 (2007) 161–175. http://www.ncbi.nlm.nih.gov/pubmed/17369606

[2] R.L. Maher, A.M. Branagan, S.W. Morrical, Coordination of DNA replication and recombination activities in the maintenance of genome stability, J. Cell. Biochem. 112 (2011) 2672–2682. http://www.ncbi.nlm.nih.gov/pubmed/21647941

[3] G. McVean, What drives recombination hotspots to repeat DNA in humans?, Philos. Trans. R. Soc. Lond., B, Biol. Sci. 365 (2010) 1213–1218. http://dx.doi.org/10.1098/rstb.2009.0299

[4]   R. Redon, S. Ishikawa, K.R. Fitch, L. Feuk, G.H. Perry, T.D. Andrews, et al., Global variation in copy number in the human genome, Nature. 444 (2006) 444–454.

http://dx.doi.org/10.1038/nature05329

[5]   P. Stankiewicz, J.R. Lupski, Genome architecture, rearrangements and genomic disorders, Trends Genet. 18 (2002) 74–82. http://www.ncbi.nlm.nih.gov/pubmed/11818139

[6]   S. Rosemblat, D. Durham-Pierre, J.M. Gardner, Y. Nakatsu, M.H. Brilliant, S.J. Orlow, Identification of a melanosomal membrane protein encoded by the pink-eyed dilution (type II oculocutaneous albinism) gene, Proc. Natl. Acad. Sci. U.S.A. 91 (1994) 12071–12075.

http://www.ncbi.nlm.nih.gov/pmc/articles/PMC45378/

[7]   R. Reliene, A.J.R. Bishop, J. Aubrecht, R.H. Schiestl, In vivo DNA deletion assay to detect environmental and genetic predisposition to cancer, Methods Mol. Biol. 262 (2004) 125–139.

http://www.ncbi.nlm.nih.gov/pubmed/14769959

[8]   A.J. Bishop, B. Kosaras, N. Carls, R.L. Sidman, R.H. Schiestl, Susceptibility of proliferating cells to benzo[a]pyrene-induced homologous recombination in mice, Carcinogenesis. 22 (2001) 641–649. http://www.ncbi.nlm.nih.gov/pubmed/11285201

[9]   A.J. Bishop, B. Kosaras, R.L. Sidman, R.H. Schiestl, Benzo(a)pyrene and X-rays induce reversions of the pink-eyed unstable mutation in the retinal pigment epithelium of mice, Mutat. Res. 457 (2000) 31–40. http://www.ncbi.nlm.nih.gov/pubmed/11106796

[10]   R.H. Schiestl, J. Aubrecht, F. Khogali, N. Carls, Carcinogens induce reversion of the mouse pink-eyed unstable mutation, Proc. Natl. Acad. Sci. U.S.A. 94 (1997) 4576–4581.

http://www.ncbi.nlm.nih.gov/pubmed/9114032

[11]   R.H. Schiestl, F. Khogali, N. Carls, Reversion of the mouse pink-eyed unstable mutation induced by low doses of x-rays, Science. 266 (1994) 1573–1576.

http://www.ncbi.nlm.nih.gov/pubmed/7985029

[12]   B. Rosenberg, Possible mechanisms for the antitumor activity of platinum coordination complexes, Cancer Chemother Rep. 59 (1975) 589–598. http://www.ncbi.nlm.nih.gov/pubmed/54213

[13]   L.S. Gold, N.B. Manley, T.H. Slone, G.B. Garfinkel, L. Rohrbach, B.N. Ames, The fifth plot of the Carcinogenic Potency Database: results of animal bioassays published in the general literature through 1988 and by the National Toxicology Program through 1989, Environ. Health Perspect. 100 (1993) 65–168. http://www.ncbi.nlm.nih.gov/pubmed/8354183

[14]   M.R. Purnell, W.J. Whish, Novel inhibitors of poly(ADP-ribose) synthetase, Biochem. J. 185 (1980) 775–777. http://www.ncbi.nlm.nih.gov/pubmed/9703762

[15]   D.A. Burden, N. Osheroff, Mechanism of action of eukaryotic topoisomerase II and drugs targeted to the enzyme, Biochim. Biophys. Acta. 1400 (1998) 139–154. http://dx.doi.org/10.1016/S0167-4781(98)00132-8

[16]   Y.H. Hsiang, M.G. Lihou, L.F. Liu, Arrest of replication forks by drug-stabilized topoisomerase I-DNA cleavable complexes as a mechanism of cell killing by camptothecin, Cancer Res. 49 (1989) 5077–5082. http://www.ncbi.nlm.nih.gov/pubmed/2548710

[17]   J.W. Yarbro, Mechanism of action of hydroxyurea, Semin. Oncol. 19 (1992) 1–10. http://www.ncbi.nlm.nih.gov/pubmed/1641648

[18]   A. Claybon, B. Karia, C. Bruce, A.J.R. Bishop, PARP1 suppresses homologous recombination events in mice in vivo, Nucleic Acids Res. 38 (2010) 7538–7545. http://dx.doi.org/10.1093/nar/gkq624

[19]   M. Lebel, Increased frequency of DNA deletions in pink-eyed unstable mice carrying a mutation in the Werner syndrome gene homologue, Carcinogenesis. 23 (2002) 213–216. http://www.ncbi.nlm.nih.gov/pubmed/11756244

[20]   L. Bodenstein, R.L. Sidman, Growth and development of the mouse retinal pigment epithelium. I. Cell and tissue morphometrics and topography of mitotic activity, Dev. Biol. 121 (1987) 192–204. http://dx.doi.org/10.1016/0012-1606(87)90152-7

[21]   A.J.R. Bishop, M.C. Hollander, B. Kosaras, R.L. Sidman, A.J. Fornace Jr, R.H. Schiestl, Atm-, p53-, and Gadd45a-deficient mice show an increased frequency of homologous recombination at different stages during development, Cancer Res. 63 (2003) 5335–5343. http://www.ncbi.nlm.nih.gov/pubmed/14500365

[22]   A. Memisoglu, L. Samson, Contribution of base excision repair, nucleotide excision repair, and DNA recombination to alkylation resistance of the fission yeast Schizosaccharomyces pombe, J. Bacteriol. 182 (2000) 2104–2112. http://www.ncbi.nlm.nih.gov/pubmed/10735851

[23]   A.D. Brown, A.B. Claybon, A.J.R. Bishop, A conditional mouse model for measuring the frequency of homologous recombination events in vivo in the absence of essential genes, Mol. Cell. Biol. 31 (2011) 3593–3602. http://www.ncbi.nlm.nih.gov/pubmed/21709021

[24]   M.H. Brilliant, The mouse p (pink-eyed dilution) and human P genes, oculocutaneous albinism type 2 (OCA2), and melanosomal pH, Pigment Cell Res. 14 (2001) 86–93. http://www.ncbi.nlm.nih.gov/pubmed/11310796

[25]   A.D. Brown, A.B. Claybon, A.J.R. Bishop, Mouse WRN Helicase Domain Is Not Required for Spontaneous Homologous Recombination-Mediated DNA Deletion, J Nucleic Acids. 2010 (2010). http://www.ncbi.nlm.nih.gov/pmc/articles/PMC2933912/

[26]   K. Trenz, S. Lugowski, U. Jahrsdörfer, S. Jainta, W. Vogel, G. Speit, Enhanced sensitivity of peripheral blood lymphocytes from women carrying a BRCA1 mutation towards the mutagenic effects of various cytostatics, Mutat. Res. 544 (2003) 279–288. http://dx.doi.org/10.1016/j.mrrev.2003.06.011

[27]   E. Sonoda, M.S. Sasaki, C. Morrison, Y. Yamaguchi-Iwai, M. Takata, S. Takeda, Sister chromatid exchanges are mediated by homologous recombination in vertebrate cells, Mol. Cell. Biol. 19 (1999) 5166–5169. http://www.ncbi.nlm.nih.gov/pmc/articles/PMC84359/

[28]   B. Kaina, Mechanisms and consequences of methylating agent-induced SCEs and chromosomal aberrations: a long road traveled and still a far way to go, Cytogenet. Genome Res. 104 (2004) 77–86. http://www.ncbi.nlm.nih.gov/pubmed/15162018

[29]   R.E. Neft, M.K. Conner, Induction of sister chromatid exchange in multiple murine tissues in vivo by various methylating agents, Teratog., Carcinog. Mutagen. 9 (1989) 219–237. http://www.ncbi.nlm.nih.gov/pubmed/2572066

[30]   D. Hellgren, S. Sahlén, B. Lambert, Mutagen-induced recombination between stably integrated neo gene fragments in CHO and EM9 cells, Mutat. Res. 226 (1989) 1–8. http://dx.doi.org/10.1016/0165-7992(89)90085-7

[31]   B.W. Durkacz, O. Omidiji, D.A. Gray, S. Shall, (ADP-ribose)n participates in DNA excision repair, Nature. 283 (1980) 593–596. http://dx.doi.org/10.1038/283593a0

[32]   T. Zaremba, N.J. Curtin, PARP inhibitor development for systemic cancer targeting, Anticancer Agents Med Chem. 7 (2007) 515–523. http://www.ncbi.nlm.nih.gov/pubmed/17896912

[33]   J.-F. Haince, D. McDonald, A. Rodrigue, U. Déry, J.-Y. Masson, M.J. Hendzel, et al., PARP1-dependent kinetics of recruitment of MRE11 and NBS1 proteins to multiple DNA damage sites, J. Biol. Chem. 283 (2008) 1197–1208. http://www.ncbi.nlm.nih.gov/pubmed/18025084

[34]   J.-F. Haince, S. Kozlov, V.L. Dawson, T.M. Dawson, M.J. Hendzel, M.F. Lavin, et al., Ataxia telangiectasia mutated (ATM) signaling network is modulated by a novel poly(ADP-ribose)-dependent pathway in the early response to DNA-damaging agents, J. Biol. Chem. 282 (2007) 16441–16453. http://www.ncbi.nlm.nih.gov/pubmed/17428792

[35]   J.L. Schwartz, W.F. Morgan, L.N. Kapp, S. Wolff, Effects of 3-aminobenzamide on DNA synthesis and cell cycle progression in Chinese hamster ovary cells, Exp. Cell Res. 143 (1983) 377–382. http://dx.doi.org/10.1016/0014-4827(83)90064-2

[36]   A.T. Natarajan, I. Csukás, A.A. van Zeeland, Contribution of incorporated 5-bromodeoxyuridine in DNA to the frequencies of sister-chromatid exchanges induced by inhibitors of poly-(ADP-ribose)-polymerase, Mutat. Res. 84 (1981) 125–132. http://www.ncbi.nlm.nih.gov/pubmed/7199115

[37]   G. Noël, N. Giocanti, M. Fernet, F. Mégnin-Chanet, V. Favaudon, Poly(ADP-ribose) polymerase (PARP-1) is not involved in DNA double-strand break recovery, BMC Cell Biol. 4 (2003) 7. http://www.ncbi.nlm.nih.gov/pubmed/12866953

[38]   J.E. Haber, DNA recombination: the replication connection, Trends Biochem. Sci. 24 (1999) 271–275. http://www.ncbi.nlm.nih.gov/pubmed/10390616

[39]   B. Modan, Low-dose radiation carcinogenesis, Eur. J. Cancer. 28A (1992) 1010–1012. http://www.ncbi.nlm.nih.gov/pubmed/22641644

[40]   Y. Yoshimoto, H. Kato, W.J. Schull, Risk of cancer among children exposed in utero to A-bomb radiations, 1950-84, Lancet. 2 (1988) 665–669. http://dx.doi.org/10.1016/S0140-6736(88)90477-1

[41]   L.F. Povirk, DNA damage and mutagenesis by radiomimetic DNA-cleaving agents: bleomycin, neocarzinostatin and other enediynes, Mutat. Res. 355 (1996) 71–89. http://dx.doi.org/10.1016/0027-5107(96)00023-1

[42]   G. Obe, C. Schunck, C. Johannes, Induction of sister-chromatid exchanges by AluI, DNase I, benzon nuclease and bleomycin in Chinese hamster ovary (CHO) cells, Mutat. Res. 307 (1994) 315–321. http://www.ncbi.nlm.nih.gov/pubmed/7513811

[43]   E.P. Rogakou, D.R. Pilch, A.H. Orr, V.S. Ivanova, W.M. Bonner, DNA double-stranded breaks induce histone H2AX phosphorylation on serine 139, J. Biol. Chem. 273 (1998) 5858–5868. http://www.ncbi.nlm.nih.gov/pubmed/9488723

[44]   H. Hashimoto, S. Chatterjee, N.A. Berger, Inhibition of etoposide (VP-16)-induced DNA recombination and mutant frequency by Bcl-2 protein overexpression, Cancer Res. 55 (1995) 4029–4035. http://www.ncbi.nlm.nih.gov/pubmed/7664276

[45]   G. Ribas, N. Xamena, A. Creus, R. Marcos, Sister-chromatid exchanges (SCE) induction by inhibitors of DNA topoisomerases in cultured human lymphocytes, Mutat. Res. 368 (1996) 205–211. http://www.ncbi.nlm.nih.gov/pubmed/8692226

[46]   P.J. Sykes, A.M. Hooker, A.A. Morley, Inversion due to intrachromosomal recombination produced by carcinogens in a transgenic mouse model, Mutat. Res. 427 (1999) 1–9. http://dx.doi.org/10.1016/S0027-5107(99)00084-6

[47]   M. Matsuoka, F. Nagawa, K. Okazaki, L. Kingsbury, K. Yoshida, U. Müller, et al., Detection of somatic DNA recombination in the transgenic mouse brain, Science. 254 (1991) 81–86. http://dx.doi.org/10.1126/science.1925563

[48]   C.C. Huang, C.S. Han, X.F. Yue, C.M. Shen, S.W. Wang, F.G. Wu, et al., Cytotoxicity and sister chromatid exchanges induced in vitro by six anticancer drugs developed in the People's

Republic of China, J. Natl. Cancer Inst. 71 (1983) 841–847.
http://www.ncbi.nlm.nih.gov/pubmed/6413744

[49] M. Lim, L.F. Liu, D. Jacobson-Kram, J.R. Williams, Induction of sister chromatid exchanges by inhibitors of topoisomerases, Cell Biol. Toxicol. 2 (1986) 485–494.
http://www.ncbi.nlm.nih.gov/pubmed/2855799

[50] F. Degrassi, R. De Salvia, C. Tanzarella, F. Palitti, Induction of chromosomal aberrations and SCE by camptothecin, an inhibitor of mammalian topoisomerase I, Mutat. Res. 211 (1989) 125–130.
http://dx.doi.org/10.1016/0027-5107(89)90112-7

[51] J.H. Zhao, H. Tohda, A. Oikawa, Camptothecin-induced sister-chromatid exchange dependent on the presence of bromodeoxyuridine and the phase of the cell cycle, Mutat. Res. 282 (1992) 49–54.
http://dx.doi.org/10.1016/0165-7992(92)90073-Q

[52] J. Piñero, M. López Baena, T. Ortiz, F. Cortés, Sister chromatid exchange induced by DNA topoisomerases poisons in late replicating heterochromatin: influence of inhibition of replication and transcription, Mutat. Res. 354 (1996) 195–201. http://www.ncbi.nlm.nih.gov/pubmed/8764948

[53] L.H. Zhang, D. Jenssen, Studies on intrachromosomal recombination in SP5/V79 Chinese hamster cells upon exposure to different agents related to carcinogenesis, Carcinogenesis. 15 (1994) 2303–2310. http://www.ncbi.nlm.nih.gov/pubmed/7955071

[54] S.G. Morham, K.D. Kluckman, N. Voulomanos, O. Smithies, Targeted disruption of the mouse topoisomerase I gene by camptothecin selection, Mol. Cell. Biol. 16 (1996) 6804–6809.
http://www.ncbi.nlm.nih.gov/pmc/articles/PMC231683/

[55] A.C. Bester, M. Roniger, Y.S. Oren, M.M. Im, D. Sarni, M. Chaoat, et al., Nucleotide deficiency promotes genomic instability in early stages of cancer development, Cell. 145 (2011) 435–446.
http://dx.doi.org/10.1016/j.cell.2011.03.044

[56] P. Chabosseau, G. Buhagiar-Labarchède, R. Onclercq-Delic, S. Lambert, M. Debatisse, O. Brison, et al., Pyrimidine pool imbalance induced by BLM helicase deficiency contributes to genetic instability in Bloom syndrome, Nat Commun. 2 (2011) 368. http://dx.doi.org/10.1038/ncomms1363

[57] C.K. Mathews, DNA precursor metabolism and genomic stability, FASEB J. 20 (2006) 1300–1314. http://www.ncbi.nlm.nih.gov/pubmed/16816105

[58] A. Matsuoka, C. Lundin, F. Johansson, M. Sahlin, K. Fukuhara, B.-M. Sjöberg, et al., Correlation of sister chromatid exchange formation through homologous recombination with ribonucleotide reductase inhibition, Mutat. Res. 547 (2004) 101–107.
http://dx.doi.org/10.1016/j.mrfmmm.2003.12.002

[59]   C. Lundin, K. Erixon, C. Arnaudeau, N. Schultz, D. Jenssen, M. Meuth, et al., Different roles for nonhomologous end joining and homologous recombination following replication arrest in mammalian cells, Mol. Cell. Biol. 22 (2002) 5869–5878. http://www.ncbi.nlm.nih.gov/pubmed/12138197

[60]   A. Hueber, P. Esser, K. Heimann, N. Kociok, S. Winter, M. Weller, The topoisomerase I inhibitors, camptothecin and beta-lapachone, induce apoptosis of human retinal pigment epithelial cells, Exp. Eye Res. 67 (1998) 525–530. http://dx.doi.org/10.1006/exer.1998.0544

[61]   C. Holm, J.M. Covey, D. Kerrigan, Y. Pommier, Differential requirement of DNA replication for the cytotoxicity of DNA topoisomerase I and II inhibitors in Chinese hamster DC3F cells, Cancer Res. 49 (1989) 6365–6368. http://www.ncbi.nlm.nih.gov/pubmed/2553254

[62]   M.A. Mackenzie, S.A. Jordan, P.S. Budd, I.J. Jackson, Activation of the receptor tyrosine kinase Kit is required for the proliferation of melanoblasts in the mouse embryo, Dev. Biol. 192 (1997) 99–107. http://www.ncbi.nlm.nih.gov/pubmed/9405100

[63]   J.M. Sidorova, K. Kehrli, F. Mao, R. Monnat Jr, Distinct functions of human RECQ helicases WRN and BLM in replication fork recovery and progression after hydroxyurea-induced stalling, DNA Repair (Amst.). 12 (2013) 128–139. http://dx.doi.org/10.1016/j.dnarep.2012.11.005

[64]   S.L. Davies, P.S. North, I.D. Hickson, Role for BLM in replication-fork restart and suppression of origin firing after replicative stress, Nat. Struct. Mol. Biol. 14 (2007) 677–679. http://dx.doi.org/10.1038/nsmb1267

[65]   V.A. Rao, A.M. Fan, L. Meng, C.F. Doe, P.S. North, I.D. Hickson, et al., Phosphorylation of BLM, dissociation from topoisomerase IIIalpha, and colocalization with gamma-H2AX after topoisomerase I-induced replication damage, Mol. Cell. Biol. 25 (2005) 8925–8937. http://www.ncbi.nlm.nih.gov/pubmed/16199871

[66]   L. Tomatis, Overview of perinatal and multigeneration carcinogenesis, IARC Sci. Publ. (1989) 1–15. http://www.ncbi.nlm.nih.gov/pubmed/2680943

[67]   L.M. Anderson, B.A. Diwan, N.T. Fear, E. Roman, Critical windows of exposure for children's health: cancer in human epidemiological studies and neoplasms in experimental animal models, Environ. Health Perspect. 108 Suppl 3 (2000) 573–594. http://www.ncbi.nlm.nih.gov/pmc/articles/PMC1637809/

[68]   F. Perera, K. Hemminki, W. Jedrychowski, R. Whyatt, U. Campbell, Y. Hsu, et al., In utero DNA damage from environmental pollution is associated with somatic gene mutation in newborns, Cancer Epidemiol. Biomarkers Prev. 11 (2002) 1134–1137. http://www.ncbi.nlm.nih.gov/pubmed/12376523

[69]   K.A. Bocskay, D. Tang, M.A. Orjuela, X. Liu, D.P. Warburton, F.P. Perera, Chromosomal aberrations in cord blood are associated with prenatal exposure to carcinogenic polycyclic aromatic hydrocarbons, Cancer Epidemiol. Biomarkers Prev. 14 (2005) 506–511. http://www.ncbi.nlm.nih.gov/pubmed/15734979

[70]   S.C. Edwards, W. Jedrychowski, M. Butscher, D. Camann, A. Kieltyka, E. Mroz, et al., Prenatal exposure to airborne polycyclic aromatic hydrocarbons and children's intelligence at 5 years of age in a prospective cohort study in Poland, Environ. Health Perspect. 118 (2010) 1326–1331. http://www.ncbi.nlm.nih.gov/pubmed/20406721

[71]   Y.R. Paashuis-Lew, J.A. Heddle, Spontaneous mutation during fetal development and post-natal growth, Mutagenesis. 13 (1998) 613–617. http://www.ncbi.nlm.nih.gov/pubmed/9862193

[72]   R. Doll, R. Wakeford, Risk of childhood cancer from fetal irradiation, Br J Radiol. 70 (1997) 130–139. http://www.ncbi.nlm.nih.gov/pubmed/9135438

[73]   S.G. Selevan, C.A. Kimmel, P. Mendola, Identifying critical windows of exposure for children's health, Environ. Health Perspect. 108 Suppl 3 (2000) 451–455. http://www.ncbi.nlm.nih.gov/pmc/articles/PMC1637810/

[74]   A.F. Olshan, L. Anderson, E. Roman, N. Fear, M. Wolff, R. Whyatt, et al., Workshop to identify critical windows of exposure for children's health: cancer work group summary, Environ. Health Perspect. 108 Suppl 3 (2000) 595–597. http://www.ncbi.nlm.nih.gov/pmc/articles/PMC1637823/

[75]   L.S. Birnbaum, S.E. Fenton, Cancer and developmental exposure to endocrine disruptors, Environ. Health Perspect. 111 (2003) 389–394. http://www.ncbi.nlm.nih.gov/pmc/articles/PMC1241417/

Specific Aim 2 and 3 References

1. Reiter LT, Murakami T, Koeuth T, Pentao L, Muzny DM, et al. (1996) A recombination hotspot responsible for two inherited peripheral neuropathies is located near a mariner transposon-like element. Nat Genet 12: 288-297.

2. Bayes M, Magano LF, Rivera N, Flores R, Perez Jurado LA (2003) Mutational mechanisms of Williams-Beuren syndrome deletions. Am J Hum Genet 73: 131-151.

3. Bi W, Park SS, Shaw CJ, Withers MA, Patel PI, et al. (2003) Reciprocal crossovers and a positional preference for strand exchange in recombination events resulting in deletion or duplication of chromosome 17p11.2. Am J Hum Genet 73: 1302-1315.

4. Barber JC, Joyce CA, Collinson MN, Nicholson JC, Willatt LR, et al. (1998) Duplication of 8p23.1: a cytogenetic anomaly with no established clinical significance. J Med Genet 35: 491-496.

5. Moog U, Engelen JJ, Albrechts JC, Baars LG, de Die-Smulders CE (2000) Familial dup(8)(p12p21.1): mild phenotypic effect and review of partial 8p duplications. Am J Med Genet 94: 306-310.

6. Lin H, Pizer ES, Morin PJ (2000) A frequent deletion polymorphism on chromosome 22q13 identified by representational difference analysis of ovarian cancer. Genomics 69: 391-394.

7. Iafrate AJ, Feuk L, Rivera MN, Listewnik ML, Donahoe PK, et al. (2004) Detection of large-scale variation in the human genome. Nat Genet 36: 949-951.

8. Sebat J, Lakshmi B, Troge J, Alexander J, Young J, et al. (2004) Large-scale copy number polymorphism in the human genome. Science 305: 525-528.

9. Tuzun E, Sharp AJ, Bailey JA, Kaul R, Morrison VA, et al. (2005) Fine-scale structural variation of the human genome. Nat Genet 37: 727-732.

10. Sharp AJ, Locke DP, McGrath SD, Cheng Z, Bailey JA, et al. (2005) Segmental duplications and copy-number variation in the human genome. Am J Hum Genet 77: 78-88.

11. Conrad DF, Andrews TD, Carter NP, Hurles ME, Pritchard JK (2006) A high-resolution survey of deletion polymorphism in the human genome. Nat Genet 38: 75-81.

12. Hinds DA, Kloek AP, Jen M, Chen X, Frazer KA (2006) Common deletions and SNPs are in linkage disequilibrium in the human genome. Nat Genet 38: 82-85.

13. McCarroll SA, Hadnott TN, Perry GH, Sabeti PC, Zody MC, et al. (2006) Common deletion polymorphisms in the human genome. Nat Genet 38: 86-92.

14. Freeman JL, Perry GH, Feuk L, Redon R, McCarroll SA, et al. (2006) Copy number variation: new insights in genome diversity. Genome Res 16: 949-961.

15. Feuk L, Marshall CR, Wintle RF, Scherer SW (2006) Structural variants: changing the landscape of chromosomes and design of disease studies. Hum Mol Genet 15 Spec No 1: R57-66.

16. Lupski JR (1998) Genomic disorders: structural features of the genome can lead to DNA rearrangements and human disease traits. Trends Genet 14: 417-422.

17. Fredman D, White SJ, Potter S, Eichler EE, Den Dunnen JT, et al. (2004) Complex SNP-related sequence variation in segmental genome duplications. Nat Genet 36: 861-866.

18. Eichler EE (2001) Recent duplication, domain accretion and the dynamic mutation of the human genome. Trends Genet 17: 661-669.

19. (2003) The International HapMap Project. Nature 426: 789-796.

20. Roth DB, Wilson JH (1986) Nonhomologous recombination in mammalian cells: role for short sequence homologies in the joining reaction. Mol Cell Biol 6: 4295-4304.

21. Bailey JA, Yavor AM, Massa HF, Trask BJ, Eichler EE (2001) Segmental duplications: organization and impact within the current human genome project assembly. Genome Res 11: 1005-1017.

22. Nguyen DQ, Webber C, Ponting CP (2006) Bias of selection on human copy-number variants. PLoS Genet 2: e20.

23. Lichtenstein P, Holm NV, Verkasalo PK, Iliadou A, Kaprio J, et al. (2000) Environmental and heritable factors in the causation of cancer--analyses of cohorts of twins from Sweden, Denmark, and Finland. N Engl J Med 343: 78-85.

24. Hoover RN (2000) Cancer--nature, nurture, or both. N Engl J Med 343: 135-136.

25. Kawajiri K, Eguchi H, Nakachi K, Sekiya T, Yamamoto M (1996) Association of CYP1A1 germ line polymorphisms with mutations of the p53 gene in lung cancer. Cancer Res 56: 72-76.

26. Ziegler A, Jonason AS, Leffell DJ, Simon JA, Sharma HW, et al. (1994) Sunburn and p53 in the onset of skin cancer. Nature 372: 773-776.

27. Nakazawa H, English D, Randell PL, Nakazawa K, Martel N, et al. (1994) UV and skin cancer: specific p53 gene mutation in normal skin as a biologically relevant exposure measurement. Proc Natl Acad Sci U S A 91: 360-364.

28. de Laat WL, Jaspers NG, Hoeijmakers JH (1999) Molecular mechanism of nucleotide excision repair. Genes Dev 13: 768-785.

29. Hoeijmakers JH (2009) DNA damage, aging, and cancer. N Engl J Med 361: 1475-1485.

30. Bennett CB, Lewis AL, Baldwin KK, Resnick MA (1993) Lethality induced by a single site-specific double-strand break in a dispensable yeast plasmid. Proc Natl Acad Sci U S A 90: 5613-5617.

31. Monneret C (2011) Platinum anticancer drugs. From serendipity to rational design. Ann Pharm Fr 69: 286-295.

32. Riley PA (1994) Free radicals in biology: oxidative stress and the effects of ionizing radiation. Int J Radiat Biol 65: 27-33.

33. Beckman KB, Ames BN (1997) Oxidative decay of DNA. J Biol Chem 272: 19633-19636.

34. Lange SS, Takata K, Wood RD (2011) DNA polymerases and cancer. Nat Rev Cancer 11: 96-110.

35. Lindahl T (1993) Instability and decay of the primary structure of DNA. Nature 362: 709-715.

36. San Filippo J, Sung P, Klein H (2008) Mechanism of eukaryotic homologous recombination. Annu Rev Biochem 77: 229-257.

37. Bode AM, Dong Z (2004) Post-translational modification of p53 in tumorigenesis. Nat Rev Cancer 4: 793-805.

38. Khanna KK, Keating KE, Kozlov S, Scott S, Gatei M, et al. (1998) ATM associates with and phosphorylates p53: mapping the region of interaction. Nat Genet 20: 398-400.

39. Fuchs B, O'Connor D, Fallis L, Scheidtmann KH, Lu X (1995) p53 phosphorylation mutants retain transcription activity. Oncogene 10: 789-793.

40. Maya R, Balass M, Kim ST, Shkedy D, Leal JF, et al. (2001) ATM-dependent phosphorylation of Mdm2 on serine 395: role in p53 activation by DNA damage. Genes Dev 15: 1067-1077.

41. Saito S, Goodarzi AA, Higashimoto Y, Noda Y, Lees-Miller SP, et al. (2002) ATM mediates phosphorylation at multiple p53 sites, including Ser(46), in response to ionizing radiation. J Biol Chem 277: 12491-12494.

42. Kim ST, Lim DS, Canman CE, Kastan MB (1999) Substrate specificities and identification of putative substrates of ATM kinase family members. J Biol Chem 274: 37538-37543.

43. Lavin MF, Gueven N (2006) The complexity of p53 stabilization and activation. Cell Death Differ 13: 941-950.

44. Saito S, Yamaguchi H, Higashimoto Y, Chao C, Xu Y, et al. (2003) Phosphorylation site interdependence of human p53 post-translational modifications in response to stress. J Biol Chem 278: 37536-37544.

45. Shieh SY, Ahn J, Tamai K, Taya Y, Prives C (2000) The human homologs of checkpoint kinases Chk1 and Cds1 (Chk2) phosphorylate p53 at multiple DNA damage-inducible sites. Genes Dev 14: 289-300.

46. Unger T, Juven-Gershon T, Moallem E, Berger M, Vogt Sionov R, et al. (1999) Critical role for Ser20 of human p53 in the negative regulation of p53 by Mdm2. EMBO J 18: 1805-1814.

47. Li M, Luo J, Brooks CL, Gu W (2002) Acetylation of p53 inhibits its ubiquitination by Mdm2. J Biol Chem 277: 50607-50611.

48. Waterman MJ, Stavridi ES, Waterman JL, Halazonetis TD (1998) ATM-dependent activation of p53 involves dephosphorylation and association with 14-3-3 proteins. Nat Genet 19: 175-178.

49. Maclaine NJ, Hupp TR (2009) The regulation of p53 by phosphorylation: a model for how distinct signals integrate into the p53 pathway. Aging (Albany NY) 1: 490-502.

50. Yu J, Zhang L, Hwang PM, Rago C, Kinzler KW, et al. (1999) Identification and classification of p53-regulated genes. Proc Natl Acad Sci U S A 96: 14517-14522.

51. Zhao R, Gish K, Murphy M, Yin Y, Notterman D, et al. (2000) Analysis of p53-regulated gene expression patterns using oligonucleotide arrays. Genes Dev 14: 981-993.

52. Kannan K, Amariglio N, Rechavi G, Jakob-Hirsch J, Kela I, et al. (2001) DNA microarrays identification of primary and secondary target genes regulated by p53. Oncogene 20: 2225-2234.

53. Kho PS, Wang Z, Zhuang L, Li Y, Chew JL, et al. (2004) p53-regulated transcriptional program associated with genotoxic stress-induced apoptosis. J Biol Chem 279: 21183-21192.

54. el-Deiry WS, Tokino T, Velculescu VE, Levy DB, Parsons R, et al. (1993) WAF1, a potential mediator of p53 tumor suppression. Cell 75: 817-825.

55. Hermeking H, Lengauer C, Polyak K, He TC, Zhang L, et al. (1997) 14-3-3 sigma is a p53-regulated inhibitor of G2/M progression. Mol Cell 1: 3-11.

56. Miyashita T, Krajewski S, Krajewska M, Wang HG, Lin HK, et al. (1994) Tumor suppressor p53 is a regulator of bcl-2 and bax gene expression in vitro and in vivo. Oncogene 9: 1799-1805.

57. Owen-Schaub LB, Zhang W, Cusack JC, Angelo LS, Santee SM, et al. (1995) Wild-type human p53 and a temperature-sensitive mutant induce Fas/APO-1 expression. Mol Cell Biol 15: 3032-3040.

58. Dameron KM, Volpert OV, Tainsky MA, Bouck N (1994) Control of angiogenesis in fibroblasts by p53 regulation of thrombospondin-1. Science 265: 1582-1584.

59. Hwang BJ, Ford JM, Hanawalt PC, Chu G (1999) Expression of the p48 xeroderma pigmentosum gene is p53-dependent and is involved in global genomic repair. Proc Natl Acad Sci U S A 96: 424-428.

60. Seo YR, Fishel ML, Amundson S, Kelley MR, Smith ML (2002) Implication of p53 in base excision DNA repair: in vivo evidence. Oncogene 21: 731-737.

61. Harper JW, Adami GR, Wei N, Keyomarsi K, Elledge SJ (1993) The p21 Cdk-interacting protein Cip1 is a potent inhibitor of G1 cyclin-dependent kinases. Cell 75: 805-816.

62. Xiong Y, Hannon GJ, Zhang H, Casso D, Kobayashi R, et al. (1993) p21 is a universal inhibitor of cyclin kinases. Nature 366: 701-704.

63. Waldman T, Kinzler KW, Vogelstein B (1995) p21 is necessary for the p53-mediated G1 arrest in human cancer cells. Cancer Res 55: 5187-5190.

64. Deng C, Zhang P, Harper JW, Elledge SJ, Leder P (1995) Mice lacking p21CIP1/WAF1 undergo normal development, but are defective in G1 checkpoint control. Cell 82: 675-684.

65. Brugarolas J, Chandrasekaran C, Gordon JI, Beach D, Jacks T, et al. (1995) Radiation-induced cell cycle arrest compromised by p21 deficiency. Nature 377: 552-557.

66. Di Leonardo A, Linke SP, Clarkin K, Wahl GM (1994) DNA damage triggers a prolonged p53-dependent G1 arrest and long-term induction of Cip1 in normal human fibroblasts. Genes Dev 8: 2540-2551.

67. Kuo ML, Chou YW, Chau YP, Huang TS (1997) Resistance to apoptosis induced by alkylating agents in v-Ha-ras-transformed cells due to defect in p53 function. Mol Carcinog 18: 221-231.

68. Yuan ZM, Huang Y, Fan MM, Sawyers C, Kharbanda S, et al. (1996) Genotoxic drugs induce interaction of the c-Abl tyrosine kinase and the tumor suppressor protein p53. J Biol Chem 271: 26457-26460.

69. Li R, Waga S, Hannon GJ, Beach D, Stillman B (1994) Differential effects by the p21 CDK inhibitor on PCNA-dependent DNA replication and repair. Nature 371: 534-537.

70. Waga S, Hannon GJ, Beach D, Stillman B (1994) The p21 inhibitor of cyclin-dependent kinases controls DNA replication by interaction with PCNA. Nature 369: 574-578.

71. Poon RY, Hunter T (1998) Expression of a novel form of p21Cip1/Waf1 in UV-irradiated and transformed cells. Oncogene 16: 1333-1343.

72. Kearsey JM, Coates PJ, Prescott AR, Warbrick E, Hall PA (1995) Gadd45 is a nuclear cell cycle regulated protein which interacts with p21Cip1. Oncogene 11: 1675-1683.

73. Takekawa M, Saito H (1998) A family of stress-inducible GADD45-like proteins mediate activation of the stress-responsive MTK1/MEKK4 MAPKKK. Cell 95: 521-530.

74. Kovalsky O, Lung FD, Roller PP, Fornace AJ, Jr. (2001) Oligomerization of human Gadd45a protein. J Biol Chem 276: 39330-39339.

75. Smith ML, Chen IT, Zhan Q, Bae I, Chen CY, et al. (1994) Interaction of the p53-regulated protein Gadd45 with proliferating cell nuclear antigen. Science 266: 1376-1380.

76. John PC, Mews M, Moore R (2001) Cyclin/Cdk complexes: their involvement in cell cycle progression and mitotic division. Protoplasma 216: 119-142.

77. Zhang H, Xiong Y, Beach D (1993) Proliferating cell nuclear antigen and p21 are components of multiple cell cycle kinase complexes. Mol Biol Cell 4: 897-906.

78. Chan TA, Hwang PM, Hermeking H, Kinzler KW, Vogelstein B (2000) Cooperative effects of genes controlling the G(2)/M checkpoint. Genes Dev 14: 1584-1588.

79. Vairapandi M, Balliet AG, Hoffman B, Liebermann DA (2002) GADD45b and GADD45g are cdc2/cyclinB1 kinase inhibitors with a role in S and G2/M cell cycle checkpoints induced by genotoxic stress. J Cell Physiol 192: 327-338.

80. Zhan Q, Antinore MJ, Wang XW, Carrier F, Smith ML, et al. (1999) Association with Cdc2 and inhibition of Cdc2/Cyclin B1 kinase activity by the p53-regulated protein Gadd45. Oncogene 18: 2892-2900.

81. Zhao H, Jin S, Antinore MJ, Lung FD, Fan F, et al. (2000) The central region of Gadd45 is required for its interaction with p21/WAF1. Exp Cell Res 258: 92-100.

82. Yang Q, Manicone A, Coursen JD, Linke SP, Nagashima M, et al. (2000) Identification of a functional domain in a GADD45-mediated G2/M checkpoint. J Biol Chem 275: 36892-36898.

83. Wang XW, Zhan Q, Coursen JD, Khan MA, Kontny HU, et al. (1999) GADD45 induction of a G2/M cell cycle checkpoint. Proc Natl Acad Sci U S A 96: 3706-3711.

84. Zhang W, Hoffman B, Liebermann DA (2001) Ectopic expression of MyD118/Gadd45/CR6 (Gadd45beta/alpha/gamma) sensitizes neoplastic cells to genotoxic stress-induced apoptosis. Int J Oncol 18: 749-757.

85. Fornace AJ, Jr., Alamo I, Jr., Hollander MC (1988) DNA damage-inducible transcripts in mammalian cells. Proc Natl Acad Sci U S A 85: 8800-8804.

86. Berger M, Stahl N, Del Sal G, Haupt Y (2005) Mutations in proline 82 of p53 impair its activation by Pin1 and Chk2 in response to DNA damage. Mol Cell Biol 25: 5380-5388.

87. Fuchs SY, Adler V, Buschmann T, Yin Z, Wu X, et al. (1998) JNK targets p53 ubiquitination and degradation in nonstressed cells. Genes Dev 12: 2658-2663.

88. Ando K, Ozaki T, Yamamoto H, Furuya K, Hosoda M, et al. (2004) Polo-like kinase 1 (Plk1) inhibits p53 function by physical interaction and phosphorylation. J Biol Chem 279: 25549-25561.

89. Mihara M, Erster S, Zaika A, Petrenko O, Chittenden T, et al. (2003) p53 has a direct apoptogenic role at the mitochondria. Mol Cell 11: 577-590.

90. Ito A, Lai CH, Zhao X, Saito S, Hamilton MH, et al. (2001) p300/CBP-mediated p53 acetylation is commonly induced by p53-activating agents and inhibited by MDM2. EMBO J 20: 1331-1340.

91. Guo A, Salomoni P, Luo J, Shih A, Zhong S, et al. (2000) The function of PML in p53-dependent apoptosis. Nat Cell Biol 2: 730-736.

92. Wesierska-Gadek J, Wojciechowski J, Schmid G (2003) Phosphorylation regulates the interaction and complex formation between wt p53 protein and PARP-1. J Cell Biochem 89: 1260-1284.

93. Sommers JA, Sharma S, Doherty KM, Karmakar P, Yang Q, et al. (2005) p53 modulates RPA-dependent and RPA-independent WRN helicase activity. Cancer Res 65: 1223-1233.

94. Hanson S, Kim E, Deppert W (2005) Redox factor 1 (Ref-1) enhances specific DNA binding of p53 by promoting p53 tetramerization. Oncogene 24: 1641-1647.

95. Wiles AM, Doderer M, Ruan J, Gu TT, Ravi D, et al. (2010) Building and analyzing protein interactome networks by cross-species comparisons. BMC Syst Biol 4: 36.

96. Soussi T, May P (1996) Structural aspects of the p53 protein in relation to gene evolution: a second look. J Mol Biol 260: 623-637.

97. Matlashewski G, Lamb P, Pim D, Peacock J, Crawford L, et al. (1984) Isolation and characterization of a human p53 cDNA clone: expression of the human p53 gene. EMBO J 3: 3257-3262.

98. Harlow E, Williamson NM, Ralston R, Helfman DM, Adams TE (1985) Molecular cloning and in vitro expression of a cDNA clone for human cellular tumor antigen p53. Mol Cell Biol 5: 1601-1610.

99. Chang J, Kim DH, Lee SW, Choi KY, Sung YC (1995) Transactivation ability of p53 transcriptional activation domain is directly related to the binding affinity to TATA-binding protein. J Biol Chem 270: 25014-25019.

100. Lin J, Chen J, Elenbaas B, Levine AJ (1994) Several hydrophobic amino acids in the p53 amino-terminal domain are required for transcriptional activation, binding to mdm-2 and the adenovirus 5 E1B 55-kD protein. Genes Dev 8: 1235-1246.

101. Unger T, Mietz JA, Scheffner M, Yee CL, Howley PM (1993) Functional domains of wild-type and mutant p53 proteins involved in transcriptional regulation, transdominant inhibition, and transformation suppression. Mol Cell Biol 13: 5186-5194.

102. Candau R, Scolnick DM, Darpino P, Ying CY, Halazonetis TD, et al. (1997) Two tandem and independent sub-activation domains in the amino terminus of p53 require the adaptor complex for activity. Oncogene 15: 807-816.

103. Venot C, Maratrat M, Dureuil C, Conseiller E, Bracco L, et al. (1998) The requirement for the p53 proline-rich functional domain for mediation of apoptosis is correlated with specific PIG3 gene transactivation and with transcriptional repression. EMBO J 17: 4668-4679.

104. Zhu J, Zhou W, Jiang J, Chen X (1998) Identification of a novel p53 functional domain that is necessary for mediating apoptosis. J Biol Chem 273: 13030-13036.

105. Wang P, Reed M, Wang Y, Mayr G, Stenger JE, et al. (1994) p53 domains: structure, oligomerization, and transformation. Mol Cell Biol 14: 5182-5191.

106. Clore GM, Ernst J, Clubb R, Omichinski JG, Kennedy WM, et al. (1995) Refined solution structure of the oligomerization domain of the tumour suppressor p53. Nat Struct Biol 2: 321-333.

107. Lee W, Harvey TS, Yin Y, Yau P, Litchfield D, et al. (1994) Solution structure of the tetrameric minimum transforming domain of p53. Nat Struct Biol 1: 877-890.

108. Jeffrey PD, Gorina S, Pavletich NP (1995) Crystal structure of the tetramerization domain of the p53 tumor suppressor at 1.7 angstroms. Science 267: 1498-1502.

109. Mittl PR, Chene P, Grutter MG (1998) Crystallization and structure solution of p53 (residues 326-356) by molecular replacement using an NMR model as template. Acta Crystallogr D Biol Crystallogr 54: 86-89.

110. Hainaut P, Hall A, Milner J (1994) Analysis of p53 quaternary structure in relation to sequence-specific DNA binding. Oncogene 9: 299-303.

111. Avantaggiati ML, Ogryzko V, Gardner K, Giordano A, Levine AS, et al. (1997) Recruitment of p300/CBP in p53-dependent signal pathways. Cell 89: 1175-1184.

112. Gu W, Shi XL, Roeder RG (1997) Synergistic activation of transcription by CBP and p53. Nature 387: 819-823.

113. Lill NL, Grossman SR, Ginsberg D, DeCaprio J, Livingston DM (1997) Binding and modulation of p53 by p300/CBP coactivators. Nature 387: 823-827.

114. Scolnick DM, Chehab NH, Stavridi ES, Lien MC, Caruso L, et al. (1997) CREB-binding protein and p300/CBP-associated factor are transcriptional coactivators of the p53 tumor suppressor protein. Cancer Res 57: 3693-3696.

115. Honda R, Tanaka H, Yasuda H (1997) Oncoprotein MDM2 is a ubiquitin ligase E3 for tumor suppressor p53. FEBS Lett 420: 25-27.

116. Shieh SY, Ikeda M, Taya Y, Prives C (1997) DNA damage-induced phosphorylation of p53 alleviates inhibition by MDM2. Cell 91: 325-334.

117. Lambert PF, Kashanchi F, Radonovich MF, Shiekhattar R, Brady JN (1998) Phosphorylation of p53 serine 15 increases interaction with CBP. J Biol Chem 273: 33048-33053.

118. Chehab NH, Malikzay A, Stavridi ES, Halazonetis TD (1999) Phosphorylation of Ser-20 mediates stabilization of human p53 in response to DNA damage. Proc Natl Acad Sci U S A 96: 13777-13782.

119. Vogelstein B, Lane D, Levine AJ (2000) Surfing the p53 network. Nature 408: 307-310.

120. Cho Y, Gorina S, Jeffrey PD, Pavletich NP (1994) Crystal structure of a p53 tumor suppressor-DNA complex: understanding tumorigenic mutations. Science 265: 346-355.

121. Rainwater R, Parks D, Anderson ME, Tegtmeyer P, Mann K (1995) Role of cysteine residues in regulation of p53 function. Mol Cell Biol 15: 3892-3903.

122. el-Deiry WS, Kern SE, Pietenpol JA, Kinzler KW, Vogelstein B (1992) Definition of a consensus binding site for p53. Nat Genet 1: 45-49.

123. Halazonetis TD, Kandil AN (1993) Conformational shifts propagate from the oligomerization domain of p53 to its tetrameric DNA binding domain and restore DNA binding to select p53 mutants. EMBO J 12: 5057-5064.

124. Halazonetis TD, Davis LJ, Kandil AN (1993) Wild-type p53 adopts a 'mutant'-like conformation when bound to DNA. EMBO J 12: 1021-1028.

125. Freeman J, Schmidt S, Scharer E, Iggo R (1994) Mutation of conserved domain II alters the sequence specificity of DNA binding by the p53 protein. EMBO J 13: 5393-5400.

126. Wieczorek AM, Waterman JL, Waterman MJ, Halazonetis TD (1996) Structure-based rescue of common tumor-derived p53 mutants. Nat Med 2: 1143-1146.

127. Hollstein M, Sidransky D, Vogelstein B, Harris CC (1991) p53 mutations in human cancers. Science 253: 49-53.

128. Joerger AC, Fersht AR (2007) Structural biology of the tumor suppressor p53 and cancer-associated mutants. Adv Cancer Res 97: 1-23.

129. Chene P (2001) The role of tetramerization in p53 function. Oncogene 20: 2611-2617.

130. Waterman JL, Shenk JL, Halazonetis TD (1995) The dihedral symmetry of the p53 tetramerization domain mandates a conformational switch upon DNA binding. EMBO J 14: 512-519.

131. Walker KK, Levine AJ (1996) Identification of a novel p53 functional domain that is necessary for efficient growth suppression. Proc Natl Acad Sci U S A 93: 15335-15340.

132. Dornan D, Shimizu H, Burch L, Smith AJ, Hupp TR (2003) The proline repeat domain of p53 binds directly to the transcriptional coactivator p300 and allosterically controls DNA-dependent acetylation of p53. Mol Cell Biol 23: 8846-8861.

133. Berger M, Vogt Sionov R, Levine AJ, Haupt Y (2001) A role for the polyproline domain of p53 in its regulation by Mdm2. J Biol Chem 276: 3785-3790.

134. Dumaz N, Milne DM, Jardine LJ, Meek DW (2001) Critical roles for the serine 20, but not the serine 15, phosphorylation site and for the polyproline domain in regulating p53 turnover. Biochem J 359: 459-464.

135. Baptiste N, Friedlander P, Chen X, Prives C (2002) The proline-rich domain of p53 is required for cooperation with anti-neoplastic agents to promote apoptosis of tumor cells. Oncogene 21: 9-21.

136. Chipuk JE, Kuwana T, Bouchier-Hayes L, Droin NM, Newmeyer DD, et al. (2004) Direct activation of Bax by p53 mediates mitochondrial membrane permeabilization and apoptosis. Science 303: 1010-1014.

137. Roth J, Koch P, Contente A, Dobbelstein M (2000) Tumor-derived mutations within the DNA-binding domain of p53 that phenotypically resemble the deletion of the proline-rich domain. Oncogene 19: 1834-1842.

138. Sakamuro D, Sabbatini P, White E, Prendergast GC (1997) The polyproline region of p53 is required to activate apoptosis but not growth arrest. Oncogene 15: 887-898.

139. Zhu J, Jiang J, Zhou W, Zhu K, Chen X (1999) Differential regulation of cellular target genes by p53 devoid of the PXXP motifs with impaired apoptotic activity. Oncogene 18: 2149-2155.

140. Kusano K, Sakaguchi M, Kagawa N, Waterman MR, Omura T (2001) Microsomal p450s use specific proline-rich sequences for efficient folding, but not for maintenance of the folded structure. J Biochem 129: 259-269.

141. Wang J, Tan NS, Ho B, Ding JL (2002) Modular arrangement and secretion of a multidomain serine protease. Evidence for involvement of proline-rich region and N-glycans in the secretion pathway. J Biol Chem 277: 36363-36372.

142. Bakalkin G, Selivanova G, Yakovleva T, Kiseleva E, Kashuba E, et al. (1995) p53 binds single-stranded DNA ends through the C-terminal domain and internal DNA segments via the middle domain. Nucleic Acids Res 23: 362-369.

143. Bakalkin G, Yakovleva T, Selivanova G, Magnusson KP, Szekely L, et al. (1994) p53 binds single-stranded DNA ends and catalyzes DNA renaturation and strand transfer. Proc Natl Acad Sci U S A 91: 413-417.

144. Jayaraman J, Prives C (1995) Activation of p53 sequence-specific DNA binding by short single strands of DNA requires the p53 C-terminus. Cell 81: 1021-1029.

145. Dudenhoffer C, Kurth M, Janus F, Deppert W, Wiesmuller L (1999) Dissociation of the recombination control and the sequence-specific transactivation function of P53. Oncogene 18: 5773-5784.

146. Dudenhoffer C, Rohaly G, Will K, Deppert W, Wiesmuller L (1998) Specific mismatch recognition in heteroduplex intermediates by p53 suggests a role in fidelity control of homologous recombination. Mol Cell Biol 18: 5332-5342.

147. Mazur SJ, Sakaguchi K, Appella E, Wang XW, Harris CC, et al. (1999) Preferential binding of tumor suppressor p53 to positively or negatively supercoiled DNA involves the C-terminal domain. J Mol Biol 292: 241-249.

148. Palecek E, Brazda V, Jagelska E, Pecinka P, Karlovska L, et al. (2004) Enhancement of p53 sequence-specific binding by DNA supercoiling. Oncogene 23: 2119-2127.

149. Zotchev SB, Protopopova M, Selivanova G (2000) p53 C-terminal interaction with DNA ends and gaps has opposing effect on specific DNA binding by the core. Nucleic Acids Res 28: 4005-4012.

150. Reed M, Woelker B, Wang P, Wang Y, Anderson ME, et al. (1995) The C-terminal domain of p53 recognizes DNA damaged by ionizing radiation. Proc Natl Acad Sci U S A 92: 9455-9459.

151. Reich NC, Oren M, Levine AJ (1983) Two distinct mechanisms regulate the levels of a cellular tumor antigen, p53. Mol Cell Biol 3: 2143-2150.

152. Momand J, Zambetti GP, Olson DC, George D, Levine AJ (1992) The mdm-2 oncogene product forms a complex with the p53 protein and inhibits p53-mediated transactivation. Cell 69: 1237-1245.

153. Wu X, Bayle JH, Olson D, Levine AJ (1993) The p53-mdm-2 autoregulatory feedback loop. Genes Dev 7: 1126-1132.

154. Lev Bar-Or R, Maya R, Segel LA, Alon U, Levine AJ, et al. (2000) Generation of oscillations by the p53-Mdm2 feedback loop: a theoretical and experimental study. Proc Natl Acad Sci U S A 97: 11250-11255.

155. Okamoto K, Li H, Jensen MR, Zhang T, Taya Y, et al. (2002) Cyclin G recruits PP2A to dephosphorylate Mdm2. Mol Cell 9: 761-771.

156. Takekawa M, Adachi M, Nakahata A, Nakayama I, Itoh F, et al. (2000) p53-inducible wip1 phosphatase mediates a negative feedback regulation of p38 MAPK-p53 signaling in response to UV radiation. EMBO J 19: 6517-6526.

157. Jimenez GS, Khan SH, Stommel JM, Wahl GM (1999) p53 regulation by post-translational modification and nuclear retention in response to diverse stresses. Oncogene 18: 7656-7665.

158. Li FP, Fraumeni JF, Jr. (1969) Rhabdomyosarcoma in children: epidemiologic study and identification of a familial cancer syndrome. J Natl Cancer Inst 43: 1365-1373.

159. Li FP, Fraumeni JF, Jr. (1969) Soft-tissue sarcomas, breast cancer, and other neoplasms. A familial syndrome? Ann Intern Med 71: 747-752.

160. Malkin D, Friend SH, Li FP, Strong LC (1997) Germ-line mutations of the p53 tumor-suppressor gene in children and young adults with second malignant neoplasms. N Engl J Med 336: 734.

161. Wu CC, Shete S, Amos CI, Strong LC (2006) Joint effects of germ-line p53 mutation and sex on cancer risk in Li-Fraumeni syndrome. Cancer Res 66: 8287-8292.

162. Li FP, Fraumeni JF, Jr., Mulvihill JJ, Blattner WA, Dreyfus MG, et al. (1988) A cancer family syndrome in twenty-four kindreds. Cancer Res 48: 5358-5362.

163. Nichols KE, Malkin D, Garber JE, Fraumeni JF, Jr., Li FP (2001) Germ-line p53 mutations predispose to a wide spectrum of early-onset cancers. Cancer Epidemiol Biomarkers Prev 10: 83-87.

164. Varley JM (2003) Germline TP53 mutations and Li-Fraumeni syndrome. Hum Mutat 21: 313-320.

165. Petitjean A, Mathe E, Kato S, Ishioka C, Tavtigian SV, et al. (2007) Impact of mutant p53 functional properties on TP53 mutation patterns and tumor phenotype: lessons from recent developments in the IARC TP53 database. Hum Mutat 28: 622-629.

166. Chompret A, Abel A, Stoppa-Lyonnet D, Brugieres L, Pages S, et al. (2001) Sensitivity and predictive value of criteria for p53 germline mutation screening. J Med Genet 38: 43-47.

167. Hisada M, Garber JE, Fung CY, Fraumeni JF, Jr., Li FP (1998) Multiple primary cancers in families with Li-Fraumeni syndrome. J Natl Cancer Inst 90: 606-611.

168. Ridley RM, Frith CD, Crow TJ, Conneally PM (1988) Anticipation in Huntington's disease is inherited through the male line but may originate in the female. J Med Genet 25: 589-595.

169. Mahadevan M, Tsilfidis C, Sabourin L, Shutler G, Amemiya C, et al. (1992) Myotonic dystrophy mutation: an unstable CTG repeat in the 3' untranslated region of the gene. Science 255: 1253-1255.

170. Kronquist KE, Sherman SL, Spector EB (2008) Clinical significance of tri-nucleotide repeats in Fragile X testing: a clarification of American College of Medical Genetics guidelines. Genet Med 10: 845-847.

171. Shlien A, Tabori U, Marshall CR, Pienkowska M, Feuk L, et al. (2008) Excessive genomic DNA copy number variation in the Li-Fraumeni cancer predisposition syndrome. Proc Natl Acad Sci U S A 105: 11264-11269.

172. Tabori U, Nanda S, Druker H, Lees J, Malkin D (2007) Younger age of cancer initiation is associated with shorter telomere length in Li-Fraumeni syndrome. Cancer Res 67: 1415-1418.

173. Fugazzola L, Cerutti N, Mannavola D, Ghilardi G, Alberti L, et al. (2002) Multigenerational familial medullary thyroid cancer (FMTC): evidence for FMTC phenocopies and association with papillary thyroid cancer. Clin Endocrinol (Oxf) 56: 53-63.

174. Martinez-Delgado B, Yanowsky K, Inglada-Perez L, Domingo S, Urioste M, et al. (2011) Genetic anticipation is associated with telomere shortening in hereditary breast cancer. PLoS Genet 7: e1002182.

175. Garber JE, Goldstein AM, Kantor AF, Dreyfus MG, Fraumeni JF, Jr., et al. (1991) Follow-up study of twenty-four families with Li-Fraumeni syndrome. Cancer Res 51: 6094-6097.

176. Bougeard G, Sesboue R, Baert-Desurmont S, Vasseur S, Martin C, et al. (2008) Molecular basis of the Li-Fraumeni syndrome: an update from the French LFS families. J Med Genet 45: 535-538.

177. Trkova M, Foretova L, Kodet R, Hedvicakova P, Sedlacek Z (2003) A Li-Fraumeni syndrome family with retained heterozygosity for a germline TP53 mutation in two tumors. Cancer Genet Cytogenet 145: 60-64.

178. Masciari S, Dewanwala A, Stoffel EM, Lauwers GY, Zheng H, et al. (2011) Gastric cancer in individuals with Li-Fraumeni syndrome. Genet Med 13: 651-657.

179. Toguchida J, Yamaguchi T, Dayton SH, Beauchamp RL, Herrera GE, et al. (1992) Prevalence and spectrum of germline mutations of the p53 gene among patients with sarcoma. N Engl J Med 326: 1301-1308.

180. Oliveira C, Ferreira P, Nabais S, Campos L, Ferreira A, et al. (2004) E-Cadherin (CDH1) and p53 rather than SMAD4 and Caspase-10 germline mutations contribute to genetic predisposition in Portuguese gastric cancer patients. Eur J Cancer 40: 1897-1903.

181. Ariffin H, Martel-Planche G, Daud SS, Ibrahim K, Hainaut P (2008) Li-Fraumeni syndrome in a Malaysian kindred. Cancer Genet Cytogenet 186: 49-53.

182. Achatz MI, Olivier M, Le Calvez F, Martel-Planche G, Lopes A, et al. (2007) The TP53 mutation, R337H, is associated with Li-Fraumeni and Li-Fraumeni-like syndromes in Brazilian families. Cancer Lett 245: 96-102.

183. Bougeard G, Limacher JM, Martin C, Charbonnier F, Killian A, et al. (2001) Detection of 11 germline inactivating TP53 mutations and absence of TP63 and HCHK2 mutations in 17 French families with Li-Fraumeni or Li-Fraumeni-like syndrome. J Med Genet 38: 253-257.

184. Malkin D (2011) Li-fraumeni syndrome. Genes Cancer 2: 475-484.

185. Lane DP (1992) Cancer. p53, guardian of the genome. Nature 358: 15-16.

186. Harvey M, Sands AT, Weiss RS, Hegi ME, Wiseman RW, et al. (1993) In vitro growth characteristics of embryo fibroblasts isolated from p53-deficient mice. Oncogene 8: 2457-2467.

187. Ishizaki K, Ejima Y, Matsunaga T, Hara R, Sakamoto A, et al. (1994) Increased UV-induced SCEs but normal repair of DNA damage in p53-deficient mouse cells. Int J Cancer 58: 254-257.

188. Rogan EM, Bryan TM, Hukku B, Maclean K, Chang AC, et al. (1995) Alterations in p53 and p16INK4 expression and telomere length during spontaneous immortalization of Li-Fraumeni syndrome fibroblasts. Mol Cell Biol 15: 4745-4753.

189. Venkatachalam S, Shi YP, Jones SN, Vogel H, Bradley A, et al. (1998) Retention of wild-type p53 in tumors from p53 heterozygous mice: reduction of p53 dosage can promote cancer formation. EMBO J 17: 4657-4667.

190. Venkatachalam S, Tyner SD, Pickering CR, Boley S, Recio L, et al. (2001) Is p53 haploinsufficient for tumor suppression? Implications for the p53+/- mouse model in carcinogenicity testing. Toxicol Pathol 29 Suppl: 147-154.

191. Ullrich RL, Bowles ND, Satterfield LC, Davis CM (1996) Strain-dependent susceptibility to radiation-induced mammary cancer is a result of differences in epithelial cell sensitivity to transformation. Radiat Res 146: 353-355.

192. Jonkers J, Meuwissen R, van der Gulden H, Peterse H, van der Valk M, et al. (2001) Synergistic tumor suppressor activity of BRCA2 and p53 in a conditional mouse model for breast cancer. Nat Genet 29: 418-425.

193. Olive KP, Tuveson DA, Ruhe ZC, Yin B, Willis NA, et al. (2004) Mutant p53 gain of function in two mouse models of Li-Fraumeni syndrome. Cell 119: 847-860.

194. Liu G, McDonnell TJ, Montes de Oca Luna R, Kapoor M, Mims B, et al. (2000) High metastatic potential in mice inheriting a targeted p53 missense mutation. Proc Natl Acad Sci U S A 97: 4174-4179.

195. Kenzelmann Broz D, Attardi LD (2010) In vivo analysis of p53 tumor suppressor function using genetically engineered mouse models. Carcinogenesis 31: 1311-1318.

196. Kato S, Han SY, Liu W, Otsuka K, Shibata H, et al. (2003) Understanding the function-structure and function-mutation relationships of p53 tumor suppressor protein by high-resolution missense mutation analysis. Proc Natl Acad Sci U S A 100: 8424-8429.

197. Milner J, Medcalf EA (1991) Cotranslation of activated mutant p53 with wild type drives the wild-type p53 protein into the mutant conformation. Cell 65: 765-774.

198. Lang GA, Iwakuma T, Suh YA, Liu G, Rao VA, et al. (2004) Gain of function of a p53 hot spot mutation in a mouse model of Li-Fraumeni syndrome. Cell 119: 861-872.

199. Terzian T, Suh YA, Iwakuma T, Post SM, Neumann M, et al. (2008) The inherent instability of mutant p53 is alleviated by Mdm2 or p16INK4a loss. Genes Dev 22: 1337-1344.

200. Wolf D, Harris N, Rotter V (1984) Reconstitution of p53 expression in a nonproducer Ab-MuLV-transformed cell line by transfection of a functional p53 gene. Cell 38: 119-126.

201. Shaulsky G, Goldfinger N, Rotter V (1991) Alterations in tumor development in vivo mediated by expression of wild type or mutant p53 proteins. Cancer Res 51: 5232-5237.

202. Dittmer D, Pati S, Zambetti G, Chu S, Teresky AK, et al. (1993) Gain of function mutations in p53. Nat Genet 4: 42-46.

203. Brosh R, Rotter V (2009) When mutants gain new powers: news from the mutant p53 field. Nat Rev Cancer 9: 701-713.

204. Song H, Hollstein M, Xu Y (2007) p53 gain-of-function cancer mutants induce genetic instability by inactivating ATM. Nat Cell Biol 9: 573-580.

205. Midgley CA, Lane DP (1997) p53 protein stability in tumour cells is not determined by mutation but is dependent on Mdm2 binding. Oncogene 15: 1179-1189.

206. Lukashchuk N, Vousden KH (2007) Ubiquitination and degradation of mutant p53. Mol Cell Biol 27: 8284-8295.

207. Bossi G, Lapi E, Strano S, Rinaldo C, Blandino G, et al. (2006) Mutant p53 gain of function: reduction of tumor malignancy of human cancer cell lines through abrogation of mutant p53 expression. Oncogene 25: 304-309.

208. Bossi G, Marampon F, Maor-Aloni R, Zani B, Rotter V, et al. (2008) Conditional RNA interference in vivo to study mutant p53 oncogenic gain of function on tumor malignancy. Cell Cycle 7: 1870-1879.

209. Amor M, Parker KL, Globerman H, New MI, White PC (1988) Mutation in the CYP21B gene (Ile-172----Asn) causes steroid 21-hydroxylase deficiency. Proc Natl Acad Sci U S A 85: 1600-1604.

210. Purandare SM, Patel PI (1997) Recombination hot spots and human disease. Genome Res 7: 773-786.

211. Gangloff S, Soustelle C, Fabre F (2000) Homologous recombination is responsible for cell death in the absence of the Sgs1 and Srs2 helicases. Nat Genet 25: 192-194.

212. Saintigny Y, Lopez BS (2002) Homologous recombination induced by replication inhibition, is stimulated by expression of mutant p53. Oncogene 21: 488-492.

213. Orr-Weaver TL, Szostak JW (1983) Multiple, tandem plasmid integration in Saccharomyces cerevisiae. Mol Cell Biol 3: 747-749.

214. Orr-Weaver TL, Szostak JW (1983) Yeast recombination: the association between double-strand gap repair and crossing-over. Proc Natl Acad Sci U S A 80: 4417-4421.

215. Szostak JW, Orr-Weaver TL, Rothstein RJ, Stahl FW (1983) The double-strand-break repair model for recombination. Cell 33: 25-35.

216. Hicks WM, Kim M, Haber JE (2010) Increased mutagenesis and unique mutation signature associated with mitotic gene conversion. Science 329: 82-85.

217. Lieber MR (2010) The mechanism of double-strand DNA break repair by the nonhomologous DNA end-joining pathway. Annu Rev Biochem 79: 181-211.

218. Takeda S, Nakamura K, Taniguchi Y, Paull TT (2007) Ctp1/CtIP and the MRN complex collaborate in the initial steps of homologous recombination. Mol Cell 28: 351-352.

219. Sartori AA, Lukas C, Coates J, Mistrik M, Fu S, et al. (2007) Human CtIP promotes DNA end resection. Nature 450: 509-514.

220. Nimonkar AV, Genschel J, Kinoshita E, Polaczek P, Campbell JL, et al. (2011) BLM-DNA2-RPA-MRN and EXO1-BLM-RPA-MRN constitute two DNA end resection machineries for human DNA break repair. Genes Dev 25: 350-362.

221. Sung P, Klein H (2006) Mechanism of homologous recombination: mediators and helicases take on regulatory functions. Nat Rev Mol Cell Biol 7: 739-750.

222. Prado F, Aguilera A (1995) Role of reciprocal exchange, one-ended invasion crossover and single-strand annealing on inverted and direct repeat recombination in yeast: different requirements for the RAD1, RAD10, and RAD52 genes. Genetics 139: 109-123.

223. Petermann E, Helleday T (2010) Pathways of mammalian replication fork restart. Nat Rev Mol Cell Biol 11: 683-687.

224. Michel B (2000) Replication fork arrest and DNA recombination. Trends Biochem Sci 25: 173-178.

225. Ralf C, Hickson ID, Wu L (2006) The Bloom's syndrome helicase can promote the regression of a model replication fork. J Biol Chem 281: 22839-22846.

226. Machwe A, Xiao L, Groden J, Orren DK (2006) The Werner and Bloom syndrome proteins catalyze regression of a model replication fork. Biochemistry 45: 13939-13946.

227. Machwe A, Karale R, Xu X, Liu Y, Orren DK (2011) The Werner and Bloom syndrome proteins help resolve replication blockage by converting (regressed) holliday junctions to functional replication forks. Biochemistry 50: 6774-6788.

228. De Haro LP, Wray J, Williamson EA, Durant ST, Corwin L, et al. (2010) Metnase promotes restart and repair of stalled and collapsed replication forks. Nucleic Acids Res 38: 5681-5691.

229. Sonoda E, Sasaki MS, Morrison C, Yamaguchi-Iwai Y, Takata M, et al. (1999) Sister chromatid exchanges are mediated by homologous recombination in vertebrate cells. Mol Cell Biol 19: 5166-5169.

230. Zhang J, Willers H, Feng Z, Ghosh JC, Kim S, et al. (2004) Chk2 phosphorylation of BRCA1 regulates DNA double-strand break repair. Mol Cell Biol 24: 708-718.

231. Johnson RD, Liu N, Jasin M (1999) Mammalian XRCC2 promotes the repair of DNA double-strand breaks by homologous recombination. Nature 401: 397-399.

232. Pierce AJ, Johnson RD, Thompson LH, Jasin M (1999) XRCC3 promotes homology-directed repair of DNA damage in mammalian cells. Genes Dev 13: 2633-2638.

233. Hendricks CA, Almeida KH, Stitt MS, Jonnalagadda VS, Rugo RE, et al. (2003) Spontaneous mitotic homologous recombination at an enhanced yellow fluorescent protein (EYFP) cDNA direct repeat in transgenic mice. Proc Natl Acad Sci U S A 100: 6325-6330.

234. Kovalchuk O, Hendricks CA, Cassie S, Engelward AJ, Engelward BP (2004) In vivo recombination after chronic damage exposure falls to below spontaneous levels in "recombomice". Mol Cancer Res 2: 567-573.

235. Wiktor-Brown DM, Hendricks CA, Olipitz W, Engelward BP (2006) Age-dependent accumulation of recombinant cells in the mouse pancreas revealed by in situ fluorescence imaging. Proc Natl Acad Sci U S A 103: 11862-11867.

236. Wiktor-Brown DM, Hendricks CA, Olipitz W, Rogers AB, Engelward BP (2006) Applications of fluorescence for detecting rare sequence rearrangements in vivo. Cell Cycle 5: 2715-2719.

237. Brilliant MH, Gondo Y, Eicher EM (1991) Direct molecular identification of the mouse pink-eyed unstable mutation by genome scanning. Science 252: 566-569.

238. Gondo Y, Gardner JM, Nakatsu Y, Durham-Pierre D, Deveau SA, et al. (1993) High-frequency genetic reversion mediated by a DNA duplication: the mouse pink-eyed unstable mutation. Proc Natl Acad Sci U S A 90: 297-301.

239. Schiestl RH, Aubrecht J, Khogali F, Carls N (1997) Carcinogens induce reversion of the mouse pink-eyed unstable mutation. Proc Natl Acad Sci U S A 94: 4576-4581.

240. Searle AG (1977) The use of pigment loci for detecting reverse mutations in somatic cells of mice. Arch Toxicol 38: 105-108.

241. Deol MS, Truslove GM (1983) The effects of the pink-eyed unstable gene on the retinal pigment epithelium of the mouse. J Embryol Exp Morphol 78: 291-298.

242. Bodenstein L, Sidman RL (1987) Growth and development of the mouse retinal pigment epithelium. I. Cell and tissue morphometrics and topography of mitotic activity. Dev Biol 121: 192-204.

243. Schiestl RH, Khogali F, Carls N (1994) Reversion of the mouse pink-eyed unstable mutation induced by low doses of x-rays. Science 266: 1573-1576.

244. Jalili T, Murthy GG, Schiestl RH (1998) Cigarette smoke induces DNA deletions in the mouse embryo. Cancer Res 58: 2633-2638.

245. Bishop AJ, Kosaras B, Sidman RL, Schiestl RH (2000) Benzo(a)pyrene and X-rays induce reversions of the pink-eyed unstable mutation in the retinal pigment epithelium of mice. Mutat Res 457: 31-40.

246. Bishop AJ, Barlow C, Wynshaw-Boris AJ, Schiestl RH (2000) Atm deficiency causes an increased frequency of intrachromosomal homologous recombination in mice. Cancer Res 60: 395-399.

247. Bishop AJ, Hollander MC, Kosaras B, Sidman RL, Fornace AJ, Jr., et al. (2003) Atm-, p53-, and Gadd45a-deficient mice show an increased frequency of homologous recombination at different stages during development. Cancer Res 63: 5335-5343.

248. Brown AD, Claybon AB, Bishop AJ (2011) A conditional mouse model for measuring the frequency of homologous recombination events in vivo in the absence of essential genes. Mol Cell Biol 31: 3593-3602.

249. Brown AD, Claybon AB, Bishop AJ (2010) Mouse WRN Helicase Domain Is Not Required for Spontaneous Homologous Recombination-Mediated DNA Deletion. J Nucleic Acids 2010.

250. Claybon A, Karia B, Bruce C, Bishop AJ (2010) PARP1 suppresses homologous recombination events in mice in vivo. Nucleic Acids Res 38: 7538-7545.

251. Bodenstein L, Sidman RL (1987) Growth and development of the mouse retinal pigment epithelium. II. Cell patterning in experimental chimaeras and mosaics. Dev Biol 121: 205-219.

252. Bishop AJ, Kosaras B, Carls N, Sidman RL, Schiestl RH (2001) Susceptibility of proliferating cells to benzo[a]pyrene-induced homologous recombination in mice. Carcinogenesis 22: 641-649.

253. Levine AJ (1997) p53, the cellular gatekeeper for growth and division. Cell 88: 323-331.

254. Agarwal ML, Taylor WR, Chernov MV, Chernova OB, Stark GR (1998) The p53 network. J Biol Chem 273: 1-4.

255. Wang XW, Yeh H, Schaeffer L, Roy R, Moncollin V, et al. (1995) p53 modulation of TFIIH-associated nucleotide excision repair activity. Nat Genet 10: 188-195.

256. Offer H, Wolkowicz R, Matas D, Blumenstein S, Livneh Z, et al. (1999) Direct involvement of p53 in the base excision repair pathway of the DNA repair machinery. FEBS Lett 450: 197-204.

257. Willers H, McCarthy EE, Alberti W, Dahm-Daphi J, Powell SN (2000) Loss of wild-type p53 function is responsible for upregulated homologous recombination in immortal rodent fibroblasts. Int J Radiat Biol 76: 1055-1062.

258. Gebow D, Miselis N, Liber HL (2000) Homologous and nonhomologous recombination resulting in deletion: effects of p53 status, microhomology, and repetitive DNA length and orientation. Mol Cell Biol 20: 4028-4035.

259. Livingstone LR, White A, Sprouse J, Livanos E, Jacks T, et al. (1992) Altered cell cycle arrest and gene amplification potential accompany loss of wild-type p53. Cell 70: 923-935.

260. Yin Y, Tainsky MA, Bischoff FZ, Strong LC, Wahl GM (1992) Wild-type p53 restores cell cycle control and inhibits gene amplification in cells with mutant p53 alleles. Cell 70: 937-948.

261. Buchhop S, Gibson MK, Wang XW, Wagner P, Sturzbecher HW, et al. (1997) Interaction of p53 with the human Rad51 protein. Nucleic Acids Res 25: 3868-3874.

262. Purdie CA, Harrison DJ, Peter A, Dobbie L, White S, et al. (1994) Tumour incidence, spectrum and ploidy in mice with a large deletion in the p53 gene. Oncogene 9: 603-609.

263. Donehower LA, Godley LA, Aldaz CM, Pyle R, Shi YP, et al. (1995) Deficiency of p53 accelerates mammary tumorigenesis in Wnt-1 transgenic mice and promotes chromosomal instability. Genes Dev 9: 882-895.

264. Aubrecht J, Secretan MB, Bishop AJ, Schiestl RH (1999) Involvement of p53 in X-ray induced intrachromosomal recombination in mice. Carcinogenesis 20: 2229-2236.

265. Zhang H, Somasundaram K, Peng Y, Tian H, Zhang H, et al. (1998) BRCA1 physically associates with p53 and stimulates its transcriptional activity. Oncogene 16: 1713-1721.

266. Marmorstein LY, Ouchi T, Aaronson SA (1998) The BRCA2 gene product functionally interacts with p53 and RAD51. Proc Natl Acad Sci U S A 95: 13869-13874.

267. Yang Q, Zhang R, Wang XW, Spillare EA, Linke SP, et al. (2002) The processing of Holliday junctions by BLM and WRN helicases is regulated by p53. J Biol Chem 277: 31980-31987.

268. Restle A, Janz C, Wiesmuller L (2005) Differences in the association of p53 phosphorylated on serine 15 and key enzymes of homologous recombination. Oncogene 24: 4380-4387.

269. Saintigny Y, Rouillard D, Chaput B, Soussi T, Lopez BS (1999) Mutant p53 proteins stimulate spontaneous and radiation-induced intrachromosomal homologous recombination independently of the alteration of the transactivation activity and of the G1 checkpoint. Oncogene 18: 3553-3563.

270. Akyuz N, Boehden GS, Susse S, Rimek A, Preuss U, et al. (2002) DNA substrate dependence of p53-mediated regulation of double-strand break repair. Mol Cell Biol 22: 6306-6317.

271. Hopfner KP, Craig L, Moncalian G, Zinkel RA, Usui T, et al. (2002) The Rad50 zinc-hook is a structure joining Mre11 complexes in DNA recombination and repair. Nature 418: 562-566.

272. Krejci L, Chen L, Van Komen S, Sung P, Tomkinson A (2003) Mending the break: two DNA double-strand break repair machines in eukaryotes. Prog Nucleic Acid Res Mol Biol 74: 159-201.

273. West SC (2003) Molecular views of recombination proteins and their control. Nat Rev Mol Cell Biol 4: 435-445.

274. Subramanian D, Griffith JD (2002) Interactions between p53, hMSH2-hMSH6 and HMG I(Y) on Holliday junctions and bulged bases. Nucleic Acids Res 30: 2427-2434.

275. Davalos AR, Campisi J (2003) Bloom syndrome cells undergo p53-dependent apoptosis and delayed assembly of BRCA1 and NBS1 repair complexes at stalled replication forks. J Cell Biol 162: 1197-1209.

276. Sengupta S, Linke SP, Pedeux R, Yang Q, Farnsworth J, et al. (2003) BLM helicase-dependent transport of p53 to sites of stalled DNA replication forks modulates homologous recombination. EMBO J 22: 1210-1222.

277. Zhivotovsky B, Kroemer G (2004) Apoptosis and genomic instability. Nat Rev Mol Cell Biol 5: 752-762.

278. Arias-Lopez C, Lazaro-Trueba I, Kerr P, Lord CJ, Dexter T, et al. (2006) p53 modulates homologous recombination by transcriptional regulation of the RAD51 gene. EMBO Rep 7: 219-224.

279. Ivanov A, Cragg MS, Erenpreisa J, Emzinsh D, Lukman H, et al. (2003) Endopolyploid cells produced after severe genotoxic damage have the potential to repair DNA double strand breaks. J Cell Sci 116: 4095-4106.

280. Meyn MS, Strasfeld L, Allen C (1994) Testing the role of p53 in the expression of genetic instability and apoptosis in ataxia-telangiectasia. Int J Radiat Biol 66: S141-149.

281. Mekeel KL, Tang W, Kachnic LA, Luo CM, DeFrank JS, et al. (1997) Inactivation of p53 results in high rates of homologous recombination. Oncogene 14: 1847-1857.

282. Bertrand P, Rouillard D, Boulet A, Levalois C, Soussi T, et al. (1997) Increase of spontaneous intrachromosomal homologous recombination in mammalian cells expressing a mutant p53 protein. Oncogene 14: 1117-1122.

283. Wiesmuller L, Cammenga J, Deppert WW (1996) In vivo assay of p53 function in homologous recombination between simian virus 40 chromosomes. J Virol 70: 737-744.

284. Xia RY, Luo YX, Wang TP (1994) Operational techniques and combination treatment for the recurrent sacro-coccygeal tumor. J Tongji Med Univ 14: 245-248.

285. Willers H, McCarthy EE, Wu B, Wunsch H, Tang W, et al. (2000) Dissociation of p53-mediated suppression of homologous recombination from G1/S cell cycle checkpoint control. Oncogene 19: 632-639.

286. Thomas AJ, Erickson CA (2008) The making of a melanocyte: the specification of melanoblasts from the neural crest. Pigment Cell Melanoma Res 21: 598-610.

287. Mayer TC (1973) The migratory pathway of neural crest cells into the skin of mouse embryos. Dev Biol 34: 39-46.

288. Bronner-Fraser M (1995) Origins and developmental potential of the neural crest. Exp Cell Res 218: 405-417.

289. Romanova LY, Willers H, Blagosklonny MV, Powell SN (2004) The interaction of p53 with replication protein A mediates suppression of homologous recombination. Oncogene 23: 9025-9033.

290. Willers H, McCarthy EE, Hubbe P, Dahm-Daphi J, Powell SN (2001) Homologous recombination in extrachromosomal plasmid substrates is not suppressed by p53. Carcinogenesis 22: 1757-1763.

291. Tang W, Willers H, Powell SN (1999) p53 directly enhances rejoining of DNA double-strand breaks with cohesive ends in gamma-irradiated mouse fibroblasts. Cancer Res 59: 2562-2565.

292. Restle A, Farber M, Baumann C, Bohringer M, Scheidtmann KH, et al. (2008) Dissecting the role of p53 phosphorylation in homologous recombination provides new clues for gain-of-function mutants. Nucleic Acids Res 36: 5362-5375.

293. Keimling M, Wiesmuller L (2009) DNA double-strand break repair activities in mammary epithelial cells--influence of endogenous p53 variants. Carcinogenesis 30: 1260-1268.

294. Yoon D, Wang Y, Stapleford K, Wiesmuller L, Chen J (2004) P53 inhibits strand exchange and replication fork regression promoted by human Rad51. J Mol Biol 336: 639-654.

295. Schallreuter KU, Kothari S, Chavan B, Spencer JD (2008) Regulation of melanogenesis--controversies and new concepts. Exp Dermatol 17: 395-404.

296. Yamaguchi Y, Brenner M, Hearing VJ (2007) The regulation of skin pigmentation. J Biol Chem 282: 27557-27561.

297. Lee ST, Nicholls RD, Bundey S, Laxova R, Musarella M, et al. (1994) Mutations of the P gene in oculocutaneous albinism, ocular albinism, and Prader-Willi syndrome plus albinism. N Engl J Med 330: 529-534.

298. Fridman C, Hosomi N, Varela MC, Souza AH, Fukai K, et al. (2003) Angelman syndrome associated with oculocutaneous albinism due to an intragenic deletion of the P gene. Am J Med Genet A 119A: 180-183.

299. Gardner JM, Nakatsu Y, Gondo Y, Lee S, Lyon MF, et al. (1992) The mouse pink-eyed dilution gene: association with human Prader-Willi and Angelman syndromes. Science 257: 1121-1124.

300. Rosemblat S, Sviderskaya EV, Easty DJ, Wilson A, Kwon BS, et al. (1998) Melanosomal defects in melanocytes from mice lacking expression of the pink-eyed dilution gene: correction by culture in the presence of excess tyrosine. Exp Cell Res 239: 344-352.

301. Gahl WA, Potterf B, Durham-Pierre D, Brilliant MH, Hearing VJ (1995) Melanosomal tyrosine transport in normal and pink-eyed dilution murine melanocytes. Pigment Cell Res 8: 229-233.

302. Lamoreux ML, Zhou BK, Rosemblat S, Orlow SJ (1995) The pinkeyed-dilution protein and the eumelanin/pheomelanin switch: in support of a unifying hypothesis. Pigment Cell Res 8: 263-270.

303. Manga P, Orlow SJ (2001) Inverse correlation between pink-eyed dilution protein expression and induction of melanogenesis by bafilomycin A1. Pigment Cell Res 14: 362-367.

304. Staleva L, Manga P, Orlow SJ (2002) Pink-eyed dilution protein modulates arsenic sensitivity and intracellular glutathione metabolism. Mol Biol Cell 13: 4206-4220.

305. Benedetto JP, Ortonne JP, Voulot C, Khatchadourian C, Prota G, et al. (1981) Role of thiol compounds in mammalian melanin pigmentation: Part I. Reduced and oxidized glutathione. J Invest Dermatol 77: 402-405.

306. Benedetto JP, Ortonne JP, Voulot C, Khatchadourian C, Prota G, et al. (1982) Role of thiol compounds in mammalian melanin pigmentation. II. Glutathione and related enzymatic activities. J Invest Dermatol 79: 422-424.

307. Jara JR, Aroca P, Solano F, Martinez JH, Lozano JA (1988) The role of sulfhydryl compounds in mammalian melanogenesis: the effect of cysteine and glutathione upon tyrosinase and the intermediates of the pathway. Biochim Biophys Acta 967: 296-303.

308. Simo R, Villarroel M, Corraliza L, Hernandez C, Garcia-Ramirez M (2010) The retinal pigment epithelium: something more than a constituent of the blood-retinal barrier--implications for the pathogenesis of diabetic retinopathy. J Biomed Biotechnol 2010: 190724.

309. Levy-Clarke G, Ding X, Gangaputra S, Yeh S, Goodglick T, et al. (2009) Recalcitrant granulomatous sclerouveitis in a patient with granulomatous ANCA-associated vasculitis. Ocul Immunol Inflamm 17: 83-87.

310. Oakey RJ, Keiper NM, Ching AS, Brilliant MH (1996) Molecular analysis of the cDNAs encoded by the pun and pJ alleles of the pink-eyed dilution locus. Mamm Genome 7: 315-316.

311. Gotow T, Hashimoto PH (1979) Fine structure of the ependyma and intercellular junctions in the area postrema of the rat. Cell Tissue Res 201: 207-225.

312. Bishop AJ, Schiestl RH (2001) Homologous recombination as a mechanism of carcinogenesis. Biochim Biophys Acta 1471: M109-121.

313. Bunting SF, Callen E, Wong N, Chen HT, Polato F, et al. (2010) 53BP1 inhibits homologous recombination in Brca1-deficient cells by blocking resection of DNA breaks. Cell 141: 243-254.

314. Cao L, Xu X, Bunting SF, Liu J, Wang RH, et al. (2009) A selective requirement for 53BP1 in the biological response to genomic instability induced by Brca1 deficiency. Mol Cell 35: 534-541.

315. Deka N, Wong E, Matera AG, Kraft R, Leinwand LA, et al. (1988) Repetitive nucleotide sequence insertions into a novel calmodulin-related gene and its processed pseudogene. Gene 71: 123-134.

316. Reliene R, Schiestl RH (2003) Mouse models for induced genetic instability at endogenous loci. Oncogene 22: 7000-7010.

317. Claybon A, Bishop AJ (2011) Dissection of a mouse eye for a whole mount of the retinal pigment epithelium. J Vis Exp.

318. Kirkland DJ, Aardema M, Banduhn N, Carmichael P, Fautz R, et al. (2007) In vitro approaches to develop weight of evidence (WoE) and mode of action (MoA) discussions with positive in vitro genotoxicity results. Mutagenesis 22: 161-175.

319. Maher RL, Branagan AM, Morrical SW (2011) Coordination of DNA replication and recombination activities in the maintenance of genome stability. J Cell Biochem 112: 2672-2682.

320. McVean G (2010) What drives recombination hotspots to repeat DNA in humans? Philos Trans R Soc Lond B Biol Sci 365: 1213-1218.

321. Redon R, Ishikawa S, Fitch KR, Feuk L, Perry GH, et al. (2006) Global variation in copy number in the human genome. Nature 444: 444-454.

322. Stankiewicz P, Lupski JR (2002) Genome architecture, rearrangements and genomic disorders. Trends Genet 18: 74-82.

323. Rosemblat S, Durham-Pierre D, Gardner JM, Nakatsu Y, Brilliant MH, et al. (1994) Identification of a melanosomal membrane protein encoded by the pink-eyed dilution (type II oculocutaneous albinism) gene. Proc Natl Acad Sci U S A 91: 12071-12075.

324. Reliene R, Bishop AJ, Aubrecht J, Schiestl RH (2004) In vivo DNA deletion assay to detect environmental and genetic predisposition to cancer. Methods Mol Biol 262: 125-139.

325. Rosenberg B (1975) Possible mechanisms for the antitumor activity of platinum coordination complexes. Cancer Chemother Rep 59: 589-598.

326. Magee PN (1966) Plant toxins and human disease. Naturally occurring alkylating agents. Proc R Soc Med 59: 751-755.

327. Szabo C, Dawson VL (1998) Role of poly(ADP-ribose) synthetase in inflammation and ischaemia-reperfusion. Trends Pharmacol Sci 19: 287-298.

328. Bryant HE, Schultz N, Thomas HD, Parker KM, Flower D, et al. (2005) Specific killing of BRCA2-deficient tumours with inhibitors of poly(ADP-ribose) polymerase. Nature 434: 913-917.

329. Farmer H, McCabe N, Lord CJ, Tutt AN, Johnson DA, et al. (2005) Targeting the DNA repair defect in BRCA mutant cells as a therapeutic strategy. Nature 434: 917-921.

330. Li S (2009) Inhibition of poly(ADP-ribose) polymerase in BRCA mutation carriers. N Engl J Med 361: 1707; author reply 1707-1708.

331. Burden DA, Osheroff N (1998) Mechanism of action of eukaryotic topoisomerase II and drugs targeted to the enzyme. Biochim Biophys Acta 1400: 139-154.

332. Hsiang YH, Lihou MG, Liu LF (1989) Arrest of replication forks by drug-stabilized topoisomerase I-DNA cleavable complexes as a mechanism of cell killing by camptothecin. Cancer Res 49: 5077-5082.

333. Pommier Y (2006) Topoisomerase I inhibitors: camptothecins and beyond. Nat Rev Cancer 6: 789-802.

334. Madaan K, Kaushik D, Verma T (2012) Hydroxyurea: a key player in cancer chemotherapy. Expert Rev Anticancer Ther 12: 19-29.

335. Yarbro JW (1992) Mechanism of action of hydroxyurea. Semin Oncol 19: 1-10.

336. Lebel M (2002) Increased frequency of DNA deletions in pink-eyed unstable mice carrying a mutation in the Werner syndrome gene homologue. Carcinogenesis 23: 213-216.

337. Memisoglu A, Samson L (2000) Contribution of base excision repair, nucleotide excision repair, and DNA recombination to alkylation resistance of the fission yeast Schizosaccharomyces pombe. J Bacteriol 182: 2104-2112.

338. Brilliant MH (2001) The mouse p (pink-eyed dilution) and human P genes, oculocutaneous albinism type 2 (OCA2), and melanosomal pH. Pigment Cell Res 14: 86-93.

339. Mir O, Berveiller P, Ropert S, Goffinet F, Goldwasser F (2008) Use of platinum derivatives during pregnancy. Cancer 113: 3069-3074.

340. Trenz K, Lugowski S, Jahrsdorfer U, Jainta S, Vogel W, et al. (2003) Enhanced sensitivity of peripheral blood lymphocytes from women carrying a BRCA1 mutation towards the mutagenic effects of various cytostatics. Mutat Res 544: 279-288.

341. Kaina B (2004) Mechanisms and consequences of methylating agent-induced SCEs and chromosomal aberrations: a long road traveled and still a far way to go. Cytogenet Genome Res 104: 77-86.

342. Neft RE, Conner MK (1989) Induction of sister chromatid exchange in multiple murine tissues in vivo by various methylating agents. Teratog Carcinog Mutagen 9: 219-237.

343. Hellgren D, Sahlen S, Lambert B (1989) Mutagen-induced recombination between stably integrated neo gene fragments in CHO and EM9 cells. Mutat Res 226: 1-8.

344. Durkacz BW, Omidiji O, Gray DA, Shall S (1980) (ADP-ribose)n participates in DNA excision repair. Nature 283: 593-596.

345. Zaremba T, Curtin NJ (2007) PARP inhibitor development for systemic cancer targeting. Anticancer Agents Med Chem 7: 515-523.

346. Haince JF, McDonald D, Rodrigue A, Dery U, Masson JY, et al. (2008) PARP1-dependent kinetics of recruitment of MRE11 and NBS1 proteins to multiple DNA damage sites. J Biol Chem 283: 1197-1208.

347. Haince JF, Kozlov S, Dawson VL, Dawson TM, Hendzel MJ, et al. (2007) Ataxia telangiectasia mutated (ATM) signaling network is modulated by a novel poly(ADP-ribose)-dependent pathway in the early response to DNA-damaging agents. J Biol Chem 282: 16441-16453.

348. Schwartz JL, Morgan WF, Kapp LN, Wolff S (1983) Effects of 3-aminobenzamide on DNA synthesis and cell cycle progression in Chinese hamster ovary cells. Exp Cell Res 143: 377-382.

349. Natarajan AT, Csukas I, van Zeeland AA (1981) Contribution of incorporated 5-bromodeoxyuridine in DNA to the frequencies of sister-chromatid exchanges induced by inhibitors of poly-(ADP-ribose)-polymerase. Mutat Res 84: 125-132.

350. Noel G, Giocanti N, Fernet M, Megnin-Chanet F, Favaudon V (2003) Poly(ADP-ribose) polymerase (PARP-1) is not involved in DNA double-strand break recovery. BMC Cell Biol 4: 7.

351. Haber JE (1999) DNA recombination: the replication connection. Trends Biochem Sci 24: 271-275.

352. Suzuki K, Yamashita S (2012) Low-dose radiation exposure and carcinogenesis. Jpn J Clin Oncol 42: 563-568.

353. Yoshimoto Y, Kato H, Schull WJ (1988) Risk of cancer among children exposed in utero to A-bomb radiations, 1950-84. Lancet 2: 665-669.

354. Povirk LF (1996) DNA damage and mutagenesis by radiomimetic DNA-cleaving agents: bleomycin, neocarzinostatin and other enediynes. Mutat Res 355: 71-89.

355. Obe G, Schunck C, Johannes C (1994) Induction of sister-chromatid exchanges by AluI, DNase I, benzon nuclease and bleomycin in Chinese hamster ovary (CHO) cells. Mutat Res 307: 315-321.

356. Rogakou EP, Pilch DR, Orr AH, Ivanova VS, Bonner WM (1998) DNA double-stranded breaks induce histone H2AX phosphorylation on serine 139. J Biol Chem 273: 5858-5868.

357. Hashimoto H, Chatterjee S, Berger NA (1995) Inhibition of etoposide (VP-16)-induced DNA recombination and mutant frequency by Bcl-2 protein overexpression. Cancer Res 55: 4029-4035.

358. Ribas G, Xamena N, Creus A, Marcos R (1996) Sister-chromatid exchanges (SCE) induction by inhibitors of DNA topoisomerases in cultured human lymphocytes. Mutat Res 368: 205-211.

359. Sykes PJ, Hooker AM, Morley AA (1999) Inversion due to intrachromosomal recombination produced by carcinogens in a transgenic mouse model. Mutat Res 427: 1-9.

360. Matsuoka M, Nagawa F, Okazaki K, Kingsbury L, Yoshida K, et al. (1991) Detection of somatic DNA recombination in the transgenic mouse brain. Science 254: 81-86.

361. Huang CC, Han CS, Yue XF, Shen CM, Wang SW, et al. (1983) Cytotoxicity and sister chromatid exchanges induced in vitro by six anticancer drugs developed in the People's Republic of China. J Natl Cancer Inst 71: 841-847.

362. Lim M, Liu LF, Jacobson-Kram D, Williams JR (1986) Induction of sister chromatid exchanges by inhibitors of topoisomerases. Cell Biol Toxicol 2: 485-494.

363. Degrassi F, De Salvia R, Tanzarella C, Palitti F (1989) Induction of chromosomal aberrations and SCE by camptothecin, an inhibitor of mammalian topoisomerase I. Mutat Res 211: 125-130.

364. Zhao JH, Tohda H, Oikawa A (1992) Camptothecin-induced sister-chromatid exchange dependent on the presence of bromodeoxyuridine and the phase of the cell cycle. Mutat Res 282: 49-54.

365. Pinero J, Lopez Baena M, Ortiz T, Cortes F (1996) Sister chromatid exchange induced by DNA topoisomerases poisons in late replicating heterochromatin: influence of inhibition of replication and transcription. Mutat Res 354: 195-201.

366. Zhang LH, Jenssen D (1994) Studies on intrachromosomal recombination in SP5/V79 Chinese hamster cells upon exposure to different agents related to carcinogenesis. Carcinogenesis 15: 2303-2310.

367. Morham SG, Kluckman KD, Voulomanos N, Smithies O (1996) Targeted disruption of the mouse topoisomerase I gene by camptothecin selection. Mol Cell Biol 16: 6804-6809.

368. Bester AC, Roniger M, Oren YS, Im MM, Sarni D, et al. (2011) Nucleotide deficiency promotes genomic instability in early stages of cancer development. Cell 145: 435-446.

369. Chabosseau P, Buhagiar-Labarchede G, Onclercq-Delic R, Lambert S, Debatisse M, et al. (2011) Pyrimidine pool imbalance induced by BLM helicase deficiency contributes to genetic instability in Bloom syndrome. Nat Commun 2: 368.

370. Mathews CK (2006) DNA precursor metabolism and genomic stability. FASEB J 20: 1300-1314.

371. Matsuoka A, Lundin C, Johansson F, Sahlin M, Fukuhara K, et al. (2004) Correlation of sister chromatid exchange formation through homologous recombination with ribonucleotide reductase inhibition. Mutat Res 547: 101-107.

372. Lundin C, Erixon K, Arnaudeau C, Schultz N, Jenssen D, et al. (2002) Different roles for nonhomologous end joining and homologous recombination following replication arrest in mammalian cells. Mol Cell Biol 22: 5869-5878.

373. Hueber A, Esser P, Heimann K, Kociok N, Winter S, et al. (1998) The topoisomerase I inhibitors, camptothecin and beta-lapachone, induce apoptosis of human retinal pigment epithelial cells. Exp Eye Res 67: 525-530.

374. Holm C, Covey JM, Kerrigan D, Pommier Y (1989) Differential requirement of DNA replication for the cytotoxicity of DNA topoisomerase I and II inhibitors in Chinese hamster DC3F cells. Cancer Res 49: 6365-6368.

375. Mackenzie MA, Jordan SA, Budd PS, Jackson IJ (1997) Activation of the receptor tyrosine kinase Kit is required for the proliferation of melanoblasts in the mouse embryo. Dev Biol 192: 99-107.

376. Aguilera A, Garcia-Muse T (2012) R loops: from transcription byproducts to threats to genome stability. Mol Cell 46: 115-124.

377. Davies SL, North PS, Hickson ID (2007) Role for BLM in replication-fork restart and suppression of origin firing after replicative stress. Nat Struct Mol Biol 14: 677-679.

378. Rao VA, Fan AM, Meng L, Doe CF, North PS, et al. (2005) Phosphorylation of BLM, dissociation from topoisomerase IIIalpha, and colocalization with gamma-H2AX after topoisomerase I-induced replication damage. Mol Cell Biol 25: 8925-8937.

379. Tomatis L (1989) Overview of perinatal and multigeneration carcinogenesis. IARC Sci Publ: 1-15.

380. Anderson LM, Diwan BA, Fear NT, Roman E (2000) Critical windows of exposure for children's health: cancer in human epidemiological studies and neoplasms in experimental animal models. Environ Health Perspect 108 Suppl 3: 573-594.

381. Perera F, Hemminki K, Jedrychowski W, Whyatt R, Campbell U, et al. (2002) In utero DNA damage from environmental pollution is associated with somatic gene mutation in newborns. Cancer Epidemiol Biomarkers Prev 11: 1134-1137.

382. Bocskay KA, Tang D, Orjuela MA, Liu X, Warburton DP, et al. (2005) Chromosomal aberrations in cord blood are associated with prenatal exposure to carcinogenic polycyclic aromatic hydrocarbons. Cancer Epidemiol Biomarkers Prev 14: 506-511.

383. Edwards SC, Jedrychowski W, Butscher M, Camann D, Kieltyka A, et al. (2010) Prenatal exposure to airborne polycyclic aromatic hydrocarbons and children's intelligence at 5 years of age in a prospective cohort study in Poland. Environ Health Perspect 118: 1326-1331.

384. Paashuis-Lew YR, Heddle JA (1998) Spontaneous mutation during fetal development and post-natal growth. Mutagenesis 13: 613-617.

385. Doll R, Wakeford R (1997) Risk of childhood cancer from fetal irradiation. Br J Radiol 70: 130-139.

386. Selevan SG, Kimmel CA, Mendola P (2000) Identifying critical windows of exposure for children's health. Environ Health Perspect 108 Suppl 3: 451-455.

387. Olshan AF, Anderson L, Roman E, Fear N, Wolff M, et al. (2000) Workshop to identify critical windows of exposure for children's health: cancer work group summary. Environ Health Perspect 108 Suppl 3: 595-597.

388. Birnbaum LS, Fenton SE (2003) Cancer and developmental exposure to endocrine disruptors. Environ Health Perspect 111: 389-394.

389. Giaccia AJ, Kastan MB (1998) The complexity of p53 modulation: emerging patterns from divergent signals. Genes Dev 12: 2973-2983.

390. Ko LJ, Prives C (1996) p53: puzzle and paradigm. Genes Dev 10: 1054-1072.

391. Lane DP (1992) Worrying about p53. Curr Biol 2: 581-583.

392. Sherr CJ (1996) Cancer cell cycles. Science 274: 1672-1677.

393. Taylor WR, Stark GR (2001) Regulation of the G2/M transition by p53. Oncogene 20: 1803-1815.

394. Malkin D, Li FP, Strong LC, Fraumeni JF, Jr., Nelson CE, et al. (1990) Germ line p53 mutations in a familial syndrome of breast cancer, sarcomas, and other neoplasms. Science 250: 1233-1238.

395. Donehower LA, Harvey M, Slagle BL, McArthur MJ, Montgomery CA, Jr., et al. (1992) Mice deficient for p53 are developmentally normal but susceptible to spontaneous tumours. Nature 356: 215-221.

396. Jacks T, Remington L, Williams BO, Schmitt EM, Halachmi S, et al. (1994) Tumor spectrum analysis in p53-mutant mice. Curr Biol 4: 1-7.

397. Nishino H, Knoll A, Buettner VL, Frisk CS, Maruta Y, et al. (1995) p53 wild-type and p53 nullizygous Big Blue transgenic mice have similar frequencies and patterns of observed mutation in liver, spleen and brain. Oncogene 11: 263-270.

398. Buettner VL, Nishino H, Haavik J, Knoll A, Hill K, et al. (1997) Spontaneous mutation frequencies and spectra in p53 (+/+) and p53 (-/-) mice: a test of the 'guardian of the genome' hypothesis in the Big Blue transgenic mouse mutation detection system. Mutat Res 379: 13-20.

399. Sands AT, Suraokar MB, Sanchez A, Marth JE, Donehower LA, et al. (1995) p53 deficiency does not affect the accumulation of point mutations in a transgene target. Proc Natl Acad Sci U S A 92: 8517-8521.

400. Greenblatt MS, Bennett WP, Hollstein M, Harris CC (1994) Mutations in the p53 tumor suppressor gene: clues to cancer etiology and molecular pathogenesis. Cancer Res 54: 4855-4878.

401. Liu G, Parant JM, Lang G, Chau P, Chavez-Reyes A, et al. (2004) Chromosome stability, in the absence of apoptosis, is critical for suppression of tumorigenesis in Trp53 mutant mice. Nat Genet 36: 63-68.

402. Albrechtsen N, Dornreiter I, Grosse F, Kim E, Wiesmuller L, et al. (1999) Maintenance of genomic integrity by p53: complementary roles for activated and non-activated p53. Oncogene 18: 7706-7717.

403. Bertrand P, Saintigny Y, Lopez BS (2004) p53's double life: transactivation-independent repression of homologous recombination. Trends Genet 20: 235-243.

404. Sengupta S, Harris CC (2005) p53: traffic cop at the crossroads of DNA repair and recombination. Nat Rev Mol Cell Biol 6: 44-55.

405. Gatz SA, Wiesmuller L (2006) p53 in recombination and repair. Cell Death Differ 13: 1003-1016.

406. Helleday T, Lo J, van Gent DC, Engelward BP (2007) DNA double-strand break repair: from mechanistic understanding to cancer treatment. DNA Repair (Amst) 6: 923-935.

407. Chaganti RS, Schonberg S, German J (1974) A manyfold increase in sister chromatid exchanges in Bloom's syndrome lymphocytes. Proc Natl Acad Sci U S A 71: 4508-4512.

408. Roy R, Chun J, Powell SN (2012) BRCA1 and BRCA2: different roles in a common pathway of genome protection. Nat Rev Cancer 12: 68-78.

409. Agam A, Yalcin B, Bhomra A, Cubin M, Webber C, et al. (2010) Elusive copy number variation in the mouse genome. PLoS One 5: e12839.

410. Bolstad BM, Irizarry RA, Astrand M, Speed TP (2003) A comparison of normalization methods for high density oligonucleotide array data based on variance and bias. Bioinformatics 19: 185-193.

411. Iwabuchi K, Li B, Massa HF, Trask BJ, Date T, et al. (1998) Stimulation of p53-mediated transcriptional activation by the p53-binding proteins, 53BP1 and 53BP2. J Biol Chem 273: 26061-26068.

412. Prives C, Hall PA (1999) The p53 pathway. J Pathol 187: 112-126.

413. Vousden KH, Lu X (2002) Live or let die: the cell's response to p53. Nat Rev Cancer 2: 594-604.

414. Vousden KH, Prives C (2009) Blinded by the Light: The Growing Complexity of p53. Cell 137: 413-431.

415. Linke SP, Sengupta S, Khabie N, Jeffries BA, Buchhop S, et al. (2003) p53 interacts with hRAD51 and hRAD54, and directly modulates homologous recombination. Cancer Res 63: 2596-2605.

416. Roy S, Musselman CA, Kachirskaia I, Hayashi R, Glass KC, et al. (2010) Structural insight into p53 recognition by the 53BP1 tandem Tudor domain. J Mol Biol 398: 489-496.

417. Cao L, Li W, Kim S, Brodie SG, Deng CX (2003) Senescence, aging, and malignant transformation mediated by p53 in mice lacking the Brca1 full-length isoform. Genes Dev 17: 201-213.

418. Cao L, Kim S, Xiao C, Wang RH, Coumoul X, et al. (2006) ATM-Chk2-p53 activation prevents tumorigenesis at an expense of organ homeostasis upon Brca1 deficiency. EMBO J 25: 2167-2177.

419. Iwabuchi K, Bartel PL, Li B, Marraccino R, Fields S (1994) Two cellular proteins that bind to wild-type but not mutant p53. Proc Natl Acad Sci U S A 91: 6098-6102.

420. Powell B, Soong R, Iacopetta B, Seshadri R, Smith DR (2000) Prognostic significance of mutations to different structural and functional regions of the p53 gene in breast cancer. Clin Cancer Res 6: 443-451.

421. Sirbu BM, Lachmayer SJ, Wulfing V, Marten LM, Clarkson KE, et al. (2011) ATR-p53 restricts homologous recombination in response to replicative stress but does not limit DNA interstrand crosslink repair in lung cancer cells. PLoS One 6: e23053.

422. Zink D, Mayr C, Janz C, Wiesmuller L (2002) Association of p53 and MSH2 with recombinative repair complexes during S phase. Oncogene 21: 4788-4800.

423. Scully R, Chen J, Plug A, Xiao Y, Weaver D, et al. (1997) Association of BRCA1 with Rad51 in mitotic and meiotic cells. Cell 88: 265-275.

424. Wu L, Davies SL, Levitt NC, Hickson ID (2001) Potential role for the BLM helicase in recombinational repair via a conserved interaction with RAD51. J Biol Chem 276: 19375-19381.

425. Ho CC, Siu WY, Lau A, Chan WM, Arooz T, et al. (2006) Stalled replication induces p53 accumulation through distinct mechanisms from DNA damage checkpoint pathways. Cancer Res 66: 2233-2241.

426. Trkova M, Hladikova M, Kasal P, Goetz P, Sedlacek Z (2002) Is there anticipation in the age at onset of cancer in families with Li-Fraumeni syndrome? J Hum Genet 47: 381-386.

427. O'Connor PM, Jackman J, Bae I, Myers TG, Fan S, et al. (1997) Characterization of the p53 tumor suppressor pathway in cell lines of the National Cancer Institute anticancer drug screen and correlations with the growth-inhibitory potency of 123 anticancer agents. Cancer Res 57: 4285-4300.

428. Dahm-Daphi J (2000) p53: biology and role for cellular radiosensitivity. Strahlenther Onkol 176: 278-285.

429. Lane DP, Cheok CF, Lain S (2010) p53-based cancer therapy. Cold Spring Harb Perspect Biol 2: a001222.

PARP1 suppresses homologous recombination events in mice *in vivo*

Alison Claybon[1,2], Bijal Karia[1,2], Crystal Bruce[3] and Alexander J. R. Bishop[1,2,*]

[1]Greehey Children's Cancer Research Institute, [2]Department of Cellular and Structural Biology, The University of Texas Health Science Center at San Antonio, San Antonio, TX 78229 and [3]Department of Biochemistry and Molecular Biology, Oklahoma State University, Stillwater, OK 74078, USA

ABSTRACT

Recent studies suggest that PARP1 inhibitors, several of which are currently in clinical trial, may selectively kill *BRCA1/2* mutant cancers cells. It is thought that the success of this therapy is based on immitigable lethal DNA damage in the cancer cells resultant from the concurrent loss or inhibition of two DNA damage repair pathways: single-strand break (SSB) repair and homologous recombination repair (HRR). Presumably, inhibition of PARP1 activity obstructs the repair of SSBs and during DNA replication, these lesions cause replication fork collapse and are transformed into substrates for HRR. In fact, several previous studies have indicated a hyper-recombinogenic phenotype in the absence of active PARP1 *in vitro* or in response to DNA damaging agents. In this study, we demonstrate an increased frequency of spontaneous HRR *in vivo* in the absence of PARP1 using the p^{un} assay. Furthermore, we found that the HRR events that occur in *Parp1* nullizygous mice are associated with a significant increase in large, clonal events, as opposed to the usually more frequent single cell events, suggesting an effect in replicating cells. In conclusion, our data demonstrates that PARP1 inhibits spontaneous HRR events, and supports the model of DNA replication transformation of SSBs into HRR substrates.

INTRODUCTION

Poly (ADP-ribosyl)ation is the posttranslational transfer of long chains of negatively charged ADP-ribose moieties to proteins. The resultant increase in negative charge causes the target protein to lose DNA-binding affinity (1). Poly (ADP-ribose) polymerases, or PARPs, comprise a large family of genes that have shared homology with the catalytic domain of the founding member, PARP1 (1). PARP1 has been widely implicated in a multitude of cellular processes including replication (2–4), transcription [reviewed in (5)], chromatin remodeling [reviewed in (5)], telomere maintenance (6) and perhaps most notably, the repair of DNA damage through the base excision repair (BER) pathway (7–9).

Current understanding is that the key BER proteins actually participate in several distinct pathways such as short-patch BER, long-patch BER, single strand break (SSB) repair and nucleotide incision repair (10). However, the common factor for all of these pathways is an SSB—be it the initiating lesion or an intermediate step in a repair process. PARP1 readily binds SSBs (11,12) and recruits the scaffolding protein XRCC1 (13). PARP1 poly (ADP-ribosyl)ates itself (13), reducing its DNA-binding affinity, thus allowing other repair factors to bind the lesion site (9,14).

A recent study demonstrated that chemical inhibition of PARP1 decreased the efficiency of SSB repair (15), conjecturing that chemically inhibited PARP1 remains bound to DNA and blocks other repair proteins from the SSB site. However, the same study revealed that despite PARP1 silencing via RNA interference, cells were able to repair SSBs (15), indicating that an alternative pathway, possibly homologous recombination repair (HRR), can compensate for this loss. Loss of *Parp1* by way of gene targeting in human cells does not hinder formation of nuclear RAD51 foci (an indicator of RAD51-dependent HRR) (16), nor does PARP1 inhibition appear to obstruct HRR *in vitro* (16,17). Waldman and Waldman (18) found a 4-fold increase in intrachromosomal homologous recombination in mouse fibroblasts grown in the poly(ADP-ribose) polymerase inhibitor, 3-methoxybenzamide, compared to controls. Furthermore, PARP1 does not co-localize to RAD51 foci following DNA damage (16) indicating that it is unlikely that PARP1 is directly involved in the HRR process. In addition, increased sister chromatid exchange has been observed with PARP1 inhibitors in Chinese

*To whom correspondence should be addressed. Tel: +1 210 562 9000; Fax: +1 210 562 9014; Email: bishopa@uthscsa.edu

hamster ovary cells (19) and in PARP1 null mice (20), whereas over-expression of *Parp1* decreases the incidence of sister chromatid exchange following DNA damage (21). Resolution of SSBs by way of HRR in the absence of PARP1 activity may be due either to stalled replication fork or DSBs resulting from replication fork collapse. The requirement of such activity is the postulated basis for synthetic lethality observed when treating breast and ovarian cancer cells deficient for either BRCA1 or BRCA2 with PARP1 inhibitors (4,22–24). This is because BRCA1 and BRCA2, amongst their various functions, are required for RAD51 dependent double-stranded DNA break induced HRR (25–27). Together, these *in vitro* observations indicate that loss or inhibition of PARP1 leads to a hyper-recombinogenic phenotype.

Here, we evaluate the spontaneous frequency of HRR *in vivo* using the well-established and highly sensitive p^{un} eye spot assay (28–30). The murine pink-eyed dilution gene, *p*, encodes a protein that functions in the pigmentation of the fur and the retinal pigment epithelium (RPE) of the mouse (31). Mice lacking a functional copy of this gene are hypopigmented, having a dilute (gray) coat and pink eyes (the cells of the RPE are rendered transparent) (31). One such mutant, the 'pink-eyed unstable' (p^{un}) allele contains a 70-kb duplication of exons 6–18 (32–34, Figure 1) and causes this autosomal recessive phenotype. However, the p^{un} allele is subject to a relatively high frequency of spontaneous, somatic reversion to wild-type (35). Reversion can only be attributed to HRR mediated deletion of the duplicated exons, which restores functionality of *p* (32,33) and consequently pigmentation to the fur and RPE. Equivalent assays in yeast have demonstrated that such intrachromosomal deletions between homologous tandem repeats may be mediated by either a RAD51-dependent pathway (canonical HRR pathway) or a RAD51-independent pathway [single strand annealing (SSA), an alternative HRR pathway)] (36). Therefore, the frequency of p^{un} reversion is indicative of the somatic occurrence of spontaneous HRR events (28,29,37). Here we use the p^{un} eye spot assay to demonstrate that the absence of PARP1 results in increased spontaneous somatic HRR events *in vivo*. The significant increase in rare multi-cell clones of eye spots in *Parp1* nullizygous mice suggests that the normal function of PARP1 is to remove DNA lesions prior to their becoming HRR substrates during DNA replication. Our observations substantiate current models of the relationship between PARP1 and HRR, providing formal *in vivo* evidence of a spontaneous, hyper-recombination phenotype.

MATERIALS AND METHODS

Generation of mice

Mice heterozygous for a targeted null allele of *Parp1*, 129S-*Parp1tm1Zqw* (38), were obtained from Jackson Laboratories (Bar Harbor, ME) and genotyped for *Parp1* as described (http://parplink.u-strasbg.fr/protocols/tools/parp1_typing.html) earlier. The $Parp1^{+/-}$ mice were made C57BL/6J congenic by five backcrosses followed by two crosses to C57BL/6J $p^{un/un}$ mice. Mice with homozygous $p^{un/un}$ genotype were selected by their phenotypic gray coat color. The resulting C57BL/6J N7 $Parp1^{+/-}$ $p^{un/un}$ mice (hereafter referred to as $Parp1^{+/-}$) were self-crossed to create the necessary experimental ($Parp1^{-/-}$) and control animals ($Parp1^{+/-}$ and $Parp1^{+/+}$).

P^{un} assay

The p^{un} frequency assay was performed as described earlier (29). Briefly, eyes were harvested, with the investigator blinded to the genotypes until after p^{un} eye spot data was collected. Three types of data were collected for each RPE: the total number of eye spots, the number of cells comprising each eye spot, and the position of each eye spot relative to the optic nerve. Following Bishop *et al.* (29), a p^{un} reversion event or eye spot was defined as 'a pigmented cell or a cluster of pigmented cells, separated by no more than one unpigmented cell'. Eyes were viewed at $15\times$ using a Zeiss Axiovert microscope and methodically scanned for pigmented spots. A $5\times$ mosaic photograph was taken of each RPE using a Zeiss Lumar V.12 stereomicroscope, Zeiss Axiovision MRm camera and Zeiss Axiovision 4.6 software (Thornwood, NY, USA). In cases where a suspected clone consisted of pigmented cells separated by clear cell(s), the Adobe Photoshop CS2 (San Jose, CA, USA) measure tool was used to assess if the unpigmented area between pigmented cells was consistent with the single cell diameter in that part of the RPE (Figure 1). The p^{un} positional assay was then performed as described earlier (28). Briefly, the position of each spot relative to the optic nerve was calculated using simple measurements. In Photoshop, the brush tool was used to mark the approximate center of the optic nerve and the measure tool was then used to obtain two distances for each eye spot: (i) from the center of the optic nerve to the proximal edge of the eye spot, and (ii) from the center of the optic nerve to the edge of the RPE. By dividing the former by the latter, the position of each eye spot relative to the optic nerve was determined.

Primary mouse embryonic fibroblasts and cell culture

Primary mouse embryonic fibroblasts (MEFs) were obtained by intercrossing *Parp1* heterozygous mice to obtain *Parp1* null embryos and littermate controls. Pregnancies were timed by the observation of a vaginal copulation plug and embryos were harvested on Day E14. Embryos were mechanically homogenized and allowed to incubate in 0.05% Trypsin–EDTA for 20 min. Cells were cultured in Dulbecco's modified Eagle's medium supplemented with 10 000 U/ml penicillin, 10 000 µg/ml streptomycin, 25 µg/ml Amphotericin B (Cellgro). The cells were grown at 37°C in the presence of 5% CO_2 in a humidified incubator.

RAD51 nuclear foci immunofluorescence

HRR frequency was determined by immunofluorescence using an antibody against RAD51 (RK-70-005, MBL) as described earlier (39). Cells were grown on acid-washed fibronectin coated cover slips at a density of 1×10^5 cells/cover slip. Cells were then fixed with 4% paraformaldehyde and permeabilized using Triton X-100
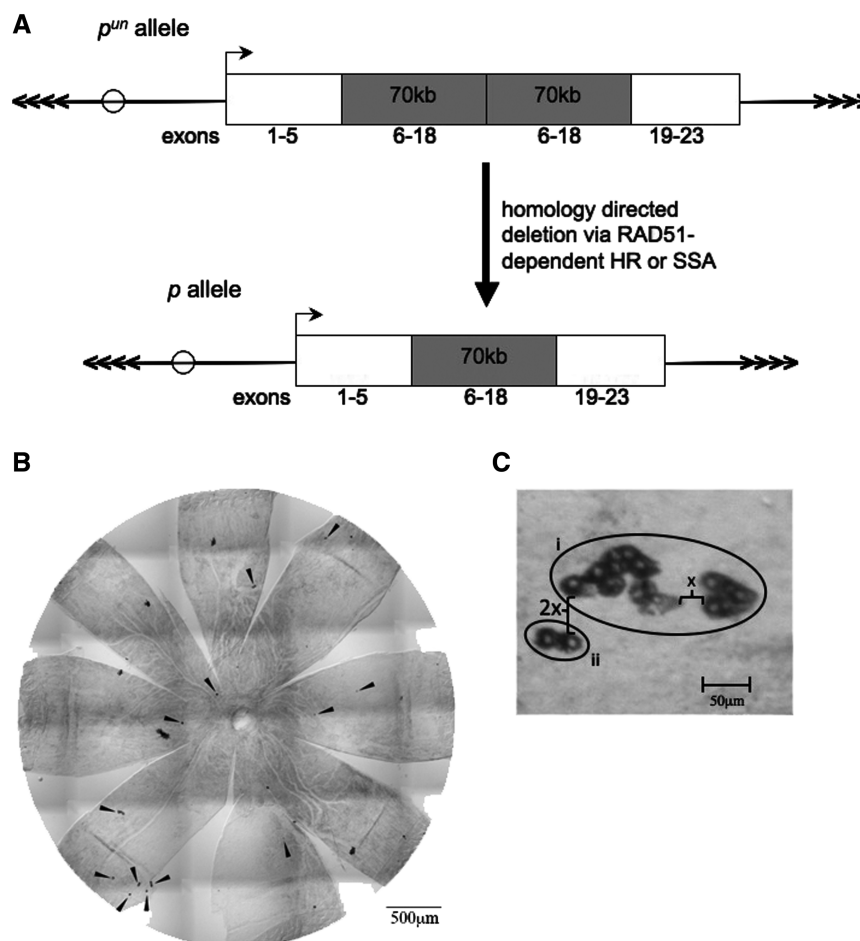
Figure 1. HR-mediated reversion of the p^{un} allele. (**A**) Schematic of the p^{un} mutation. HR events mediate the deletion of one copy of a tandem repeat (of Exons 6–18) rendering the p gene functional, thus causing pigmentation of RPE cells. Circles represent centromeres and arrows telomere DNA. (**B**) Mosaic image of a $Parp1^{-/-}$ RPE wholemount. The 13 p^{un} reversion spots are indicated with black arrowheads. (**C**) Example of two distinct p^{un} reversion events within a cluster of pigmented cells. x is the diameter of one cell in this region of the RPE and $2\times$ is twice this diameter. For example, the two clusters of cells labeled i, are separated by a distance of x and are scored as one event. The cluster labeled ii is a distance of $2\times$ from cluster i, and therefore represents a distinct event.

for 10 min at room temperature. Blocking was performed with 1% BSA–4% goat serum for 1 h followed by an overnight incubation with RAD51 antibody (1:2000) in a humidified chamber. Goat antichicken Alexa Fluor 488 (Invitrogen) diluted 1:1000 was applied to each cover slip for 1 h followed by DAPI staining and Fluoromount G slide mounting. A minimum of 100 nuclei were examined for each genotype, repeated with three technical replicates per genotype.

Statistics

Parametric analysis of variance was performed in Microsoft Excel 1994 for Mac (Redmond, Washington). The F_{max} test was done by hand per Hartley (40) and Rohlf and Sokal (41). Measurements of skew and kurtosis were obtained using descriptive statistics in Microsoft Excel 1994 for Mac (Redmond, Washington). Non-parametric Kruskal–Wallis test was performed using Stata (College Station, TX, USA). Dunn's test was done by hand per Siegel (42). Chi-squared contingency analysis was performed using the VasserStats online calculator

(http://faculty.vasser.edu/lowry/VasserStats.html, accessed 11/2009). Fisher's Exact test (43) was used to compare RAD51 foci quantification using the sum of the technical replicates per genotype.

RESULTS

Loss of *Parp1* leads to a significant increase in HRR *in vivo*

PARP1, amongst its various activities, is involved in SSB repair (11,12). Inhibition of the PARP1 protein in BRCA1 and BRCA2 mutant cells leads to their selective cell death (23,44). This has led to the working model that the observed cell death is due to immitigable DNA damage caused by the loss of two key DNA repair pathways: (i) HRR, due to loss of *BRCA1/2*, and (ii) SSB repair due to inhibition of PARP1 (4,23,24). This model suggests that lack of PARP1 alone will cause an increase in HRR frequency in the absence of exogenous damage. To test this assumption, we determined the spontaneous frequency of

HRR in $Parp1^{-/-}$, $^{+/-}$ and $^{+/+}$ animals using the *in vivo* p^{un} assay.

The frequency of p^{un} reversion was determined in $Parp1^{-/-}$, $^{+/-}$ and $^{+/+}$ animals using p^{un} eye spot assay (Table 1 and Figure 2). There is a clear increase in the frequency of p^{un} reversion events observed in the absence of PARP1 compared to wild-type and heterozygous littermate controls. Considering that the data is non-parametric and not normal, we used the non-parametric Kruskal–Wallis test (followed by Dunn's test to determine which groups are different from one another). This analysis revealed that $Parp1^{-/-}$ animals had a highly statistically significant increase in p^{un} reversion, and thus increased HRR, compared to controls ($P = 0.0001$).

$Parp1$ null mice have an earlier incidence of p^{un} reversion than controls

The RPE develops radially outward from the optic nerve during development (45), therefore, much like the concentric annual rings of a tree, the positions of eye spots indicate the developmental time at which they occurred (28,29). p^{un} reversion events closer to the optic nerve occurred earlier in development and events further from the optic nerve occurred later in development (29). To investigate whether the increased number of events occurred at a particular time during development, we analyzed the relative positions of the p^{un} reversion events on the RPE of differing $Parp1$ genotype (35 wild-type, 28 heterozygous and 24 $Parp1$ null RPE). A Kruskal–Wallis test was used to compare the positional distribution of spots and indicated that there is a significant difference between genotypes ($P = 0.0043$, Figure 3). Subsequently, a Dunn's test indicated that the $Parp1$ null group is different from the control groups.

To determine whether the difference in the positions of spots was due to early or late events, comparison was done between the numbers of events with proximal positions (earlier in development, 0–0.50) versus the numbers of events with distal positions (later in development, 0.51–1.0). A 2×3 contingency table analysis comparing wild-type, heterozygous and null revealed a highly statistically significant difference in the proportion of spots on the proximal half of the RPE ($\chi^2 = 32.09$, $P < 0.0001$). To verify that the difference was due to the null group, groups were analyzed pairwise. There was no significant difference between wild-type and heterozygous ($P = 0.865$), whereas the null group was significantly different from each of them ($P = 0.005$ and $P = 0.004$, respectively).

Finally, 2×2 analysis was performed comparing the null group against the combined heterozygotes and wild-type, confirming a highly statistically significant difference ($\chi^2 = 17.86$, $P < 0.0001$), indicating that there is a shift of p^{un} reversion events to earlier in development. One interpretation of this result is that there is an increased rate of homologous recombination that occurs in the absence of PARP1.

Clonal expansion of p^{un} reversion events is associated with PARP1 absence

On initial analysis of the RPE, there appeared be a greater number of large (consisting of multiple cells) spots in the $Parp1^{-/-}$ RPE (Table 1). Previous studies have shown that spots with greater than 10 cells are very rare (28,30, Bishop, unpublished data). Therefore, a 2×3 contingency table analysis (Chi-square) was computed comparing the number of spots with 10 or fewer cells and the number of spots with 11 or more cells between genotypes ($\chi^2 = 32.65$, $P < 0.0001$, Figure 4). To determine if the null group is
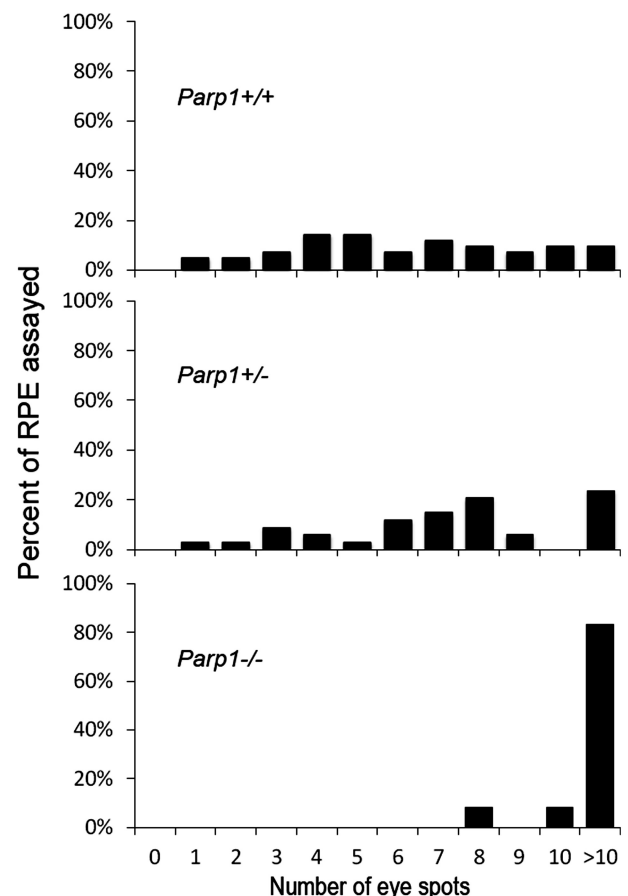

Figure 2. The frequency of p^{un} reversion events in the RPE (pigmented eye spots) in mice with differing $Parp1$ genotypes. There is a highly statistically significant difference between the frequency of eye spots in $Parp1^{-/-}$ mice compared to wild-type and heterozygous controls ($P = 0.0001$ using the non-parametric Kruskal-Wallis test. A Dunn's test determined that the null group is different from the other two). The *x*-axis is expressed as whole number counts of eye spots, while the *y*-axis is expressed as percent of RPE assayed for that genotype. For example, over 80% of the $Parp1^{-/-}$ RPE had greater than 10 eye spots.

Table 1. Summary of RPE examined and p^{un} reversion frequency by $Parp1$ genotype

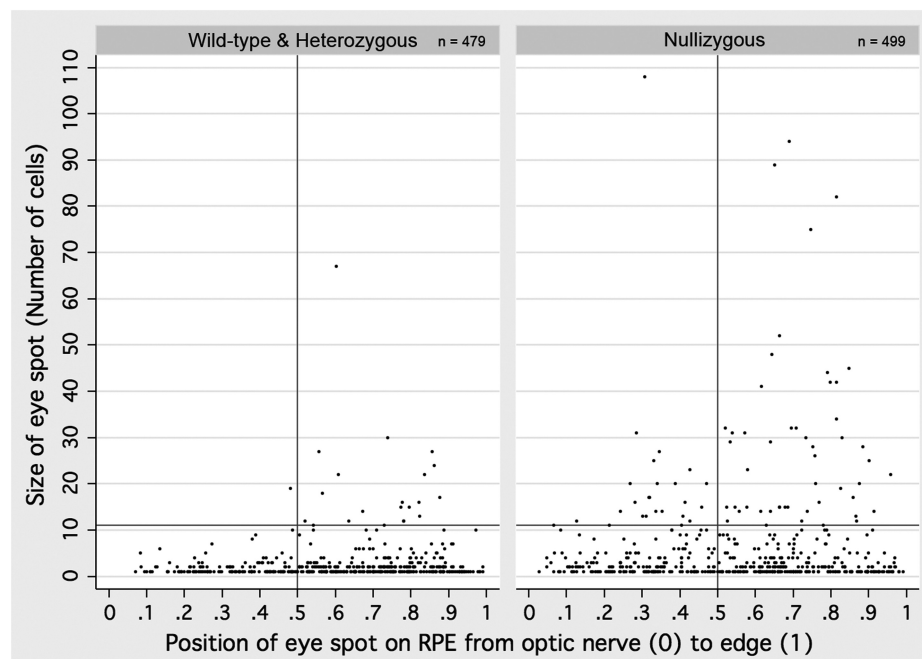| Genotype	No. of RPE	Total no. of spots	Average no. of spots/RPE	Average spot size (no. cells)
$Parp1^{+/+}$	42	287	6.8	3.5
$Parp1^{+/-}$	34	264	7.8	2
$Parp1^{-/-}$	28	545	19.5	6.2

Figure 3. Positional distribution of spots in mice with differing *Parp1* genotypes. The position of an eyespot is a measurement relative to the optic nerve head. The position '0', which represents the optic nerve head, correlates to p^{un} reversion events that occurred relatively early in eye development. The position '1', which represents spots at the edge of the RPE, correlates to reversion events that occurred at a later time in eye development. Non-parametric analysis with a Kruskal–Wallis test ($P = 0.013$) followed by a Dunn's Test indicated that there is an increase in HRR more proximal to the optic nerve, and presumably earlier in eye development, in *Parp1* null mice compared to wild-type and heterozygous controls. Wild-type and heterozygous controls showed no difference, so data were combined in this graphical representation to compensate visually for disparity in sample sizes between the null group and either of the controls. The position (along the *x*-axis) and size (along the *y*-axis) of each individual eye spot is represented as a dot. The vertical marker delineates the position that is halfway between the optic nerve head and the edge of the RPE. The horizontal marker represents the divide between large and small eye spots and is therefore at the 11-cell size marker. Any dot on or above this line represents a 'large' eye spot.

the cause of statistical significance and because our frequency and positional analysis showed no difference between wild-type and heterozygous, the data for these two groups were combined and compared against the null group in a 2×2 contingency table analysis ($\chi^2 = 28.64$, $P < 0.0001$). These results indicate that there is a significant increase in the incidence of large spots in the *Parp1* null mice compared to controls, indicating an increase in HRR in proliferating cells.

To investigate whether a particular subset of spots (single cell or multi-cell) caused the observed shift in spots to an earlier time in development in *Parp1* null mice, a Kruskal–Wallis test was used to analyze the relative positions of these subsets of eye spots between genotypes. This test revealed that multi-cell eye spots are shifted toward the optic nerve in the null mice as compared to heterozygous and wild-type ($P = 0.0001$). Furthermore, analysis of the single-cell eye spots showed no difference between groups ($P = 0.5762$, Kruskal–Wallis test), indicating that the positional shift observed when analyzing all spots is in fact due to the multi-cell eye spots. Considering that the *Parp1* null mice display both an increase in the large eye spots and the position of these eye spots, we examined whether these large eye spots are significantly increased in the proximal half of the RPE in the absence of PARP1. A 2×2 contingency table analysis revealed that indeed there was a significant increase in

large, multi-cell events (≥ 11 cells) in the proximal half of the RPE in null mice compared to control RPE ($\chi^2 = 5.49$, $P = 0.019$, Figure 3). This suggests that many more highly replicative cells are prone to p^{un} reversion events during early RPE development in the absence of PARP1.

Loss of *Parp1* leads to an increase in RAD51 nuclear foci

It has been previously reported that human cells either deficient or inhibited for PARP1 have increased RAD51 nuclear foci, an indicator of increased HRR (16,17). To demonstrate that the same cellular phenomenon is observed here with the mouse *Parp1* knockout model, we examined spontaneous levels of RAD51 nuclear foci in MEFs isolated from these mice (Figure 5). As expected, the observed frequency of spontaneous RAD51 foci for wild-type MEFs displayed a very low background, mostly in the category of 0–5 RAD51 foci per cell. However, *Parp1* null MEFs showed a high number of cells with RAD51 foci with 68.3% having >6 foci per cell compared to wild-type MEFs (23.5%) ($P = 2.6e{-}29$). In addition, comparing 0 foci to either the 6–10 or >10 foci per cell groups demonstrates a significant increase in numbers of foci per cell in the *Parp1* null cells ($P = 3.3e{-}15$ and $P = 8.3e{-}25$, respectively). This data suggests a significantly higher frequency of HRR in
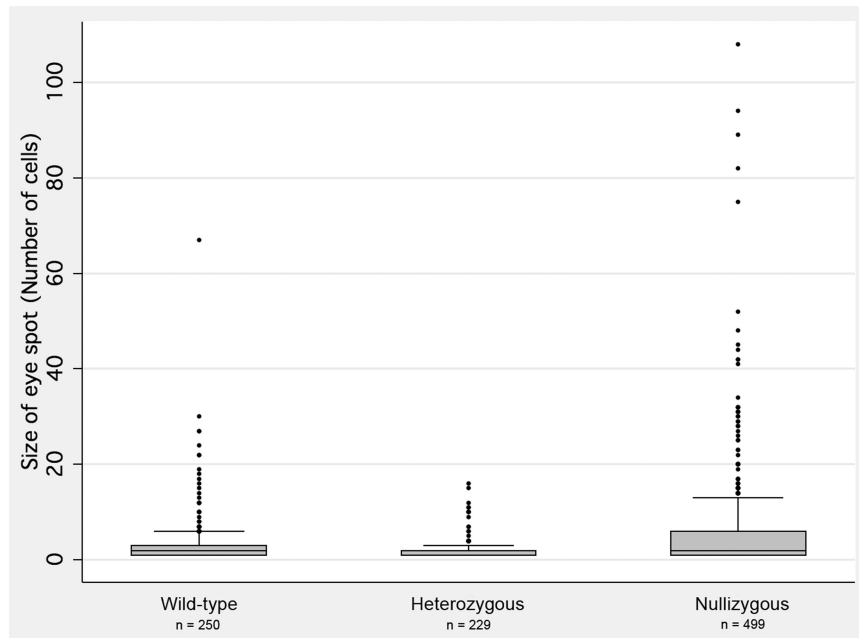
Figure 4. The size of eye spots in mice with differing *Parp1* genotypes. Eye spot size is expressed as the number of pigmented RPE cells comprising the eye spot (*y*-axis). A statistically significant increase in the number of large eye spots in *Parp1* null mice ($\chi^2 = 32.65$, $p < 0.0001$) compared to wild-type and heterozygous controls is shown by using a 2×3 contingency table. Comparison of null against combined wild-type and heterozygous data in a 2×2 contingency table also demonstrated a statistically significant difference in the null group ($\chi^2 = 28.64$, $p < 0.0001$).

Parp1 null MEFs compared to wild-type, correlating well with our *in vivo* p^{un} assay observations.

DISCUSSION

The inhibition of PARP1 activity is an exciting novel therapy used in the treatment of BRCA1 and BRCA2 hereditary breast and ovarian cancers (22). The mechanism by which this therapy is thought to work is by synthetic lethality resulting from an inability to repair SSBs by either PARP1-dependent SSB repair or BRCA1/2-dependent HRR (after replication fork stall/ collapse) (4,23,24). This model would suggest an increase in the spontaneous frequency of HRR in the absence of PARP1. *In vitro* evidence for a hyper-recombination phenotype has been presented in various tissue culture experiments (16,17,19–21). Here, we provide *in vivo* evidence that spontaneous HRR frequency is indeed increased in the absence of PARP1 protein by using an established mouse model for measuring HRR events. HRR dependent repair of SSBs has been proposed to be due to DNA replication fork collapse at the SSB that converts these lesions into HRR substrates. Our data supports this notion, with a significant increase in large clonal eye spots in the *Parp1* null background compared to controls. There is no selective advantage for p^{un} reversion, thus it is likely that similar somatic homologous recombination events are occurring in replicating cells throughout all tissues of the body and not just in the developing RPE and at the p^{un} locus.

The p^{un} HRR assay is based on the loss of one copy of a DNA duplication that encompasses exons 6–18 of the

A RAD51 foci frequency

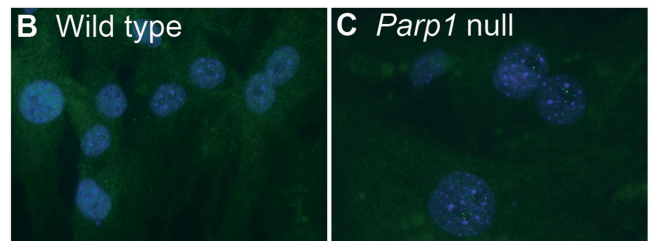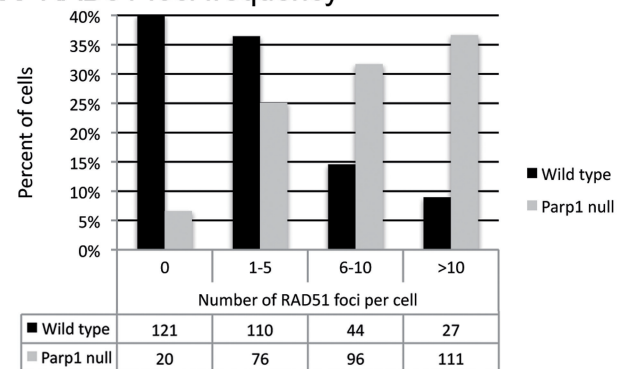|	0	1-5	6-10	>10
Wild type	121	110	44	27
Parp1 null	20	76	96	111

Figure 5. Spontaneous frequency of RAD51 nuclear foci in wild-type and *Parp1* null MEFs. (**A**) Frequency of RAD51 foci per cell by genotype categorized in 0, 1–5, 6–10 and >10 foci by *Parp1* genotype provided as a percentage of cells in the bar graph and actual numbers of cells in the table. There is a statistically significant increase in cells with RAD51 foci in *Parp1* null MEFs compared to wild-type MEFs (comparing 0–5 foci per cell to >6 foci, $P = 2.6e-29$). Furthermore, there are more RAD51 foci present per cell in the absence of PARP1. Representative field of cells with RAD51 foci positive cells are presented in (**B**) for wild-type and (**C**) for *Parp1* null MEFs. Blue is DAPI and green is RAD51, taken with a 40× objective.

p gene, restoring the function of this pigmentation gene. Theoretically the p^{un} reversion event, a homology directed deletion, may be mediated by either of two alternative mechanisms (36). First, there is the canonical, RAD51/BRCA1-dependent HRR pathway and is likely instigated by either a double-stranded DNA break or DNA replication fork collapse. The alternative homology-dependent repair pathway is SSA. SSA is a RAD51-independent pathway that can mediate intrachromosomal deletions between homologous DNA sequences, but is unlikely to be dependent upon the DNA replication process and is more likely to act in response to a double-stranded DNA break than an SSB-induced replication fork collapse (46,47). In contrast, RAD51-dependent HRR is considered a high fidelity DNA repair pathway and is likely a favored mechanism in replicating cells. Therefore, RAD51-dependent HRR provides the most obvious explanation for the observation that earlier p^{un} reversion events in proliferating cells will lead to larger eye spots.

Using the p^{un} assay, we previously reported that there is a significant increase in HRR in *Atm*, *p53* and *Gadd45a* null mice compared to controls (28). While these models showed differing shifts in the timing of events (position of eye spots) (28), the distribution of eye spot size was equivalent to wild-type (a majority of single cell eye spots, fewer two cell eye spots, and so forth, Bishop, unpublished data). In contrast, in the *Parp1* null mice we observed a significant increase in the number of multi-cell spots, particularly those greater than 10 cells (Figure 4). It is possible that different HRR pathways are at work in these different mutant mice, with a preference for replication-tied RAD51-dependent HRR events observed in PARP1 null mice.

It has already been postulated that the mechanism by which *Parp1* nullizygosity increases HRR is through replication fork collapse. Therefore, it is probable that it is the RAD51/BRCA1-dependent HRR pathway that results in the hyper-recombination phenotype we have observed in the *Parp1* null animals. In such a case, it would logically follow that more of the spots consist of a greater number of cells because the original cell in which the p^{un} reversion occurred was a proliferating cell; the daughter cells would have inherited the reverted *p* allele and thus will also be pigmented. However, in wild-type, as well as in *Atm*, *p53* and *Gadd45a* null mice, the majority of spots are single-cell events. These events follow the same general pattern of positions as larger spots, but with a phase shift toward the optic nerve. This relative distribution suggests that the single-cell events were likely to have occurred in cells that were in their terminal division at the rear of the proliferating region of the RPE (28). Therefore, it is possible that these single-cell events were not necessarily tied to active replication machinery, but rather could be due to SSA, in a DNA replication-independent manner. BRCA1-dependent HRR is thought necessarily to involve RAD51 (48) yet SSA is thought to be a RAD51-independent event (36). In support of this, we observe a significant increase in spontaneous nuclear RAD51 foci in the absence of PARP1. Though we cannot determine the proportion of p^{un} reversions that result from SSA events, it appears that the absence of PARP1 results in a clear increase in p^{un} reversion events that are tied to cellular proliferation and DNA replication. Overall, our observations provide formal evidence that the absence of PARP1 protein results in a spontaneous hyper-homologous recombination phenotype that supports the proposed mechanisms of PARP1 inhibition and BRCA1/2 null synthetic lethality.

REFERENCES

1. Diefenbach,J. and Burkle,A. (2005) Introduction to poly(ADP-ribose) metabolism. *Cell. Mol. Life Sci.*, **62**, 721–730.
2. Simbulan-Rosenthal,C.M., Rosenthal,D.S., Boulares,A.H., Hickey,R.J., Malkas,L.H., Coll,J.M. and Smulson,M.E. (1998) Regulation of the expression or recruitment of components of the DNA synthesome by poly(ADP-ribose) polymerase. *Biochemistry*, **37**, 9363–9370.
3. Dantzer,F., Nasheuer,H.P., Vonesch,J.L., de Murcia,G. and Menissier-de Murcia,J. (1998) Functional association of poly(ADP-ribose) polymerase with DNA polymerase alpha-primase complex: a link between DNA strand break detection and DNA replication. *Nucleic Acids Res.*, **26**, 1891–1898.
4. Bryant,H.E., Petermann,E., Schultz,N., Jemth,A.S., Loseva,O., Issaeva,N., Johansson,F., Fernandez,S., McGlynn,P. and Helleday,T. (2009) PARP is activated at stalled forks to mediate Mre11-dependent replication restart and recombination. *EMBO J.*, **28**, 2601–2615.
5. Kim,M.Y., Zhang,T. and Kraus,W.L. (2005) Poly(ADP-ribosyl)ation by PARP-1: 'PAR-laying' NAD+ into a nuclear signal. *Genes Dev.*, **19**, 1951–1967.
6. d'Adda di Fagagna,F., Hande,M.P., Tong,W.M., Lansdorp,P.M., Wang,Z.Q. and Jackson,S.P. (1999) Functions of poly(ADP-ribose) polymerase in controlling telomere length and chromosomal stability. *Nat. Genet.*, **23**, 76–80.
7. Dantzer,F., Schreiber,V., Niedergang,C., Trucco,C., Flatter,E., De La Rubia,G., Oliver,J., Rolli,V., Menissier-de Murcia,J. and de Murcia,G. (1999) Involvement of poly(ADP-ribose) polymerase in base excision repair. *Biochimie*, **81**, 69–75.
8. Dantzer,F., de La Rubia,G., Menissier-De Murcia,J., Hostomsky,Z., de Murcia,G. and Schreiber,V. (2000) Base excision repair is impaired in mammalian cells lacking Poly(ADP-ribose) polymerase-1. *Biochemistry*, **39**, 7559–7569.
9. Herceg,Z. and Wang,Z.Q. (2001) Functions of poly(ADP-ribose) polymerase (PARP) in DNA repair, genomic integrity and cell death. *Mutat. Res.*, **477**, 97–110.

10. Almeida,K.H. and Sobol,R.W. (2007) A unified view of base excision repair: lesion-dependent protein complexes regulated by post-translational modification. *DNA Rep.*, **6**, 695–711.

11. de Murcia,G. and Menissier de Murcia,J. (1994) Poly(ADP-ribose) polymerase: a molecular nick-sensor. *Trends Biochem. Sci.*, **19**, 172–176.

12. Gradwohl,G., Menissier de Murcia,J.M., Molinete,M., Simonin,F., Koken,M., Hoeijmakers,J.H. and de Murcia,G. (1990) The second zinc-finger domain of poly(ADP-ribose) polymerase determines specificity for single-stranded breaks in DNA. *Proc. Natl Acad. Sci. USA*, **87**, 2990–2994.

13. Masson,M., Niedergang,C., Schreiber,V., Muller,S., Menissier-de Murcia,J. and de Murcia,G. (1998) XRCC1 is specifically associated with poly(ADP-ribose) polymerase and negatively regulates its activity following DNA damage. *Mol. Cell. Biol.*, **18**, 3563–3571.

14. Satoh,M.S. and Lindahl,T. (1992) Role of poly(ADP-ribose) formation in DNA repair. *Nature*, **356**, 356–358.

15. Godon,C., Cordelieres,F.P., Biard,D., Giocanti,N., Megnin-Chanet,F., Hall,J. and Favaudon,V. (2008) PARP inhibition versus PARP-1 silencing: different outcomes in terms of single-strand break repair and radiation susceptibility. *Nucleic Acids Res.*, **36**, 4454–4464.

16. Schultz,N., Lopez,E., Saleh-Gohari,N. and Helleday,T. (2003) Poly(ADP-ribose) polymerase (PARP-1) has a controlling role in homologous recombination. *Nucleic Acids Res.*, **31**, 4959–4964.

17. Yang,Y.G., Cortes,U., Patnaik,S., Jasin,M. and Wang,Z.Q. (2004) Ablation of PARP-1 does not interfere with the repair of DNA double-strand breaks, but compromises the reactivation of stalled replication forks. *Oncogene*, **23**, 3872–3882.

18. Waldman,A.S. and Waldman,B.C. (1991) Stimulation of intrachromosomal homologous recombination in mammalian cells by an inhibitor of poly(ADP-ribosylation). *Nucleic Acids Res.*, **19**, 5943–5947.

19. Oikawa,A., Tohda,H., Kanai,M., Miwa,M. and Sugimura,T. (1980) Inhibitors of poly(adenosine diphosphate ribose) polymerase induce sister chromatid exchanges. *Biochem. Biophys. Res. Commun.*, **97**, 1311–1316.

20. de Murcia,J.M., Niedergang,C., Trucco,C., Ricoul,M., Dutrillaux,B., Mark,M., Oliver,F.J., Masson,M., Dierich,A., LeMeur,M. *et al.* (1997) Requirement of poly(ADP-ribose) polymerase in recovery from DNA damage in mice and in cells. *Proc. Natl Acad. Sci. USA*, **94**, 7303–7307.

21. Meyer,R., Muller,M., Beneke,S., Kupper,J.H. and Burkle,A. (2000) Negative regulation of alkylation-induced sister-chromatid exchange by poly(ADP-ribose) polymerase-1 activity. *Int. J. Cancer*, **88**, 351–355.

22. Fong,P.C., Boss,D.S., Yap,T.A., Tutt,A., Wu,P., Mergui-Roelvink,M., Mortimer,P., Swaisland,H., Lau,A., O'Connor,M.J. *et al.* (2009) Inhibition of poly(ADP-ribose) polymerase in tumors from BRCA mutation carriers. *N Engl. J. Med.*, **361**, 123–134.

23. Farmer,H., McCabe,N., Lord,C.J., Tutt,A.N., Johnson,D.A., Richardson,T.B., Santarosa,M., Dillon,K.J., Hickson,I., Knights,C. *et al.* (2005) Targeting the DNA repair defect in BRCA mutant cells as a therapeutic strategy. *Nature*, **434**, 917–921.

24. Turner,N., Tutt,A. and Ashworth,A. (2005) Targeting the DNA repair defect of BRCA tumours. *Curr. Opin. Pharmacol.*, **5**, 388–393.

25. Bhattacharyya,A., Ear,U.S., Koller,B.H., Weichselbaum,R.R. and Bishop,D.K. (2000) The breast cancer susceptibility gene BRCA1 is required for subnuclear assembly of Rad51 and survival following treatment with the DNA cross-linking agent cisplatin. *J. Biol. Chem.*, **275**, 23899–23903.

26. Moynahan,M.E., Chiu,J.W., Koller,B.H. and Jasin,M. (1999) Brca1 controls homology-directed DNA repair. *Mol. Cell.*, **4**, 511–518.

27. Moynahan,M.E., Pierce,A.J. and Jasin,M. (2001) BRCA2 is required for homology-directed repair of chromosomal breaks. *Mol. Cell.*, **7**, 263–272.

28. Bishop,A.J., Hollander,M.C., Kosaras,B., Sidman,R.L., Fornace,A.J. Jr and Schiestl,R.H. (2003) Atm-, p53-, and Gadd45a-deficient mice show an increased frequency of homologous recombination at different stages during development. *Cancer Res.*, **63**, 5335–5343.

29. Bishop,A.J., Kosaras,B., Carls,N., Sidman,R.L. and Schiestl,R.H. (2001) Susceptibility of proliferating cells to benzo[a]pyrene-induced homologous recombination in mice. *Carcinogenesis*, **22**, 641–649.

30. Bishop,A.J., Kosaras,B., Sidman,R.L. and Schiestl,R.H. (2000) Benzo(a)pyrene and X-rays induce reversions of the pink-eyed unstable mutation in the retinal pigment epithelium of mice. *Mutat. Res.*, **457**, 31–40.

31. Brilliant,M.H. (2001) The mouse p (pink-eyed dilution) and human P genes, oculocutaneous albinism type 2 (OCA2), and melanosomal pH. *Pigment Cell Res.*, **14**, 86–93.

32. Brilliant,M.H., Gondo,Y. and Eicher,E.M. (1991) Direct molecular identification of the mouse pink-eyed unstable mutation by genome scanning. *Science*, **252**, 566–569.

33. Gondo,Y., Gardner,J.M., Nakatsu,Y., Durham-Pierre,D., Deveau,S.A., Kuper,C. and Brilliant,M.H. (1993) High-frequency genetic reversion mediated by a DNA duplication: the mouse pink-eyed unstable mutation. *Proc. Natl Acad. Sci. USA*, **90**, 297–301.

34. Oakey,R.J., Keiper,N.M., Ching,A.S. and Brilliant,M.H. (1996) Molecular analysis of the cDNAs encoded by the pun and pJ alleles of the pink-eyed dilution locus. *Mamm. Genome*, **7**, 315–316.

35. Melvold,R.W. (1971) Spontaneous somatic reversion in mice. Effects of parental genotype on stability at the p-locus. *Mutat. Res.*, **12**, 171–174.

36. Ira,G. and Haber,J.E. (2002) Characterization of RAD51-independent break-induced replication that acts preferentially with short homologous sequences. *Mol. Cell. Biol.*, **22**, 6384–6392.

37. Bodenstein,L. and Sidman,R.L. (1987) Growth and development of the mouse retinal pigment epithelium. II. Cell patterning in experimental chimaeras and mosaics. *Dev. Biol.*, **121**, 205–219.

38. Wang,Z.Q., Auer,B., Stingl,L., Berghammer,H., Haidacher,D., Schweiger,M. and Wagner,E.F. (1995) Mice lacking ADPRT and poly(ADP-ribosyl)ation develop normally but are susceptible to skin disease. *Genes Dev.*, **9**, 509–520.

39. Busuttil,R.A., Munoz,D.P., Garcia,A.M., Rodier,F., Kim,W.H., Suh,Y., Hasty,P., Campisi,J. and Vijg,J. (2008) Effect of Ku80 deficiency on mutation frequencies and spectra at a LacZ reporter locus in mouse tissues and cells. *PLoS ONE*, **3**, e3458.

40. Hartley,H.O. (1950) The use of range in analysis of variance. *Biometrika*, **37**, 271–280.

41. Rohlf,F.J. and Sokal,R.R. (1995) *Statistical Tables*, 3rd edn. Freeman and Company, New York.

42. Siegel,S. and Castellan,N.J. (1956) *Non-Parametric Statistics for Behavioral Sciences*. McGraw Hill, New York.

43. Fisher,R. (1922) On the interpretation of $\chi 2$ from contingency tables, and the calculation of P. *J. Roy. Statist. Soci.*, **85**, 87–94.

44. Bryant,H.E., Schultz,N., Thomas,H.D., Parker,K.M., Flower,D., Lopez,E., Kyle,S., Meuth,M., Curtin,N.J. and Helleday,T. (2005) Specific killing of BRCA2-deficient tumours with inhibitors of poly(ADP-ribose) polymerase. *Nature*, **434**, 913–917.

45. Bodenstein,L. and Sidman,R.L. (1987) Growth and development of the mouse retinal pigment epithelium. I. Cell and tissue morphometrics and topography of mitotic activity. *Dev. Biol.*, **121**, 192–204.

46. Galli,A. and Schiestl,R.H. (1998) Effect of Salmonella assay negative and positive carcinogens on intrachromosomal recombination in S-phase arrested yeast cells. *Mutat. Res.*, **419**, 53–68.

47. Galli,A. and Schiestl,R.H. (1998) Effects of DNA double-strand and single-strand breaks on intrachromosomal recombination events in cell-cycle-arrested yeast cells. *Genetics*, **149**, 1235–1250.

48. Cousineau,I., Abaji,C. and Belmaaza,A. (2005) BRCA1 regulates RAD51 function in response to DNA damage and suppresses spontaneous sister chromatid replication slippage: implications for sister chromatid cohesion, genome stability, and carcinogenesis. *Cancer Res.*, **65**, 11384–11391.

Shu Lin, Lan Yu, Junhua Yang, Zhao Liu, Bijal Karia, Alexander J. R. Bishop, James Jackson, Guillermina Lozano, John A. Copland, Xiaoxin Mu, Beicheng Sun and Lu-Zhe Sun

Access the most updated version of this article at doi: 10.1074/jbc.M111.265397

Find articles, minireviews, Reflections and Classics on similar topics on the JBC Affinity Sites.

Alerts:
- When this article is cited
- When a correction for this article is posted

Click here to choose from all of JBC's e-mail alerts

Supplemental material:

http://www.jbc.org/content/suppl/2011/10/28/M111.265397.DC1.html

This article cites 56 references, 17 of which can be accessed free at
http://www.jbc.org/content/286/51/44023.full.html#ref-list-1

APPENDIX 2

Mutant p53 Disrupts Role of ShcA Protein in Balancing Smad Protein-dependent and -independent Signaling Activity of Transforming Growth Factor-β (TGF-β)*[S]

Shu Lin[‡], **Lan Yu**[‡], **Junhua Yang**[‡], **Zhao Liu**[‡], **Bijal Karia**[‡§], **Alexander J. R. Bishop**[‡§¶], **James Jackson**[‖], **Guillermina Lozano**[‖], **John A. Copland****, **Xiaoxin Mu**[‡‡‡], **Beicheng Sun**[‡‡], and **Lu-Zhe Sun**[‡¶1]

From the ‡Department of Cellular and Structural Biology, §Greehey Children's Cancer Research Institute, and ¶Cancer Therapy and Research Center, University of Texas Health Science Center, San Antonio, Texas 78229, ‖Department of Genetics, The University of Texas M. D. Anderson Cancer Center, Houston, Texas 77030, **Department of Cancer Biology, Mayo Clinic, Jacksonville, Florida 32224, and ‡‡Key Laboratory of Living Donor Liver Transplantation, First Affiliated Hospital of Nanjing Medical University, Nanjing, China 210009

Background: Biomarkers driving TGF-β from tumor-suppressing to tumor-promoting remain elusive.
Results: p53 mutation inhibits TGF-β-induced ShcA/ERK signaling and enhances Smad signaling. Elevated p-p52ShcA levels shift the role of TGF-β from growth suppression to migration promotion.
Conclusion: Mutant p53 disrupts the role of ShcA in balancing Smad-dependent and -independent signaling activity of TGF-β.
Significance: Elevated p-p52ShcA levels are a promising biomarker for TGF-β as a tumor promoter.

Biomarkers are lacking for identifying the switch of transforming growth factor-β (TGF-β) from tumor-suppressing to tumor-promoting. Mutated p53 (mp53) has been suggested to switch TGF-β to a tumor promoter. However, we found that mp53 does not always promote the oncogenic role of TGF-β. Here, we show that endogenous mp53 knockdown enhanced cell migration and phosphorylation of ERK in DU145 prostate cancer cells. Furthermore, ectopic expression of mp53 in p53-null PC-3 prostate cancer cells enhanced Smad-dependent signaling but inhibited TGF-β-induced cell migration by downregulating activated ERK. Reactivation of ERK by the expression of its activator, MEK-1, restored TGF-β-induced cell migration. Because TGF-β is known to activate the MAPK/ERK pathway through direct phosphorylation of the adaptor protein ShcA and MAPK/ERK signaling is pivotal to tumor progression, we investigated whether ShcA contributed to mp53-induced ERK inhibition and the conversion of the role of TGF-β during carcinogenesis. We found that mp53 expression led to a decrease of phosphorylated p52ShcA/ERK levels and an increase of phosphorylated Smad levels in a panel of mp53-expressing cancer cell lines and in mammary glands and tumors from mp53 knock-in mice. By manipulating ShcA levels to regulate ERK and Smad signaling in human untransformed and cancer cell lines, we showed that the role of TGF-β in regulating anchorage-dependent and -independent growth and migration can be shifted between growth suppression and migration promotion.

Thus, our results for the first time suggest that mp53 disrupts the role of ShcA in balancing the Smad-dependent and -independent signaling activity of TGF-β and that ShcA/ERK signaling is a major pathway regulating the tumor-promoting activity of TGF-β.

Transforming growth factor-β (TGF-β) is a tumor suppressor during early tumor outgrowth. However, carcinogenesis-mediated elevation of TGF-β production and signaling is often tumor-promoting at later stages, leading to enhanced tumor cell migration, invasion, and metastasis (1). Increased TGF-β is often associated with the loss of the growth-inhibitory activity of TGF-β and its conversion to promote malignant progression of cancers (2), making TGF-β a potential therapeutic target. Indeed, many preclinical studies have shown the efficacy of various types of TGF-β inhibitors in blocking tumor growth, angiogenesis, and metastasis in animal models of human and rodent cancer (3–5). However, biomarkers are lacking for signifying the complicated molecular alterations mediating the switch of TGF-β from tumor suppression to tumor promotion and for identifying appropriate cancer patients for therapy with TGF-β inhibitors.

As a homodimeric polypeptide in humans and mice, TGF-β signals through cell surface receptors called TGF-β type I (RI)[2] and type II (RII) receptors to regulate multiple cellular functions including cell proliferation, differentiation, migration, and wound healing (1). RI and RII are transmembrane serine/threonine kinase receptors that also contain tyrosine kinase activity (6). Active TGF-β ligands bind first to RII, which then

---

[2] The abbreviations used are: RI, TGF-β type I receptor; RII, TGF-β type II receptor; mp53, mutant p53; SBE, Smad-binding element; R-Smad, receptor-regulated class of Smads; DNRII, dominant-negative RII; MTT, 3-(4,5-dimethylthiazol-2-yl)-2,5-diphenyltetrazolium bromide; MMTV, murine mammary tumor virus; p-ERK, phosphorylated ERK; *MEK-1, constitutively active form of MEK-1.

recruits RI, leading to the phosphorylation and activation of RI. Active RI directly phosphorylates the receptor-regulated class of Smads (R-Smad), Smad2/3. Phosphorylated R-Smads in turn associate with Smad4 and translocate into the nucleus to regulate the transcription of TGF-β-responsive target genes (1).

Besides Smad-mediated canonical signaling, TGF-β also signals through Smad-independent pathways including the Ras/Raf/ERK pathway (7). The integration of TGF-β-mediated-Smad-dependent and -independent signaling is believed to contribute to the key events of TGF-β-induced tumor progression including ERK signaling-mediated cell migration (8, 9). TGF-β activates Ras/ERK signaling through the direct phosphorylation of the adaptor protein ShcA (10). ShcA belongs to the family of Shc adaptor proteins, which are substrates of receptor tyrosine kinases (11). ShcA consists of three isoforms, p46, p52, and p66. They are derived from two different transcripts, called p66 and p52/p46 mRNAs (12). Compared with p52ShcA, p46ShcA results from a different in-frame ATG transcript and is predominantly expressed in mitochondria with an elusive role (13). Following the TGF-β engagement, tyrosine-phosphorylated RI recruits and directly phosphorylates p52/46ShcA proteins on tyrosine sites, leading to their association with Grb2 adaptor protein and Sos GTP exchange factor (14). The ShcA-Grb2-Sos complex activates Ras (15), thereby initiating the sequential activation of c-Raf, MEK, and ERK1/2. Among the three tyrosine phosphorylation sites at residues 239/240 (Tyr-239/240) and 317 (Tyr-317) in the CH1 domain of p52/46ShcA, Tyr-317 plays the major role in Ras/ERK signaling activation (11, 16). Clinical studies have shown that a high amount of Tyr-317-phosphorylated p52/46ShcA alone with a low amount of p66ShcA serves as an efficient predictor for identifying aggressive breast tumors with a high risk of recurrence (17, 18). High levels of TGF-β are also associated with poor outcome of human cancer (1). However, it is unclear whether ShcA-mediated activation of ERK signaling contributes to the switch of TGF-β function during carcinogenesis.

A recently published study has shown that the presence of mutated p53 (mp53) in the DNA-binding domain in certain cells together with additional Ras activation can switch TGF-β activity to that of a tumor promoter in the MDA-MB-231 breast cancer cell line and H1299 non-small cell lung cancer cell line (19). Somatic mutation-induced inactivation of p53 occurs in about 50% of human cancers including breast and prostate cancer (20). p53 mutation is considered a biomarker of advanced prostate cancer in which prostate cancer cells lose differentiated phenotypes and transit from androgen-dependent to androgen-independent growth (21). Rather than losing the wild-type p53 (WTp53), the tumor with retention of mp53 has been shown to be more aggressive and associated with poor outcome in certain cancer types (22). For example, mp53 was shown to enhance the cell migration and invasion in breast and lung cancer cell lines (23). However, the role of mp53 in mediating the key steps of cancer progression including cell migration and invasion is largely cell context-dependent and controversial (24). For example, in human endometrial cancer cells, the p53 R213Q mutation does not promote cell migration (25). As shown in another study using the H1299 cell line, p53 R175H negatively regulates cell migration when TGF-β/Smad

signaling is repressed (26). At present, the cellular context for mp53 to exert its oncogenic activity is underexplored. In addition, little is known about whether mp53 alone is sufficient to activate the switch of TGF-β during tumor progression.

To gain a more thorough understanding of the effect of mp53 on tumor progression, particularly with respect to the role of TGF-β signaling, we investigated whether mp53 contributes to the conversion of the role of TGF-β in the regulation of cell growth and migration. Here, we show that mp53 alone is not sufficient to promote the oncogenic role of TGF-β. We further demonstrate that mp53 disrupts the role of ShcA in altering the signaling strength of TGF-β through ERK and Smad pathways in certain human untransformed and cancer cell lines and mice with mp53 knock-in. ShcA-mediated ERK signaling appears to play a more dominant role in conferring the tumor-promoting activity of TGF-β in the regulation of cell growth and migration. Our finding provides novel insight into the role of ShcA as a promising biomarker in driving TGF-β signaling toward tumor promotion.

EXPERIMENTAL PROCEDURES

Ethics Statement—All animal experiments were conducted following appropriate guidelines. They were approved by the Institutional Animal Care and Use Committee and monitored by the Department of Laboratory Animal Resources at the University of Texas Health Science Center at San Antonio (protocol identification numbers 99142-34-11-A and 05054-34-01-A) and the M. D. Anderson Institutional Animal Care and Use Committee (protocol identification number 079906634).

Cell Culture—Human untransformed mammary epithelial cell line MCF-10A was obtained from the Michigan Cancer Foundation. These cells were grown in DMEM/F-12 supplemented with 5% horse serum, EGF, NaHCO$_3$, hydrocortisone, insulin, Fungizone, CaCl$_2$, cholera toxin, and antibiotics. Human prostate carcinoma cell lines PC-3, DU145, and 22Rv-1 and human breast cancer cell line BT20 was purchased from the American Type Culture Collection (ATCC, Manassas, VA). The human breast cancer MCF-7 control cell line and the dominant-negative RII (DNRII)-transfected cell line were provided by Dr. Michael G. Brattain (27). All these cells were cultured in McCoy's 5A medium with 10% fetal bovine serum (FBS) and other supplements as described previously (28). The human breast cancer cell line BT474 was obtained from ATCC and cultured in DMEM (low glucose) with 10% FBS. Cells were maintained at 37 °C in a 5% CO$_2$ humidified incubator.

Chemicals—The small RI kinase inhibitor HTS466284 reported previously to be an ATP-competitive inhibitor of RI kinase (29) was synthesized by the Chemical Synthesis Core of Vanderbilt University. U0126 is an MEK-1/2 inhibitor from Calbiochem.

Plasmids and Transfection—p52/46ShcA plasmid was purchased from Origene. p53 R175H-pCMV-Neo-Bam plasmid was provided by Dr. Harikrishna Nakshatri. p53 R273H-pCDNA3 plasmid was provided by Dr. Zhi-Min Yuan. Human WTp53 expression plasmid pRc/CMV hp53 was obtained from Dr. Arnold Levine. Constitutively active MEK-1 plasmid was provided by Dr. Kun-Liang Guan. Stable transfection of p53 R175H into PC-3 cells was performed by using Lipo-

fectamine 2000 (Invitrogen). Forty-eight hours after the transfection, G418 selection of neomycin-resistant cells was conducted for 1 week. The sequence of p53 siRNA 1 is 5′-CCG GAC GAU AUU GAA CAA UGG UUC A-3′, and the sequence of p53 siRNA 2 is 5′-GCU-UCG AGA UGU UCC GAG AGC UGA A-3′ (Invitrogen). The sequence of ShcA siRNA is 5′-GAC UAA GGA UCA CCG CUU U-3′ (Dharmacon, Lafayette, CO). All transient transfections were performed by using Lipofectamine 2000 according to the manufacturer's protocol. The pLKO.1-puro lentiviral RII shRNA and control shRNA were purchased from Sigma. The sequence of RII shRNA is 5′-CCG GCC TGA CTT GTT GCT AGT CAT ACT CGA GTA TGA CTA GCA ACA AGT CAG GTT TTG-3′. The process of generating MCF-10A cells with stable knockdown of RII was conducted according to the manufacturer's protocol.

Immunoblotting Analysis—Immunoblotting analyses were performed as described previously (30). Primary antibodies were obtained from the following sources: p-Smad2, p-ERK (Thr-202/Tyr-204), p-ShcA (Tyr-317), total-ERK, and MEK-1/2 from Cell Signaling Technology (Danvers, MA); p-Smad3 from Epitomics (Burlingame, CA); total Smad2/3 from BD Transduction Laboratories; p53 from Santa Cruz Biotechnology (Santa Cruz, CA); total ShcA from BD Biosciences; and RII from Abcam (Cambridge, MA). Relative expression levels of the indicated genes were quantified with ImageJ software (National Institutes of Health).

Cell Migration Assay—Cell migration assays were performed in 24-well Boyden chambers with 8-μm pore polycarbonate membranes (BD Biosciences). Cells at the indicated number in serum-free medium were seeded in the upper insert. Complete medium with or without treatment was added in the lower chamber. After 18 h, cells that had migrated through the membrane were stained with the Hema 3 Stain 18 kit (Fisher Scientific) according to the manufacturer's protocol. Migrated cells were counted under a microscope with 100× magnification.

3-(4,5-Dimethylthiazol-2-yl)-2,5-diphenyltetrazolium Bromide (MTT) Assay—Cells were plated in a 96-well plate at 2,500 cells/well with or without TGF-β1 treatment. Two hours before each time point, 50 μl of MTT (2 mg/ml in PBS) was added into each well, and cells were incubated at 37 °C for another 2 h. DMSO (100 μl) was added into each well after the medium was removed. For dissolving the precipitate, the plate was gently shaken on a shaker for 10 min. The absorbance was measured at 595 nm with a microplate reader (BioTek Instrument, Winooski, VT).

Soft Agar Colony Formation Assay—Cells in 1 ml of 0.4% low melting agarose (Invitrogen) with culture medium were plated at 6,000 cells/well on top of existing 0.8% agarose in 6-well plates. The wells were covered with 1 ml of culture medium containing various treatments and incubated at 37 °C in a 5% CO_2 incubator for the indicated number of days. Visualized colonies were counted after staining with *p*-iodonitrotetrazolium violet (Sigma) overnight.

SBE-Luciferase Reporter Assay—The pSBE4-Luc plasmid with Smad-responsive promoter and luciferase reporter gene was used to measure the TGF-β-induced transcriptional activity (31). Cells at 100,000 cells/well were plated in 12-well plates. After 24 h, the pSBE4-Luc plasmid (0.4 μg) was transiently co-transfected with a β-galactosidase expression plasmid (0.1 μg) into the cells by using Lipofectamine 2000. TGF-β1 was added to the transfected cells 5 h later. After an additional 20 h of incubation, cells were lysed, and the activities of luciferase and β-galactosidase of the cell lysates were assayed as described previously (32). Luciferase activity was normalized to β-galactosidase activity.

Animal Tissue Protein Extraction—C57BL/6 mice with a heterozygous $p53^{R172H}$ mutation were described previously (33). Heterozygous $p53^{R172P}$ mice were generated in a similar way (34). They were crossed to C57BL/6 $p^{un/un}$ mice (The Jackson Laboratory, Bar Harbor, ME) (35). Heterozygous breeding cohorts of $p53^{R172P/+}$ $p^{un/un}$ and $p53^{R172H/+}$ $p^{un/un}$ were intercrossed to produce the $p53^{R172P/R172P}$ $p^{un/un}$, $p53^{R172H/R172H}$ $p^{un/un}$, and $p53^{+/+}$ $p^{un/un}$ mice. MMTV-*Wnt1* mice were bred with $p53^{+/+}$ or $p53^{R172H/+}$ mice to generate MMTV-*Wnt1* mice in $p53^{+/+}$, $p53^{R172H/+}$, and $p53^{R172H/R172H}$ backgrounds. A fraction of tumors in the $p53^{R172H/+}$ background undergo loss of heterozygosity (herein referred to as $p53^{R172H/O}$) and thus are functionally p53 mutants. Loss of heterozygosity analysis was performed as described previously (36). The tumor sizes were measured regularly with a caliper in two dimensions. Tumor volumes (V) were calculated with the equation $V = (L \times W^2) \times 0.5$ where L is length and W is width. When tumors reached a volume of ~500 mm^3, mice were sacrificed, and the tumors were collected.

The isolated mammary tissues from $p53^{R172P/R172P}$ $p^{un/un}$, $p53^{R172H/R172H}$ $p^{un/un}$, and $p53^{+/+}$ $p^{un/un}$ mice or breast tumors from MMTV-*Wnt1*-$p53^{+/+}$, -$p53^{R172H/R172H}$ and -$p53^{R172H/O}$ mice were snap frozen in liquid nitrogen. Proteins for immunoblotting analysis were isolated from liquid nitrogen by grinding tissues using T-Per extraction reagent (Thermo Fisher Scientific Inc., Rockford, IL) according to the manufacturer's protocol.

Statistical Analysis—Two-tailed Student's *t* tests were used to determine the significant difference between two mean values from the control and experimental data. All statistical analysis was performed with GraphPad Prism 3.03 software (GraphPad Software, La Jolla, CA).

RESULTS

Mutant p53 Inhibits Cell Migration and Down-regulates ERK Signaling in Prostate Cancer Cell Lines—To investigate whether mp53 alone can promote tumor migration, we knocked down mp53 in the human prostate cancer cell line DU145 containing inactivating endogenous p53 P223L and V274F mutations in its DNA-binding domain (37). We found that instead of making cells less migratory mp53 knockdown significantly enhanced cell migration accompanied by the activation of ERK via phosphorylation (p-ERK) (Fig. 1, *A* and *B*). Active ERK signaling is reported to be essential for tumor metastasis progression including cell migration (9), suggesting that the mp53 depletion-induced migration was likely caused by the up-regulated ERK signaling. We further stably introduced mutant p53 R175H with a mutation in its DNA-binding domain into the p53-null human prostate cancer cell line PC-3 (PC-3/mp53). This resulted in the repression of cell migration as well as the down-regulation of ERK signaling (Fig. 1, *C* and
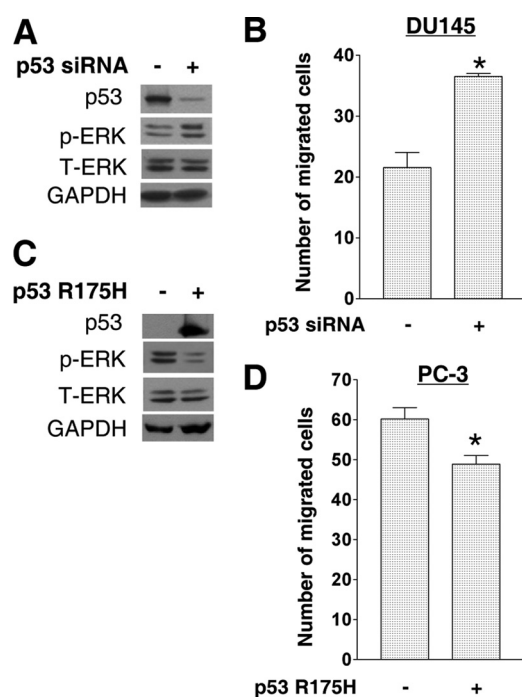
FIGURE 1. **Mutant p53 inhibits cell migration and ERK signaling in prostate cancer cell lines.** *A*, immunoblotting analysis of the indicated gene expression in DU145 cells, which were transfected with control or p53 siRNA for 72 h. *B*, cell migration was assessed in DU145 cells 48 h after the transfection. Cells were plated at 40,000 cells/insert and incubated for 18 h as described under "Experimental Procedures." Data represent mean ± S.E. from three inserts. *, $p < 0.05$. *C*, immunoblotting analysis of the indicated gene expression in PC-3 cells with stable introduction of p53 R175H expression plasmid (PC-3/mp53) or empty vector. *D*, cell migration was assessed in PC-3/mp53 and control cells plated at 70,000 cells/insert and incubated for 18 h. Data represent mean ± S.E. from three inserts. *, $p < 0.05$. *T-ERK*, total ERK. *Error bars* represent S.E.

D). These data indicate that mp53 in certain prostate cell lines attenuates cell migration, which is a key step of procancer metastasis.

Mutant p53 Represses Oncogenic Role of TGF-β and Enhances TGF-β/Smad Signaling in Prostate Cancer Cell Line— The presence of mp53 has been shown to facilitate the tumor-promoting activity of TGF-β in some breast cancer models (19). Because mp53 was found not to enhance cell migration in our studies with two prostate cancer cells, we explored whether mp53 showed a different effect on the oncogenic role of TGF-β. We observed that TGF-β significantly increased migration of the control PC-3 cells, whereas it suppressed migration in the PC-3/mp53 cells, suggesting that the activity of TGF-β is affected by the presence of mp53 (Fig. 2*A*). Because PC-3 is a tumorigenic cell line, we next performed a soft agar colony formation assay to assess the effect of p53 R175H on the growth of PC-3 cells in an anchorage-independent manner. We found that the presence of p53 R175H repressed the anchorage-independent growth ability of PC-3/mp53 cells compared with cells without mp53. Interestingly, the colony formation was more dramatically inhibited by TGF-β, and the treatment with HTS466284, an RI kinase inhibitor (29), significantly stimulated colony formation in PC-3/mp53 cells (Fig. 2, *B* and *C*). To rule out the possibility that the p53 R175H-reduced cell migration in PC-3 cells was due to an altered cell growth rate, we verified that the presence of p53 R175H in PC-3 cells showed

little effect on cell growth but that TGF-β treatment induced a moderate growth inhibition in a dose-dependent manner (Fig. 2*D*). Thus, these results indicate that p53 R175H alone is not sufficient to switch TGF-β to be more tumor-promoting in the PC-3 cell line. Considering that TGF-β-inhibited anchorage-dependent and -independent cell growth is mainly due to Smad-dependent signaling (38, 39), we investigated whether p53 R175H could alter the activation of TGF-β/Smad signaling in PC-3/mp53 cells. We found that p53 R175H made PC-3 cells more sensitive to TGF-β in a dose-dependent manner as evidenced by higher levels of TGF-β-induced phosphorylation of Smad2/3 (Fig. 2*E*). Additionally, the transcriptional activity of TGF-β was also increased in PC-3/mp53 cells when compared with the control cells as detected with transfection of a Smad-responsive promoter-luciferase reporter plasmid (SBE-Luc) (Fig. 2*F*), further indicating that the presence of p53 R175H enhanced the Smad-dependent signaling. These results revealed that the addition of p53 R175H to PC-3 cells enhanced TGF-β/Smad-signaling while inhibiting TGF-β-induced cell migration.

Mutant p53 Represses Activation of ShcA/ERK Signaling—It is suggested that Smad-dependent and -independent signaling pathways work together to drive the key events of TGF-β-induced cell migration and metastasis (8). However, our observations indicate that Smad-dependent signaling is not responsible for the loss of TGF-β-induced migration in PC-3/mp53 cells as reflected by the enhanced TGF-β/Smad signaling. Consequently, we speculated that MAPK/ERK signaling might be involved in the loss of TGF-β-induced cell migration of PC-3/mp53 cells. Consistent with our observation above (Fig. 1*C*), we found that the basal level of p-ERK was markedly reduced in the PC-3/mp53 cells when compared with control cells (Fig. 3*A*). Additionally, TGF-β was unable to further activate ERK in PC-3/mp53 cells (Fig. 3*A*). To confirm that this observation was specifically due to mp53 expression and not an aberrant selection of a pool of antibiotic-resistant clones, we transiently introduced p53 R175H into PC-3 cells and found that p-ERK was greatly reduced when compared with PC-3 cells transfected with a control plasmid or a WTp53 expression plasmid (Fig. 3*B*). In parallel, p53 R175H knockdown in PC-3/mp53 cells with p53 siRNA restored the p-ERK level (Fig. 3*C*). We additionally used another p53 mutation in the DNA-binding domain, p53 R273H, which also enhanced TGF-β-stimulated phosphorylation of Smad2/3 and inhibited the basal and TGF-β-stimulated p-ERK levels. Consistently, p53 R273H also significantly attenuated TGF-β-induced cell migration of PC-3 cells in comparison with the control cells (Fig. 3*D* and supplemental Fig. 1*A*). However, exogenous human WTp53 expression in PC-3 cells showed no effect on the level of TGF-β-induced cell migration, TGF-β-induced activation of ERK, or Smad signaling (Fig. 3*E* and supplemental Fig. 1*B*). Because tyrosine-phosphorylated p52ShcA has been shown to positively mediate TGF-β-activated Ras/ERK signaling (10), we next examined whether the mp53-inhibited phosphorylation of ERK was linked to the down-regulation of p-p52ShcA. Indeed, the expression of p53 R175H and p53 R273H, but not WTp53, in PC-3 cells inhibited TGF-β-induced phosphorylation of p52ShcA
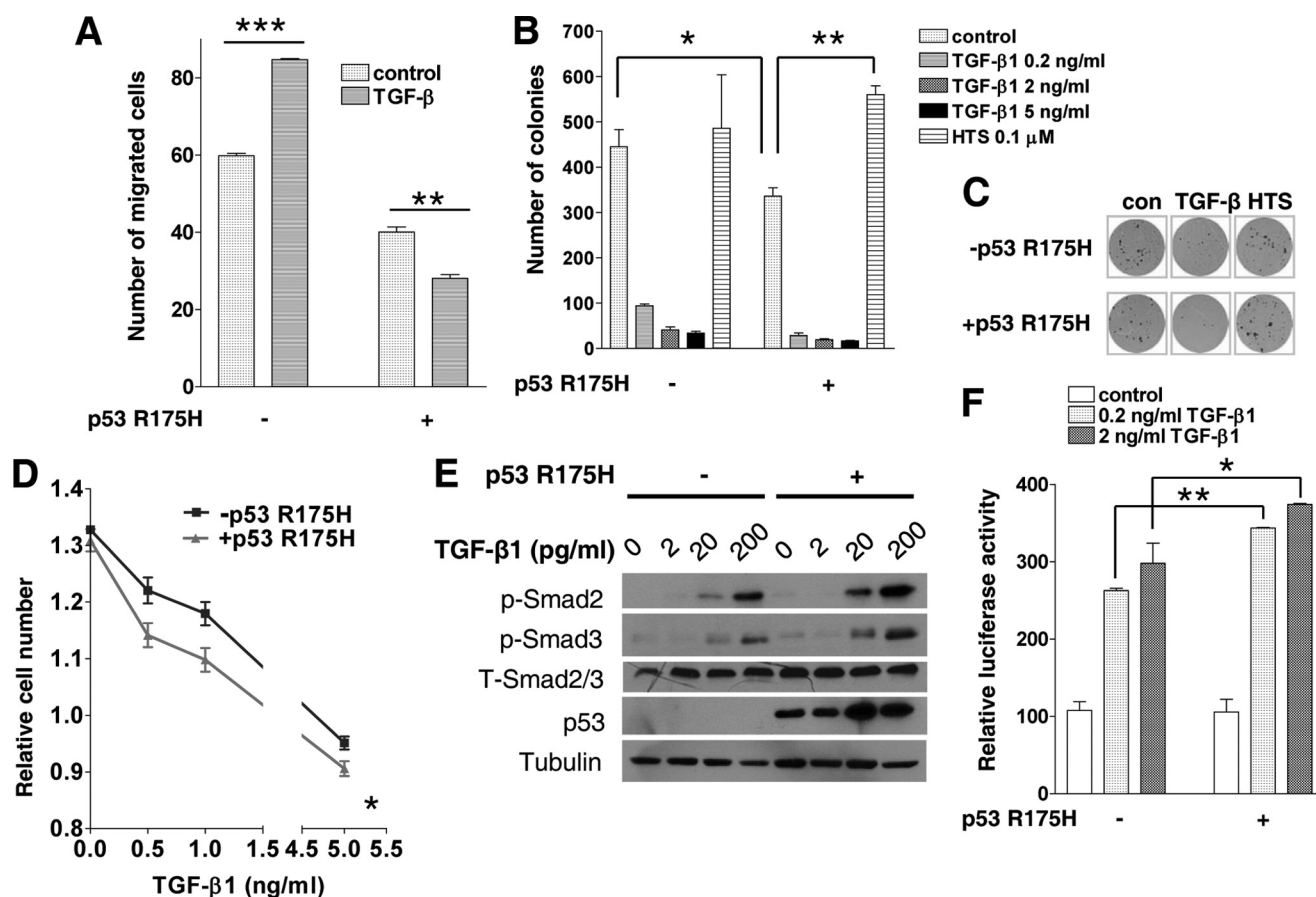
FIGURE 2. **Mutant p53 inhibits oncogenic role of TGF-β and enhances TGF-β/Smad signaling.** *A*, cell migration was assayed with PC-3/mp53 and PC-3 control cells plated at 70,000 cells/insert with or without TGF-β1 (2 ng/ml) for 18 h. Data represent mean ± S.E. from three inserts. **, $p < 0.01$; ***, $p < 0.0001$. *B*, soft agar colony formation ability was assessed in PC-3/mp53 and PC-3 control cells under the indicated TGF-β1 or HTS466284 (*HTS*) treatment for 12 days. Data represent mean ± S.E. from three wells. *, $p < 0.05$; **, $p < 0.01$. *C*, representative pictures of soft agar colonies of PC-3/mp53 and PC-3 control cells were taken after 12-day treatment with 2 ng/ml TGF-β1 or 0.1 μM HTS466284. *D*, effect of TGF-β1 on cell proliferation was measured with the MTT assay at day 6 after incubation with the indicated dose of TGF-β1. Data represent mean ± S.E. from five wells. A two-tailed *t* test was performed to compare the mean of relative cell number between PC-3/mp53 and PC-3 control cells for all treatments. *, $p < 0.05$. *E*, immunoblotting analysis for the indicated gene expression was performed in PC-3/mp53 and PC-3 control cells under TGF-β1 treatment for 40 min. *F*, SBE-luciferase assay was performed using PC-3/mp53 and PC-3 control cells after TGF-β1 treatment as described under "Experimental Procedures." Data represent mean ± S.E. from three independent transfections of relative luciferase units normalized to β-galactosidase activity. *, $p < 0.05$; **, $p < 0.01$. *T-Smad2/3*, total Smad2/3. *Error bars* represent S.E.

compared with control cells (Fig. 3*F*). Thus, these data revealed that mp53, but not WTp53, has the ability to down-regulate ShcA-mediated ERK signaling.

Expression of MEK-1 or ShcA Restores Active ERK Level and TGF-β-induced Cell Migration—To determine whether the attenuated ERK signaling led to the loss of TGF-β-induced cell migration in PC-3/mp53 cells, we examined whether TGF-β-induced cell migration could be rescued by the reactivation of ERK. As shown in Fig. 4*A*, ectopic expression of the ERK activator, a constitutively active form of MEK-1 (*MEK-1), was able to restore the level of p-ERK in PC-3/mp53 cells. More importantly, compared with control plasmid-transfected cells, PC-3/mp53 cells with *MEK-1 expression-rescued p-ERK became responsive again to TGF-β in cell migration (Fig. 4*B*). These results suggest the need for active ERK signaling to mediate the migration-promoting activity of TGF-β in the presence of mp53. To further confirm our results, we used DU145 cells to test whether manipulating the active ERK by elevated ShcA activation also affected TGF-β-induced cell migration in a different mp53-containing model system. We found that TGF-β slightly induced the phosphorylation of ShcA and did not

induce the phosphorylation of ERK (Fig. 4*C*). Neither was TGF-β able to induce DU145 cell migration (Fig. 4*D*), reca-pitulating the results with PC-3/mp53 (Fig. 2*A*). Conversely, ectopic overexpression of p52/46ShcA in the presence of TGF-β expression resulted in the clear activation of p52ShcA and ERK as well as the stimulation of cell migra-tion. These findings are highly consistent with the findings from PC-3/mp53 cells with reactivated ERK (Fig. 4*B*). Our observations thus far have demonstrated that TGF-β is able to induce cell migration in the context of mp53 when p-p52ShcA is elevated and that this correlates with activa-tion of ERK. To verify that the increase of TGF-β-induced cell migration after overexpression of p52/46ShcA was in fact mediated by the activation of ERK, we treated the PC-3 cells with an ERK signaling inhibitor, U0126, and found that TGF-β-induced cell migration was totally abolished (Fig. 4*E*). Thus, these findings indicate that TGF-β-induced cell migration is dependent on its activation of ERK signaling in prostate cancer cells in which mp53 tends to attenuate TGF-β-induced cancer malignancy.
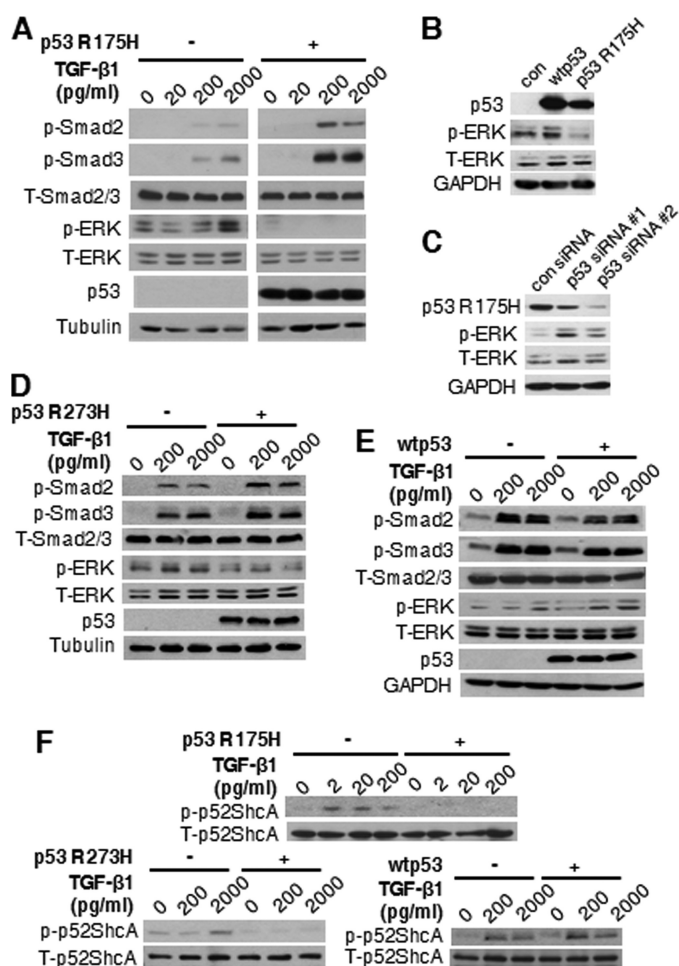
FIGURE 3. ShcA-mediated ERK signaling is down-regulated in presence of mutated p53. *A*, immunoblotting analysis for the indicated gene expression was performed in PC-3/mp53 and PC-3 control cells after TGF-β1 treatment for 40 min. *B*, immunoblotting analysis for p-ERK and p53 was performed in PC-3 cells 72 h after transfection of p53 R175H expression plasmid, human WTp53 expression plasmid, or the empty vector. *C*, immunoblotting analysis for the indicated gene expression was performed in PC-3/mp53 cells 72 h after transfection of p53 siRNA 1, p53 siRNA 2, or control siRNA. *D*, immunoblotting analysis for the indicated gene expression was assessed in PC-3 cells 72 h after transfection of a p53 R273H expression plasmid or empty vector followed by TGF-β1 treatment for 40 min. *E*, immunoblotting analysis for the indicated gene expression was assessed in PC-3 cells 72 h after transfection of a human WTp53 expression plasmid or empty vector followed by TGF-β1 treatment for 40 min. *F*, immunoblotting analysis for the indicated gene expression was conducted in PC-3/mp53 and PC-3 control cells and PC-3 cells transfected with p53 R273H or WTp53 expression plasmid for 72 h followed by TGF-β1 treatment for 40 min. *T-ERK*, total ERK; *T-Smad2/3*, total Smad2/3; *con*; control.

ShcA Alters Role of TGF-β in Cellular Migration and Anchorage-dependent and -independent Growth in Transformed Cells— To this point, we have demonstrated that mp53-induced alteration of Smad-dependent and -independent TGF-β signaling is due to altered ShcA activation. Therefore, we next investigated whether ShcA could serve as a biomarker in converting the role of TGF-β from growth suppression to migration promotion in cancer cells. To this end, we examined the effect of manipulating the expression level of ShcA in PC-3 cells on growth and migration. Interestingly, we found that knockdown of ShcA isoforms by pan-ShcA siRNA decreased TGF-β-induced phosphorylation of ERK and increased TGF-β-induced phosphorylation of Smad2/3 (Fig. 5A). Conversely, the ectopic

overexpression of p52/46ShcA raised TGF-β-induced phosphorylated ERK levels and reduced TGF-β-induced phosphorylated Smad2/3 levels (Fig. 5B). Consistently, we found that knockdown of p52/46ShcA enhanced, but ectopic overexpression of p52/46ShcA reduced, TGF-β-inhibited anchorage-dependent (Fig. 5, *C* and *D*) and -independent cell growth (Fig. 5, *E* and *F*). TGF-β-induced cell migration was significantly diminished in ShcA-depleted cells but significantly increased in p52/46ShcA-overexpressing cells (Fig. 5, *G* and *H*). Because anchorage-independent growth ability is associated with tumorigenicity *in vivo* and cell migration is a key step of tumor progression, our results suggest that ShcA attenuates the tumor suppressor activity of TGF-β while enhancing its tumor promoter activity.

ShcA Alters Role of TGF-β in Cellular Migration and Cell Growth in Untransformed Cells— To further investigate the effect of ShcA on TGF-β-mediated cellular growth and migration, we introduced pan-ShcA siRNA or p52/46ShcA cDNA into untransformed MCF-10A cells, which lack complicated alterations of tumor suppressor genes and oncogenes. By using this spontaneously immortalized and non-tumorigenic human mammary epithelial cell line, we were able to examine the transition of the role of TGF-β in the early stage of transformation. We essentially observed the same phenotypic changes as in the transformed PC-3 cells. Specifically, knockdown of ShcA isoforms down-regulated TGF-β-induced phosphorylation of ERK and up-regulated TGF-β-induced phosphorylation of Smad2/3 (Fig. 6A). In cells with knockdown of ShcA, we found that TGF-β-inhibited cell growth was significantly enhanced (Fig. 6C) and that TGF-β-induced cell migration was significantly reduced (Fig. 6E) in comparison with the control siRNA-transfected cells. In contrast, when compared with vehicle-transfected cells, ectopic overexpression of p52/46ShcA augmented TGF-β-induced phosphorylation of ERK (Fig. 6B) and TGF-β-induced cell migration (Fig. 6F) but repressed TGF-β-induced phosphorylation of Smad2/3 (Fig. 6B) and significantly attenuated TGF-β-inhibited cell growth (Fig. 6D). Thus, our data suggest that ShcA can alter the role of TGF-β in controlling cellular growth and migration by balancing its signaling between the ERK and Smad pathways. We next asked whether TGF-β-induced tyrosine phosphorylation of p52ShcA by RI requires RII. Therefore, we knocked down RII in MCF-10A cells by using an RII shRNA and found that the depletion of RII led to the attenuation of TGF-β-induced phosphorylation of p52ShcA and ERK (Fig. 6G). Additionally, we have previously shown that ectopic expression of a DNRII blocked TGF-β signaling and reduced the level of active ERK in the human MCF-7 breast cancer cell line, which contains a high level of autocrine TGF-β activity (40). Interestingly, we found that this DNRII-expressing MCF-7 cell line also has a lower level of the tyrosine-phosphorylated p52ShcA than the control vector-transfected cells (Fig. 6H). Thus, our observations suggest that RII is required for the activation of p52ShcA by TGF-β.

Mutant p53 Positively Correlates with Activation of Smad-dependent Signaling and Negatively Correlates with Active ShcA/ERK Signaling in Human Cancer Cell Lines and Transgenic Mouse Models— To further generalize our findings, we tested the correlation among the presence of mp53, activation of ShcA/ERK signaling, and Smad-dependent signaling in a
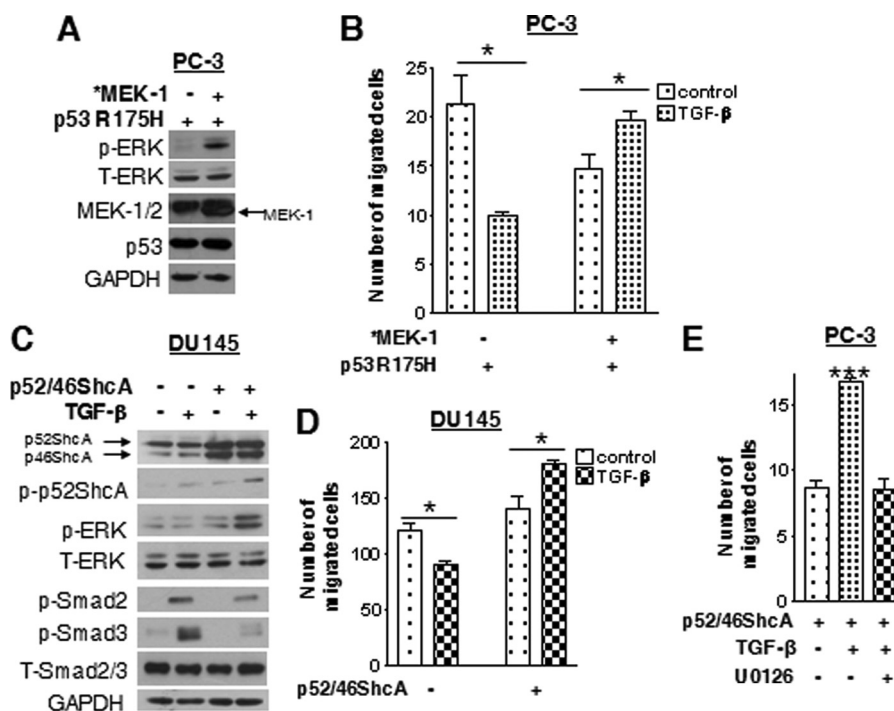
FIGURE 4. **Expression of MEK-1 or ShcA restores active ERK level and TGF-β-induced cell migration.** *A*, immunoblotting analysis for the indicated gene expression was assessed in PC-3/mp53 cells 72 h after transfection of an *MEK-1expression plasmid or empty vector. *B*, cell migration was assayed in PC-3/mp53 cells 48 h after *MEK-1 transfection. Cells were plated at 70,000 cells/insert with or without TGF-β1 (2 ng/ml) for 18 h. Data represent mean ± S.E. from three inserts. *, $p < 0.05$. *C*, 72 h post-transfection with an empty vector or p52/46ShcA expression plasmid, immunoblotting analysis for the indicated gene expression was performed in DU145 cells with or without 2 ng/ml TGF-β1 treatment for 40 min. *D*, cell migration was assessed in DU145 cells 48 h after transfection of p52/46ShcA or empty vector. Cells were plated at 40,000 cells/insert with or without TGF-β1 (2 ng/ml) for 18 h. Data represent mean ± S.E. from three inserts. *, $p < 0.05$. *E*, cell migration was assessed in PC-3 cells 48 h after transfection of p52/46ShcA or empty vector. Cells were plated at 100,000 cells/insert and treated with TGF-β1 (2 ng/ml) or U0126 (10 μM) for 18 h. Data represent mean ± S.E. from three inserts. ***, $p < 0.0001$. *T-ERK*, total ERK; *T-Smad2/3*, total Smad2/3. *Error bars* represent S.E.

panel of human breast and prostate cancer cell lines, each expressing varying p53 mutations, although all mutations were within the DNA-binding domain. Human breast cancer cell lines BT20 with p53 K132Q mutation, BT474 with p53 E285K mutation (41), and DU145 were used in our study. We also included human prostate cancer cell line 22Rv1 with p53 Q331R mutation in the dimerization domain (42). mp53 knockdown in those cell lines increased the phosphorylation of p52ShcA and ERK, whereas it decreased the phosphorylation of Smad2 or Smad3 (Fig. 7*A*). In mammary gland tissues from $WTp53^{+/+}$, $p53^{R172H/R172H}$ mutant, or $p53^{R172P/R172P}$ mutant (equivalent to human p53 R175H and R175P mutations, respectively) female mice on a C57BL/6 $p^{un/un}$ genetic background, we found that the total ERK-normalized phosphorylation of ERK was down-regulated, whereas the total Smad2/3-normalized phosphorylation of Smad3 was up-regulated in the tissues bearing the mp53 when compared with WTp53-expressing tissues (Fig. 7*B*). We also normalized the p-ERK and p-Smad3 expression levels with GAPDH protein levels and obtained a similar outcome (supplemental Fig. 2*A*). The p-ShcA expression levels were undetectable, and we speculated that the normal murine mammary tissues might express low levels of p-ShcA (data not shown). Furthermore, to evaluate the correlation among mp53, ShcA/ERK signaling, and Smad signaling in a more clinically relevant setting, we collected mammary tumor tissues with $WTp53^{+/+}$, $p53^{R172H/R172H}$ mutation, or $p53^{R172H/O}$ (p53 R172H heterozygous with loss of heterozy-

gosity) on the background of the MMTV-*Wnt1* transgenic mice, a well established model of breast cancer development and progression. The presence of mp53 showed negative correlation with the active ShcA/ERK signaling and positive correlation with the active Smad-dependent signaling (Fig. 7*C* and supplemental Fig. 2*B*). These observations further support the conclusion that p53 mutation disrupts the role of ShcA in balancing the Smad-dependent and Smad-independent signaling activity of TGF-β.

DISCUSSION

The cross-talk between p53 mutation and oncogenic Ras/ERK signaling has been demonstrated to promote TGF-β-induced cell migration and metastasis in certain breast cancer models (19). However, it is still unclear whether mp53 alone can act as a tumor promoter and cause TGF-β signaling to become oncogenic. Several studies have revealed that the malignancy gained from mp53 is cell context-dependent and controversial (24). For example, mp53 can enhance the cell migration and invasion via up-regulation of the epithelial-mesenchymal transition factor Slug in human non-small cell lung cancer and breast cancer cell lines (23). In contrast, p53 R312Q mutation does not positively regulate migration of human endometrial cancer cells (25). p53 R175H mutation was shown to inhibit the migration of the H1299 lung cancer cell line when its RII was down-regulated and TGF-β/Smad signaling was repressed (26). Here, we focused on the p53 DNA-binding domain mutations,
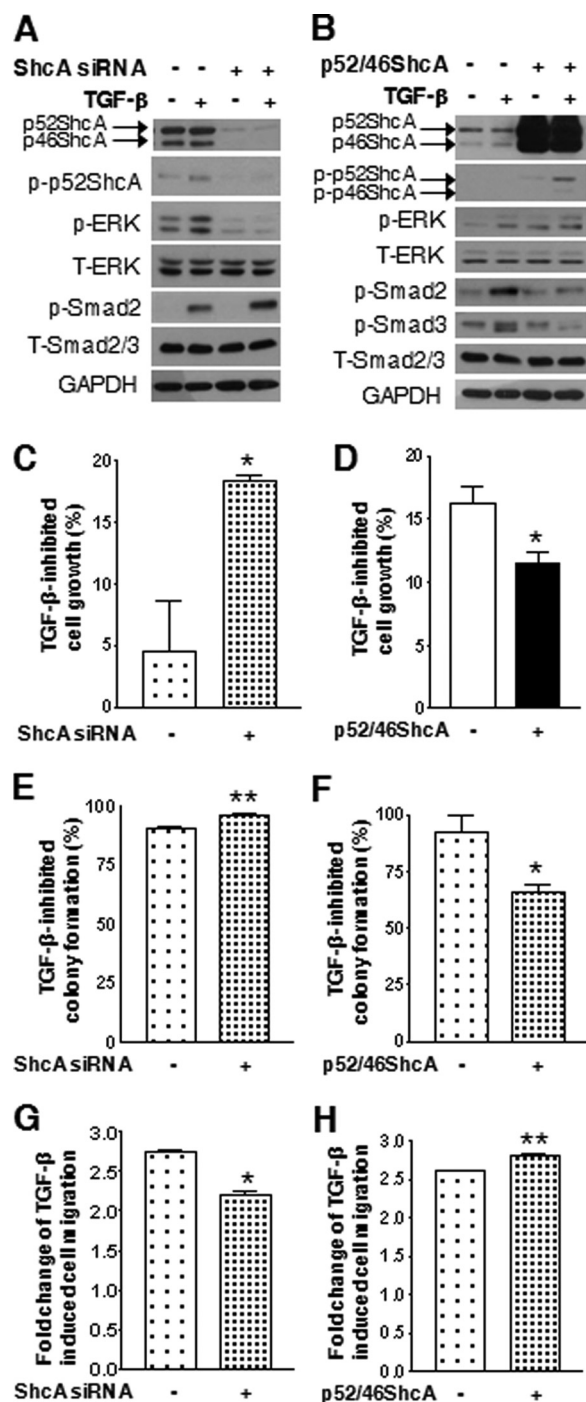
FIGURE 5. ShcA alters TGF-β-mediated Smad and ERK signaling and activity in human cancer cell. PC-3 cells were transfected with a pan-ShcA siRNA or a p52/46ShcA expression plasmid as shown in *A* and *B*, respectively. Seventy-two hours post-transfection, immunoblotting analysis for the indicated gene expression was performed using the transfected cells treated with or without 2 ng/ml TGF-β1 for 40 min. *C* and *D*, TGF-β1 (2 ng/ml)-induced cell growth inhibition was measured with the MTT assay in cells 72 h after transfection. Data are presented as the percentage of TGF-β-induced inhibition of cell growth or colony formation (shown in *E* and *F*) relative to untreated cells. Data represent mean ± S.E. from four wells. *E* and *F*, soft agar colony formation ability was assessed in cells 24 h after transfection. Cells were treated with or without 2 ng/ml TGF-β1 for 6 days. Data represent mean ± S.E. from three wells. *G* and *H*, cell migration was assessed in cells 48 h after transfection. Cells were plated at 70,000 cells/insert with or without TGF-β1 (2 ng/ml) for 18 h. Data are presented as the -fold change of TGF-β-induced migration relative to untreated cells. Data represent mean ± S.E. from three inserts. *, $p < 0.05$; **, $p < 0.01$. *T-ERK*, total ERK; *T-Smad2/3*, total Smad2/3. *Error bars* represent S.E.

which have been reported as the majority of p53 mutations in human breast and prostate cancer cell lines (43). We found that in DU145 and PC-3 human prostate cancer cells the endogenous or ectopic expression of p53 with a point mutation in its DNA-binding domain does not enhance the cell migration or cause TGF-β to be more migration-promoting. Hence, our results from these models indicate that mp53 alone does not always function as a promoter of migration in already transformed cells, and its function is likely context-dependent. Indeed, p53 mutation has been shown to occur relatively late during multistage oncogenic progression and often follows Ras mutation-induced ERK signaling (44). It has been shown that mp53 works together with oncogenic Ras to induce the expression of several protumorigenesis and prometastasis genes in gene expression profiling studies (45). Our finding that mp53 repressed the oncogenic role of TGF-β in the model systems we used suggests that additional signaling activation and genetic alterations such as ERK signaling activation and attenuation of TGF-β-induced growth inhibition appear necessary to collaboratively confer the tumor-promoting activity of mp53 and TGF-β during cancer progression. Although the sequestration of metastasis suppressor p63 by the formation of an mp53-Smad-p63 ternary complex has been shown to enhance the oncogenic activity of TGF-β (19), an additional mechanism involving mp53 but not the formation of the ternary complex has also been shown to drive TGF-β to become more tumor-promoting (46). DU145 cells are negative for p63 expression (47). Thus, the conversion of TGF-β is independent of the ternary complex formation in DU145 cells with restored ShcA/ERK signaling. The presence of mp53 repressed the basal level of phosphorylated p52ShcA and also abolished the activation of p52ShcA by TGF-β, suggesting that mp53 could be the upstream regulator of p52ShcA. We speculate that the mechanism by which mp53 down-regulates the phosphorylation of p52ShcA is perhaps through an aberrant or dysregulated protein interaction. However, further investigation is needed to elucidate the mechanism.

TGF-β receptors have been shown to possess dual tyrosine and serine kinase activity and can directly tyrosine phosphorylate ShcA to activate Ras/MAPK signaling or serine phosphorylate ShcA with an unclear consequence (10). The same study suggests that tyrosine phosphorylation of p66Shc, the inhibitory isoform of ShcA, is more dependent on RI in untransformed cells. On the other hand, it is unclear whether RI alone is sufficient to induce tyrosine phosphorylation of p52ShcA. In our study, the depletion of RII in the untransformed human breast cells attenuated the TGF-β-induced activation of the ShcA/ERK cascade as well as Smad signaling. DNRII has the intact extracellular and transmembrane domains of the wild-type RII and is capable of forming a functional complex with TGF-β and RI. By introducing this DNRII into a human breast cancer cell line that has autocrine TGF-β activity, we found that the dysfunctional RII caused the inhibition of ShcA/ERK activation. Our observations suggest that RII is required for TGF-β to activate the p52ShcA/ERK pathway. It is worth mentioning that other tyrosine kinase receptors such as epidermal growth factor receptor and insulin receptor also have the ability to tyrosine phosphorylate p52/46ShcA and consequently activate Ras/
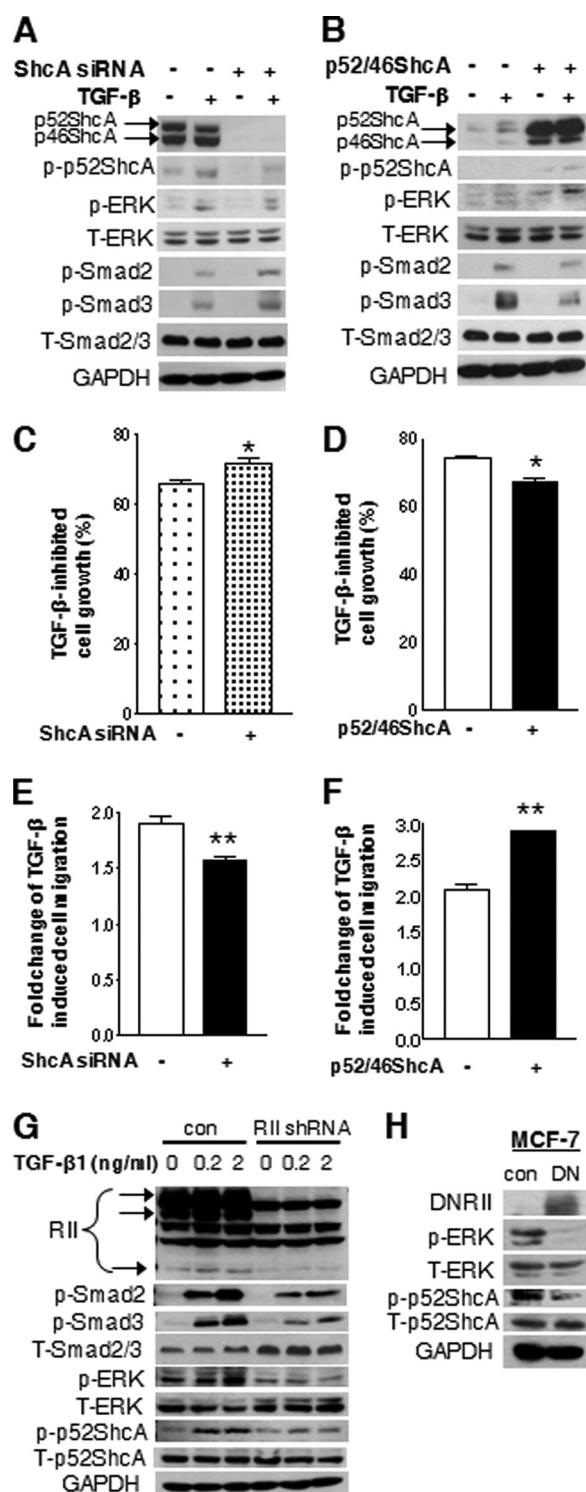
FIGURE 6. **ShcA alters TGF-β-mediated Smad and ERK signaling and activity in untransformed human cells.** MCF-10A cells were transfected with a pan-ShcA siRNA or a p52/46ShcA expression plasmid as shown in *A* and *B*, respectively. Seventy-two hours post-transfection, immunoblotting analysis for the indicated gene expression was performed using the transfected cells treated with or without 2 ng/ml TGF-β1 for 40 min. *C* and *D*, TGF-β1 (2 ng/ml)-induced cell growth inhibition was measured with the MTT assay in cells 72 h after transfection. Data are presented as the percentage of TGF-β-induced growth inhibition relative to the untreated cells. Data represent mean ± S.E. from four wells. *E* and *F*, cell migration was assayed in cells 48 h after transfection. Cells were plated at 70,000 cells/insert with or without TGF-β1 (2 ng/ml) for 18 h. Data are presented as the fold change of TGF-β-induced migration relative to untreated cells. Data represent mean ± S.E. from three inserts. *, $p < 0.05$; **, $p < 0.01$. *G*, immunoblotting analysis of the indicated gene

ERK signaling (48). We speculate that RI and other tyrosine receptors may compete for available ShcA. This competition may further influence the signaling strength of TGF-β between Smad and ERK signaling. Currently, how those pathways may affect the Smad-dependent and -independent signaling of TGF-β via p52/46ShcA is also under investigation.

The activation of TGF-β/Smad-dependent signaling requires the serine/threonine kinase activity of RII and RI. Tyrosine kinases, instead of serine/threonine kinases, have been reported as the catalytic center of RI in certain structural features (49). Conceivably, R-Smads and ShcA may compete for RI kinase, and the balance between the tyrosine phosphorylation of ShcA and serine phosphorylation of R-Smads could determine the signaling strength of TGF-β through the Smad-independent and -dependent pathways, respectively.

It is well known that TGF-β-induced cell growth inhibition in epithelial cells depends on Smad-dependent signaling (38, 39). Loss of Smad4 during cancer progression has been shown to contribute to the resistance of TGF-β-inhibited cell growth, which is considered one mechanism for the TGF-β to be tumor-promoting (1). However, it is less clear what other mechanistic biomarkers can indicate the change of TGF-β signaling in favor of tumor progression during tumorigenesis. Our study showed that knockdown of ShcA isoforms enhanced, whereas overexpression of p52/46ShcA attenuated, TGF-β-inhibited anchorage-dependent and independent-growth of tumor cells, implicating ShcA as a negative mediator of TGF-β-induced tumor suppression. For the Smad-dependent TGF-β signaling, TGF-β-mediated cell cycle arrest involves a Smad-dependent induction of cyclin-dependent kinase inhibitors p15 and p21. On the other hand, the activation of MAPK/ERK signaling is pivotal for the TGF-β-induced epithelial-mesenchymal transition and cell migration, both of which are considered important steps of prometastatic progression (1). Thus, it is conceivable that the mechanism by which p52/46ShcA regulates TGF-β-induced cell migration or growth inhibition is cell context-dependent. For DU145, PC-3, and MCF-10A cells, we found that the cells are sensitive to TGF-β as evidenced by the increased p-Smad2/3 and that manipulating ShcA enhanced TGF-β-induced cell migration accompanied by increased TGF-β/ShcA/ERK signaling and decreased TGF-β/Smad signaling. Because TGF-β/Smad-dependent stimulation of p21 expression has been observed in these cells and p21 was shown to be up-regulated by the Smad3-FoxO Forkhead transcription factor transcriptional complex (50), it is likely that the altered cell growth we observed was due to the manipulation of p52/46ShcA and altered Smad/FOXO/p21 cascade. On the other hand, in cancer cells with Smad4 mutation or aberrant regulation of p21 and/or p15, the alteration of Smad signaling due to a change in ShcA activity may not result in TGF-β-inhibited cell growth.

It is believed that p66ShcA is not involved in the activation of MAPK signaling (51). In fact, p66ShcA was shown to

expression was performed in MCF-10A cells with or without RII knockdown after TGF-β1 treatment for 40 min. *H*, immunoblotting analysis for the indicated gene expression was performed in MCF-7 cells with or without DNRII expression. *T-ERK*, total ERK; *T-Smad2/3*, total Smad2/3; *T-p52ShcA*, total p52ShcA; *con*, control. *Error bars* represent S.E.
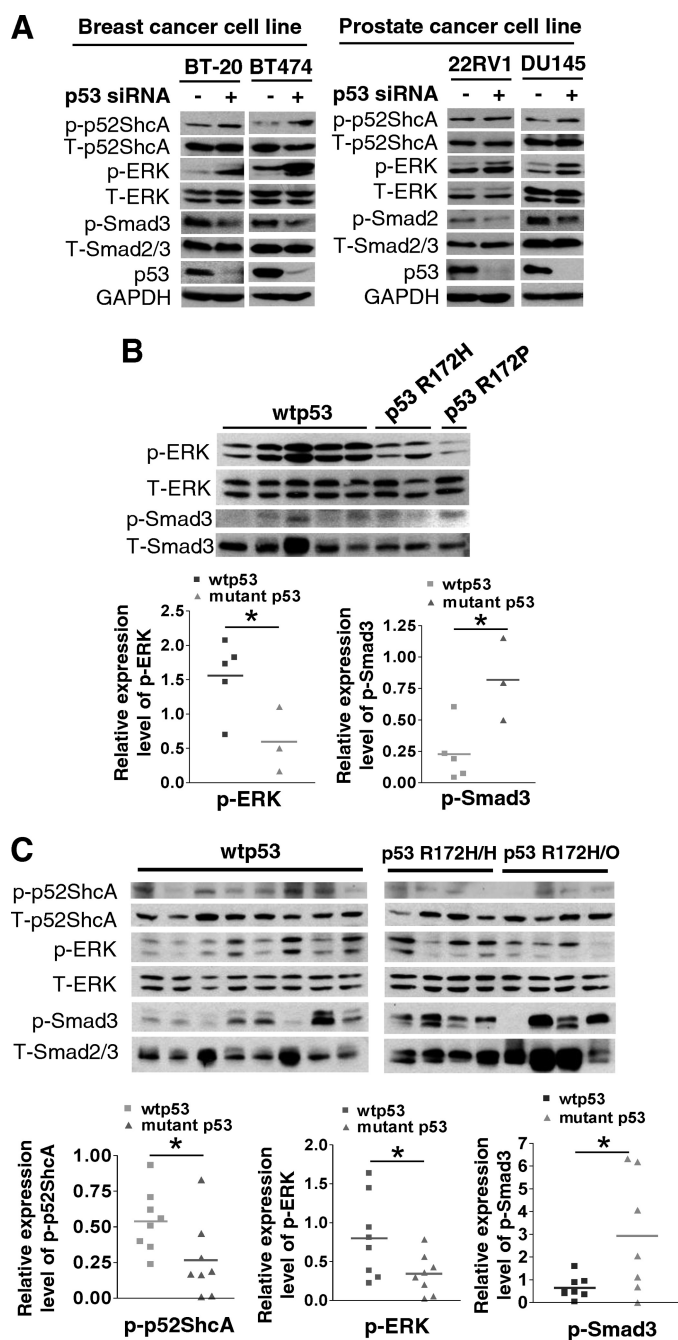
FIGURE 7. Mutant p53 correlates with higher level of Smad-dependent signaling and lower level of ShcA/ERK signaling in human cancer cell lines and genetically altered mouse models. *A*, immunoblotting analysis for the indicated gene expression was performed in BT-20, BT474, 22Rv1, and DU145 cells 72 h after transfection of p53 siRNA 1 or control siRNA. *B*, immunoblotting analysis for the indicated gene expression was performed in the tissue lysates from mammary gland of $p53^{R172H/R172H} p^{un/un}$ (p53 R172H; $n = 2$) and $p53^{R172P/R172P} p^{un/un}$ (p53 R172P; $n = 1$) mice and the littermate $p53^{+/+} p^{un/un}$ (WTp53; $n = 5$). The scatter plot figures under the immunoblots are the total ERK-normalized p-ERK levels and the total Smad2/3-normalized p-Smad3 levels quantified with ImageJ software. *C*, immunoblotting analysis for the indicated gene expression was performed in the tissue lysates from mammary tumors of MMTV-*Wnt1*-*WTp53*$^{+/+}$ (WTp53; $n = 8$), MMTV-*Wnt1*-$p53^{R172H/R172H}$ (p53 R172H/H; $n = 4$), and MMTV-*Wnt1*-$p53^{R172H/O}$ (p53 R172H/O; $n = 4$) mice. The scatter plot figures under the immunoblots are the total p52ShcA-normalized p-p52ShcA levels, total ERK-normalized p-ERK levels, and the total Smad2/3-normalized p-Smad3 levels for each sample quantified with ImageJ software. *, $p < 0.05$. *T-ERK*, total ERK; *T-Smad2/3*, total Smad2/3; *T-p52ShcA*, total p52ShcA.

antagonize ERK activation via negative regulation of c-*fos* promoter activity (52) and to be mainly involved in oxidative stress signaling (53). Additionally, the role of p66ShcA in tumor metastasis is controversial (54, 55). Therefore, the reduction of the p-ERK level after ShcA knockdown with the pan-ShcA siRNA was likely due to the depletion of p52/46ShcA.

Consistent with a previous study demonstrating that knockdown of ShcA or a dominant-negative form of ShcA inhibited TGF-β-induced cell migration and invasion of murine breast cancer cells bearing activated Neu/ErbB-2 receptor (56), our study showed that ShcA depletion-caused down-regulation of ERK signaling resulted in the attenuation of TGF-β-induced cell migration in human untransformed and transformed cells. On the other hand, we found that increased ShcA/ERK signaling augmented TGF-β-induced cell migration. We further showed that in DU145 cells the restored activation of p52/46ShcA/ERK signaling completely switched the role of TGF-β from suppression to promotion of cell migration. ERK signaling-induced cell migration is a key sign of tumor progression (9); therefore, our results provide a novel concept that the ShcA/ERK pathway acts as a pivotal driver of the oncogenic role of TGF-β. In an unpublished study,[3] we found that knockdown of Smad4 in MCF-10A cells moderately reduced TGF-β-induced cell migration in comparison with control siRNA-transfected cells, indicating that Smad-dependent signaling partially contributes to TGF-β-induced cell migration. Here, we showed that the ShcA-mediated increase of TGF-β-induced migration was in the presence of down-regulated Smad signaling. These observations suggest that ShcA-enhanced ERK signaling appears to play a dominant role in TGF-β-induced cell migration. Thus, the down-regulation of p-Smad2/3 is not likely necessary for the ShcA/ERK signaling-mediated increase of TGF-β-induced migration.

In our study, we found that mp53 positively correlates with phosphorylation of R-Smads, whereas it negatively correlates with phosphorylation of p52ShcA and ERK in a panel of mp53-expressing breast and prostate cancer cell lines as well as in mp53 mouse models. We demonstrated that ShcA tipped the balance of the role of TGF-β in tumor progression as evidenced by enhanced migration and attenuated proliferation in the presence of TGF-β. The earlier clinical studies reported that high levels of tyrosine-phosphorylated p52/46Shc in primary tumors might actually identify patients with malignant breast tumors (17, 18). Increased levels of TGF-β are also positively related to poor outcome of human cancer (1). Our finding that overexpression of ShcA enhanced the tumor-promoting activity of TGF-β provides insight in linking these two biomarkers to the disease outcome. In the preclinical models, we and others have shown that anti-TGF-β therapies are potent in treating cancer in which TGF-β functions as a tumor promoter (3–5). However, the lack of knowledge about when TGF-β is switched from a tumor suppressor to a tumor promoter is a major

---

obstacle for the utility of TGF-β antagonists for treating metastatic carcinomas. Thus, our study indicates that the TGF-β-dependent increase of tyrosine-phosphorylated p52/46ShcA may be a promising biomarker for an effective anti-TGF-β cancer therapy. Biomarkers identified by this type of research may help cancer patients benefit from anti-TGF-β therapy in blocking tumor progression in the future.

REFERENCES

1. Massagué, J. (2008) *Cell* **134,** 215–230
2. Sun, L. (2004) *Front. Biosci.* **9,** 1925–1935
3. Bandyopadhyay, A., Agyin, J. K., Wang, L., Tang, Y., Lei, X., Story, B. M., Cornell, J. E., Pollock, B. H., Mundy, G. R., and Sun, L. Z. (2006) *Cancer Res.* **66,** 6714–6721
4. Muraoka, R. S., Dumont, N., Ritter, C. A., Dugger, T. C., Brantley, D. M., Chen, J., Easterly, E., Roebuck, L. R., Ryan, S., Gotwals, P. J., Koteliansky, V., and Arteaga, C. L. (2002) *J. Clin. Investig.* **109,** 1551–1559
5. Yang, Y. A., Dukhanina, O., Tang, B., Mamura, M., Letterio, J. J., MacGregor, J., Patel, S. C., Khozin, S., Liu, Z. Y., Green, J., Anver, M. R., Merlino, G., and Wakefield, L. M. (2002) *J. Clin. Investig.* **109,** 1607–1615
6. Manning, G., Whyte, D. B., Martinez, R., Hunter, T., and Sudarsanam, S. (2002) *Science* **298,** 1912–1934
7. Mulder, K. M. (2000) *Cytokine Growth Factor Rev.* **11,** 23–35
8. Davies, M., Robinson, M., Smith, E., Huntley, S., Prime, S., and Paterson, I. (2005) *J. Cell. Biochem.* **95,** 918–931
9. Reddy, K. B., Nabha, S. M., and Atanaskova, N. (2003) *Cancer Metastasis Rev.* **22,** 395–403
10. Lee, M. K., Pardoux, C., Hall, M. C., Lee, P. S., Warburton, D., Qing, J., Smith, S. M., and Derynck, R. (2007) *EMBO J.* **26,** 3957–3967
11. Ravichandran, K. S. (2001) *Oncogene* **20,** 6322–6330
12. Luzi, L., Confalonieri, S., Di Fiore, P. P., and Pelicci, P. G. (2000) *Current Opin. Genet. Dev.* **10,** 668–674
13. Ventura, A., Maccarana, M., Raker, V. A., and Pelicci, P. G. (2004) *J. Biol. Chem.* **279,** 2299–2306
14. van der Geer, P., Wiley, S., Gish, G. D., and Pawson, T. (1996) *Curr. Biol.* **6,** 1435–1444
15. Lotti, L. V., Lanfrancone, L., Migliaccio, E., Zompetta, C., Pelicci, G., Salcini, A. E., Falini, B., Pelicci, P. G., and Torrisi, M. R. (1996) *Mol. Cell. Biol.* **16,** 1946–1954
16. Ursini-Siegel, J., and Muller, W. J. (2008) *Cell Cycle* **7,** 1936–1943
17. Davol, P. A., Bagdasaryan, R., Elfenbein, G. J., Maizel, A. L., and Frackelton, A. R., Jr. (2003) *Cancer Res.* **63,** 6772–6783
18. Frackelton, A. R., Jr., Lu, L., Davol, P. A., Bagdasaryan, R., Hafer, L. J., and Sgroi, D. C. (2006) *Breast Cancer Res.* **8,** R73
19. Adorno, M., Cordenonsi, M., Montagner, M., Dupont, S., Wong, C., Hann, B., Solari, A., Bobisse, S., Rondina, M. B., Guzzardo, V., Parenti, A. R., Rosato, A., Bicciato, S., Balmain, A., and Piccolo, S. (2009) *Cell* **137,** 87–98
20. Levine, A. J. (1997) *Cell* **88,** 323–331
21. Navone, N. M., Troncoso, P., Pisters, L. L., Goodrow, T. L., Palmer, J. L., Nichols, W. W., von Eschenbach, A. C., and Conti, C. J. (1993) *J. Natl. Cancer Inst.* **85,** 1657–1669
22. Soussi, T., and Béroud, C. (2001) *Nat. Rev. Cancer* **1,** 233–240
23. Wang, S. P., Wang, W. L., Chang, Y. L., Wu, C. T., Chao, Y. C., Kao, S. H., Yuan, A., Lin, C. W., Yang, S. C., Chan, W. K., Li, K. C., Hong, T. M., and Yang, P. C. (2009) *Nat. Cell Biol.* **11,** 694–704
24. Oren, M., and Rotter, V. (2010) *Cold Spring Harb. Perspect. Biol.* **2,** a001107
25. Dong, P., Tada, M., Hamada, J., Nakamura, A., Moriuchi, T., and Sakuragi, N. (2007) *Clin. Exp. Metastasis* **24,** 471–483
26. Kalo, E., Buganim, Y., Shapira, K. E., Besserglick, H., Goldfinger, N., Weisz, L., Stambolsky, P., Henis, Y. I., and Rotter, V. (2007) *Mol. Cell. Biol.* **27,** 8228–8242
27. Ko, Y., Koli, K. M., Banerji, S. S., Li, W., Zborowska, E., Willson, J. K., Brattain, M. G., and Arteaga, C. L. (1998) *Int. J. Oncol.* **12,** 87–94
28. Bandyopadhyay, A., Wang, L., López-Casillas, F., Mendoza, V., Yeh, I. T., and Sun, L. (2005) *Prostate* **63,** 81–90
29. Singh, J., Chuaqui, C. E., Boriack-Sjodin, P. A., Lee, W. C., Pontz, T., Corbley, M. J., Cheung, H. K., Arduini, R. M., Mead, J. N., Newman, M. N., Papadatos, J. L., Bowes, S., Josiah, S., and Ling, L. E. (2003) *Bioorg. Med. Chem. Lett.* **13,** 4355–4359
30. Lei, X., Bandyopadhyay, A., Le, T., and Sun, L. (2002) *Oncogene* **21,** 7514–7523
31. Zawel, L., Dai, J. L., Buckhaults, P., Zhou, S., Kinzler, K. W., Vogelstein, B., and Kern, S. E. (1998) *Mol. Cell* **1,** 611–617
32. Chen, C., Wang, X. F., and Sun, L. (1997) *J. Biol. Chem.* **272,** 12862–12867
33. Lang, G. A., Iwakuma, T., Suh, Y. A., Liu, G., Rao, V. A., Parant, J. M., Valentin-Vega, Y. A., Terzian, T., Caldwell, L. C., Strong, L. C., El-Naggar, A. K., and Lozano, G. (2004) *Cell* **119,** 861–872
34. Liu, G., Parant, J. M., Lang, G., Chau, P., Chavez-Reyes, A., El-Naggar, A. K., Multani, A., Chang, S., and Lozano, G. (2004) *Nat. Genet.* **36,** 63–68
35. Aubrecht, J., Secretan, M. B., Bishop, A. J., and Schiestl, R. H. (1999) *Carcinogenesis* **20,** 2229–2236
36. Post, S. M., Quintás-Cardama, A., Terzian, T., Smith, C., Eischen, C. M., and Lozano, G. (2010) *Oncogene* **29,** 1260–1269
37. Isaacs, W. B., Carter, B. S., and Ewing, C. M. (1991) *Cancer Res.* **51,** 4716–4720
38. Liu, X., Sun, Y., Constantinescu, S. N., Karam, E., Weinberg, R. A., and Lodish, H. F. (1997) *Proc. Natl. Acad. Sci. U.S.A.* **94,** 10669–10674
39. Ramachandra, M., Atencio, I., Rahman, A., Vaillancourt, M., Zou, A., Avanzini, J., Wills, K., Bookstein, R., and Shabram, P. (2002) *Cancer Res.* **62,** 6045–6051
40. Lei, X., Yang, J., Nichols, R. W., and Sun, L. Z. (2007) *Exp. Cell Res.* **313,** 1687–1695
41. Bartek, J., Iggo, R., Gannon, J., and Lane, D. P. (1990) *Oncogene* **5,** 893–899
42. van Bokhoven, A., Varella-Garcia, M., Korch, C., Johannes, W. U., Smith, E. E., Miller, H. L., Nordeen, S. K., Miller, G. J., and Lucia, M. S. (2003) *Prostate* **57,** 205–225
43. Berglind, H., Pawitan, Y., Kato, S., Ishioka, C., and Soussi, T. (2008) *Cancer Biol. Ther.* **7,** 699–708
44. Vogelstein, B., and Kinzler, K. W. (1993) *Trends Genet.* **9,** 138–141
45. Buganim, Y., Solomon, H., Rais, Y., Kistner, D., Nachmany, I., Brait, M., Madar, S., Goldstein, I., Kalo, E., Adam, N., Gordin, M., Rivlin, N., Kogan, I., Brosh, R., Sefadia-Elad, G., Goldfinger, N., Sidransky, D., Kloog, Y., and Rotter, V. (2010) *Cancer Res.* **70,** 2274–2284
46. Muller, P. A., Caswell, P. T., Doyle, B., Iwanicki, M. P., Tan, E. H., Karim, S., Lukashchuk, N., Gillespie, D. A., Ludwig, R. L., Gosselin, P., Cromer, A., Brugge, J. S., Sansom, O. J., Norman, J. C., and Vousden, K. H. (2009) *Cell* **139,** 1327–1341
47. Signoretti, S., Waltregny, D., Dilks, J., Isaac, B., Lin, D., Garraway, L., Yang, A., Montironi, R., McKeon, F., and Loda, M. (2000) *Am. J. Pathol.* **157,** 1769–1775
48. Okada, S., Yamauchi, K., and Pessin, J. E. (1995) *J. Biol. Chem.* **270,** 20737–20741
49. Huse, M., Chen, Y. G., Massagué, J., and Kuriyan, J. (1999) *Cell* **96,** 425–436
50. Seoane, J., Le, H. V., Shen, L., Anderson, S. A., and Massagué, J. (2004) *Cell* **117,** 211–223
51. Jackson, J. G., Yoneda, T., Clark, G. M., and Yee, D. (2000) *Clin. Cancer*

Res. **6,** 1135–1139

52. Migliaccio, E., Mele, S., Salcini, A. E., Pelicci, G., Lai, K. M., Superti-Furga, G., Pawson, T., Di Fiore, P. P., Lanfrancone, L., and Pelicci, P. G. (1997) *EMBO J.* **16,** 706–716

53. Migliaccio, E., Giorgio, M., Mele, S., Pelicci, G., Reboldi, P., Pandolfi, P. P., Lanfrancone, L., and Pelicci, P. G. (1999) *Nature* **402,** 309–313

54. Ma, Z., Liu, Z., Wu, R. F., and Terada, L. S. (2010) *Oncogene* **29,** 5559–5567

55. Rajendran, M., Thomes, P., Zhang, L., Veeramani, S., and Lin, M. F. (2010) *Cancer Metastasis Rev.* **29,** 207–222

56. Northey, J. J., Chmielecki, J., Ngan, E., Russo, C., Annis, M. G., Muller, W. J., and Siegel, P. M. (2008) *Mol. Cell. Biol.* **28,** 3162–3176

Mice heterozygous for *CREB binding protein* are hypersensitive to γ-radiation and invariably develop myelodysplastic/myeloproliferative neoplasm

Stephanie N. Zimmer[a,b,*], Madeleine E. Lemieux[c,*], Bijal P. Karia[a,b], Claudia Day[b], Ting Zhou[a,b], Qing Zhou[b], Andrew L. Kung[c], Uthra Suresh[b], Yidong Chen[b,d], Marsha C. Kinney[e], Alexander J.R. Bishop[a,b], and Vivienne I. Rebel[a,b]

[a]Department of Cellular and Structural Biology; [b]Greehey Children's Cancer Research Institute, University of Texas Health Science Center at San Antonio, Tx., USA; [c]Department of Pediatric Oncology, Dana-Farber Cancer Institute and Harvard Medical School, Boston, Mass., USA; [d]Department of Epidemiology and Biostatistics; [e]Department of Pathology, University of Texas Health Science Center at San Antonio, Tx., USA

Myelodysplastic syndrome is a complex family of preleukemic diseases in which hematopoietic stem cell defects lead to abnormal differentiation in one or more blood lineages. Disease progression is associated with increasing genomic instability and a large proportion of patients go on to develop acute myeloid leukemia. Primarily a disease of the elderly, it can also develop after chemotherapy. We have previously reported that *CREB binding protein (Crebbp)* heterozygous mice have an increased incidence of hematological malignancies, and others have shown that *CREBBP* is one of the genes altered by chromosomal translocations found in patients suffering from therapy-related myelodysplastic syndrome. This led us to investigate whether hematopoietic tumor development in *Crebbp*^{+/−} mice is preceded by a myelodysplastic phase and whether we could uncover molecular mechanisms that might contribute to its development. We report here that *Crebbp*^{+/−} mice invariably develop myelodysplastic/myeloproliferative neoplasm within 9 to 12 months of age. They are also hypersensitive to ionizing radiation and show a marked decrease in poly(ADP-ribose) polymerase-1 activity after irradiation. In addition, protein levels of XRCC1 and APEX1, key components of base excision repair machinery, are reduced in unirradiated *Crebbp*^{+/−} cells or upon targeted knockdown of CREBBP levels. Our results provide validation of a novel myelodysplastic/myeloproliferative neoplasm mouse model and, more importantly, point to defective repair of DNA damage as a contributing factor to the pathogenesis of this currently incurable disease. © 2012 ISEH - Society for Hematology and Stem Cells. Published by Elsevier Inc.

Myelodysplastic syndromes (MDS) is a complex family of preleukemic diseases in which hematopoietic stem cell (HSC) defects lead to abnormal differentiation in one or more blood lineages. Disease progression is associated with increasing genomic instability and a large proportion of patients go on to develop acute myeloid leukemia (AML) (reviewed in [1]). Primarily a disease of the elderly, MDS/AML can also develop after treatment with alkylating agents, radiation, and topoisomerase II inhibitors [2,3]. The

poor outcomes and increasing incidence of MDS, due to an aging population and increasing numbers of cancer survivors, motivated our efforts to better understand the pathogenesis of this disease.

Studies in marrow or blood cells from patients suffering from AML or myeloproliferative neoplasms (MPNs) suggest that inadequate DNA repair may play an important role in the etiology of these diseases. It has been shown that some of the frequently observed genomic aberrations in these diseases [4–7] cause excessive DNA damage by increasing the production of reactive oxygen species and/ or usage of alternative, error-prone DNA repair pathways. This mechanism of genomic instability, or mutator phenotype, as proposed by Loeb [8], explains why progression of many of these diseases is associated with increasing genetic abnormalities. MDS patient samples have been less extensively investigated in this context; however,

increased oxidative DNA damage has been observed in blood cells from MDS patients [9,10] and DNA repair deficiencies have been demonstrated in MDS patients with a high risk of progressing toward leukemia [9,11]. Moreover, children suffering from diseases due to mutated genes essential for DNA repair, such as Fanconi anemia [12], Bloom disease [13,14], and Rothmund-Thomson syndrome [15,16], have an increased risk of developing MDS.

CREB binding protein (CREBBP) interacts with DNA damage response/repair proteins, such as TP53 [17,18] and BRCA1 [19], among others, to enhance their function. CREBBP also helps remodel chromatin through its histone acetyltransferase activity, thereby facilitating DNA repair [20,21]. Finally, CREBBP modulates the activity of poly(ADP-ribose) polymerase-1 (PARP1), an accessory factor in transcriptional regulation and base-excision repair (BER) (reviewed in [22]). Because the amount of CREBBP is dose-limiting within the cell [23,24], a decrease in its availability is likely to impair its ability to enhance DNA repair.

We previously reported that $\sim$40% of *Crebbp* heterozygous mice develop hematological malignancies [25] and others have shown that *CREBBP* is one of the genes involved in chromosomal translocations found in patients suffering from therapy-related MDS [26]. We now report that *Crebbp*$^{+/-}$ mice invariably develop MDS/MPN within 9 to 12 months of age and are hypersensitive to γ-radiation. Mechanistically, we find a marked decrease in PARP1 activity upon exposure to ionizing radiation and a reduction of key BER proteins in progenitor and stem cell-enriched bone marrow (BM), suggesting deficient DNA repair as a contributing factor to their disease.

Material and methods

Mice

Crebbp$^{+/-}$ mice [25] were fully backcrossed onto a C57BL/6 background. Wild-type (WT) littermates served as controls. Mice were bred and maintained under microisolator conditions at the animal facility of University of Texas Health Science Center at San Antonio. All animal procedures were in accordance with University policies regarding animal care and use.

Total body irradiation (TBI) and survival analysis

WT and *Crebbp*$^{+/-}$ mice (3- to 6-month-old) received a total dose of 10 or 11 Gy (90–100 cGy/min from a Co^{60} source (Theratron T-780 unit; Atomic Energy of Canada Limited, Chalk River, Ontario, Canada), delivered as two equal doses of 5 or 5.5 Gy, respectively, 5 hours apart. Kaplan-Meier curves and log rank survival statistics were generated using the R-project survival package [27,28].

Blood analysis, histology, flow cytometry, and in vitro methylcellulose assays

Standard techniques were used. See Supplementary Materials and Methods for details (online only, available at www.exphem.org).

Short hairpin RNA (shRNA) knockdown of CREBBP in EML1 cells

A lentivirus-encoded shRNA targeting the sequence 5′-CAAG CACTGGGAATTCTCT-3′ from mouse *Crebbp* was created by cloning oligonucleotides into the FSIPPW vector as described previously [29]. A lentivirus targeting enhanced green fluorescent protein (5′-AAGAACGGCATCAAGGTGAACTT-3′) was used as a control. Both were packaged as described previously [30]. Cotransfection of 293TD cells was performed using lipofectamine 2000 as per manufacturer's instructions (Invitrogen, Carlsbad, CA, USA).

EML1 cells (CRL-11691; ATCC, Manassas, VA, USA) [31], were cultured in Iscove's modified Dulbecco's medium supplemented with 20% fetal bovine serum (StemCell Technologies, Vancouver, BC, Canada) and recombinant murine stem cell factor (100 ng/mL; R&D Systems, Minneapolis, MN, USA) and were never carried for more than 3 months. Undifferentiated EML1 cells were split 1 day before infection. Virus-containing supernatant supplemented with 8 μg/mL protamine was added to the cells and left until a complete medium change the next morning. At the end of day 2, another round of infection was performed using a flow-through infection protocol, as described previously [32]. On day 3, infected cells were selected in puromycin (3 μg/mL). EML1 cells were cloned in methylcellulose-based medium (M3234, StemCell Technologies) and expanded in liquid medium.

Gene expression and network analysis

Total RNA was isolated in two independent experiments from HSCs sorted from WT and *Crebbp*$^{+/-}$ day 14.5 fetal livers as described in the Supplementary Material and Methods (online only, available at www.exphem.org). For each, 12 ng were amplified, in duplicate, using the Ovation RNA Amplification Kit (NuGen Technologies, Inc., San Carlos, CA, USA) and hybridized to Affymetrix Gene Chip Mouse Genome 430 2.0. Data files are MIAME-compliant and available from the Gene Expression Omnibus (accession GSE18061). Arrays were normalized, corrected for background and analyzed using R and the Bioconductor *gcrma* package [27,33]. After averaging technical replicates, litter-paired *t*-tests with *p* values <0.05 and a fold-change >1.5 were used as the cutoff for calling significant change. Quantitative reverse transcription polymerase chain reaction for two genes on three independent samples were consistent with the microarray results (*Klf6* average $\pm$ standard deviation: on microarray = 1.8 $\pm$ 0.0, by quantitative reverse transcription polymerase chain reaction = 2.8 $\pm$ 1.4; *Tcf4* average $\pm$ standard deviation on microarray = 1.1 $\pm$ 0.03, by quantitative reverse transcription polymerase chain reaction = 1.1 $\pm$ 0.09). To generate protein interaction networks (PINs), murine genes were mapped via the National Center for Biotechnology Information HomoloGene database (May 2009) to their human homologs (Supplementary Table E1; online only, available at www.exphem.org). The human proteins were used to retrieve direct binding partners from the human interactome [34], where both binding partners were called "present" by Affymetrix MAS5 (Bioconductor *affy* package implementation [35]) in at least one sample, resulting in a reference "HSC PIN" of 4,237 proteins and 14,704 interactions. Similarly, the 93 distinct genes we found significantly altered in *Crebbp*$^{+/-}$ HSCs relative to WT corresponded to 39 human homologs that were represented in the HSC PIN. Together, these 39 proteins and their direct interactors comprise the *Crebbp*-target PIN of 258 proteins and 257 interactions. Cytoscape [36] was used to

visualize the resulting networks and its BinGO plugin [37] to determine Gene Ontology (GO) annotation enrichment. We used our HSC PIN as the background for enrichment with a *p* value <0.01 as cutoff.

Protein extracts
Peripheral blood (PB) cells were obtained from more than three mice and pooled. Leukocytes were irradiated with 6 Gy (1 Gy/min) using a Gammacell 40 Cesium Unit (Atomic Energy of Canada Limited). Postirradiation cells were either put on ice directly or incubated for various times at 37°C to allow DNA repair to occur. Cells were lyzed in RIPA buffer for CREBBP Westerns or in NaCl lysis buffer (0.1 M NaCl, 50 mM Tris-HCl [pH 7.2], 1 mM dithiothreitol) containing phosphatase and protease inhibitors in other cases. After lysis, CREBBP and PARP1 samples were centrifuged at 14,000 rpm for 10 minutes at 4°C and supernatant protein concentrations determined by BCA protein assays (Pierce, Rockford, IL, USA). For BER protein Westerns, lysates were passed five times through a QIAshredder homogenizer (Qiagen, Valencia, CA, USA), then centrifuged at 16,000 rcf for 10 minutes at 4°C and the supernatants concentrated for 40 minutes at 14,800 rcf in Amicon Ultra-0.5 filter devices (Millipore, Billerica, MA, USA). After concentration, the protein lysates were diluted 1:1 with a 10 mM Tris-HCl (pH 7.5), 1 mM EDTA, 1 mM dithiothreitol, 20% glycerol solution, and protein concentrations determined by Bradford assays (Sigma, St Louis, MO, USA).

Western blots
Equal amounts of protein extract were separated on 12% Bis-Tris gels and transferred to nitrocellulose membranes (Invitrogen). Primary antibodies used: CREBBP (AC26 [38]), XRCC1 (Santa Cruz Biotechnology, Inc., Santa Cruz, CA, USA) and from Abcam, Cambridge, MA, USA: ACTB, LIG1, POLB, APEX1, TRP53, phospho-TRP53 (Ser15), PARP1. They were visualized with horseradish peroxidase–coupled secondary antibodies (Cell Signaling, Danvers, MA, USA) and ECL Plus solution (Amersham, Piscataway, NJ, USA) and quantified with densitometry using Image J software (National Institutes of Health, Bethesda, MD, USA).

PARP1 activity assay
PARP1 activity in protein extracts from PB and BM (200 ng/25 μL), or EML1 cells (400 ng/25 μL) was measured using the HT Colorimetric PARP1/Apoptosis Assay Kit (Trevigen, Gaithersburg, MD, USA) following manufacturer's instructions. The absorbance of the colorimetric substrate was read at 450 nm on a Spectramax M5 spectrophotometer (Molecular Devices, Sunnyvale, CA, USA).

Statistical analysis
Unless otherwise indicated, Excel (Microsoft, Redmond, WA, USA) was used to perform *t*-tests. The R *stats* package [27] was used for the paired condition and time-series *t*-test and the Kolmogorov-Smirnov distribution test. In all cases, *p* values <0.05 were considered statistically significant.

Results

Myelodysplastic features of Crebbp^{+/−} mice
To determine whether *Crebbp*^{+/−} mice might harbor previously undetected MDS, we compared the hematopoietic system of 3- to 4-month-old and 9- to 12-month-old *Crebbp*^{+/−} mice with that of age-matched WT controls. The number of cells harvested from two femurs was similar for both age groups and genotypes (Fig. 1A), but *Crebbp*^{+/−} mice were significantly smaller by weight than their WT counterpart (Fig. 1B). When BM cellularity was corrected for weight, we found that the marrow of *Crebbp*^{+/−} mice was significantly more cellular than WT (Fig. 1C). At both ages, a mild but significant splenomegaly was also observed in *Crebbp*^{+/−} mice (Fig. 1D).

This marrow hypercellularity was not accompanied by an increase in the number of colony-forming cells (CFCs). On the contrary, 9- to 12-month-old *Crebbp*^{+/−} mice had significantly fewer CFCs in their marrow than WT mice, most notably granulocytic and monocytic CFCs (Fig. 1E). No significant differences were detectable between young *Crebbp*^{+/−} and WT mice (data not shown). A decrease in the numbers of myeloid CFCs in the context of an overall increase in BM cellularity and splenomegaly is indicative of abnormal myeloid differentiation.

Histological examination of blood smears and BM preparations revealed distinct dysplastic features [39,40] of *Crebbp*^{+/−} blood cell differentiation (Fig. 2), including hypersegmented granulocytes (Fig. 2B; 55% of 9- to 12-month-old mice) and leukocytes with a pseudo Pelger-Huët anomaly (Fig. 2C; 22%). *Crebbp*^{+/−} BM preparations confirmed the hypercellularity and showed an increased myeloid to erythroid ratio, mostly due to an excess of mature granulocytes (Fig. 2E). More than half of the 9- to 12-month-old *Crebbp*^{+/−} mice exhibited either increased numbers of megakaryocytes or abnormal forms such as hyperlobulated cells (Fig. 2F) or naked nuclei (Fig. 2G).

Unlike older mice, 3- to 4-month-old *Crebbp*^{+/−} mice displayed none of these characteristics; interestingly, however, 2 of 14 young animals examined had small clusters of immature cells in the center of the marrow space (Fig. 2H and inset). This atypical localization of immature precursors is indicative of very early stages of myelodysplastic hematopoiesis and possibly the onset of leukemia. Another common finding in MDS, particularly in its early stages, is an increase in apoptosis in marrow progenitors (reviewed in [1]). Consistent with this, Figure 2I shows a significant increase in Annexin V$^+$ cells in the lineage-depleted (Lin$^−$) fraction of marrow enriched for stem and progenitor cells but not in whole BM.

Altered numbers of HSCs and myeloid progenitors in Crebbp^{+/−} mice
Fluorescence-activated cell sorting analysis at 3 to 4 months of age showed that the only significant, albeit small, difference in hematopoietic cell populations between *Crebbp*^{+/−} and WT mice was an increased proportion of Gr-1^{lo}Mac-1^{++} myeloid cells in the BM (15.3% ± 2.4% vs 12.7% ± 1.3%; *p* = 0.015). By 9 to 12 months of age, however, the frequency of long-term HSCs was
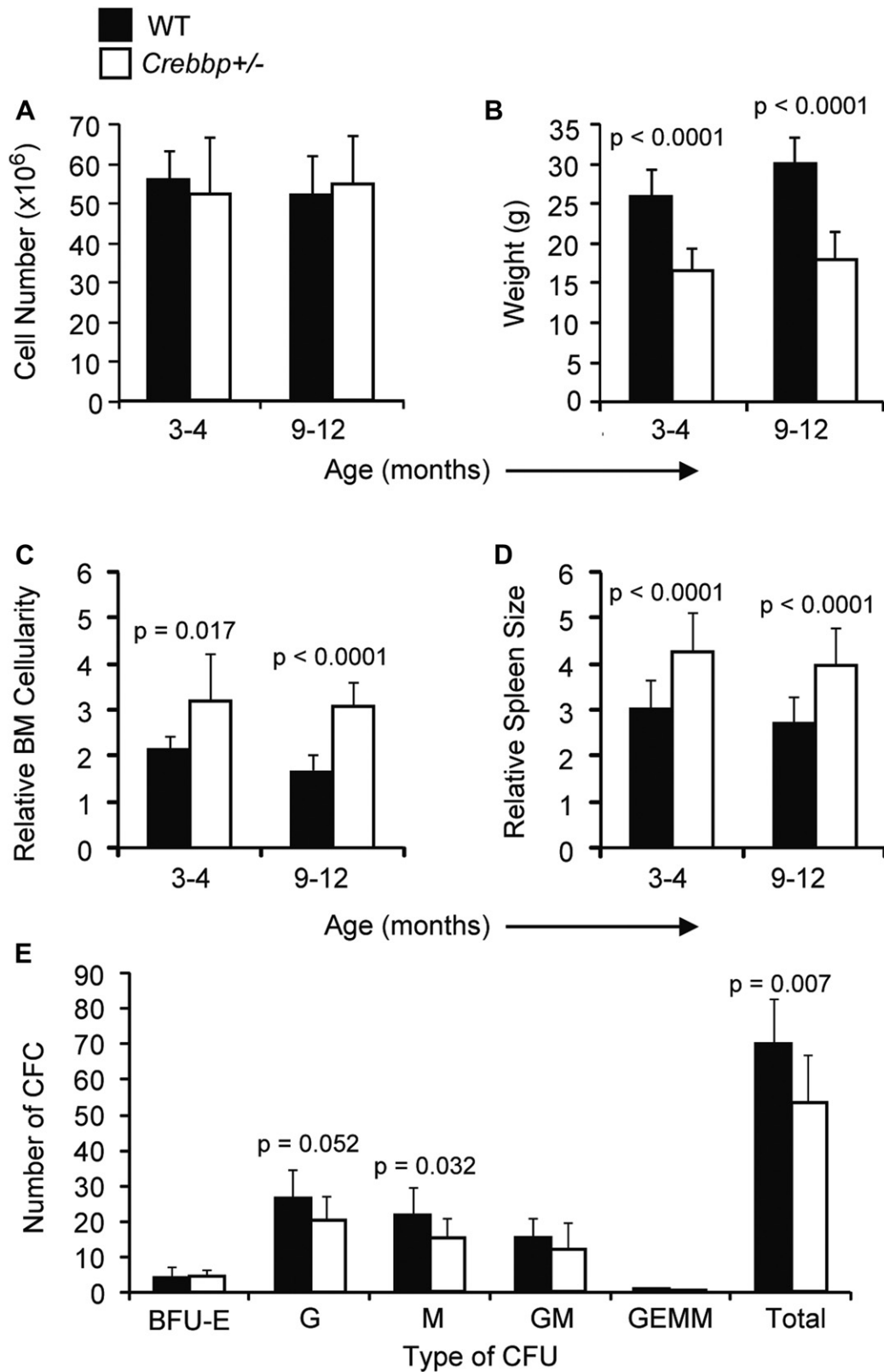
Figure 1. Hypercellularity, mild splenomegaly, and low CFC counts in $Crebbp^{+/-}$ mice (**A**) Number of BM cells in two femurs ($\times 10^6$) and (**B**) body weights of 3- to 4- or 9- to 12-month-old mice, as indicated. (**C**) Relative BM cellularity and (**D**) spleen size (in mg) corrected for body weight (g). (**E**) Number and type of colony-forming units (CFU) from an input of 1×10^4 BM cells from 9- to 12-month-old mice. Bars represent average ($\pm$standard deviation). Seven to 10 animals were used per group. Significant differences are indicated by *p* values.
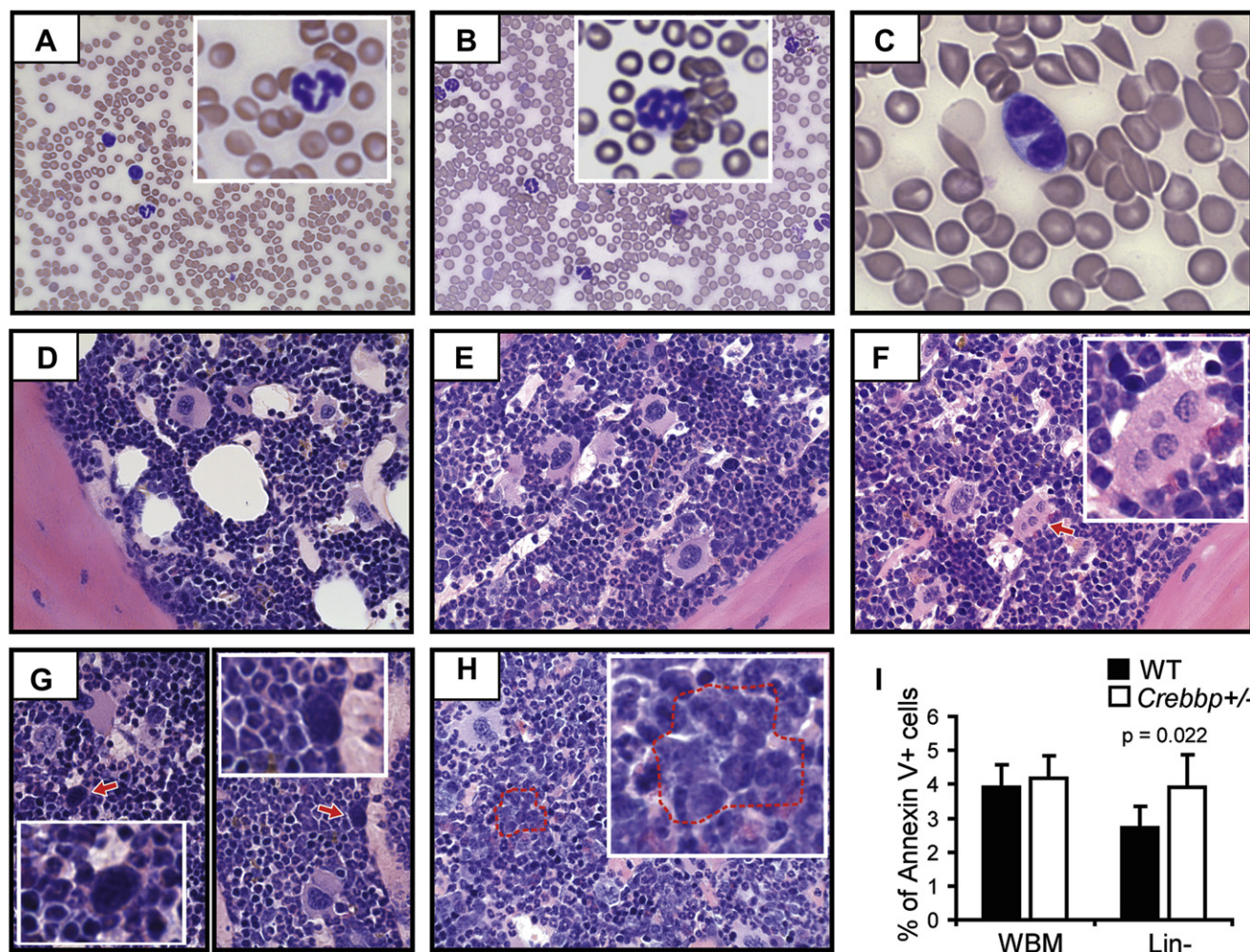
Figure 2. Histopathology and Annexin V staining of WT and *Crebbp*^{+/−} animals. (A–C) Wright-stained PB cells from 9- to 12-month-old mice. (A) WT control. (B, C) *Crebbp*^{+/−} blood smears showing hypersegmented granulocytes (i.e., granulocytes with more than six segments of irregular size) (B, inset) and (C) a pseudo Pelger-Huët anomaly. (D–H) Bone sections from 9- to 12-month-old mice. (D) WT control. (E–H) *Crebbp*^{+/−} sections. (E) Hypercellular marrow and an increased myeloid to erythroid ratio due to increased mature granulocytes, particularly near the bony trabeculae. (F, G) Abnormal megakaryocytic differentiation with hyperlobulated megakaryocytes (F, arrow and inset) and naked megakaryocytic nuclei (G, arrow and inset). (H, and inset) Clusters of immature precursor cells present in the middle of the marrow cavity. Magnification: 40× (A, B, D–H), 60× (C). (I) Quantification of apoptosis by Annexin V staining of whole (WBM) and lineage-depleted (Lin−) bone marrow isolated from WT and *Crebbp*^{+/−} mice (n = 7). *p* value indicated where significant.

significantly lower in *Crebbp*^{+/−} BM compared to control (Fig. 3A), resulting in ∼2-fold fewer long-term HSCs per femur (2300 ± 1100 vs 4400 ± 1900, respectively; *p* = 0.007). These mice also showed a decrease in common myeloid progenitors and an expansion of granulocyte/macrophage progenitors (Fig. 3B). No differences between *Crebbp*^{+/−} and WT mice were found with respect to megakaryocyte/erythroid progenitors (Fig. 3B) or common lymphoid progenitors (Fig. 3C).

Because primitive BM progenitors represent only a very small proportion of the total BM content, the expansion of granulocyte/macrophage progenitors alone cannot explain the greater marrow cellularity observed in the older *Crebbp*^{+/−} mice relative to controls. Moreover, histological analysis suggested that the difference was due to an increase in mature myeloid cells in the marrow (Fig. 2E).

Indeed, relative to controls, *Crebbp*^{+/−} marrow contained significantly more Gr-1^{lo}Mac-1^{+/+} and Gr-1^{+/+}Mac-1^{+/+} myeloid cells (Fig. 4A). Concurrent PB cell analysis of 9- to 12-month-old mice by fluorescence-activated cell sorting (Fig. 4B) and complete blood count (Fig. 4C) showed a significant increase in granulocytes, while the lymphoid cell compartment contracted. In contrast, total leukocyte, erythrocyte, and platelet numbers measured by complete blood count were similar to age-matched controls (data not shown). By 1 year of age, the relative number of myeloid cells had therefore significantly increased in *Crebbp*^{+/−} mice at the expense of lymphoid cells.

Taken together, the hematopoietic characteristics of 9- to 12-month-old *Crebbp*^{+/−} mice are clearly different from those found in *Crebbp*^{+/−} mice suffering from myeloid leukemia, as described previously [25] and shown in
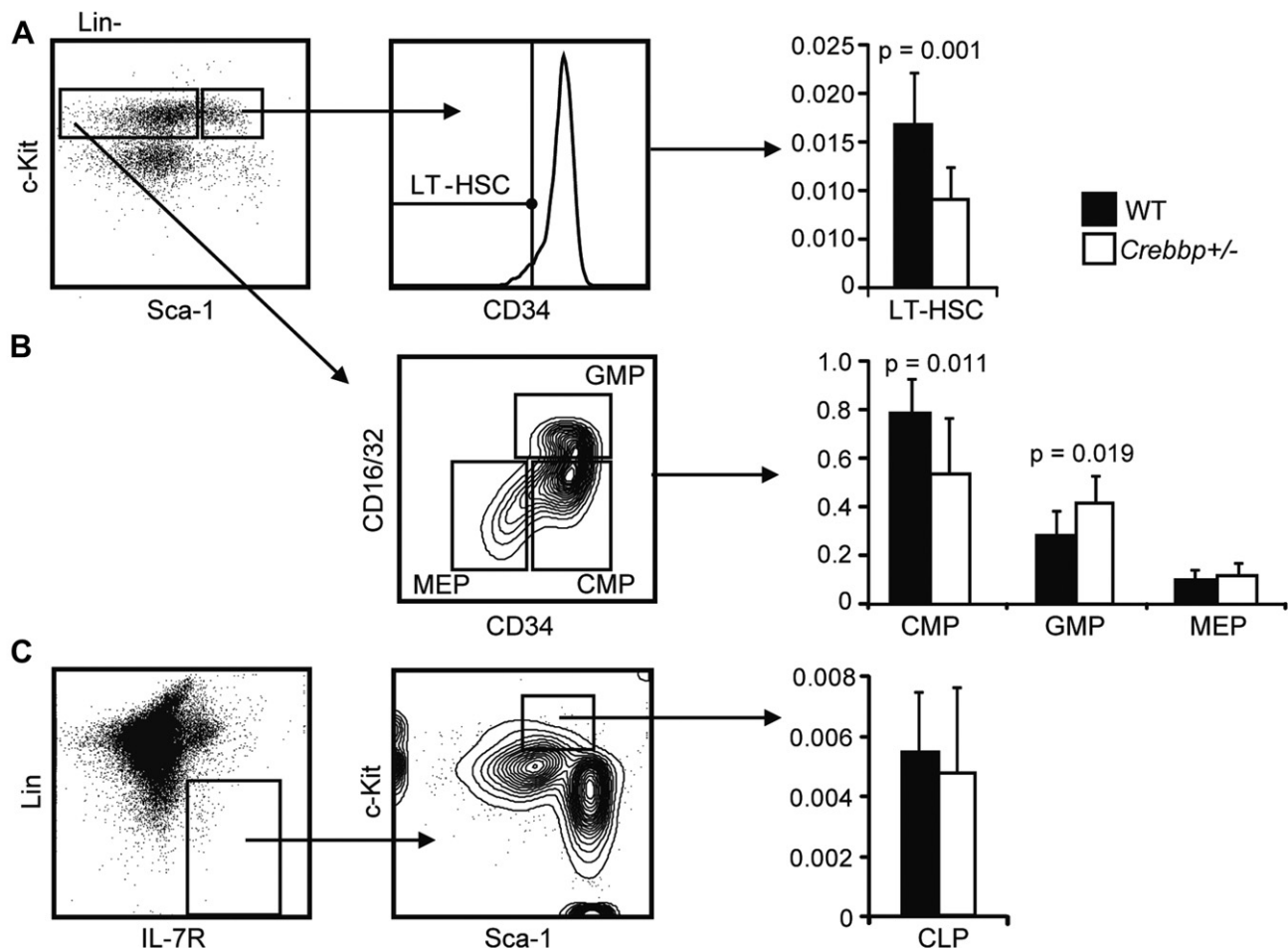
Figure 3. Abnormal numbers of HSCs, common myeloid progenitors, and granulocyte/macrophage progenitors in $Crebbp^{+/-}$ mice. (A–C) Left and middle panels depict the sorting strategy used for each BM population, and bar graphs on the right show average percentages ($\pm$standard deviation) for the corresponding cell population(s). (A) Long-term HSCs (LT-HSCs) are selected from mature lineage marker–negative (Lin$^-$) c-Kit^{++}Sca-1$^+$ cells (rightmost sorting gate of the dot plot) that are also CD34$^-$ (histogram). (B) Immature myeloid progenitors are identified by separating Lin$^-$Sca-1$^-$c-Kit^{++} BM cells on the basis of CD16/32 and CD34 expression as shown. (C) Common lymphoid progenitors (CLPs) are purified from whole BM (WBM) based first on expression of interleukin-7R but not of other mature lineage markers. Cells in the sorting gate of the dot plot are then further analyzed for c-Kit and Sca-1 expression (contour plot). CLPs are c-Kit$^+$ Sca-1(intermediate) cells. Significant differences are indicated by *p* values with 9 to 12 mice used in each analysis.

Supplementary Figure E1 (online only, available at www.exphem.org). These features are reminiscent of human MDS, most consistent with MDS/MPN according to the current World Health Organization classification [41].

Changes in apoptosis and DNA damage repair pathways predicted by expression profiling of Crebbp$^{+/-}$ HSCs
As MDS is considered a stem cell disease, we compared gene expression profiles of $Crebbp^{+/-}$ and WT HSCs in the hope of uncovering molecular mechanisms that might be at its root. We chose to isolate HSCs from fetal livers because at this stage there were no overt differences between $Crebbp^{+/-}$ and WT hematopoiesis (data not shown). Any differences in gene expression found in $Crebbp^{+/-}$ fetal liver HSCs would thus more likely reflect the initially altered genetic program of HSC regulation as opposed to adaptation to a compromised or failing hematopoietic system.

GO annotation analysis of the protein-coding genes differentially expressed in $Crebbp^{+/-}$ HSCs (Supplementary Table E1; online only, available at www.exphem.org) showed little enrichment in any particular pathway or process. However, it has been shown that PINs can be used to predict loss-of-function phenotypes through so-called "guilt by association" [42]. Because there is better coverage of the human than of the murine interactome, we generated a reference PIN consisting of human proteins corresponding to all genes expressed in fetal liver HSCs (HSC PIN) and assumed that key hematopoietic pathways and processes are preserved in both species. We next generated a CREBBP PIN nucleated by the human homologs of genes differentially expressed in $Crebbp^{+/-}$ fetal liver HSCs relative to WT ("seed proteins," Fig. 5A larger nodes) and their coexpressed, direct binding partners (Fig. 5A, smaller nodes). By comparing the HSC and CREBBP PINs, we sought to identify pathways that might be altered by
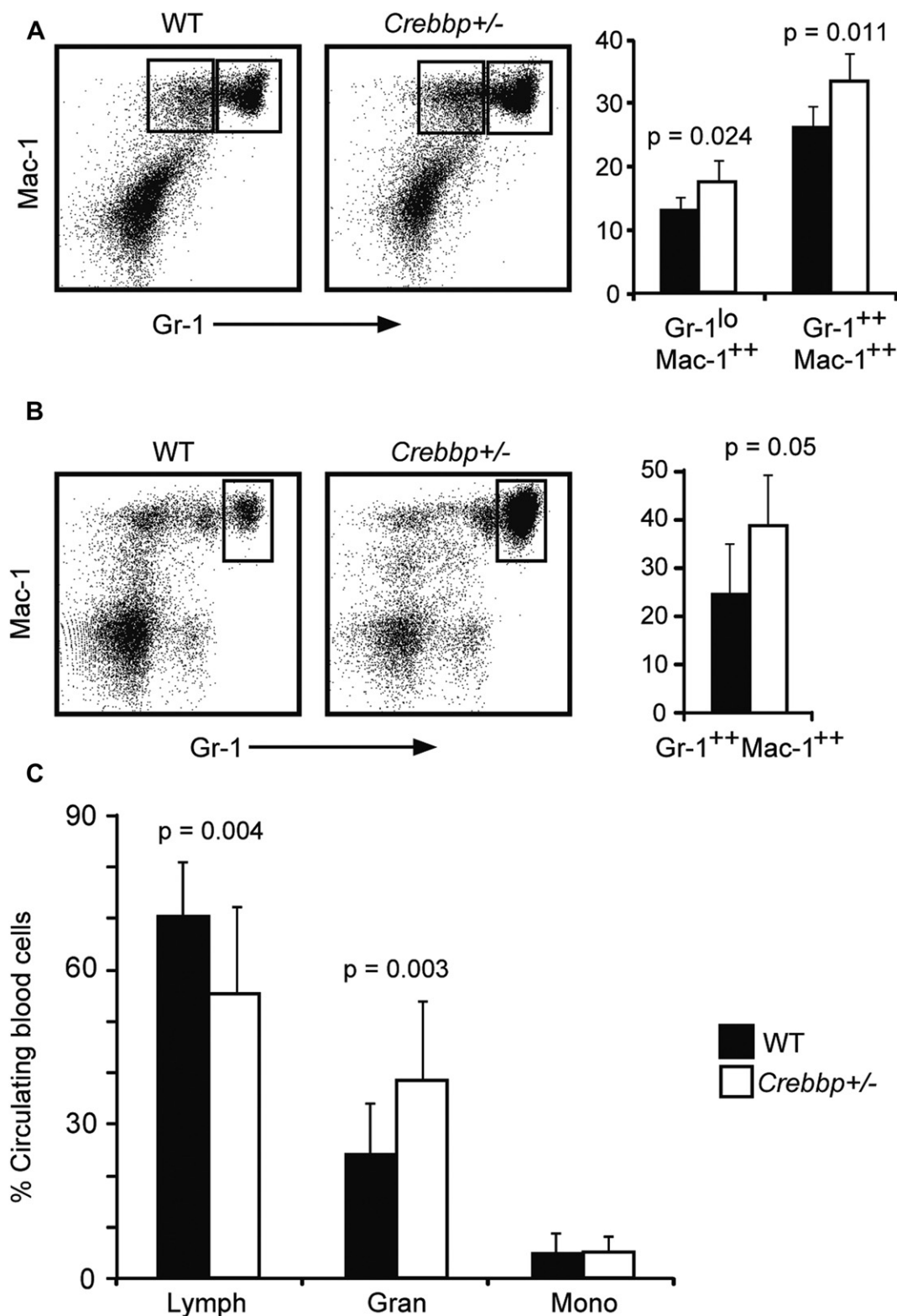
Figure 4. Increased mature myeloid cells in the BM and PB of *Crebbp*^{+/−} mice. (**A, B**) Representative fluorescence-activated cell sorting a profiles of WT (left) and *Crebbp*^{+/−} cells (middle) immunostained for Mac-1 and Gr-1 expression. Right panels show average percentages (±standard deviation [SD]) from profiles of five to eight mice for the indicated cell populations. (**A**) Identification of granulocytes (Mac-1^{++}Gr-1^{++}, right gate) and more immature myeloid cells (Mac-1^{++}Gr-1^{lo} cells, left dot plot gate) in BM. (**B**) Identification of granulocytes (as indicated by the gate) in PB. (**C**) Average proportion (±SD) of lymphocytes (LYMPH), granulocytes (GRAN), and monocytes (MONO) in PB measured by complete blood count (n = 16–17). In all bar graphs, significant differences are indicated by *p* values.

"guilty" interactions between the primary CREBBP target genes and other HSC-expressed proteins.

GO term enrichment analysis of the CREBBP PIN identified two interesting pathways significantly enriched above the HSC PIN background. First, 28 proteins were annotated to the GO term *programmed cell death* (GO:0012501; black and green nodes in Fig. 5A and Supplementary Table E2 [online only, available at www.exphem.org], $p = 5 \times 10^{-3}$). Of those, 20 were annotated to the more specific term *positive regulation of apoptosis* (GO:0043065). Second, 25 proteins were annotated to the GO term *response to DNA damage stimulus* (GO:0006974; blue and green nodes in Fig. 5A, Supplementary Table E2 [online only, available at www.exphem.org], $p = 9 \times 10^{-3}$), 20 of which corresponded to the more specific term *DNA repair* (GO:0006281).

As a control, we randomly selected 10,000 sets of 39 proteins normally expressed in HSCs, retrieved their interaction partners as before and determined the proportion of cases in which the overlap was greater than for the CREBBP PIN as an empirical test of significance. For programmed cell death and response to DNA damage stimulus, the *p* values were 0.033 and 0.045, respectively, supporting our contention that both these pathways might be indirectly affected in *Crebbp*$^{+/-}$ HSCs through direct interaction with primary CREBBP targets. The involvement of apoptotic pathways is consistent with our finding, described here, of increased apoptosis in *Crebbp*$^{+/-}$ Lin$^-$ cells (Fig. 2I). Analysis of purified adult BM HSCs revealed a similar, significant increase in apoptosis in *Crebbp*$^{+/-}$ HSCs (Fig. 5B, paired *t*-test; $p = 0.021$).

Increased hypersensitivity of Crebbp$^{+/-}$ *mice to ionizing radiation*

The possibility that responses to DNA damage, and particularly DNA repair functions, might be altered in *Crebbp*$^{+/-}$ HSCs was of considerable interest because this has only been linked fairly recently to the development of chromosomal abnormalities in MDS and its progression to AML [9,11]. If the CREBBP PIN prediction of impaired DNA repair were correct, one might expect *Crebbp*$^{+/-}$ animals to have an altered sensitivity to DNA-damaging agents.

We tested this hypothesis by subjecting groups of mice to a split-dose of 11 Gy TBI. Immediately after TBI, mice received various doses of BM cells (Fig. 5C) or no cells at all (Fig. 5D). As expected, WT controls not transplanted with a supportive hematopoietic graft all died 11 to 13 days after irradiation. All WT animals receiving a transplant of 5.0×10^6 marrow cells survived, as did 9 of 11 receiving a ∼30-fold smaller graft of 1.5×10^5 cells. In contrast, 5 of 22 *Crebbp*$^{+/-}$ mice receiving the high-dose graft died and only 1 of 11 recipients of the low dose BM cells survived the first 2 weeks after TBI (Fig. 5C). To rule out the possibility that differences in survival were due to the *Crebbp*$^{+/-}$ microenvironment having a negative impact on homing of the transplanted cells, we also compared the

intrinsic sensitivity of mice to a 10-Gy split-dose TBI in the absence of supporting BM cells (Fig. 5D). In this case, all *Crebbp*$^{+/-}$ mice died before the first WT mouse succumbed to hematopoietic failure. Moreover, approximately one third of the WT mice survived a 10-Gy split-dose TBI.

Decreased PARP1 activity and BER protein levels in Crebbp$^{+/-}$ *cells*

Two notable players in the detection and repair of DNA lesions present in the CREBBP PIN by association with a direct target are TP53 and PARP1 (Fig. 5A). We decided to examine both more closely. Western blot analysis of PB leukocytes obtained before and after γ-irradiation showed no clear differences in total or Ser15-phosphorylated TRP53 levels between the two genotypes (Supplementary Figure E2A; online only, available at www.exphem.org), nor did we find any clear differences in full-length or cleaved PARP1 protein levels (Supplementary Figure E2B; online only, available at www.exphem.org). PARP1 activity was slightly, but not significantly, lower in *Crebbp*$^{+/-}$ cells before irradiation (Fig. 6A). However, immediately after irradiation, *Crebbp*$^{+/-}$ leukocytes showed significantly lower levels in enzymatic activity at several time points (Fig. 6A, asterisks). Comparing responses between *Crebbp*$^{+/-}$ and WT cells during the entire 12-hour period revealed that PARP1 activity is significantly dampened by the reduction of CREBBP levels (*t*-test paired by condition and time point; $p = 8.8 \times 10^{-6}$). We next looked in unirradiated whole BM and Lin$^-$ BM to see whether PARP1 activity was reduced in more primitive hematopoietic cell populations. Similar to unirradiated PB, *Crebbp*$^{+/-}$ BM samples showed decreased PARP1 activity compared to WT but not to a statistically significant level (Fig. 6B).

PARP1 plays an important, although not enzymatic, role in BER by protecting single-strand breaks until repair can proceed. Consistent with this, cells that lack PARP1 rapidly accumulate DNA breaks and *Parp1*$^{-/-}$ animals are extremely sensitive to γ-irradiation (reviewed in [22]). Because we had observed the same radiation hypersensitivity in *Crebbp*$^{+/-}$ mice, and because MDS patients are thought to have deficiencies in BER [9], we wondered whether other BER proteins were affected by a reduction in CREBBP. When we measured the abundance of several key BER proteins in *Crebbp*$^{+/-}$ and WT Lin$^-$ BM cells, we found a modest reduction in XRCC1 and DNA polymerase β (POLB) and a significant decrease in AP endonuclease (APEX1) abundance in *Crebbp*$^{+/-}$ Lin$^-$ cells (Fig. 6C). To determine whether the changes in PARP1 activity and BER protein levels were directly related to reduced CREBBP levels, we knocked down *Crebbp* expression in the multipotential hematopoietic EML1 cell line [31]. Consistent with the *Crebbp*$^{+/-}$ Lin$^-$ BM cells, shRNA-mediated reduction of CREBBP levels in unirradiated EML1 cells resulted in a marked decrease in XRCC1 levels and more modest changes in other BER protein levels (Fig. 6D, E), whereas
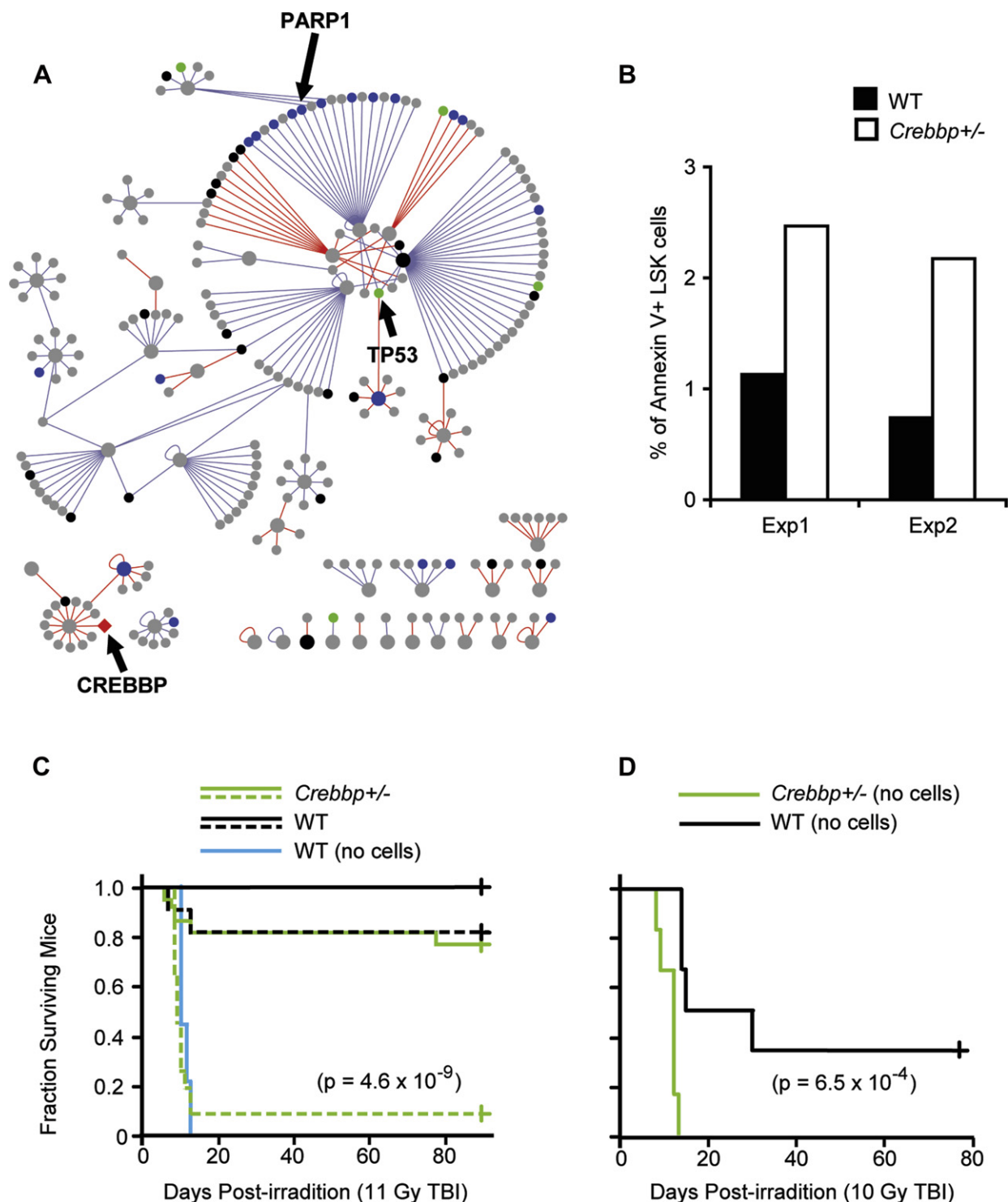
Figure 5. Decreased survival of *Crebbp*^{+/−} mice in response to ionizing radiation consistent with CREBBP PIN predictions. (**A**) Predicted interaction network of proteins encoded by genes differentially expressed in *Crebbp*^{+/−} HSCs relative to WT (larger circles) and their direct interaction partners (smaller circles). Red edges indicate interactions with proteins encoded by genes upregulated in *Crebbp*^{+/−} HSCs, while blue edges mark interactions with proteins encoded by downregulated genes. Black nodes mark proteins implicated in programmed cell death and blue nodes those involved in responses to DNA damage. Green nodes are annotated to both processes and gray nodes to neither. See Supplementary Tables E1 and E2 [online only, available at www. exphem.org] for full lists of genes. (**B**) Quantification of apoptosis by Annexin V staining in the stem cell compartment (LSK; Lin[−];Sca-1^{+};cKit[++]) of WT and *Crebbp*^{+/−} mice. Depicted is the data of two independent experiments. (**C**) Kaplan-Meier curves for WT (black and blue lines) and *Crebbp*^{+/−} mice (green lines) after exposure to 11 Gy γ-radiation. Mice received either no cells (control, blue line [n = 9]), a single dose of 1×10^5 BM cells (dashed lines; n = 11) or 5×10^6 BM cells (solid lines, n = 22). (**D**) Kaplan-Meier curves for WT (black line) and *Crebbp*^{+/−} (green line) mice after exposure to 10 Gy of γ-radiation with no injected cells. (**C, D**) Log-rank *p* values for the difference in survival between WT (excluding control animals) and *Crebbp*^{+/−} as indicated.
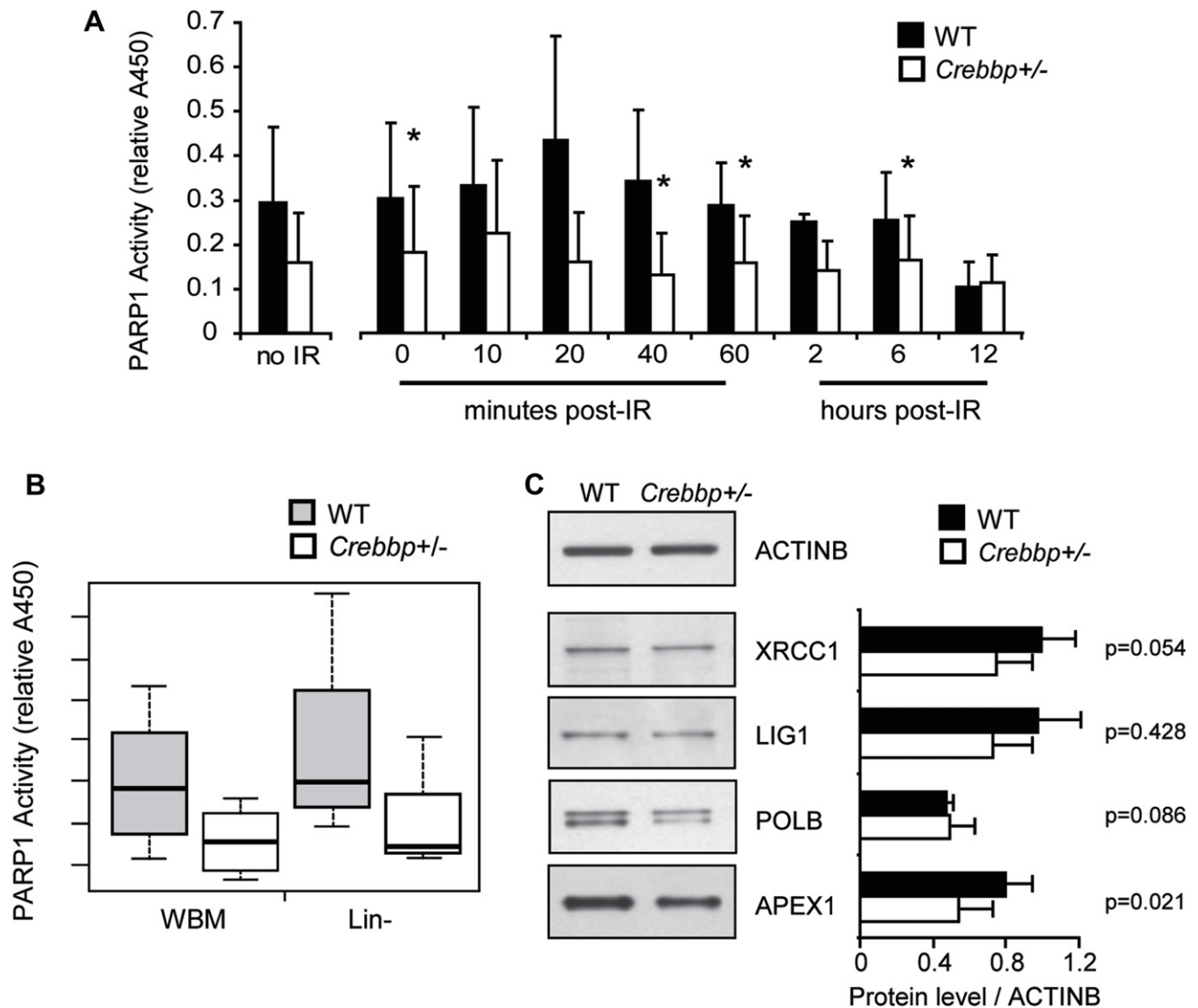
Figure 6. PARP1 enzymatic activity and BER protein levels in cells with reduced CREBBP levels. (**A**) PARP1 enzymatic activity measured in PB cells of WT and $Crebbp^{+/-}$ mice before (no irradiation [IR]) and at various time points after 6 Gy of radiation exposure (post-IR). Presented are average values (±standard error of mean) of three independent experiments. Asterisks indicate statistical significance at individual time points between WT and $Crebbp^{+/-}$ cells (paired t-test; *$p < 0.05$). (**B**) PARP1 activity in nonirradiated WBM and Lin$^-$ cells from WT and $Crebbp^{+/-}$ animals (n = 3–4). In the boxplot, the horizontal line represents the median and the boxes extend from the 25th to 75th percentile. The whiskers extend to the maximum and minimum values. (**C**) Representative Western blots (left) of the indicated BER proteins in unirradiated Lin$^-$ BM and corresponding average levels (±standard deviation) relative to ACTB in four experiments (right). Probabilities that protein levels are significantly reduced in $Crebbp^{+/-}$ cells (one-sided paired t-test) as shown.

an irrelevant shRNA against enhanced green fluorescent protein had no effect. Decreased availability of CREBBP thus has a negative impact on the abundance of BER proteins, which may explain the increased radiosensitivity of $Crebbp^{+/-}$ mice and their predisposition for developing MDS.

Discussion

Several MDS mouse models have been described to date (reviewed in [39]), each capturing some features of this notoriously variable disease. The histopathology, hemato-

logical characteristics, and increased progenitor/stem cell apoptosis of our $Crebbp^{+/-}$ mice constitute a good model for human MDS/MPN as defined in the current World Health Organization classification [41].

Our protein network analysis predicted an impaired ability to respond to and repair DNA damage in $Crebbp^{+/-}$ cells. Consistent with this, our study revealed a significant hypersensitivity of $Crebbp^{+/-}$ mice to high-dose ionizing TBI. TP53 and PARP1 are both present in the CREBBP PIN and their functions are known to be modulated through acetylation by CREBBP/EP300

Figure 6. *(Cotinued).* (**D**) Western blots of CREBBP and BER proteins in parental EML1 cells, control enhanced green fluorescent protein (eGFP) knockdown cells and in five independent *Crebbp* knockdown (KD) clones. (**E**) Quantification of CREBBP and BER proteins in t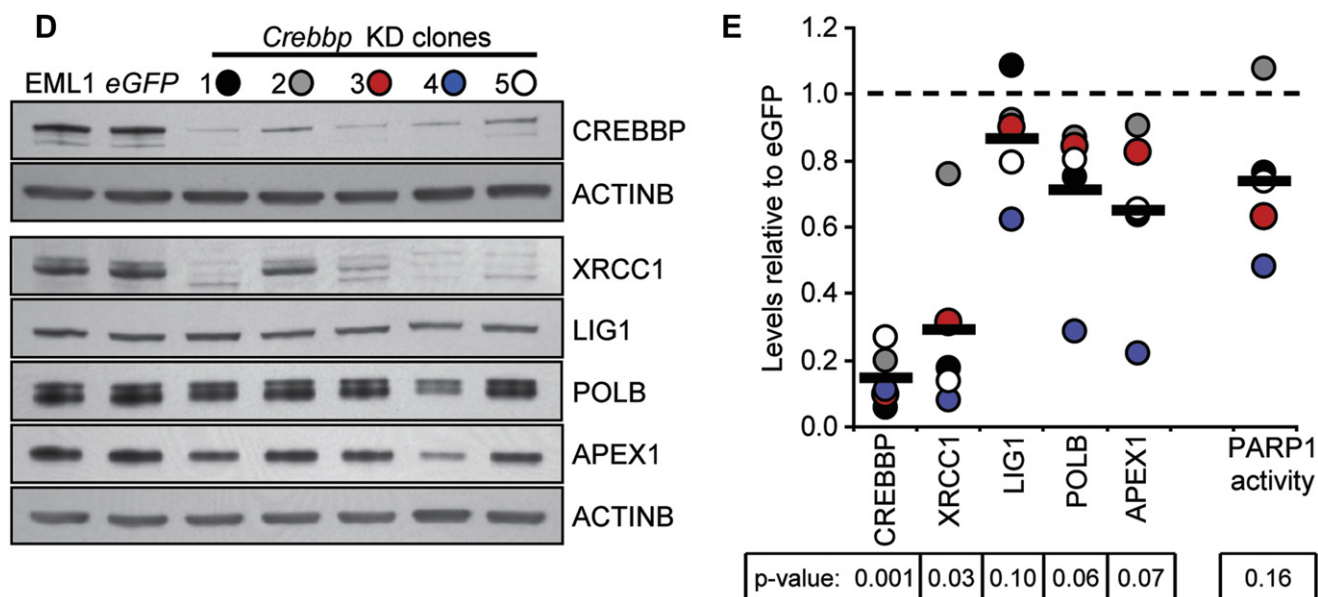he *Crebbp* KD clones color-coded as in (**D**) relative to eGFP control levels (dashed line). PARP1 activity in unirradiated cells in the corresponding clones is shown on the right. Horizontal bars indicate mean values. Likelihood that values are normally distributed around 1 (P(X ∼ Norm(1,1)), Kolmogorov-Smirnov Test) are indicated below the figure.

[17,18,22]. However, a recent report showed that neither CREBBP nor its paralog EP300 are required for TRP53-dependent upregulation of *Cdkn1a* and *Mdm2* following DNA damage [43]. Consistent with this observation, we found that neither total nor Ser15-phosphorylated TRP53 protein levels were altered in PB by a reduction in CREBBP levels. Nor could we detect any significant differences in PARP1 abundance between WT and *Crebbp*^{+/−} cells, before or after irradiation. In contrast, PARP1 enzymatic activity tended to be lower in cells with reduced levels of CREBBP and was dampened in PB cells in response to radiation. An interesting question arises from this observation: does acetylation by CREBBP/EP300 of PARP1 enhance not only PARP1's transcriptional coactivation functions [22], but also its enzymatic or repair-associated activities? Further studies will be required to formally address this.

The majority of endogenous DNA damage, such as caused by reactive oxygen species, is repaired by BER. PARP1 binds and protects single strand DNA breaks and further facilitates BER by recruiting other BER proteins such as APEX1, LIG3, POLB, and XRCC1 to the site of damage (reviewed in [44]). In this study, we demonstrate that a reduction in CREBBP causes these BER protein levels to decline, some more than others. There is evidence to suggest that even small changes in the relative abundance of these essential BER proteins can cause aberrant BER, which can lead to increased mutagenesis and genomic instability [44]. This raises the possibility that loss of a single copy of *Crebbp* constitutes a mutator phenotype [8] predisposing *Crebbp*^{+/−} animals to MDS/AML.

In summary, we have demonstrated a previously undetected but highly penetrant MDS/MPN in *Crebbp*^{+/−} mice. These animals are also radiosensitive, a common feature of human MDS [11], although not shown yet for MDS/MPN in particular. In addition, we found significantly decreased PARP1 enzymatic activity in *Crebbp*^{+/−} blood cells and an imbalance of BER proteins. Further studies will be required to fully elucidate the molecular mechanisms at play and determine the direct impact of these CREBBP-associated changes on BER activity and genomic instability.

Conflict of interest disclosure
No financial interest/relationships with financial interest relating to the topic of this article have been declared.

References

1. Corey SJ, Minden MD, Barber DL, Kantarjian H, Wang JC, Schimmer AD. Myelodysplastic syndromes: the complexity of stem-cell diseases. Nat Rev Cancer. 2007;7:118–129.
2. Godley LA, Larson RA. Therapy-related myeloid leukemia. Semin Oncol. 2008;35:418–429.
3. Vardiman JW, Harris NL, Brunning RD. The World Health Organization (WHO) classification of the myeloid neoplasms. Blood. 2002;100: 2292–2302.
4. Sallmyr A, Fan J, Datta K, et al. Internal tandem duplication of FLT3 (FLT3/ITD) induces increased ROS production, DNA damage, and misrepair: implications for poor prognosis in AML. Blood. 2008; 111:3173–3182.
5. Koptyra M, Falinski R, Nowicki MO, et al. BCR/ABL kinase induces self-mutagenesis via reactive oxygen species to encode imatinib resistance. Blood. 2006;108:319–327.
6. Nowicki MO, Falinski R, Koptyra M, et al. BCR/ABL oncogenic kinase promotes unfaithful repair of the reactive oxygen species-dependent DNA double-strand breaks. Blood. 2004;104:3746–3753.
7. Plo I, Nakatake M, Malivert L, et al. JAK2 stimulates homologous recombination and genetic instability: potential implication in the heterogeneity of myeloproliferative disorders. Blood. 2008;112: 1402–1412.
8. Loeb LA. A mutator phenotype in cancer. Cancer Res. 2001;61: 3230–3239.
9. Jankowska AM, Gondek LP, Szpurka H, Nearman ZP, Tiu RV, Maciejewski JP. Base excision repair dysfunction in a subgroup of patients with myelodysplastic syndrome. Leukemia. 2008;22:551–558.
10. Novotna B, Bagryantseva Y, Siskova M, Neuwirtova R. Oxidative DNA damage in bone marrow cells of patients with low-risk myelodysplastic syndrome. Leuk Res. 2009;33:340–343.
11. Kuramoto K, Ban S, Oda K, Tanaka H, Kimura A, Suzuki G. Chromosomal instability and radiosensitivity in myelodysplastic syndrome cells. Leukemia. 2002;16:2253–2258.
12. Alter BP, Giri N, Savage SA, et al. Malignancies and survival patterns in the National Cancer Institute inherited bone marrow failure syndromes cohort study. Br J Haematol. 2010;150:179–188.
13. Iwahara Y, Ishii K, Watanabe S, Taguchi H, Hara H, Miyoshi I. Bloom's syndrome complicated by myelodysplastic syndrome and multiple neoplasia. Intern Med. 1993;32:399–402.
14. Poppe B, Van Limbergen H, Van Roy N, et al. Chromosomal aberrations in Bloom syndrome patients with myeloid malignancies. Cancer Genet Cytogenet. 2001;128:39–42.
15. Narayan S, Fleming C, Trainer AH, Craig JA. Rothmund-Thomson syndrome with myelodysplasia. Pediatr Dermatol. 2001;18:210–212.
16. Pianigiani E, De Aloe G, Andreassi A, Rubegni P, Fimiani M. Rothmund-Thomson syndrome (Thomson-type) and myelodysplasia. Pediatr Dermatol. 2001;18:422–425.
17. Gu W, Roeder RG. Activation of p53 sequence-specific DNA binding by acetylation of the p53 C-terminal domain. Cell. 1997;90:595–606.
18. Gu W, Shi XL, Roeder RG. Synergistic activation of transcription by CBP and p53. Nature. 1997;387:819–823.
19. Pao GM, Janknecht R, Ruffner H, Hunter T, Verma IM. CBP/p300 interact with and function as transcriptional coactivators of BRCA1. Proc Natl Acad Sci U S A. 2000;97:1020–1025.
20. Karagiannis TC, Harikrishnan KN, El-Osta A. Disparity of histone deacetylase inhibition on repair of radiation-induced DNA damage on euchromatin and constitutive heterochromatin compartments. Oncogene. 2007;26:3963–3971.
21. Masumoto H, Hawke D, Kobayashi R, Verreault A. A role for cell-cycle-regulated histone H3 lysine 56 acetylation in the DNA damage response. Nature. 2005;436:294–298.
22. Krishnakumar R, Kraus WL. The PARP side of the nucleus: molecular actions, physiological outcomes, and clinical targets. Mol Cell. 2010; 39:8–24.
23. Horvai AE, Xu L, Korzus E, et al. Nuclear integration of JAK/STAT and Ras/AP-1 signaling by CBP and p300. Proc Natl Acad Sci U S A. 1997;94:1074–1079.
24. Kamei Y, Xu L, Heinzel T, et al. A CBP integrator complex mediates transcriptional activation and AP-1 inhibition by nuclear receptors. Cell. 1996;85:403–414.
25. Kung AL, Rebel VI, Bronson RT, et al. Gene dose-dependent control of hematopoiesis and hematologic tumor suppression by CBP. Genes Dev. 2000;14:272–277.
26. Bedford DC, Kasper LH, Fukuyama T, Brindle PK. Target gene context influences the transcriptional requirement for the KAT3 family of CBP and p300 histone acetyltransferases. Epigenetics. 2010;5:9–15.
27. R: A language and environment for statistical computing. Vienna, Austria: R Foundation for Statistical Computing; 2009.
28. Harrington DP, Fleming TR. A class of rank test procedures for sensored survival data. Biometrika. 1982;69:553–566.
29. Kanellopoulou C, Muljo SA, Kung AL, et al. Dicer-deficient mouse embryonic stem cells are defective in differentiation and centromeric silencing. Genes Dev. 2005;19:489–501.
30. Lois C, Hong EJ, Pease S, Brown EJ, Baltimore D. Germline transmission and tissue-specific expression of transgenes delivered by lentiviral vectors. Science. 2002;295:868–872.
31. Tsai S, Bartelmez S, Sitnicka E, Collins S. Lymphohematopoietic progenitors immortalized by a retroviral vector harboring a dominant-negative retinoic acid receptor can recapitulate lymphoid, myeloid, and erythroid development. Genes Dev. 1994;8:2831–2841.
32. Chuck AS, Palsson BO. Consistent and high rates of gene transfer can be obtained using flow-through transduction over a wide range of retroviral titers. Hum Gene Ther. 1996;7:743–750.
33. Gentleman RC, Carey VJ, Bates DM, et al. Bioconductor: open software development for computational biology and bioinformatics. Genome Biol. 2004;5:R80.
34. Rual JF, Venkatesan K, Hao T, et al. Towards a proteome-scale map of the human protein-protein interaction network. Nature. 2005;437:1173–1178.
35. Gautier L, Cope L, Bolstad BM, Irizarry RA. affy–analysis of Affymetrix GeneChip data at the probe level. Bioinformatics. 2004;20:307–315.
36. Cline MS, Smoot M, Cerami E, et al. Integration of biological networks and gene expression data using Cytoscape. Nat Protoc. 2007;2:2366–2382.
37. Maere S, Heymans K, Kuiper M. BiNGO: a Cytoscape plugin to assess overrepresentation of gene ontology categories in biological networks. Bioinformatics. 2005;21:3448–3449.
38. Yao TP, Oh SP, Fuchs M, et al. Gene dosage-dependent embryonic development and proliferation defects in mice lacking the transcriptional integrator p300. Cell. 1998;93:361–372.
39. Beachy SH, Aplan PD. Mouse models of myelodysplastic syndromes. Hematol Oncol Clin North Am. 2010;24:361–375.
40. Brunning RD, Orazi A, Germing U, Le Beau MM. Myelodysplastic syndromes/neoplasms, overview. In: Swerdlow SH, Campo E, Harris NL, et al., eds. WHO classification of tumours of haematopoietic and lymphoid tissues. Lyon: International Agency for Research on Cancer (IARC); 2008. p. 88–93.
41. Vardiman JW, Thiele J, Arber DA, et al. The 2008 revision of the World Health Organization (WHO) classification of myeloid neoplasms and acute leukemia: rationale and important changes. Blood. 2009;114:937–951.
42. McGary KL, Lee I, Marcotte EM. Broad network-based predictability of Saccharomyces cerevisiae gene loss-of-function phenotypes. Genome Biol. 2007;8:R258.
43. Kasper LH, Thomas MC, Zambetti GP, Brindle PK. Double null cells reveal that CBP and p300 are dispensable for p53 targets p21 and Mdm2 but variably required for target genes of other signaling pathways. Cell Cycle. 2011;10:212–221.
44. Nemec AA, Wallace SS, Sweasy JB. Variant base excision repair proteins: contributors to genomic instability. Semin Cancer Biol. 2010;20:320–328.

Supplementary materials and methods

Blood analysis

Complete blood counts (i.e., red blood cells, white blood cells, and differential counts) were performed on a VetScan HM2 hematology system (Abaxis, Union City, CA, USA).

Histology

Histological analysis of the BM was performed on Wright-stained touch preparations and whole BM tissue sections. For the latter, tibias were fixed at room temperature in 10% formalin for 24 hours (Fisher Diagnostics, ThermoFisher Scientific, Waltham, MA, USA). After decalcification in CalRite solution (Richard-Allan Scientific, ThermoFisher Scientific,Waltham, MA, USA) for 15 hours, the bones were stored in 70% ethanol before embedding in paraffin and sectioning and staining with hematoxylin and eosin for analysis. Images were produced using an Olympus BX51 microscope and an Infinity1 camera. Infinity Analyze software v.4.6 (http/www.lumenera.com) was used to capture the images.

Flow cytometry

Well-established fluorescence-activated cell sorting protocols were used to purify long-term HSCs and progenitor cells from the BM [1–3]. Myeloid cells were stained with antibodies against Gr-1 and Mac-1. PB lymphocytes were detected with antibodies against B cells (CD45R) and T cells (CD4, CD8). Fetal liver HSCs were obtained by first performing a positive selection for $AA4.1^+$ cells (Easysep; StemCell Technologies) and then sorting for $Sca-1^+Lin^-AA4.1^+c-Kit^{++}$ [4]. To measure apoptosis, 1.0×10^5 cells were resuspended in 100 μL $1\times$ binding buffer and stained with 1.5 μL Annexin V-fluorescence isothiocyanate and 5 μL propidium iodide according to manufacturer's instructors (BD Biosciences). Sorting and analyses were performed on a dual-laser BD FACSAria or a BD FACSCanto (BD Biosciences). Antibodies were purchased from BD Biosciences.

In vitro methylcellulose assay

Unfractionated BM cells (1.5×10^4 cells/dish) were plated in duplicate in methylcellulose-containing medium (M3434; StemCell Technologies). Burst-forming units-erythroid, colony-forming units (CFU)-granulocyte, CFU-macrophage, CFU-mixed granulocyte-macrophage, and CFU-mixed granulocyte-erythrocyte-macrophage-megakaryocyte colonies were scored 12 to 14 days later on standard morphological criteria (http://www.stemcell.com/technical/28405_methocult%20M.pdf).

References

1. Akashi K, Traver D, Miyamoto T, Weissman IL. A clonogenic common myeloid progenitor that gives rise to all myeloid lineages. Nature. 2000;404:193–197.
2. Kondo M, Weissman IL, Akashi K. Identification of clonogenic common lymphoid progenitors in mouse bone marrow. Cell. 1997;91:661–672.
3. Osawa M, Hanada K, Hamada H, Nakauchi H. Long-term lymphohematopoietic reconstitution by a single CD34-low/negative hematopoietic stem cell. Science. 1996;273:242–245.
4. Ivanova NB, Dimos JT, Schaniel C, Hackney JA, Moore KA, Lemischka IR. A stem cell molecular signature. Science. 2002;298:601–604.

A

Mac-1 (log intensity)

BM

PB

Gr-1 (log intensity)

B

i ii iii iv

C

i ii iii iv
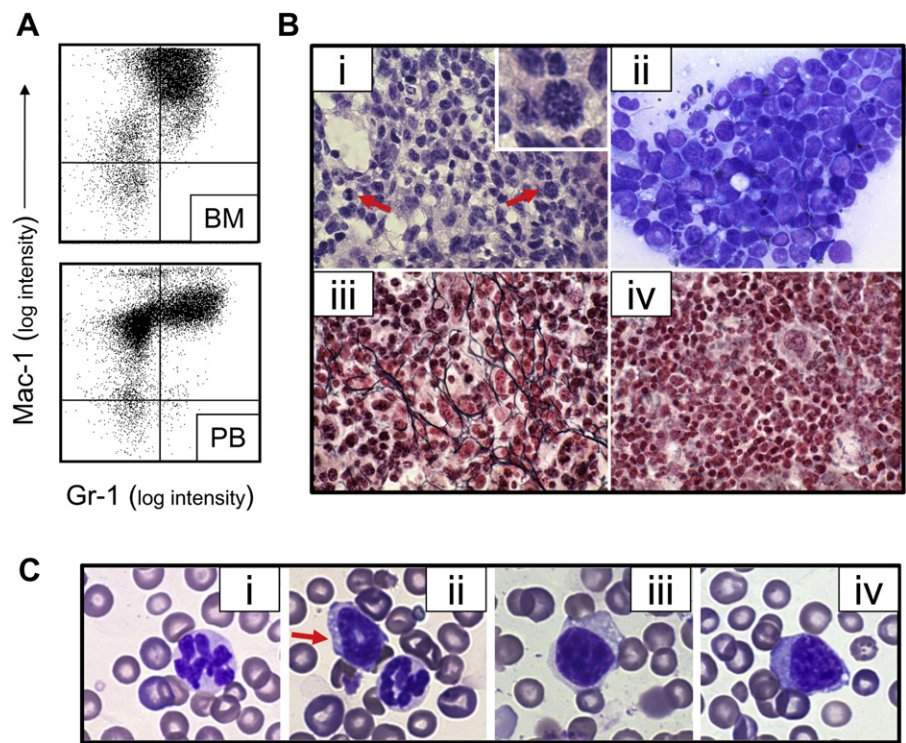
Supplementary Figure E1. Fluorescence-activated cell sorting (FACS) and histopathology of a young *Crebbp*^{+/−} mouse with leukemic disease. As we have previously reported, hematopoietic malignances do not typically become apparent in *Crebbp*^{+/−} mice before 12 months of age; reference [25] in main article; however, one of the mice in the 9- to 12-month-old age group showed early signs of acute leukemic disease progression. Its BM was hypocellular and its spleen enlarged to 283 mg. (**A**) FACS profiles of BM and PB stained with antibodies against Gr-1 and Mac-1, indicating that the majority of cells in these tissues are myeloid. (**B**) Bone sections (**i**, **iii**, and **iv**) and BM touch-prep (**ii**) of the same mouse. Histological examination reveals the hypocellularity of the marrow (**i**) and the prevalence of immature myeloid cells (**I, ii**). The arrows and inset (**i**) indicate cells actively undergoing mitosis, indicative of the high mitotic index of this marrow. (**iii**, **iv**) Reticulin staining (black fibers) indicates a high degree of myelofibrosis in the marrow of this *Crebbp*^{+/−} mouse (**iii**) compared to an age-matched WT control (**iv**). (**C**) Presence of hypersegmented granulocytes (**i**), myeloid precursor cells (**ii**, arrow) and blast cells (**iii** and **iv**) in the PB of this *Crebbp*^{+/−} mouse. Magnification: $60\times$ for all images.

A

	WT							*Crebbp+/-*						

No IR | 20 min | 40 min | 60 min | 2 hr | 6 hr | 12 hr | No IR | 20 min | 40 min | 60 min | 2 hr | 6 hr | 12 hr

TRP53

- total

- phospho-

B-ACTIN

B

PARP1

- Full length

- Cleaved

B-ACTIN
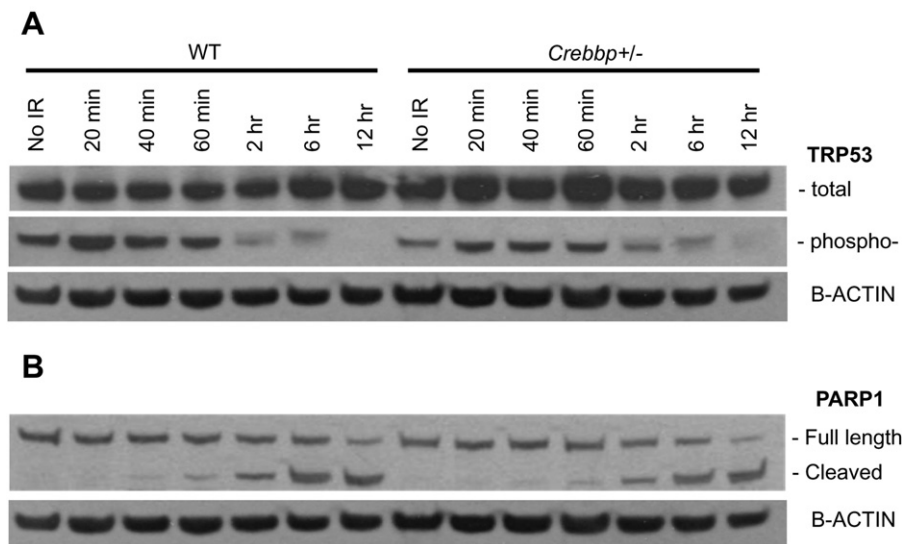
Supplementary Figure E2. No overt changes in TRP53 or PARP in *Crebbp*^{+/−} PB cells compared to WT. (**A**) Western blot of total- and Ser15-phosphorylated TRP53 and in PB cells from WT and *Crebbp*^{+/−} mice. Measurements were taken before and at different time points after irradiation (6 Gy). The 20-minute time point represents the maximum response, earlier time points not shown. (**B**) Western blot of full-length and cleaved PARP1 protein in PB cells from WT and *Crebbp*^{+/−} mice.

Table E1. Probe sets significantly altered in *Crebbp*+/− HSCs relative to wild-type

Probe set ID	Mouse gene	Mouse gene ID	CBP vs WT	Human homolog	Human gene ID
1444262_at	1110017F19Rik	68528	down		
1457062_at	1700081L11RIK	76719	down	KIAA1267	284058
1439112_at	2810442I21RIK	72735	down		
1446425_at	4732418C07RIK	230648	down	KIAA0494	9813
1426936_at	629242	629242	down		
1435684_at	ABCC5	27416	down	ABCC5	10057
1442071_at	ABCE1	24015	down	ABCE1	6059
1421168_at	ABCG3	27405	down		
1440392_at	AKAP13	75547	down	AKAP13	11214
1430047_at	ANKRD32	105377	down	ANKRD32	84250
1430127_a_at	CCND2	12444	down	CCND2	894
1424051_at	COL4A2	12827	down	COL4A2	1284
1430681_at	CRYL1	68631	down	CRYL1	51084
1438211_s_at	DBP	13170	down	DBP	1628
1451363_a_at	DENND2D	72121	down	DENND2D	79961
1439226_at	DOCK8	76088	down	DOCK8	81704
1453753_at	DTL	76843	down	DTL	51514
1437543_at	FUBP1	51886	down	FUBP1	8880
1437171_x_at	GSN	227753	down	GSN	2934
1417184_s_at	HBB-B1	15129	down	HBB	3043
1444942_at	HELZ	78455	down	HELZ	9931
1448152_at	IGF2	16002	down	IGF2	3481
1418280_at	KLF6	23849	down	KLF6	1316
1440315_at	MBNL1	56758	down	MBNL1	4154
1443260_at	MEIS1	17268	down	MEIS1	4211
1438157_s_at	NFKBIA	18035	down	NFKBIA	4792
1427005_at	PLK2	20620	down	PLK2	10769
1429639_at	PREI4	74182	down	RP5-1022P6.2	56261
1429196_at	RABGAP1L	29809	down	RABGAP1L	9910
1428961_a_at	SFRS16	53609	down	SFRS16	11129
1438160_x_at	SLCO4A1	108115	down	SLCO4A1	28231
1436737_a_at	SORBS1	20411	down	SORBS1	10580
1441802_at	SPRED2	114716	down	SPRED2	200734
1421664_a_at	STYX	56291	down	STYX	6815
1437277_x_at	TGM2	21817	down	TGM2	7052
1455900_x_at	TGM2	21817	down	TGM2	7052
1424966_at	TMEM40	94346	down	TMEM40	55287
1438495_at	TOP1	21969	down	TOP1	7150
1430575_a_at	TPP2	22019	down	TPP2	7174
1428992_at	UNC13D	70450	down	UNC13D	201294
1428564_at	ZFP579	68490	down	ZNF579	163033
1424982_a_at	2700078E11RIK	78832	up	C10orf46	143384
1435070_at	AEBP2	11569	up	AEBP2	121536
1437743_at	AEBP2	11569	up	AEBP2	121536
1434266_at	AI847670	330050	up		
1454982_at	ARFGEF2	99371	up	ARFGEF2	10564
1418523_at	ARIH2	23807	up	ARIH2	10425
1457139_at	AUTS2	319974	up	AUTS2	26053
1452346_at	B3GNT1	108902	up	B3GNT1	11041
1443688_at	BC050092	235048	up		
1439783_at	C330018D20RIK	77422	up		
1427419_x_at	CCR9	12769	up	CCR9	10803
1449932_at	CSNK1D	104318	up	CSNK1D	1453
1429301_at	CSNK2A2	13000	up	CSNK2A2	1459
1428794_at	CYTSB	432572	up	SPECC1	92521
1428267_at	DHX40	67487	up	DHX40	79665
1449116_a_at	DTYMK	21915	up	DTYMK	1841
1418699_s_at	FECH	14151	up	FECH	2235
1431645_a_at	GDI2	14569	up	GDI2	2665
1424076_at	GDPD1	66569	up	GDPD1	284161
1418839_at	GLMN	170823	up	GLMN	11146

(continued)

S.N. Zimmer et al./ Experimental Hematology 2012;40:295–306

Table E1. (*continued*)

Probe set ID	Mouse gene	Mouse gene ID	CBP vs WT	Human homolog	Human gene ID
1426463_at	GPHN	268566	up	GPHN	10243
1455007_s_at	GPT2	108682	up	GPT2	84706
1451490_at	LYPLAL1	226791	up	LYPLAL1	127018
1420977_at	MAN1A2	17156	up	MAN1A2	10905
1426850_a_at	MAP2K6	26399	up	MAP2K6	5608
1435285_at	MPPED2	77015	up	MPPED2	744
1452740_at	MYH10	77579	up	MYH10	4628
1429584_at	MYNN	80732	up	MYNN	55892
1421321_a_at	NET1	56349	up	NET1	10276
1428951_at	NOL8	70930	up	NOL8	55035
1430875_a_at	PAK1IP1	68083	up	PAK1IP1	55003
1428543_at	PPAT	231327	up	PPAT	5471
1423903_at	PVR	52118	up	PVR	5817
1451074_at	RNF13	24017	up	RNF13	11342
1451108_at	RNF185	193670	up	RNF185	91445
1437532_at	RNF216	108086	up	RNF216	54476
1448127_at	RRM1	20133	up	RRM1	6240
1415957_a_at	RRP1	18114	up	RRP1	8568
1440275_at	RUNX3	12399	up	RUNX3	864
1437088_at	SDAD1	231452	up	SDAD1	55153
1429459_at	SEMA3D	108151	up		
1452059_at	SLC35F5	74150	up	SLC35F5	80255
1436867_at	SRL	106393	up	SRL	6345
1450420_at	STAG1	20842	up	STAG1	10274
1431115_at	TGIF2	228839	up	TGIF2	60436
1420868_s_at	TMED2	56334	up	TMED2	10959
1427314_at	TMED7	66676	up	TMED7	51014
1452290_at	TMEM106B	71900	up	TMEM106B	54664
1448863_a_at	TNFAIP1	21927	up	TNFAIP1	7126
1418132_a_at	UBFD1	28018	up	UBFD1	56061
1423675_at	USP1	230484	up	USP1	7398
1427991_s_at	USP45	77593	up	USP45	85015
1429393_at	WDR40A	68970	up	WDR40A	25853
1449353_at	ZMAT3	22401	up	ZMAT3	64393

Table E2. Programmed cell death and DNA damage response proteins present in the PIN shown in Figure 5A

	Programmed cell death	Response to DNA damage stimulus
GO ID#:	12501	6974
Gene symbols:	APP	ABL1
	BCAP31	CCNH
	CASP3	CDKN1A
	CDKN1B	CDKN2D
	CDKN2D	CIB1
	CIB1	**CSNK1D**
	CUL1	DDIT3
	DYNLL1	GTF2H1
	GJA1	**MAP2K6**
	HTT	MCM7
	MET	PARP1
	NFKB1	PCNA
	NFKBIA	PRKDC
	PAK1	RAD21
	PFN1	RBBP8
	PTK2B	RPA1
	RAD21	RRM2B
	RIPK3	SFPQ
	RNF216	SMC1A
	RRAGA	SMC3
	SMAD3	TOPORS
	TNFRSF1A	TP53
	TNFRSF1B	VCP
	TP53	XRCC5
	TRAF2	XRCC6
	VCP	
	VDAC1	
	YWHAB	

The gene symbols in bold are direct target genes.

14-3-3 σ Expression Effects G2/M Response to Oxygen and Correlates with Ovarian Cancer Metastasis

Dashnamoorthy Ravi[1,2], Yidong Chen[1,3,], Bijal Karia[1,2], Adam Brown[1,2], Ting Ting Gu[1], Jie Li[4], Mark S. Carey[4,5], Bryan T. Hennessy[4,6], Alexander J. R. Bishop[1,2]*

1 Greehey Children's Cancer Research Institute, University of Texas Health Science Center, San Antonio, Texas, United States of America, 2 Department of Cellular and Structural Biology, University of Texas Health Science Center, San Antonio, Texas, United States of America, 3 Department of Epidemiology and Biostatistics, University of Texas Health Science Center, San Antonio, Texas, United States of America, 4 Department of Gynecologic Medical Oncology, University of Texas MD Anderson Cancer Center, Houston, Texas, United States of America, 5 Division of Gynecologic Oncology, Department of Obstetrics and Gynecology, University of British Columbia, Vancouver, Canada, 6 Department of Medical Oncology, Beaumont Hospital, Dublin, Ireland

Abstract

Background: In vitro cell culture experiments with primary cells have reported that cell proliferation is retarded in the presence of ambient compared to physiological O_2 levels. Cancer is primarily a disease of aberrant cell proliferation, therefore, studying cancer cells grown under ambient O_2 may be undesirable. To understand better the impact of O_2 on the propagation of cancer cells in vitro, we compared the growth potential of a panel of ovarian cancer cell lines under ambient (21%) or physiological (3%) O_2.

Principal Findings: Our observations demonstrate that similar to primary cells, many cancer cells maintain an inherent sensitivity to O_2, but some display insensitivity to changes in O_2 concentration. Further analysis revealed an association between defective G2/M cell cycle transition regulation and O_2 insensitivity resultant from overexpression of 14-3-3 σ. Targeting 14-3-3 σ overexpression with RNAi restored O_2 sensitivity in these cell lines. Additionally, we found that metastatic ovarian tumors frequently overexpress 14-3-3 σ, which in conjunction with phosphorylated RB, results in poor prognosis.

Conclusions: Cancer cells show differential proliferative sensitivity to changes in O_2 concentration. Although a direct link between O_2 insensitivity and metastasis was not determined, this investigation showed that an O_2 insensitive phenotype in cancer cells to correlate with metastatic tumor progression.

Introduction

Cell lines derived from cancer patients provide an experimentally manipulable model system that facilitates investigations into cancer biology and its therapy. The unlimited proliferation potential of cancer cells is a major hallmark of malignancy, however the use of standard tissue culture protocols often restricts cell proliferation, as observed with primary cell lines [1,2,3,4]. Although the use of physiological conditions is known to impact in vitro proliferation of cancer cells [5,6,7] and primary cells are known to propagate better at physiological O_2, the impact of physiological O_2 on in vitro cancer cell proliferation is relatively unexplored. However, it has been reported that altered concentrations of O_2 results in clear differences in cell proliferation and response to drug treatment in the cancer cells [8,9,10].

Oxygen, in addition to nutrients and growth factors, is vital for proper cell growth and its availability has a direct impact on cellular metabolism, signaling pathways, proliferation, differentiation and survival [3,11,12,13]. Many in vitro investigations have demonstrated the advantages of physiological O_2 for tissue culture. For example, the biological behavior of primary cell cultures with a physiological concentration of O_2 (2.7–5.3%) is far superior compared to the standard practice of growing cells under atmospheric or "ambient" O_2 concentration (21% O_2) [4]. In fact, these two growth conditions are known to result in distinct metabolic and molecular characteristics [13].

The importance of considering O_2 tension in cancer biology is well established. For example, the fact that many cancers exist in a 'hypoxic' state has led to the development of hypoxia-targeted therapy [14,15]. In general the hypoxic concentration of O_2 is

<1% for most solid tumors, however the hypoxic concentration could vary based on the cell types and the normal perfusion status [16] and additionally, hypoxia tends to inhibit cell proliferation [17]. Physiological O_2 tension varies from 2.7–5.3% in the interstitial space [18], where many primary tumors reside, to 14.7% in the arterial circulation and lungs, where migrating and potentially metastatic cancer cells are often found. Therefore, cancer studies that are only conducted in ambient (21%) O_2 may miss pertinent biological observations. This may be particularly important when attempting to study the progression of cancer to metastatic disease, which is a significant event in cancer etiology and is associated with poor prognosis [19]. Considering the differences in O_2 tension in different compartments of the body, an understanding of the effect of O_2 concentration on cancer cell proliferation could provide useful insights into the mechanisms involved in the pathological progression of cancer.

Cancer cells that have acquired mutations in either oncogenes or tumor suppressor genes display a characteristic uncontrolled proliferation phenotype [20]. For example, tumor suppressors such as p53 or RB act as "molecular gatekeepers" known to affect cell cycle progression. Mutation of such factors facilitates unlimited proliferation in cancer cells [20]. Cell cycle progression involves a sequential series of events catalyzed by cyclins and cyclin-dependent kinases (CDKs) [21], and in normal cells is a tightly regulated process. The tumor suppressor p53 is a master regulator of G1/S and G2/M phase transition in the cell cycle [22] and is known to have an important role in responding to oxygen concentration, particularly hypoxia (<1% O_2) [23] or hyperoxia (95% O_2) [24]. Although examining the effect of extreme O_2 conditions is both important and revealing, it must be noted that these previous studies did not investigate the response of p53 at physiological (3%) O_2 and ambient (21%) O_2. p21 and 14-3-3 σ are transcriptional targets of p53 that are involved in regulating G1/S and G2/M transitions of the cell cycle by targeting CDK2 and CDC2 (also known as CDK1), respectively [22,25]. The CDKs, in turn, regulate RB protein function, to mediate cell cycle progression through G1/S and G2/M [26]. Therefore, disruption of RB function could also impact the control of cell cycle progression [26]. Considering that differences in O_2 concentration result in altered cell cycle progression in primary cells but cancer cells frequently display cell cycle control defects, there is clearly the potential that these defects may impact how cancer cells respond to altered O_2 levels in a manner that could have a profound influence on cancer progression.

Here we examined the biological behavior of ovarian cancer cells under physiological and ambient O_2. Interestingly, some of the ovarian cancer cell lines had a normal response to O_2 concentration, (i.e. reduced cell proliferation with increased O_2 concentration) while the proliferation of other ovarian cancer cell lines was unaffected by this O_2 increase. Further, our investigations revealed that 14-3-3 σ and its role in the cell cycle influence the proliferative response to altered O_2 levels. Considering the variation in partial pressure of oxygen throughout the body and the potential importance that this context may have on cancer progression, it is crucial to understand the affect of O_2 concentration on cancer cell proliferation and cancer progression. We provide evidence that acquisition of O_2 insensitivity may be a component in cancer progression and a hallmark of successful metastatic disease.

Results

Physiological oxygen results in increased cell proliferation in ovarian cancer cells

In our initial studies we compared the effect of physiological (3% O_2) and ambient (21% O_2) oxygen concentration using A2780

ovarian cancer cells and observed that 12 days of cell culture under these conditions resulted in a 2.6 fold growth suppression under 21% O_2 (Figure 1). Therefore, we examined the affect of O_2 concentration on the growth potential of six ovarian cancer cell lines using physiological (3% O_2) and ambient (21% O_2) oxygen concentrations. Since the serum present in cell culture medium can also have a dominant influence on growth, we also tested the affect of various concentrations of serum. Regardless of the amount of serum present in the growth medium, culturing in 21% O_2 generally resulted in a significant decrease in cell proliferation for four of the ovarian cancer cell lines (A2780, OVCAR5, OVCAR8 and HOC8) compared to 3% O_2 (Figure 2). The only exception observed was with HOC8 cells in the presence of the highest concentration of serum (10% v/v), where an insignificant O_2-dependent growth effect was observed (Figure 2). Presumably the lack of response in Hoc8 results from a dominant influence of serum, which was not observed with A2780, OVCAR5 and OVCAR8. In contrast, there was no significant effect on the growth of SKOV3 and HeyA8 cell lines by increasing the O_2 concentration to 21%, irrespective of serum concentrations (Figure 2). The observed exception was HeyA8 cultured under 2% serum, which showed decreased cell proliferation at 21% O_2 compared to 3% O_2 ($p<0.001$). In contrast to the effect of O_2 levels, increasing the concentration of serum resulted in a proportional growth increase in the ovarian cancer cell lines A2780, OVCAR5 and OVCAR8 ($p<10^{-5}$, Figure 2). The concentration of serum had a moderate influence on growth in SKOV3 and HeyA8 (Figure 2); a serum concentration between 2 and 6% had a significant effect ($p<10^{-5}$) in SKOV3, while HeyA8 serum concentration between 2 and 10% serum had the greatest effect at 3% O_2 ($p<10^{-5}$) (Figure 2). Increasing serum concentration from 6% to 10% had little effect on growth of HeyA8, SKOV3 and HOC8 (Figure 2). Together, it appears that both oxygen levels and serum concentration affect the growth of these ovarian cancer cell lines, but in an independent fashion. As expected from work by others with primary cells [4], we observed that the majority of the ovarian cancer cells displayed decreased cell proliferation at ambient O_2 concentration compared to physiological O_2 concentration. However, two cell lines did not appear to have inhibited cell proliferation at the higher (ambient) O_2 levels. We therefore categorized the ovarian cancer cell lines based on these differences, being either O_2 sensitive (A2780, OVCAR5, OVCAR8 and HOC8) or insensitive (SKOV3 and HeyA8) (Figure 2). Overall, these differences suggest heterogeneity in growth regulation responses to physiological cues of O_2 levels in these cultured cell lines.

It is possible that the apparent O_2 insensitivity and differences in proliferation resulted from differences in the doubling time of each cell line. For example, if SKOV3 and HeyA8 (the O_2 insensitive cell lines) proliferate more slowly, O_2 dependent proliferation changes may be too trivial to measure. Therefore, we measured the cell doubling time for all ovarian cancer cell lines. Our results showed that under standard tissue culture conditions (10% serum and 21% O_2) the doubling time for all ovarian cancer cell lines were somewhat similar (<24 hours) except for HOC8, which had an extended doubling time of about 45.5±4.9 hours (Table S1, and see Methods S1). Therefore, most of the ovarian cancer cell lines were dividing at an approximately equal rate, and gross difference in doubling time is unlikely to be a factor in the observed proliferation differences between cell lines under different conditions.

Oxygen sensitivity correlates with dynamic changes in the S and G2 phases of the cell cycle

Considering the differences in proliferation observed for ovarian cancer cell lines grown under either 3% or 21% O_2, we examined
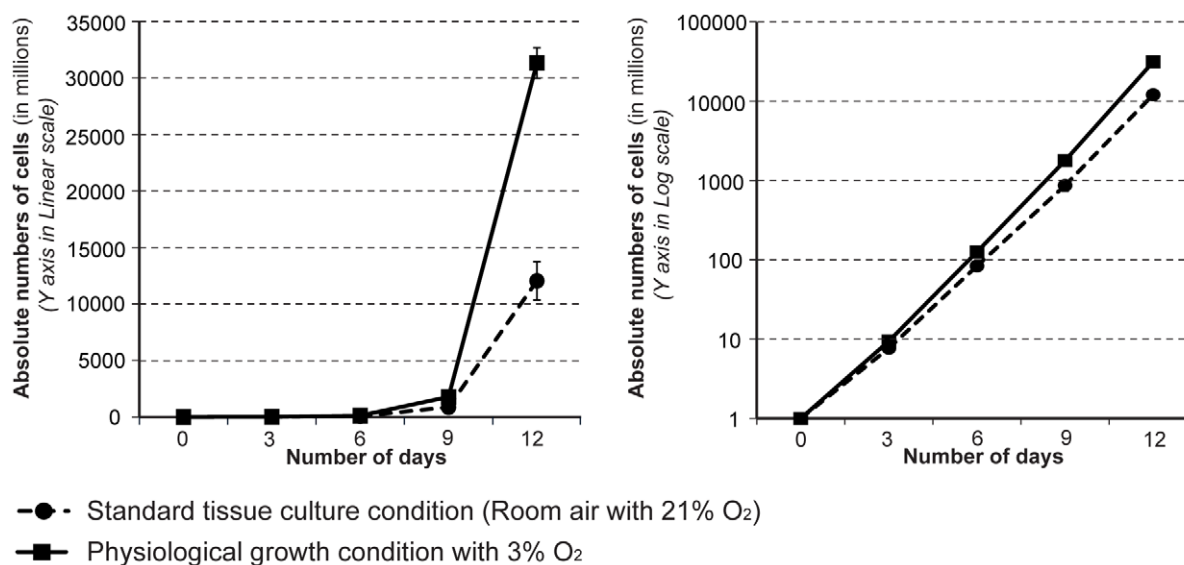
Figure 1. Cancer cell proliferation is markedly suppressed by the standard cell culture conditions used for *in vitro* experiments. Equal numbers of A2780 ovarian cancer cells were seeded in a 10 cm petri dish and were routinely maintained under 3% O_2 (physiological) or 21% O_2 (ambient). The increase in cell numbers was determined by counting manually once in three days, and the total cell numbers were estimated and plotted using linear scale (in Graph A) and log scale (in Graph B).
doi:10.1371/journal.pone.0015864.g001

whether O_2 concentration alters the cell cycle profile of each cell line. Irrespective of serum concentration, comparing 3% O_2 to 21% O_2 resulted in a significant decrease in the percentage of cells that were in the G1 phase of the cell cycle and a significant increase in the percentage of cells in S phase (Table 1), which was

expected based on previous observations made with primary cells [27]. Furthermore, in three of the O_2 sensitive cell lines (A2780, OVCAR5 and OVCAR8) the percentage of the cell population in the G2 phase was increased significantly in 21% O_2. However a significant increase in G2 was not observed in the fourth O_2
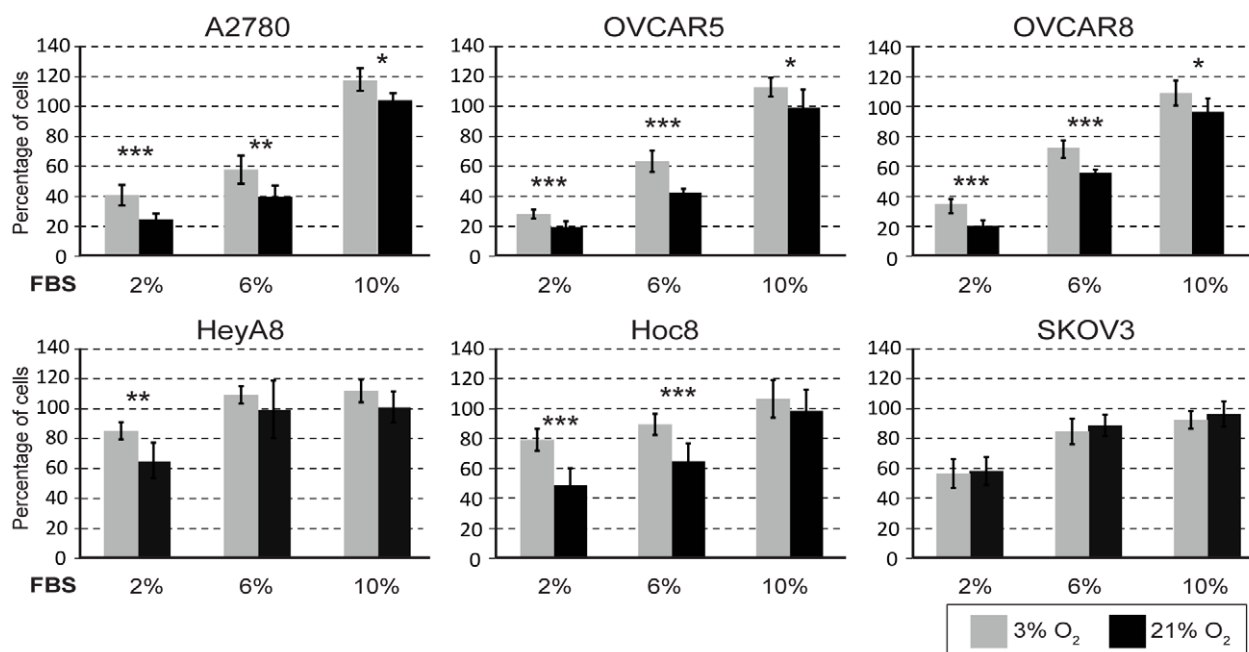
Figure 2. Ovarian cancer cells grown under physiological and ambient O_2 show differential proliferation response. Ovarian cancer cell lines were cultured under 3% or 21% O_2 and the extent of proliferation was determined following 3 days of growth (see Materials and Methods section). For each cell line, the percent of cell proliferation at 3% O_2 (light shaded bars) and at different concentrations of serum was compared with proliferation under standard tissue culture conditions consisting of 21% (ambient) O_2 (dark shaded bars) and 10% FBS. The error bars represent the standard deviations of mean and statistical significant (by student T Test) differences in proliferation between 3% and 21% O_2 for each concentration of serum is indicated by an asterisk [(*) $p < 0.05$, (**) $p < 0.001$ and (***) $p < 0.0001$].
doi:10.1371/journal.pone.0015864.g002

sensitive cell line, HOC8 (Table 1). Similar to HOC8, the O_2 insensitive cell lines, SKOV3 and HeyA8, did not display a significant alteration in the proportion of cells in the G2 phase of the cell cycle when grown under 3% O_2 or 21% O_2 (Table 1). Considering that the O_2 sensitive cell lines proliferated more slowly at 21% O_2 compared to 3% O_2 despite having smaller proportions of their cell population in G1 and a increased proportions in S and G2, we conclude that these cells must be progressing more slowly through the cell cycle. However, for the O_2 insensitive cell lines and HOC8 (with the significantly extended doubling time), we did not observe a significant increase in the percentage of cells in G2 when the O_2 levels were increased. These results suggest that although the G1 and S phases of the cell cycle are responding similarly to changes in O_2 concentration in both O_2 sensitive and insensitive cell lines, it is the G2 phase of the cell cycle that is not responsive to O_2 concentration in the O_2 insensitive cell lines. Therefore, the difference in cell cycle response observed with these ovarian cancer cell lines might be at the level of regulation during the cell cycle progression from G2 to M phase. It is also possible that the changes observed with G2 and O_2 sensitivity in these cancer cell lines is reflected in the mitotic component of the cell cycle. Our observation of the mitotic cells present in the O_2 sensitive and insensitive cell lines grown under 3% and 21% O_2 supports this conclusion; the O_2 sensitive cell lines show a proportionate decrease in the mitotic cell population observed at 21% O_2 compared to 3% O_2, (Figure 3), corresponding to an accumulation of cells at G2 at 21% O_2 (Table 1). Similarly, in the O_2 insensitive cell lines (HeyA8 and SKOV3) the proportion of mitotic cells remained unaltered regardless of O_2 concentrations (Figure 3). This is expected because, as noted previously (Table 1), the proportion of cells at G2 in the O_2 insensitive cell lines were also unaffected by O_2 concentration. We conclude that most cancer cells retain an ability to regulate cell cycle in response to changes in O_2 concentration comparable to wild type cells [27]. However, some cancer cells may lose O_2 concentration dependent control of cell cycle (as in the O_2 insensitive cancer cell lines), resulting in a distinct phenotype.

Oxygen insensitivity correlates with altered G2/M components

Thus far we have demonstrated that O_2 sensitive cell cycle response at the G2/M transition is lacking in the O_2 insensitive cell lines. We therefore went on to characterize this observation further by determining what component of G2/M regulation is deficient in the O_2-insensitive cancer cells. The major effector of G2/M transition is CDC2 [22,28]. CDC2 forms a complex with cyclin B [29,30], which phosphorylates various structural proteins resulting in the collapse of the nuclear envelope, condensation and segregation of chromosomes [30,31] and inactivation of other cell cycle regulatory proteins such as WEE1, RB and CDC25C [30,32]. In normal cells, the overall levels of CDC2 protein are kept constant throughout the cell cycle [33] and are regulated by post-translational modification [33] and cellular localization [30,31]. Once the Tyr15 residue on CDC2 is dephosphorylated by CDC25C, activated CDC2 forms a complex with cyclin B, accumulates in the nucleus, and promotes the G2/M transition[30,33,34]. This occurs in a stepwise fashion through increasing amounts of nuclear CDC2 protein [30]. Our examination of total CDC2 protein and phosphorylated CDC2 protein revealed that both are considerably lower in the O_2-insensitive cell lines (HeyA8 and SKOV3) compared to the O_2-sensitive cell lines (Figure 4A). Although the levels of CDC2 were relatively high in the O_2-sensitive cell lines (A2780, OVCAR5 and OVCAR8) (Figure 2), we observed a decrease in Tyr15 phosphorylation status regardless of O_2
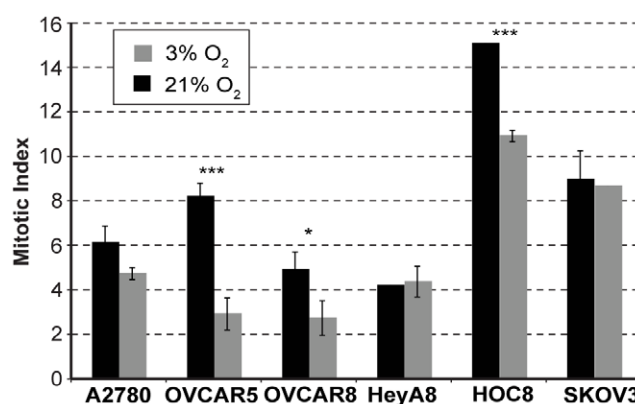

Figure 3. Mitotic index in the ovarian cancer cell lines grown under 3% or 21% O_2. Mitotic index in the ovarian cancer cell lines that were cultured under 3% or 21% O_2 for 3 days were determined by counting nuclei with condensed chromosomes, among the minimum of 1000 cells present in each experiment. Statistical significance was determined by ANOVA and the significant difference in the mitotic index between 3% and 21% O_2 is denoted by an asterisk [(*) $p < 0.05$, (***) $p < 0.0001$].
doi:10.1371/journal.pone.0015864.g003

concentration for A2780, OVCAR5 and OVCAR8 with increasing serum levels (Figure 4A). This correlates with the observation that increasing serum concentration causes increased cellular proliferation and results in a concomitant reduction in the proportion of cells in G2/M (compare with Table 1). However, no overt O_2-dependent alteration in either total or phosphorylated cyclin B or CDC25C was observed in the O_2 sensitive cell lines (A2780, OVCAR5, OVCAR8 and HOC8) compared to O_2 insensitive cell lines (HeyA8 and SKOV3) (Figure 4A). Therefore, it appears that the observed decrease in the cell population in G2 in 21% O_2 might not be dependent on phosphorylation-mediated inactivation of CDC2. It should be noted that these experiments were performed in asynchronously growing cells, and therefore it is possible that transient differences in CDC2 status were missed. Interestingly, the levels of CDC2, Cyclin B and CDC25c (the negative regulator of CDC2) were considerably lower in O_2 insensitive cell lines (HeyA8 and SKOV3) compared to O_2 sensitive cell lines (A2780, OVCAR5, OVCAR8 and HOC8) (Figure 4A). These observations suggest an inherent deficiency in the core components involved in the G2/M progression in the O_2 insensitive cell lines.

p53, p21 and 14-3-3 σ are factors which have the ability negatively to influence CDC2 activity and G2/M transition [22]. Current understanding is that p53 and p21 influence cell cycle in hypoxic and hyperoxic conditions [23,24,35,36]. Considering the reduced levels of CDC2 and the apparently defective G2/M checkpoint in the O_2 insensitive cell lines (HeyA8 and SKOV3), we explored the possibility that impairment was due to a defect in any of these molecular regulators. Western blot analysis found p53 and p21 to be overexpressed in one O_2-insensitive cell line (HeyA8). However, both were absent in the other O_2-insensitive cell line (SKOV3), and the expression pattern for these proteins remained unaltered regardless of changes in O_2 or serum concentration (Figure S1), suggesting that neither p53 nor p21 is relevant to CDC2's function in O_2 sensitivity. Interestingly, we observed a considerable elevation in the expression of 14-3-3 σ (Figure 4A) in the O_2 insensitive cell lines (HeyA8 and SKOV3) compared to the O_2-sensitive cell lines. Although, the level of 14-3-3 σ expression was considerably lower in all O_2-sensitive cell lines compared to HeyA8 and SKOV3, we did observe an increase in the expression of 14-3-3 σ at 21% O_2 with A2780 (Figure 4A). Although

Table 1. FACS profile for cell cycle analysis with ovarian cancer cells that were grown under cell culture conditions consisting of increasing serum and O_2 concentration.

Cells	Serum	G1			S			G2		
		3% O_2	21% O_2	*p*-value	3% O_2	21% O_2	*p*-value	3% O_2	21% O_2	*p*-value
	2%	66.8±0.9	62.5±0.2	0.0011	25.6±1	27.5±0.1	0.02800	7.6±0.4	9.96±0.1	0.0007
A2780	6%	76.9±2.1	64.3±0.7	0.0006	17.5±0.9	29±0.1	<0.0001	5.6±1.4	6.7±0.6	**NS**
	10%	84.1±3.2	69.5±1.4	0.0028	14.3±1.9	26.5±1.3	0.0080	1.5±1.3	4±0.7	0.0411
	2%	66.4±0.7	60.2±0.4	0.0001	25.8±0.2	29.3±0.6	0.0006	7.7±0.5	10.4±0.3	0.0017
OVCAR5	6%	79±1.5	70.2±0.5	0.0014	17.4±1.5	25.1±0.9	0.0015	3.4±0.4	4.7±0.6	**NS**
	10%	90.6±1.2	84±1.6	0.0077	8.2±1.4	14.6±1.5	0.0052	1.1±0.1	1.2±2.1	**NS**
	2%	74.7±10.7	69±1	**NS**	15.5±2.5	23.7±0.6	0.0052	13.7±2.3	6±0	0.0043
OVCAR8	6%	66±1	59±1	0.0010	25.7±1.5	30±0	0.0079	7±0	9.7±0.6	0.0013
	10%	69±4.6	61.7±1.5	0.0582	24.3±1.5	30.7±1.2	0.0045	5.3±3.8	6.3±0.6	**NS**
	2%	69.3±1.5	58.7±2.1	0.0020	25±1	34±1	0.0003	4.3±1.5	5.7±1.5	**NS**
HeyA8	6%	62.7±0.6	53.7±1.5	0.0006	30.3±1.2	37.3±2.5	0.0118	5.3±0.6	8±3.5	**NS**
	10%	61.7±1.2	50.3±2.3	0.0016	30.7±1.2	37.3±1.2	0.0021	6.7±2.3	11±1.6	**NS**
	2%	80±1.7	72.3±1.5	0.0045	15±0	18.7±1.5	0.0141	5±1.7	8±1	**NS**
HOC8	6%	80.3±1.2	72.7±1.2	0.0012	15.3±1.5	22.7±1.5	0.0041	3.3±1.5	3.7±1.5	**NS**
	10%	78.7±2.5	73.3±0.6	0.0232	16.3±0.6	23.7±0.6	<0.0001	4.3±2.5	3±1	**NS**
	2%	74±2	62.1±1.7	0.0014	13.5±3.5	27.7±1.2	0.0026	12±2	10.3±2.5	**NS**
SKOV3	6%	76.7±1.5	65.3±3.2	0.0052	14±1	25.7±1.5	0.0003	9.3±1.5	9±2	**NS**
	10%	80.3±1.2	68±1.7	0.0005	12.7±1.5	26±1	0.0002	7±1	6.3±0.6	**NS**

NS "Not Significant"
doi:10.1371/journal.pone.0015864.t001

contradictory to the known inhibitory role of 14-3-3 σ on CDC2 activity, we concluded that high levels of 14-3-3 σ combined with reduced levels of CDC2 in a proliferating cancer cell may indicate a lack of control of G2/M progression in response to O_2 levels.

To clarify the consequence of the low levels of CDC2 protein observed in the O_2-insensitive cell lines, we determined the functional activity of the remaining CDC2 by examining the phosphorylation of two of its substrates, RB and WEE1. Phosphorylation of RB at the Ser 807 residue is mediated by CDC2 [32], and we observed this phosphorylation regardless of CDC2 levels or O_2 levels with 10% serum for all cell lines except HOC8 (Figure 4B), indicating unimpaired CDC2 activity in these cell lines. A reduction in phosphorylated RB correlated with reduction of serum concentration (Figure 4B) and correlated with increased accumulation of total RB in the O_2-sensitive cell lines (A2780, OVCAR5 and OVCAR8), but not in HOC8 (Figure 4B). Total RB was barely detectable in the O_2-insensitive cell lines (HeyA8 and SKOV3) (Figure 4B), with the exception of 2% serum at 3% O_2 condition in the HeyA8 cell line. Interestingly, a comparison between the RB expression pattern (Figure 4B) and cell proliferation (Figure 2) revealed that HOC8, HeyA8 and SKOV3 cells grow better in cell culture medium with a low concentration of serum (2%) compared to A2780, OVCAR5 and OVCAR8. It therefore appears that the total RB protein level response remains intact in O_2-sensitive cell lines and that this response is probably more relevant to serum concentrations than O_2 levels. The other target for CDC2-mediated inactivation by phosphorylation is WEE1, which can also reciprocally inhibit CDC2 function by phosphorylation [37]. We observed increased phosphorylation of WEE1 in the O_2 sensitive cell lines (A2780, OVCAR5 and OVCAR8), barely detectable levels in HOC8, (Figure 4B) and a complete absence in the O_2-insensitive cell lines (HeyA8 and SKOV3, Figure 4B). This pattern was largely recapitulated for total WEE1 protein levels (Figure 4B). Therefore, the absence of phospho-WEE1 in the O_2-insensitive cell lines does not indicate an absence of CDC2 activity, but rather an absence of the WEE1 substrate. From these results we concluded that despite the reduced amounts of CDC2 in the O_2-insensitive cell lines, CDC2 is functionally active and uninhibited by the increased levels of 14-3-3 σ. It should be noted that RB and CDC2 act upon each other to regulate each others function [38], and phosphorylation status of RB [26] or CDC2 [39] could influence E2F mediated expression of cyclins that are essential for cell cycle progression. Therefore, considering this complex relationship between RB and CDC2, the phosphorylation pattern of RB is insufficient to predict G2/M progression.

In summary, the O_2-sensitive cell lines (A2780, OVCAR5 and HOC8) showed increased expression of CDC2 and cyclin B combined with low level of 14-3-3 σ expression. This suggests that the cell cycle components required for a dynamic proliferative response to differences in the O_2 concentration is present in these cell lines. However in the O_2-insensitive cell lines that express high levels of 14-3-3 σ and low levels of CDC2 and CDC25C such a dynamic cell cycle response to changes in O_2 concentration could be impaired. We therefore pursued the possibility that this inverse correlation between 14-3-3 σ and CDC2 might be important for the O_2-sensitive regulation of G2/M transition.

14-3-3 σ and mitotic progression in oxygen sensitivity

Our previous observations suggest an association between elevated level of 14-3-3 σ and O_2-insensitivity that needs to be confirmed. Therefore, we wanted to confirm that 14-3-3 σ does indeed affect O_2-dependent proliferation. For this part of the study, we restricted our analysis to two cell lines with wild type p53: the O_2-sensitive A2780 [40], and O_2-insensitive HeyA8 cell lines [41].
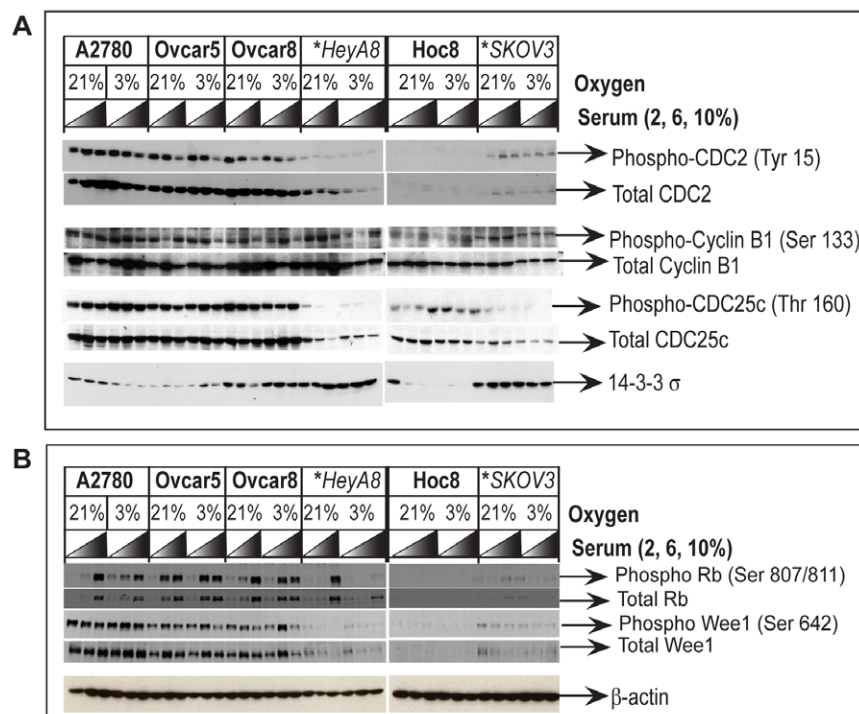
Figure 4. Western blot analysis of G2 cell cycle regulatory proteins and the relevance to O₂ sensitivity in the ovarian cancer cell lines. Protein lysates prepared from the ovarian cancer cell lines maintained in growth medium consisting of increasing concentrations of serum and 21% or 3% O_2 were analyzed by Western blot. (A) Compared to O_2 sensitive cell lines, decreased expression of the core components involved in G2/M cell cycle progression CDC2/cyclin B1 complex and its activator CDC25c is observed in the O_2 insensitive cell lines (indicated by asterisk and italics), while the expression of 14-3-3 σ, a protein that inhibits CDC2 is elevated in the O_2 insensitive cell lines. (B) Phosphorylation of RB and Wee1 were monitored as an indicator for CDC2 function because both RB and Wee1 are known targets for phosphorylation by CDC2. Equal loading of protein extracts were monitored by probing the stripped Western blots with the primary antibody for β-actin.
doi:10.1371/journal.pone.0015864.g004

So far we have used Western blot analysis to monitor the overall expression levels of 14-3-3 σ and CDC2 (Figure 4A). However, since the functional responses of these proteins are dependent on their cellular localization, we used immunofluorescence to determine their cellular location under 3% O_2 and 21% O_2. In the O_2-sensitive A2780 cell line, the localization of 14-3-3 σ was restricted to the cytoplasm under 3% O_2 (Figure 5A), but was found in both the nucleus and cytoplasm at 21% O_2 (Figure 5A). CDC2 was distributed throughout the cell and its localization was unaffected by O_2 concentration. It therefore appears that nuclear exclusion of 14-3-3 σ correlates with a decreased fraction of cells in the G2/M phase and an uninhibited cell cycle progression when A2780 is grown at 3% O_2, as noted before (Table 1). In contrast, the O_2-insensitive HeyA8 cell line showed high levels of 14-3-3 σ and low levels of CDC2 (Figure 4A), with a considerable amount of 14-3-3 σ in the cytoplasm (Figure 5A). Further, 14-3-3 σ remained excluded from the nucleus even at 21% O_2 in the HeyA8 cells (Figure 5A). These observations were further verified by Western blot analysis of nuclear and cytosolic cell fractions obtained from these cells (Figure 5B). Finally, to confirm the effect on G2/M transition, we determined the proportion of those cells in M phase for different O_2 concentrations using the mitosis specific marker phospho-histone H3. In the O_2-sensitive A2780 cells, under 21% O_2, we observed a decrease in the mitotic index (P<0.001), compared to 3% O_2 (Figure 5C). No such O_2-dependent change in mitotic index was observed for the O_2-insensitive HeyA8 cells (Figure 5C). These results support our initial conclusion, that the O_2-insensitive cells lines have a deficiency in regulating cell cycle progression at G2/M in response to increased O_2 levels (Figure 2).

The levels and cellular localization of 14-3-3 σ correlate with O_2-sensitive proliferation. To demonstrate a direct relationship, we examined whether over-expression of 14-3-3 σ could render O_2-sensitive A2780 cells insensitive to O_2 and conversely whether reducing the levels of 14-3-3 σ in O_2-insensitive HeyA8 cells could restore O_2-sensitivity. Transient over-expression of 14-3-3 σ in A2780 cells reduced cell proliferation (Figure 5D) and resulted in loss of O_2-sensitivity. Therefore, merely increasing 14-3-3 σ expression results in its inability to regulate G2/M in the absence of any further genetic alterations. Conversely, RNAi-mediated silencing of 14-3-3 σ expression in HeyA8 cells (Figure 5E - Western blot) resulted in a substantial increase in proliferation under 3% O_2 (Figure 5E - Bar graph). Interestingly, when the cells from the same siRNA transfection were placed at 21% oxygen, 14-3-3 σ protein expression was induced, reducing the knockdown effect of the siRNA. This observation also suggests an O_2-dependent transcriptional response by 14-3-3 σ. Despite this transcriptional response, we still observed a muted growth phenotype at 21% O_2 under these conditions. Together these experiments demonstrate that 14-3-3 σ is a critical factor for controlling ovarian cancer cell proliferation in response to O_2 concentration.

14-3-3 σ is frequently highly expressed in ovarian cancer and its ineffectiveness in controlling CDC2 is relevant to ovarian tumor pathology

Considering that increased expression of 14-3-3 σ provides some indication of impaired G2/M control, it is possible that cancer cell lines that express high levels of 14-3-3 σ are O_2-insensitive. The O_2-insensitive ovarian cancer cell lines we have
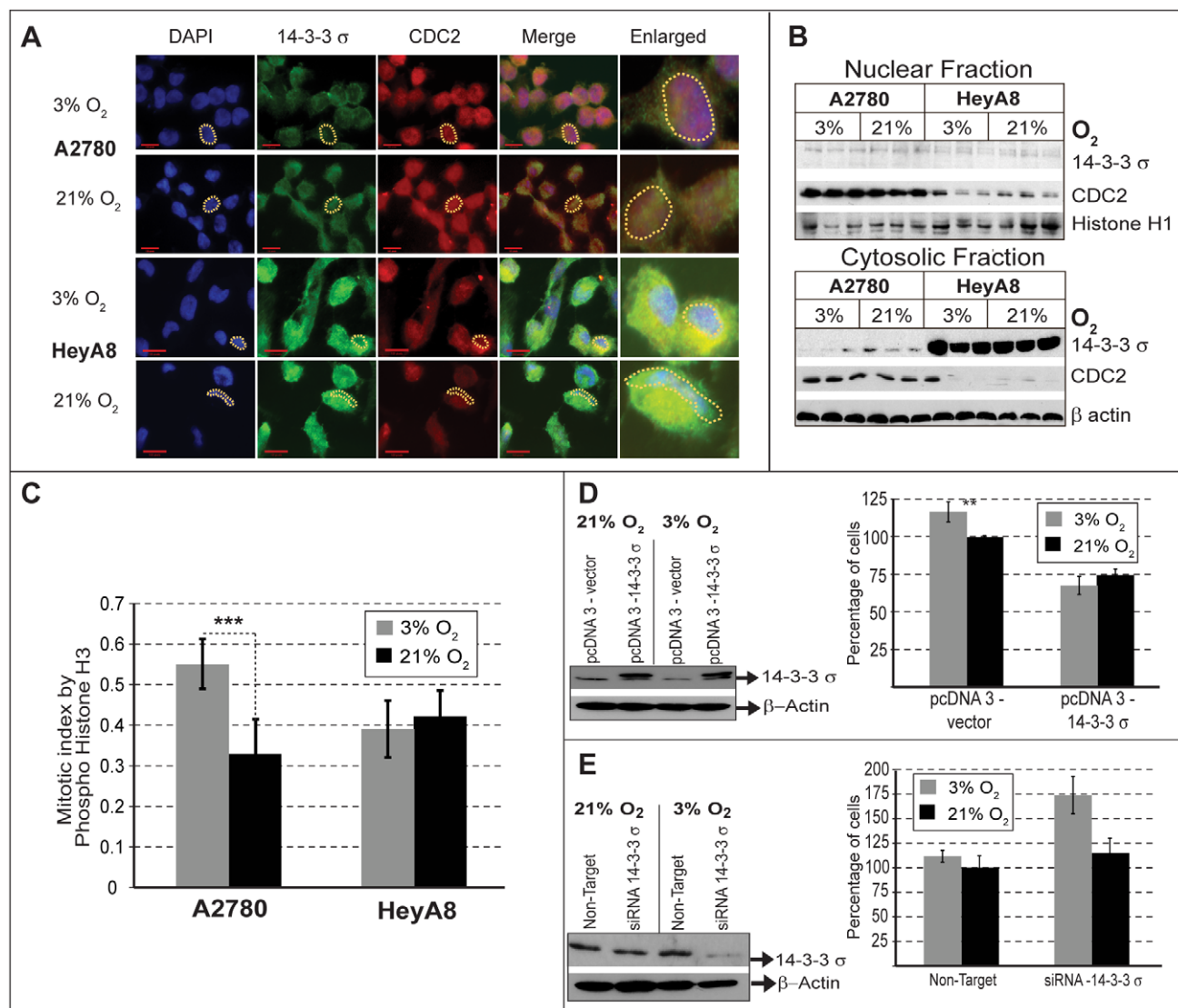
Figure 5. 14-3-3 σand O₂ sensitivity. (A) Cellular localization by immunofluoresence shows that 14-3-3 σ (Green) is located in the cytoplasm and CDC2 (Red) is present in the nucleus (Blue). Compared to O₂ sensitive A2780 cells, the level of 14-3-3 σ is higher and CDC2 is low in the O₂ insensitive HeyA8 cells. In the O₂ sensitive A2780, 14-3-3 σ is localized both in the nucleus and cytoplasm at 21% O₂. (A dotted yellow line, outlines a representative nuclei to indicate relative localization of 14-3-3 σ and CDC2 in these cells). (B) Western blot analysis of nuclear and cytoplasmic fractions show low levels of 14-3-3 σ in the nucleus compared to cytoplasm, with increased amounts of 14-3-3 σ being present in the cytoplasm of the O₂ insensitive HeyA8 cells. The level of CDC2 is higher both in the nucleus and cytoplasm of the O₂ sensitive A2780, but present in lower amount only in the nucleus of O₂ insensitive HeyA8 cells. Histone H1 and β−actin were used as loading controls for nuclear and cytoplasmic fractions, respectively. (C) Mitotic cells were determined by counting the cells that stained positively for a mitosis specific marker, Phospho-Histone H3 from the total cell population. Mitotic fractions present at 3% or 21% O₂ were counted in both A2780 and HeyA8 and represented as bar graph. A significant increase in mitotic index (p>0.001, indicated by asterisk) was observed in the O₂ sensitive A2780 at 3% O₂, but not in the O₂ insensitive HeyA8 cells. (D) Over-expression of 14-3-3 σ in the O₂ sensitive A2780 (Western Blot) results in loss of O₂ sensitivity (Bar graph). For the cells transfected with empty vector (mock transfection) or 14-3-3 σ over-expression construct, the percent of cell proliferation was compared with proliferation of mock transfected cells grown under standard tissue culture conditions consisting of 21% O₂ (ambient), and (E) in the converse experiment performed with O₂ insensitive HeyA8, reducing the levels of 14-3-3 σ by siRNA (Western blot) results in restoration of O₂ sensitivity (Bar graph). For the cells transfected with scrambled siRNA (mock transfection) or siRNA against 14-3-3 σ, the percent of cell proliferation was compared with proliferation of mock transfected cells grown under standard tissue culture conditions consisting of 21% O₂.
doi:10.1371/journal.pone.0015864.g005

thus far characterized have high 14-3-3 σ (Figure 5A) and low CDC2 protein levels. It is conceivable that the same phenotypic defect might result from cells with unchecked CDC2 activity, irrespective of 14-3-3 σ levels. To determine the frequency of commonly available cancer cell lines that have the hallmarks of O₂-insensitivity, we used a reverse phase protein array (RPPA) and screened 57 different ovarian cancer cell lines for the levels of

14-3-3 σ and CDC2, as well as phospho-RB as an indicator of CDC2 activity. Cell lines with the same name but from different labs or different passages were considered to be different. We therefore set the analysis criteria on the RPPA array to detect high phospho-RB (P-RB) and either high 14-3-3 σ or high CDC2. In the context of high levels of P-RB, this criteria should indicate that either 14-3-3 σis dysfunctional or that active CDC2 is uninhibited,

perhaps due to methylated 14-3-3 σ or inhibition of CDC2 degradation [42] We observed that of the 57 ovarian cancer cell lines represented in the RPPA, 28 cell lines (49%) showed high levels of 14-3-3 σ (Figure 6A) of which 16 cell lines (28%) also had increased P-RB, corresponding to the O_2 insensitivity pattern we have described. Amongst these 16 cell lines, 6 also have increased levels of CDC2 while the remainder had decreased levels of CDC2. This suggests that this protein profile is not exclusive to the cell lines we originally identified and might be representative of a relatively common phenomenon. We therefore determined whether this O_2-insensitive associated 14-3-3 σ/CDC2/P-RB protein profile is also observed in ovarian tumor samples. Using the same criteria as with the cell line RPPA, we examined 205 ovarian tumor specimens using RPPA. This analysis revealed that 27% of ovarian tumors (56) had elevated levels of both 14-3-3 σ and P-RB, and amongst these, 34 also had elevated levels of CDC2 expression (Figure 6B). These results are very comparable with the RPPA analysis of the ovarian cancer cell lines (Figure 6A).

Ovarian cancer has a poor survival rate and this is often associated with metastatic progression [43]. The O_2-insensitive associated 14-3-3 σ/CDC2/P-RB protein profile suggests an unrestricted G2/M control in response to changes in O_2 levels, such as a migrating or metastatic cancer would encounter. Therefore, it is possible that this protein profile is associated with poor prognosis. Using the O_2-insensitive associated protein profile (high P-RB with either high 14-3-3 σ or high CDC2) we identified 47 of 158 tumors with associated clinical data. A Kaplan-Meier survival estimate shows that patients with the O_2-insensitive associated protein profile have a poor survival outcome (less than 90 months compared to 200 months observed otherwise, $p = 0.016$, Figure 6C). Altogether it appears that the O_2-insensitive associated protein profile suggests that unrestricted G2/M accompanies a substantial proportion of ovarian cancer cells and primary tumor samples. Further, this O_2-insensitive profile is associated with poor prognosis for this disease.

Elevated 14-3-3 σ expression in metastatic ovarian tumors

Having observed that the O_2-insensitive associated protein profile (high P-RB with either high 14-3-3 σ or high CDC2) is both relatively common in ovarian cancer and associated with poor prognosis, we went on to determine directly whether metastatic ovarian tumors exhibit an overt 14-3-3 σ signature. Of note, the ovarian tumors represented in the ovarian tumor RPPA are from primary sites and thus do not necessarily provide an accurate representation of the protein profile in the metastatic cancer. We therefore expect that metastatic tumors or primary tumors that give rise to metastatic tumors will exhibit a more overt 14-3-3 σ signature than primary tumors. In fact, an increased expression of 14-3-3 σ has been previously reported with other tumors [44] and a functional involvement for 14-3-3 σ in metastatic disease is known [45,46]. We analyzed 14-3-3 σ expression using immunohistochemistry on paraffin embedded tissues obtained from 10 different metastatic ovarian tumors and their corresponding primary site tumors. We consistently observed intense immunostaining of 14-3-3 σ in 8/10 metastatic tumors and the corresponding primary tumors (Figure 7j–l). In contrast, the primary tumors without metastasis at diagnosis showed moderate immunostaining for 14-3-3 σ, and occasionally intense staining was also noted (Figure 7i). Borderline tumors showed a mild to moderate staining pattern for 14-3-3 σ, while in normal tissues, protein levels were absent or diffusely present (Figure 7 a–c). Increased expression of 14-3-3 σ in the metastatic primary tumors compared to normal tissue or malignant tumors without

metastasis were observed to be statistically significant by the Fisher's exact test (Figure 7, Bar Graph). The high level of 14-3-3 σ expression offers the first indication of the manner in which regulation of G2/M may be dysfunctional in these tumors.

Over-expression of 14-3-3 σ in metastatic disease is not unexpected and has been previously noted [45,46,47]. However, we speculate the reason for this association is due to a loss of O_2-sensitivity and that this provides a selective advantage for metastatic progression. Our conclusion is that O_2-sensitive and insensitive patterns of 14-3-3 σ and CDC2 expression are readily detectable and common to cancer cells, regardless of whether they are grown *in vivo* or *in vitro*. Further, these expression patterns may have prognostic implications, but additional experiments will be required to confirm the mechanistic relevance of O_2-sensitivity in the clinical progression of cancer.

Discussion

There is an increasing interest to study cell biology under the context of physiological O_2 levels. Investigations with primary mouse embryonic fibroblasts comparing the effects of physiological (3%) and ambient (21%) oxygen, show that 21% O_2 causes increased oxidative stress and induces senescence [4]. Several studies conducted with embryonic stem (ES) cells reported that characteristic stem cell properties are preserved only when ES cells are maintained under physiological O_2- ES cells otherwise differentiate under ambient O_2 as reviewed in [2]. This prompted us to investigate the effects of physiological (3%) and ambient (21%) oxygen in the context of cancer. With A2780 ovarian cancer cells grown under 21% or 3% O_2, a 20% growth suppression was observed with 21% O_2 by three days (Figure 2) and although the proportional changes to cell cycle profile appear small, they were significant (Table 1). The accumulated effect of these differences in proliferation and cell cycle resulted in a 2.6 fold difference to the growth of the cancer cells by 12 days in the presence of different O_2 concentrations (Figure 1). This observation demonstrates that standard tissue culture conditions may adversely impact the *in vitro* proliferation of cancer, which is primarily a disease of proliferation. Previous studies compared the growth of primary mouse embryonic fibroblast cells [4], adult human fibroblasts [48] and human cancer cells [8] grown under physiological (3–5%) or ambient (21%) O_2 and observed increased cell proliferation under physiological O_2. In this study, we observed similar effects with ovarian cancer cells (A2780, OVCAR5, OVCAR8 and HOC8 - Figure 2), however other cells lines failed to respond to O_2 concentration (HeyA8 and SKOV3) (Figure 2). These proliferative responses to O_2 seem to affect all phases of the cell cycle, particularly the G1 and S phases of cell cycle, in all cell lines. However, only the G2 phase was affected in cell lines which displayed proliferative response to 3% O_2 (Table 1), suggesting the possibility that the G2 phase transition of the cell cycle is crucial for regulating proliferation in response to differences in 3% O_2 levels. A change in the G2 phase in response to O_2 levels was reported in only one other study performed with Fanconi anemia (FA) cell lines [49]. Analogous to our study, the experiments with FA cells demonstrated a characteristic G2 delay with standard tissue culture conditions (20% O_2), but a reduced proportion of cells in G2 and increased proliferation when cultured at 5% O_2 [49]. Furthermore, growth of different human fibroblast cells under physiological O_2 has also been observed to be accompanied by a reduction in the G2 cell population [27,48]. Overall, it appears that the G2 phase is the most O_2-sensitive phase of the cell cycle. Exploring the possible molecular mechanisms that render ovarian cancer cells either sensitive or insensitive to oxygen has
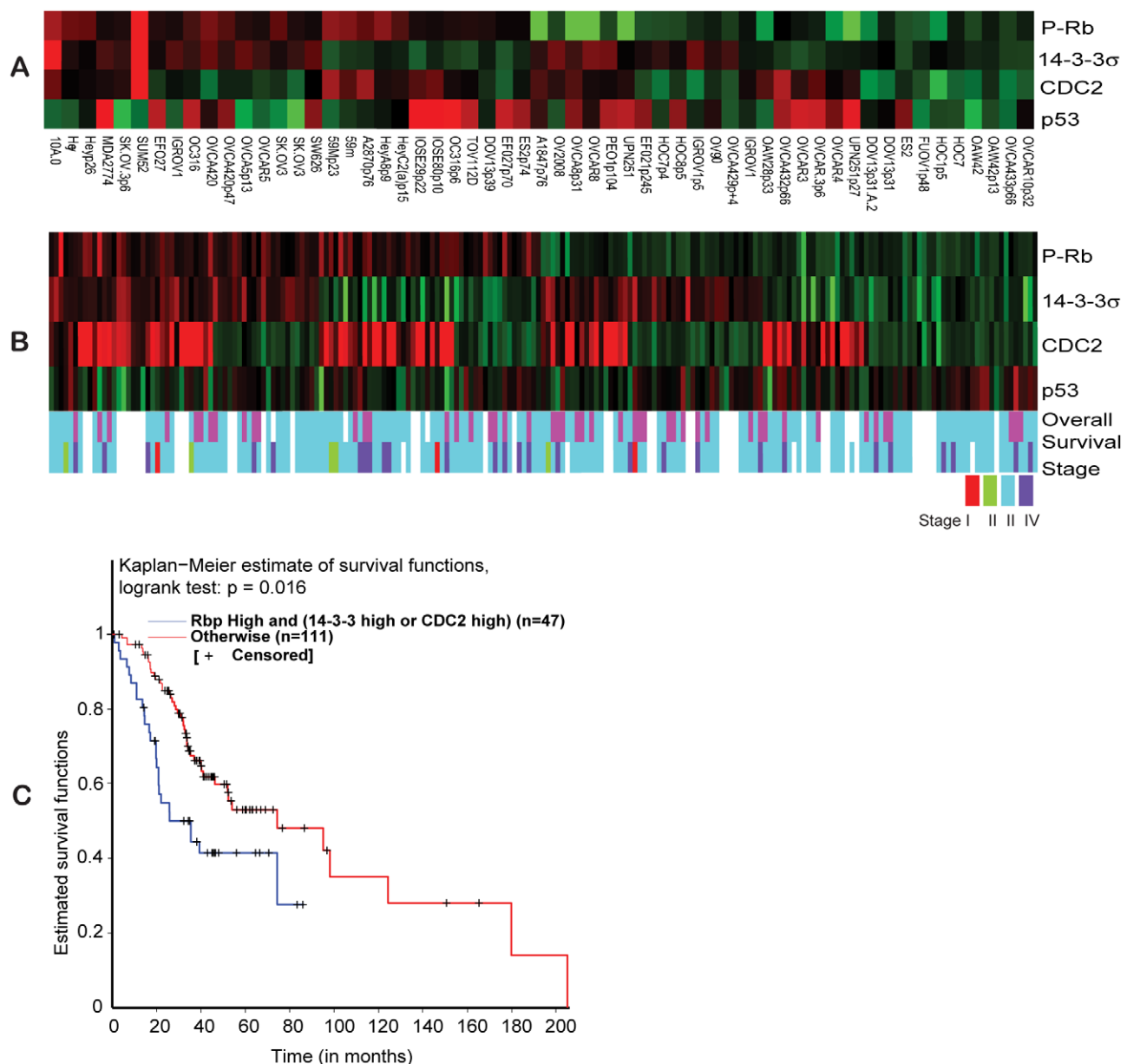
Figure 6. Reverse phase protein array data analysis. (A) Hierarchical clustering of normalized RPPA data over Phospho-RB (Ser 807/811), 14-3-3 σ, CDC2 and p53 across 57 ovarian cancer cell lines. (B) Hierarchical clustering of normalized RPPA data over Phospho-RB (Ser 807/811), 14-3-3 σ, CDC2 and p53 across 205 ovarian tumors. The color codes for overall survival represents overall survival >24 months (blue) and overall survival <24 months (pink). The color codes for tumor stage represent stage I (red), stage II (green), stage III (light-blue) and stage IV (dark-blue). (C). Kaplan-Meier survival curve for the RPPA results comparing the group of ovarian tumors with high Phospho-RB and high 14-3-3 σ or CDC2 (blue line) with other expression profiles (red line).

doi:10.1371/journal.pone.0015864.g006

clearly demonstrated that it is 14-3-3 σ and its inability to control CDC2 dependent G2/M transition in response to O_2 levels that results in oxygen-insensitive cell lines. Although expression of 14-3-3 σ is regulated by p53 [25], we observed no difference in the levels of p53 expression under different oxygen concentrations (Figure S1), suggesting that the involvement of 14-3-3 σ in O_2-sensitivity is independent of p53. If the decrease in 14-3-3 σ is associated with oxygen-sensitive increase in proliferation, then silencing the expression of 14-3-3 σ in oxygen-insensitive cell lines should restore proliferative sensitivity to oxygen. In fact, our experiments show that RNAi mediated silencing of 14-3-3 σ in HeyA8 cells restored oxygen sensitivity (Figure 5E) and in a

converse experiment, over-expression of 14-3-3 σ abolished oxygen sensitivity in the A2780 cell line (Figure 5D). This suggests that high levels of 14-3-3 σ protein is sufficient to restrict the regulation of CDC2 mediated G2/M progression. The cytoplasmic restriction of overexpressed 14-3-3 σ in the O_2-insensitive HeyA8 cells provides the first indication for the possible mechanistic basis of this dysregulation (Figure 5A). Other reports also show preferential changes to cellular localization of 14-3-3 σ during different phases of the cell cycle [50], suggesting that cell cycle changes observed with oxygen could be relevant to the 14-3-3 σ localization and pattern in our experiments. Furthermore, 14-3-3 σ is actively exported out of nucleus by CRM1, [51], a nuclear
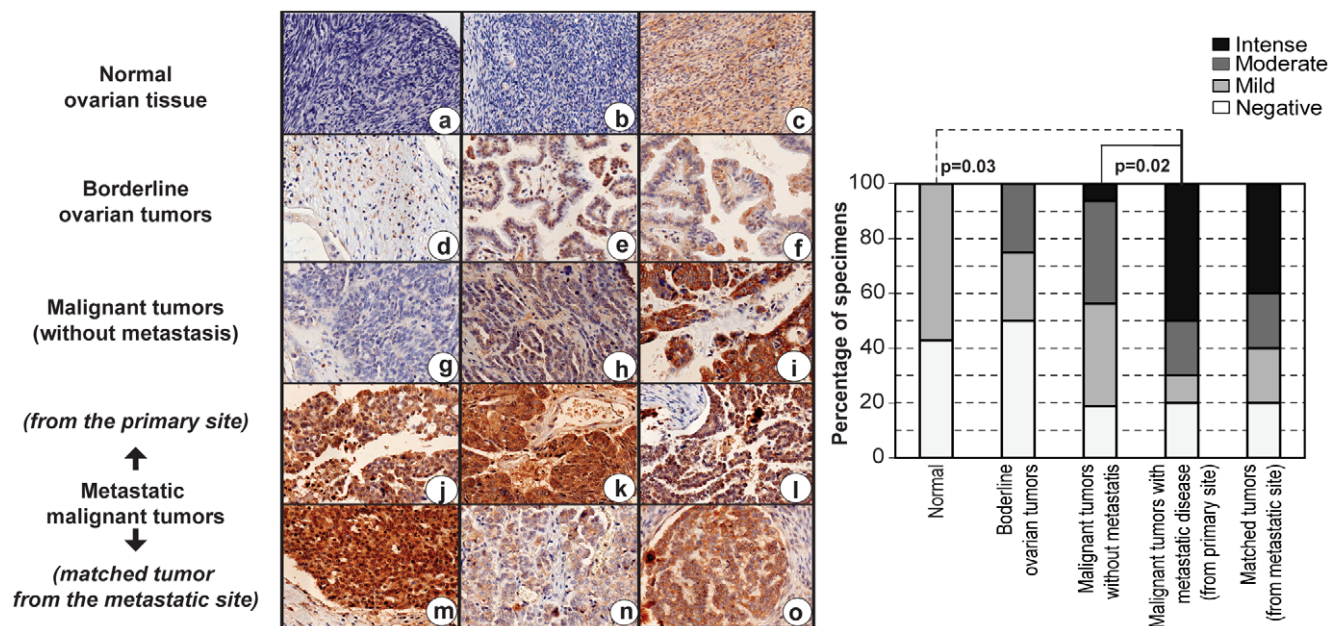
Figure 7. 14-3-3 σ expression and ovarian tumor metastasis. Immunohistochemical analysis of 14-3-3 σ in ovarian tissues show negative (hematoxylin stained blue nucleus) to diffuse staining pattern for 14-3-3 σ (brown) in normal ovarian tissues (a–c), and a moderate increase in the staining intensity localized to the cytoplasm is observed in the borderline ovarian tumors (d–f). In the malignant tumors without any metastatic disease at diagnosis, 14-3-3 σ expression was either absent (g), or stained at moderate to intense levels (h–i), with occasional nuclear staining (i). Intense nuclear and cytoplasmic staining for 14-3-3 σ was observed in ovarian tumors with metastatic disease, obtained from the primary site of the disease, and a moderate to intense staining for 14-3-3 σ in the cytoplasm or both nucleus and cytoplasm of the corresponding tumors obtained from the metastatic site was observed [site of metastasis - (m) appendix, (n) lymph node and (o) omentum]. The quantitative relationship between 14-3-3 σ expression and various stages of ovarian cancer progression is represented in the bar graph, and the statistical analysis for correlation of expression with pathological grades were determined by a Fisher's exact test.
doi:10.1371/journal.pone.0015864.g007

protein that is frequently over-expressed in ovarian cancer [52]. A host of other factors such as, BRCA1, p63 and estrogen induced zinc finger protein (EFP) are also known to regulate the levels of 14-3-3 σ [53]. Therefore, it is possible that 14-3-3 σ expression and its cellular distribution could be influenced by several factors, independent of p53 (as must be the situation in the O_2 insensitive p53 null cell line SKOV3).

The differences in O_2-sensitivity and, consequently, cell proliferation is most important when trying to recapitulate *in vivo* responses where physiological O_2 tensions vary from 2.7–5% in the interstitial space (where many cancer cells reside) to 14.7% in the arterial circulation and lung [18]. Thus, it is reasonable to predict that if O_2-sensitive cancer cells were to dislodge from a primary interstitial space and migrate to the lungs via blood circulation, the increased O_2 concentration would restrict proliferation. In contrast, we speculate that oxygen insensitive cancer cells would have a selective advantage compared to sensitive ones, being better able to thrive in the conditions of increased oxygen concentration. In fact, 14-3-3 σ is frequently over-expressed in many thyroid [54], colorectal [55] and prostate [56] tumors, and is also a potential target for therapeutic modulation [55,56]. Our results provide one rationale for selecting the cancers best suited for 14-3-3 σ targeted therapy. Oxygen insensitivity observed in HeyA8 or SKOV3 is less likely an adaptation to *in vitro* growth conditions because transient over-expression of 14-3-3 σ renders O_2-sensitive A2780 cell line insensitive to increased levels of O_2 (Figure 5D), and over-expression of 14-3-3 σ is observable in primary tumors with metastatic potential (Figure 7). Oxygen sensitivity could therefore be an important factor in the context of metastatic spread of

cancer because over-expression of 14-3-3 σ is frequently observed in metastatic cancers, including this study (Figure 7) and others (gastric [57], endometrial [58] and pancreatic [59]). However, epigenetic inactivation of 14-3-3 σ by gene methylation has also been reported to correlate with decreased expression of 14-3-3 σ in cancer progression [60] and metastasis of certain types of tumors [61]. Further, a correlation with a functional role for 14-3-3 σ in promoting tumor invasion and metastasis has also been demonstrated [45,47,62]. Taken together, there is ample evidence to support that over-expression of 14-3-3 σ is relevant to tumor metastasis and therefore, it is likely that O_2 insensitivity associated with over-expression of 14-3-3 σ may have a pivotal role in metastatic dissemination of tumors. Further support to demonstrate the explicit role of 14-3-3 σ in *in vivo* O_2 sensitivity and its relevance to metastasis would require experiments with animal models.

In conclusion, there are many advantages to studying cancer biology under physiological O_2. In fact, compared to cell propagation under physiological O_2, ambient O_2 levels are expected to result in oxidative stress [4], mutation proneness and persistence of transformation [63]. In this context, we have demonstrated that growing cancer cells *in vitro* at low physiological O_2 (not hypoxia), compared with ambient (21%) O_2 is a prudent approach to identify and understand some of the behavioral diversity observed in cancer.

Materials and Methods

Cell culture and Transfection

Ovarian cancer cells were grown in RPMI 1640 (A2780, OVCAR5, OVCAR8, SKOV3) or DMEM (HeyA8 and HOC8)

supplemented with 10% heat inactivated Fetal Bovine Serum (Sigma Aldrich, St.Louis, MO, Cat# F6178) and 200 units of penicillin/streptomycin and 0.5 µg amphotericin-B. Transfection was performed using Amaxa Nucleofector technology (Lonza) as described previously [64]. Plasmid pcDNA 3.0 HA 14-3-3 σ was obtained from Addgene (plasmid 11946 [65]) and pcDNA 3.0 HA empty vector was a gift from Dr. Y. Shiio, UTHSCSA. 14-3-3 σ siRNA and non-targeting dsRNA were purchased from Dharmacon. For oxygen exposures we used Forma Series II 3110 water-jacketed multigas incubator (Thermo Fisher scientific, Waltham, MA) with built-in CO_2 and O_2 monitors and controllers. To maintain 3% O_2, the incubator received an additional supply of nitrogen gas.

Cell proliferation

Cell proliferation was determined using Celltitre-Glo (Promega, Madison, WI) per manufacturer instructions, as described previously [64]. Cells were seeded to a final density of 100, 200 or 400 cells per well in a 384 well plate containing 40 µl of growth medium consisting of 2%, 6% or 10% FBS and antibiotics. Plates were then placed in a humid chamber and returned to the incubators of appropriate oxygen pressure. After 3 days of incubation, the number of cells present per well was measured using Celltitre-Glo reagent, as described previously [64]. The number of cells per well was determined using a standard curve based on ATP concentration, as recommended by the manufacturer.

Mitotic Index

The number of mitotic cells were quantified based the method as described [66]. Briefly, 96 well collagen coated plates were used to seed cells at a final concentration of 1000 cells/well in their respective media. Cells were then incubated for three days at 37°C in 3% or 21% O_2. Finally, cells were washed, resuspended in phosphate buffered saline and stained with DAPI, as described [66]. Images of stained cells were acquired using a Zeiss Axiovert 200M inverted fluorescent microscope using 10X magnification and Openlab (PerkinElmer) image acquisition software. Using Image J, a set threshold for staining intensity was used to count the brightly stained nuclei, with obvious chromatin condensation and the mitotic index was determined based on the ratio of number of mitotic cells present in 1000 cells, as described [66].

Protein isolation and Western blot analysis

Protein lysates and western blot analysis were preformed as previously described [64]. The immunoblots were probed with the appropriate dilutions of primary antibody and visualized using either Lumiglo (Cell signaling technology) or the ECL plus system (GE Healthcare) with the appropriate horseradish peroxidase-conjugated secondary antibody. The primary antibodies used were Phospho - p53 (Ser 15), total p53, Phospho - CDC2 (Tyr 15) and Total CDC2, Phospho - Cyclin B1 (Ser 133), total Cyclin B1, Phospho - CDC25C (Thr 160), total CDC25C, Phsopho RB (Ser 807/811), total RB, Phospho - WEE1 (Ser 642) and total WEE1 (Cell signaling technology), p21, 14-3-3 σ (Millipore) and β-actin (Abcam). Primary antibody dilutions were used as per manufacturer instructions. RB and WEE1 immunoblots were performed using 4–15% gradient gel (Criterion precast gel, Biorad).

Flow Cytometry

Cells were trypsinized and seeded to a final density of 1×10^6 cells per well in a 10 cm dish containing growth medium, antibiotics and appropriate concentrations of FBS. Dishes were then returned to the incubators set for the different oxygen conditions. Following three days of incubation, cells were harvested and prepared for FACS analysis as described previously [67]. Experiments were performed in triplicate. Stained cells were analyzed using a FACS Canto I (BD Biosciences) flow cytometer using an argon laser at 488 nm wavelength. Cell cycle analysis was performed using Modfit LT (version 3.2) software (Verity Software House).

Quantification of M phase cells

The number of cells in M phase were quantified based on mitosis-specific histone H3 phosphorylation in the ovarian cancer cell lines using the Cellomics® Cell Cycle Kit I (Thermo Scientific) as per the manufacturer's recommended protocol. Briefly, 96 well collagen coated plates were used to seed cells at a final concentration of 1000 cells/well in their respective media. Cells were then incubated for three days at 37°C in 3% or 21% O_2. Control wells were treated with 1.5 µg/ml nocodazole (Sigma Aldrich) for 16 hours, fixed with 16% formaldehyde, permeabilized, blocked and stained with reagents consisting anti-phospho-histone H3 primary antibody, as per instructions provided in the kit. Stained cells were analyzed with a Zeiss Axiovert 200M inverted fluorescent microscope using 10X magnification and Openlab (PerkinElmer) image acquisition software. 100–250 cells per replicate were counted for phospho-histone H3 positive cells.

Immunolocalization of 14-3-3 σ and CDC2

A2780 cells transfected with a 14-3-3 σ cDNA expression construct or HeyA8 cells transfected with 14-3-3 σ siRNA were seeded at a final density of 10^5 cells per fibronectin (Sigma) coated 12.5 mm^2 glass coverslip mounted in each well of a 12-well plate. Cells were maintained in complete growth medium supplemented with 10% fetal bovine serum and allowed to grow for three days in the presence of 21% or 3% oxygen. For the detection of 14-3-3 σ or CDC2 by immunofluorescence, cells were processed as described previously [68]. The primary antibodies used were mouse monoclonal 14-3-3 σ at 1.0 µg/mL (Upstate) and rabbit polyclonal total CDC2 at 1:1000 (Cell Signaling). Following a PBS wash, the cells were incubated with secondary antibodies, goat anti-mouse AlexaFluor 488 and goat anti-rabbit AlexaFluor 568 (Invitrogen) at 1:1000 dilution in blocking buffer for 1 hour at room temperature. Cells were then counterstained with DAPI (1:3000 dilution in PBS) and mounted onto microscope slides using Fluoromount-G. Images were taken at 63X magnification using the Zeiss Axiovert 200M inverted fluorescent microscope and Openlab software (PerkinElmer).

Reverse Phase Protein Array

Protein lysates from 57 cancer cell lines or 205 primary ovarian cancer tumors were spotted in RPPA slides and processed for expression analysis, as described previously [69,70]. Data acquisition and processing were performed as described previously [69]. Ovarian cancer specimens were obtained from Gynecology Tumor Tissue Bank at MD Anderson Cancer Center, following approval from the Institutional Review Board (BT).

Normalization and Clustering

log-transformed RPPA data was first examined to remove non ovarian cancer cell lines. We then examined all replicated representations from the same source as annotated to reduce down to 57 ovarian cancer cell lines or 205 patient samples (from each source) by taking the median protein expression level of all replicates. An additional cell-line specific normalization step was performed in which median expression levels for each protein was

first determined and then subtracted from individual RPPA experiments. The anchored heatmap (termed after anchored over/under-expression orientation) was generated by requiring RB, 14-3-3 σ and CDC2 to be arranged from over-expressed to under-expressed recursively from the given cell-line order, but exact positions of each protein was determined by hierarchical clustering algorithm with Euclidean distance as similarity measure and average lineage from all cell-lines, as shown in Figure 6 A&B). Raw data obtained from RPPA for the expression of Phospho RB, 14-3-3 σ and CDC2 is provided in the supplementary tables (for ovarian cancer cell lines, see Table S2, and for ovarian cancer patient specimens, see Table S3)

Immunohistochemistry

Tissue arrays (OV951-1) consisting of normal and malignant tissues from primary or metastatic sites were purchased from US Biomax Inc. Slides were processed for immunohistochemistry and analyzed, as described previously [71]. 14-3-3 σ (Upstate) was used at 1:50 dilution for incubation with primary antibody and subsequent steps were performed using the Dako universal LSAB kit with DAB as described by the manufacturer.

Statistical Analyses

To determine significant differences to proliferation under 3% or 21% O_2, a Student *t-test* was performed, and *ANOVA* was performed to compare the different cell cycle profiles with the panel of ovarian cancer cell lines. Kaplan-Meier survival analysis with p-value determined with log-rank test was performed using MATLAB (Mathworks, Natick, MA) for RPPA data consisting patient specimens. For Kaplan-Meier survival analysis the data was censored based on patient's vital status. Statistical analysis for the correlation of 14-3-3 σ expression with the various pathological grades of ovarian tumors determined based on immunohistochemistry was analyzed by a Fisher's exact test using R.

Supporting Information

Figure S1 Western blot analysis of phospho and total p53, and p21, which are major upstream regulators of G2/M cell cycle progression and the relevance to 21% or 3% O_2 in ovarian cancer cells. O_2 insensitive cell lines are indicated by asterisk and italics.
(EPS)

Table S1 *In vitro* cell doubling time for the ovarian cancer cell lines.
(XLS)

Table S2 Raw data from cell line RPPA for Phospho-Rb, p53, CDC2 and 14-3-3 σ expression. The table contains following columns: 1) Unique ID, 2) Original cell-line or with treatment, 3) Cell-line's contributing Lab/source; 4) Cell type, 5) Cell-line name, 6–9) log2 transformed protein expression ratios (14-3-3 σ, CDC2, p-Rb, and p53) as the raw measurement provided by the MD Anders Cancer Center RPPA core facility.
(XLS)

Table S3 Raw data from OVSS2 RPPA for Phospho Rb, CDC2 and 14-3-3 σ expression. The table contains following columns: 1) Unique ID, 2) Tumor ID in various databases (DBs), 3) Tumor source institution; 4) patient age at diagnosis (in months), 5) tumor stage, 6) grade (HG: high grade, LG: low grade, empty: unknown), 7) Overall survival (in months), 8) Vital Status (0: alive, 1: dead), 9–12) log2 transformed protein expression ratios (14-3-3 σ, CDC2, p53 and p-Rb) as the raw measurement provided by the MD Anderson Cancer Center RPPA core facility.
(XLS)

Author Contributions

Conceived and designed the experiments: DR AJRB. Performed the experiments: DR BK AB TTG. Analyzed the data: DR YC BK AB AJRB. Contributed reagents/materials/analysis tools: YC JL MSC BTH AJRB. Wrote the paper: DR YC BK AB AJRB.

References

1. Sullivan M, Galea P, Latif S (2006) What is the appropriate oxygen tension for in vitro culture? Mol Hum Reprod 12: 653.
2. Csete M (2005) Oxygen in the cultivation of stem cells. Ann N Y Acad Sci 1049: 1–8.
3. Hornsby PJ (2003) Mouse and human cells versus oxygen. Sci Aging Knowledge Environ 2003: PE21.
4. Parrinello S, Samper E, Krtolica A, Goldstein J, Melov S, et al. (2003) Oxygen sensitivity severely limits the replicative lifespan of murine fibroblasts. Nat Cell Biol 5: 741–747.
5. Shay JW, Wright WE (2007) Tissue culture as a hostile environment: identifying conditions for breast cancer progression studies. Cancer Cell 12: 100–101.
6. Ince TA, Richardson AL, Bell GW, Saitoh M, Godar S, et al. (2007) Transformation of different human breast epithelial cell types leads to distinct tumor phenotypes. Cancer Cell 12: 160–170.
7. Frieboes HB, Edgerton ME, Fruehauf JP, Rose FR, Worrall LK, et al. (2009) Prediction of drug response in breast cancer using integrative experimental/computational modeling. Cancer Res 69: 4484–4492.
8. Sridhar KS, Plasse TF, Holland JF, Shapiro M, Ohnuma T (1983) Effects of physiological oxygen concentration on human tumor colony growth in soft agar. Cancer Res 43: 4629–4631.
9. Gupta V, Krishan A (1982) Effect of oxygen concentration on the growth and drug sensitivity of human melanoma cells in soft-agar clonogenic assay. Cancer Res 42: 1005–1007.
10. Carrera S, de Verdier PJ, Khan Z, Zhao B, Mahale A, et al. (2010) Protection of cells in physiological oxygen tensions against DNA damage-induced apoptosis. J Biol Chem 285: 13658–13665.
11. Laser H (1937) Tissue metabolism under the influence of low oxygen tension. Biochem J 31: 1671–1676.
12. Green DR, Chipuk JE (2006) p53 and metabolism: Inside the TIGAR. Cell 126: 30–32.
13. Powers DE, Millman JR, Huang RB, Colton CK (2008) Effects of oxygen on mouse embryonic stem cell growth, phenotype retention, and cellular energetics. Biotechnol Bioeng 101: 241–254.
14. Pouyssegur J, Dayan F, Mazure NM (2006) Hypoxia signalling in cancer and approaches to enforce tumour regression. Nature 441: 437–443.
15. Magagnin MG, Koritzinsky M, Wouters BG (2006) Patterns of tumor oxygenation and their influence on the cellular hypoxic response and hypoxia-directed therapies. Drug Resist Updat 9: 185–197.
16. Brizel DM, Rosner GL, Prosnitz LR, Dewhirst MW (1995) Patterns and variability of tumor oxygenation in human soft tissue sarcomas, cervical carcinomas, and lymph node metastases. Int J Radiat Oncol Biol Phys 32: 1121–1125.
17. Brown JM, Giaccia AJ (1998) The unique physiology of solid tumors: opportunities (and problems) for cancer therapy. Cancer Res 58: 1408–1416.
18. Treacher DF, Leach RM (1998) Oxygen transport-1. Basic principles. Bmj 317: 1302–1306.

19. Pantel K, Brakenhoff RH (2004) Dissecting the metastatic cascade. Nat Rev Cancer 4: 448–456.

20. Sherr CJ (2004) Principles of tumor suppression. Cell 116: 235–246.

21. Payton M, Chung G, Yakowec P, Wong A, Powers D, et al. (2006) Discovery and evaluation of dual CDK1 and CDK2 inhibitors. Cancer Res 66: 4299–4308.

22. Taylor WR, Stark GR (2001) Regulation of the G2/M transition by p53. Oncogene 20: 1803–1815.

23. Graeber TG, Peterson JF, Tsai M, Monica K, Fornace AJ, Jr., et al. (1994) Hypoxia induces accumulation of p53 protein, but activation of a G1-phase checkpoint by low-oxygen conditions is independent of p53 status. Mol Cell Biol 14: 6264–6277.

24. Das KC, Dashnamoorthy R (2004) Hyperoxia activates the ATR-Chk1 pathway and phosphorylates p53 at multiple sites. Am J Physiol Lung Cell Mol Physiol 286: L87–97.

25. Hermeking H, Lengauer C, Polyak K, He TC, Zhang L, et al. (1997) 14-3-3 sigma is a p53-regulated inhibitor of G2/M progression. Mol Cell 1: 3–11.

26. Eguchi T, Takaki T, Itadani H, Kotani H (2007) RB silencing compromises the DNA damage-induced G2/M checkpoint and causes deregulated expression of the ECT2 oncogene. Oncogene 26: 509–520.

27. Balin AK, Goodman DB, Rasmussen H, Cristofalo VJ (1978) Oxygen-sensitive stages of the cell cycle of human diploid cells. J Cell Biol 78: 390–400.

28. Stark GR, Taylor WR (2006) Control of the G2/M transition. Mol Biotechnol 32: 227–248.

29. Kaldis P, Aleem E (2005) Cell cycle sibling rivalry: Cdc2 vs. Cdk2. Cell Cycle 4: 1491–1494.

30. Lindqvist A, Rodriguez-Bravo V, Medema RH (2009) The decision to enter mitosis: feedback and redundancy in the mitotic entry network. J Cell Biol 185: 193–202.

31. Kishimoto T (1994) Cell reproduction: induction of M-phase events by cyclin-dependent cdc2 kinase. Int J Dev Biol 38: 185–191.

32. Lees JA, Buchkovich KJ, Marshak DR, Anderson CW, Harlow E (1991) The retinoblastoma protein is phosphorylated on multiple sites by human cdc2. Embo J 10: 4279–4290.

33. Berry LD, Gould KL (1996) Regulation of Cdc2 activity by phosphorylation at T14/Y15. Prog Cell Cycle Res 2: 99–105.

34. Shibuya EK (2003) G2 cell cycle arrest—a direct link between PKA and Cdc25C. Cell Cycle 2: 39–41.

35. Roy S, Khanna S, Bickerstaff AA, Subramanian SV, Atalay M, et al. (2003) Oxygen sensing by primary cardiac fibroblasts: a key role of p21(Waf1/Cip1/Sdi1). Circ Res 92: 264–271.

36. Lees SJ, Childs TE, Booth FW (2008) p21(Cip1) expression is increased in ambient oxygen, compared to estimated physiological (5%) levels in rat muscle precursor cell culture. Cell Prolif 41: 193–207.

37. Kim SY, Ferrell JE, Jr. (2007) Substrate competition as a source of ultrasensitivity in the inactivation of Wee1. Cell 128: 1133–1145.

38. Dalton S (1992) Cell cycle regulation of the human cdc2 gene. Embo J 11: 1797–1804.

39. Smith EM, Proud CG (2008) cdc2-cyclin B regulates eEF2 kinase activity in a cell cycle- and amino acid-dependent manner. Embo J 27: 1005–1016.

40. Astanehe A, Arenillas D, Wasserman WW, Leung PC, Dunn SE, et al. (2008) Mechanisms underlying p53 regulation of PIK3CA transcription in ovarian surface epithelium and in ovarian cancer. J Cell Sci 121: 664–674.

41. Armaiz-Pena GN, Mangala LS, Spannuth WA, Lin YG, Jennings NB, et al. (2009) Estrous cycle modulates ovarian carcinoma growth. Clin Cancer Res 15: 2971–2978.

42. Urano T, Saito T, Tsukui T, Fujita M, Hosoi T, et al. (2002) Efp targets 14-3-3 sigma for proteolysis and promotes breast tumour growth. Nature 417: 871–875.

43. Ramirez PT, Landen CN, Jr., Coleman RL, Milam MR, Levenback C, et al. (2008) Phase I trial of the proteasome inhibitor bortezomib in combination with carboplatin in patients with platinum- and taxane-resistant ovarian cancer. Gynecol Oncol 108: 68–71.

44. Li Z, Liu JY, Zhang JT (2009) 14-3-3sigma, the double-edged sword of human cancers. Am J Transl Res 1: 326–340.

45. Ghahary A, Karimi-Busheri F, Marcoux Y, Li Y, Tredget EE, et al. (2004) Keratinocyte-releasable stratifin functions as a potent collagenase-stimulating factor in fibroblasts. J Invest Dermatol 122: 1188–1197.

46. Ghahary A, Marcoux Y, Karimi-Busheri F, Li Y, Tredget EE, et al. (2005) Differentiated keratinocyte-releasable stratifin (14-3-3 sigma) stimulates MMP-1 expression in dermal fibroblasts. J Invest Dermatol 124: 170–177.

47. Lam E, Kilani RT, Li Y, Tredget EE, Ghahary A (2005) Stratifin-induced matrix metalloproteinase-1 in fibroblast is mediated by c-fos and p38 mitogen-activated protein kinase activation. J Invest Dermatol 125: 230–238.

48. Poot M, Schindler D, Kubbies M, Hoehn H, Rabinovitch PS (1988) Bromodeoxyuridine amplifies the inhibitory effect of oxygen on cell proliferation. Cytometry 9: 332–338.

49. Poot M, Gross O, Epe B, Pflaum M, Hoehn H (1996) Cell cycle defect in connection with oxygen and iron sensitivity in Fanconi anemia lymphoblastoid cells. Exp Cell Res 222: 262–268.

50. Moreira JM, Shen T, Ohlsson G, Gromov P, Gromova I, et al. (2008) A combined proteome and ultrastructural localization analysis of 14-3-3 proteins in transformed human amnion (AMA) cells: definition of a framework to study isoform-specific differences. Mol Cell Proteomics 7: 1225–1240.

51. van Hemert MJ, Niemantsverdriet M, Schmidt T, Backendorf C, Spaink HP (2004) Isoform-specific differences in rapid nucleocytoplasmic shuttling cause distinct subcellular distributions of 14-3-3 sigma and 14-3-3 zeta. J Cell Sci 117: 1411–1420.

52. Noske A, Weichert W, Niesporek S, Roske A, Buckendahl AC, et al. (2008) Expression of the nuclear export protein chromosomal region maintenance/exportin 1/Xpo1 is a prognostic factor in human ovarian cancer. Cancer 112: 1733–1743.

53. Mhawech P (2005) 14-3-3 proteins—an update. Cell Res 15: 228–236.

54. Ito Y, Miyoshi E, Uda E, Yoshida H, Uruno T, et al. (2003) 14-3-3 sigma possibly plays a constitutive role in papillary carcinoma, but not in follicular tumor of the thyroid. Cancer Lett 200: 161–166.

55. Perathoner A, Pirkebner D, Brandacher G, Spizzo G, Stadlmann S, et al. (2005) 14-3-3sigma expression is an independent prognostic parameter for poor survival in colorectal carcinoma patients. Clin Cancer Res 11: 3274–3279.

56. Quayle SN, Sadar MD (2007) 14-3-3 sigma increases the transcriptional activity of the androgen receptor in the absence of androgens. Cancer Lett 254: 137–145.

57. Tanaka K, Hatada T, Kobayashi M, Mohri Y, Tonouchi H, et al. (2004) The clinical implication of 14-3-3 sigma expression in primary gastrointestinal malignancy. Int J Oncol 25: 1591–1597.

58. Nakayama H, Sano T, Motegi A, Oyama T, Nakajima T (2005) Increasing 14-3-3 sigma expression with declining estrogen receptor alpha and estrogen-responsive finger protein expression defines malignant progression of endometrial carcinoma. Pathol Int 55: 707–715.

59. Okada T, Masuda N, Fukai Y, Shimura T, Nishida Y, et al. (2006) Immunohistochemical expression of 14-3-3 sigma protein in intraductal papillary-mucinous tumor and invasive ductal carcinoma of the pancreas. Anticancer Res 26: 3105–3110.

60. Cheng L, Pan CX, Zhang JT, Zhang S, Kinch MS, et al. (2004) Loss of 14-3-3sigma in prostate cancer and its precursors. Clin Cancer Res 10: 3064–3068.

61. Yi B, Tan SX, Tang CE, Huang WG, Cheng AL, et al. (2009) Inactivation of 14-3-3 sigma by promoter methylation correlates with metastasis in nasopharyngeal carcinoma. J Cell Biochem 106: 858–866.

62. Chavez-Munoz C, Morse J, Kilani R, Ghahary A (2008) Primary human keratinocytes externalize stratifin protein via exosomes. J Cell Biochem 104: 2165–2173.

63. Busuttil RA, Rubio M, Dolle ME, Campisi J, Vijg J (2003) Oxygen accelerates the accumulation of mutations during the senescence and immortalization of murine cells in culture. Aging Cell 2: 287–294.

64. Ravi D, Wiles AM, Bhavani S, Ruan J, Leder P, et al. (2009) A network of conserved damage survival pathways revealed by a genomic RNAi screen. PLoS Genet 5: e1000527.

65. Wilker EW, Grant RA, Artim SC, Yaffe MB (2005) A structural basis for 14-3-3sigma functional specificity. J Biol Chem 280: 18891–18898.

66. Tarnowski BI, Sens DA, Nicholson JH, Hazen-Martin DJ, Garvin AJ, et al. (1993) Automatic quantitation of cell growth and determination of mitotic index using DAPI nuclear staining. Pediatr Pathol 13: 249–265.

67. Ravi D, Muniyappa H, Das KC (2005) Endogenous thioredoxin is required for redox cycling of anthracyclines and p53-dependent apoptosis in cancer cells. J Biol Chem 280: 40084–40096.

68. Ravi D, Das KC (2004) Redox-cycling of anthracyclines by thioredoxin system: increased superoxide generation and DNA damage. Cancer Chemother Pharmacol 54: 449–458.

69. Zhang L, Wei Q, Mao L, Liu W, Mills GB, et al. (2009) Serial dilution curve: a new method for analysis of reverse phase protein array data. Bioinformatics 25: 650–654.

70. Stemke-Hale K, Gonzalez-Angulo AM, Lluch A, Neve RM, Kuo WL, et al. (2008) An integrative genomic and proteomic analysis of PIK3CA, PTEN, and AKT mutations in breast cancer. Cancer Res 68: 6084–6091.

71. Ravi D, Ramadas K, Mathew BS, Nalinakumari KR, Nair MK, et al. (1999) De novo programmed cell death in oral cancer. Histopathology 34: 241–249.

Elsevier Editorial System(tm) for DNA Repair
Manuscript Draft

Corresponding Author: Dr. Alexander J R Bishop, DPhil

Corresponding Author's Institution: UTHSCSA

First Author: Bijal Karia, BS

Order of Authors: Bijal Karia, BS; Jo Ann Martinez; Alexander J R Bishop, DPhil

Abstract: Much of our understanding of homologous recombination, as well as the development of the working models for these processes, has been derived from extensive work in model organisms, such as yeast and fruit flies, and mammalian systems by studying the repair of induced double strand breaks or repair following exposure to genotoxic agents in vitro. We therefore set out to expand this in vitro work to ask whether DNA-damaging agents with varying modes of action could induce somatic change in an in vivo mouse model of homologous recombination. We exposed pregnant dams to DNA-damaging agents, conferring a variety of lesions at a specific time in embryo development. To monitor homologous recombination frequency, we used the well-established retinal pigment epithelium pink-eyed unstable assay. Homologous recombination resulting in the deletion of a duplicated 70 kb fragment in the coding region of the Oca2 gene renders this gene functional and can be visualized as a pigmented eyespot in the retinal pigment epithelium. We observed an increased frequency of pigmented eyespots in resultant litters following exposure to cisplatin, methyl methanesulfonate, ethyl methanesulfonate, 3-aminobenzamide, bleomycin, and etoposide with a contrasting decreased frequency of reversion events following camptothecin and hydroxyurea exposure. The somatic genomic rearrangements that result from such a wide variety of differently acting damaging agents implies long-term potential effects from even short-term in utero exposures.

ELSEVIER

DNA Repair
Conflict of Interest Policy

Manuscript number (if applicable): Article Title: Induction of Homologous Recombination Following *in utero* Exposure to DNA Damaging Agents	Author name: Jo Ann Martinez

Declarations

DNA Repair requires that all authors sign a declaration of conflicting interests. If you have nothing to declare in any of these categories then this should be stated.

Conflict of Interest

A conflicting interest exists when professional judgement concerning a primary interest (such as patient's welfare or the validity of research) may be influenced by a secondary interest (such as financial gain or personal rivalry). It may arise for the authors when they have financial interest that may influence their interpretation of their results or those of others. Examples of potential conflicts of interest include employment, consultancies, stock ownership, honoraria, paid expert testimony, patent applications/registrations, and grants or other funding.

Please state any competing interests

> The authors declare that there are no conflicts of interest

Funding Source

All sources of funding should also be acknowledged and you should declare any involvement of study sponsors in the study design; collection, analysis and interpretation of data; the writing of the manuscript; the decision to submit the manuscript for publication. If the study sponsors had no such involvement, this should be stated.

Please state any sources of funding for your research

Signature (a scanned signature is acceptable, but each author must sign)

Jo Ann Martinez (signature)

Print name

Jo Ann Martinez

DNA Repair
Conflict of Interest Policy

Manuscript number (if applicable): Article Title: Induction of Homologous Recombination Following *in utero* Exposure to DNA Damaging Agents

Author name: Alexander J.R. Bishop

Declarations

DNA Repair requires that all authors sign a declaration of conflicting interests. If you have nothing to declare in any of these categories then this should be stated.

Conflict of Interest

A conflicting interest exists when professional judgement concerning a primary interest (such as patient's welfare or the validity of research) may be influenced by a secondary interest (such as financial gain or personal rivalry). It may arise for the authors when they have financial interest that may influence their interpretation of their results or those of others. Examples of potential conflicts of interest include employment, consultancies, stock ownership, honoraria, paid expert testimony, patent applications/registrations, and grants or other funding.

Please state any competing interests

The authors declare that there are no conflicts of interest

Funding Source

All sources of funding should also be acknowledged and you should declare any involvement of study sponsors in the study design; collection, analysis and interpretation of data; the writing of the manuscript; the decision to submit the manuscript for publication. If the study sponsors had no such involvement, this should be stated.

Please state any sources of funding for your research

NIH NCI (1R01CA152063-01A1) NIH NIEHS (1R15ES019128-01) NIH NIEHS (K22ES012264) GCCRI AMBASSADOR'S CIRCLE RESEARCH SUPPORT AWARD

Signature (a scanned signature is acceptable, but each author must sign)

Digitally signed by Alex Bishop
DN: cn=Alex Bishop, o=UTHSCSA,
ou=GCCRI,
email=bishopa@uthscsa.edu, c=US
Date: 2013.03.28 12:48:55 -05'00'

Print name

Alexander Bishop_____

ELSEVIER

DNA Repair
Conflict of Interest Policy

Manuscript number (if applicable):	Author name: Bijal Karia
Article Title: Induction of Homologous Recombination Following in utero Exposure to DNA Damaging Agents	

Declarations

DNA Repair requires that all authors sign a declaration of conflicting interests. If you have nothing to declare in any of these categories then this should be stated.

Conflict of Interest

A conflicting interest exists when professional judgement concerning a primary interest (such as patient's welfare or the validity of research) may be influenced by a secondary interest (such as financial gain or personal rivalry). It may arise for the authors when they have financial interest that may influence their interpretation of their results or those of others. Examples of potential conflicts of interest include employment, consultancies, stock ownership, honoraria, paid expert testimony, patent applications/registrations, and grants or other funding.

Please state any competing interests

The author declares that there are no conflicts of interest

Funding Source

All sources of funding should also be acknowledged and you should declare any involvement of study sponsors in the study design; collection, analysis and interpretation of data; the writing of the manuscript; the decision to submit the manuscript for publication. If the study sponsors had no such involvement, this should be stated.

Please state any sources of funding for your research

DOD CDMRP Breast Cancer Research Program Predoctoral Traineeship Award (W81XWH-10-1-0026)

Signature (a scanned signature is acceptable, but each author must sign)

Print name

Bijal Karia

*Cover Letter

WE MAKE LIVES BETTER
UT HEALTH SCIENCE CENTER™
SAN ANTONIO

Alex Bishop, D. Phil
UTHSCSA
Department of Cellular and Structural Biology,
Greehey Children's Cancer Research Institute,
7703 Floyd Curl Drive,
San Antonio, TX 78229

Phone: 210-562-9060
Fax: 210-562-9014
Email: bishopa@uthscsa.edu

Samuel H. Wilson
Editor-in-Chief,
Lab. of Structural Biology, National Institutes of Health (NIH),
National Institute of Environmental Health Sciences (NIEHS)
Research Triangle Park,
NC 27709-2233, USA
Tel. (919) 541-4701
Fax. (919) 541-4724

March 28, 2013

To the Managing Editor,

Please find attached our manuscript entitled "Induction of Homologous Recombination following *in utero* Exposure to DNA-Damaging Agents" for your kind consideration as a research article in DNA Repair.

In this paper we set out to ask whether DNA-damaging agents with varying modes of action can induce somatic change in the *in vivo* p^{un} mouse model of homologous recombination. Extensive tissue culture work has been done to study the repair of induced double strand breaks or repair following exposure to genotoxic agents, but here we look at the role of homologous recombination in an *in vivo* model system and its ability to repair strand breaks, alkylation damage and replication block associated damage, among others. Further, the fact that these DNA damaging agents are used in chemotherapy may have implications when administered *in utero* to a developing fetus; in the context of increased somatic genetic variation providing an environment conducive to increased cancer risk. We believe that this is a timely and thought provoking manuscript that will be of interest to your readers. Of note, this manuscript is not being sent to any other journal for consideration for publication.

We would like to suggest the following scientists as potential reviewers who may be familiar with the subject:

Bevin Engelward, *Department of Biological Engineering, Massachusetts Institute of Technology 77 Massachusetts Avenue, Rm. 16-267, Cambridge, MA 02139, Tel. (617) 258-0260, Fax. (617) 258-0499, email: bevin@mit.edu*

Thomas Helleday, *Department of Genetics Microbiology and Toxicology, Stockholm University, S-106 91 Stockholm, Sweden, email: helleday@gmt.su.se*

Helen E Bryant, *Institute for Cancer Studies, Department of Oncology, The Medical School Beech Hill Road, Sheffield S10 2RX, UK, Tel: +44 (0)114 271 2993, Fax: +44 (0)114 271 1602, email: h.bryant@sheffield.ac.uk*

Bernard S. Lopez, *Institut de radiobiologie Cellulaire et moléculaire, 18 route du panorama, Fontenay aux Roses F-92265, France. Tel: 33-1-4654-8835; Fax: 33-1-4654-8955; email: bernard.lopez@cea.fr*

Thomas J. Begley, *Department of Biomedical Sciences, School of Public Health, Ge*NY*sis Center for Excellence in Cancer Genomics, University at Albany, State University of New York, email: tbegley@albany.edu*

Niall G. Howlett, *University of Rhode Island, College of the Environment and Life Sciences, 379 CBLS Building, Tel: 401-874-4306, email: nhowlett@mail.uri.edu*

We would like to suggest the following editors for their expertise:

Philip C. Hanawalt
Leona D. Samson
Bennett Van Houten
Rodney Rothstein

Thank you again for considering our manuscript and I look forward to hearing from you.

Sincerely yours,

Alex Bishop, D.Phil.
Assistant Professor of Cellular & Structural Biology

Highlights

- HR repairs a variety of DNA lesions as measured by the p^{un} assay
- *In utero* exposure to cisplatin and alkylation damage increased HR frequency
- *In utero* exposure to PARP inhibition and bleomycin increased HR frequency
- *In utero* exposure to etoposide increased HR frequency
- *In utero* exposure to camptothecin and HU decreased HR frequency

Abstract

Much of our understanding of homologous recombination, as well as the development of the working models for these processes, has been derived from extensive work in model organisms, such as yeast and fruit flies, and mammalian systems by studying the repair of induced double strand breaks or repair following exposure to genotoxic agents *in vitro.* We therefore set out to expand this *in vitro* work to ask whether DNA-damaging agents with varying modes of action could induce somatic change in an *in vivo* mouse model of homologous recombination. We exposed pregnant dams to DNA-damaging agents, conferring a variety of lesions at a specific time in embryo development. To monitor homologous recombination frequency, we used the well-established retinal pigment epithelium pink-eyed unstable assay. Homologous recombination resulting in the deletion of a duplicated 70 kb fragment in the coding region of the Oca2 gene renders this gene functional and can be visualized as a pigmented eyespot in the retinal pigment epithelium. We observed an increased frequency of pigmented eyespots in resultant litters following exposure to cisplatin, methyl methanesulfonate, ethyl methanesulfonate, 3-aminobenzamide, bleomycin, and etoposide with a contrasting decreased frequency of reversion events following camptothecin and hydroxyurea exposure. The somatic genomic rearrangements that result from such a wide variety of differently acting damaging agents implies long-term potential effects from even short-term *in utero* exposures.

Dear Dr. Samson,   July 5, 2013

We wish to thank the reviewers for their thoughtful and thorough review of our manuscript. We appreciate their overall positive response to the manuscript and have carefully considered each of their comments. In general the introduction and discussion of the manuscript has been greatly revised and shortened from the original version, as suggested by the Reviewer. Otherwise we have addressed each comment as outlined below hopefully to their satisfaction.

<u>Reviewer #1</u>

1) *Therefore, the camptothecin result is particularly puzzling and potentially warrants deeper analysis, ideally with follow up studies to test resulting hypotheses.*

   - We are in agreement that camptothecin and HU resulted in a surprising result and a deeper analysis would be very interesting but this is beyond the scope of the current study (as further noted below).

2) *The manuscript is well written, although it would benefit from being shortened overall.*

   - Thank you for the comment. To reduce the overall length of the manuscript the overlapping points in the introduction and discussion have been condensed and only pertinent information regarding the action and mechanism of the drugs has been retained for better readability of the manuscript.

3) *Additionally, the impact of this study would be greater if more attention were put to the overriding differences in the mechanism of action of the different agents, and the implication of those differences in terms of the types of HR events that might ensue (and the likelihood that such events would be detectable)*

   - The reviewer makes a good point and something that would be worth pursuing. The HR event that reconstitutes the *p* gene can result from single strand annealing (SSA) or unequal crossover between sister chromatids or between homologues or an unequal gene conversion type event or possibly a template switch either during replication or replication restart. We have shown here that the resulting fur or eyespots exhibit increased frequency after exposure to different DNA-damaging

agents, and previously the effect of different genetic backgrounds. The mechanisms of HR utilized to repair each differing DNA damaging agent is an interesting question, but would require specific substrates to be examined (that distinguished each of the above possibilities) and would probably have to be conducted using tissue culture systems. As such, we believe that such an extensive study would be well suited for a future study while we attempt here to present a more generalized theme. In this manuscript we show the *in vivo in utero* effect of these exposures on the genome, without necessarily concentrating on the exact type of HR used.

4) *Describing and interpreting the experiments in more generalizable terms would strengthen this study*

- In addressing other points by the Reviewer (see point 12) and Reviewer #2 we have worked to focus on the general findings of changes in HR frequency in the context of differing DNA lesions.

5) *One concern of this reviewer is that the statement that "in utero exposure to camptothecin and HU decreased HR frequency" could be misleading. It may be the case that these exposures induced HR significantly, but that cells that underwent HR died. Therefore, a more conservative statement might be that "camptothecin and HU did not lead to a detectable increase in cells that had undergone HR", or perhaps it could be stated that "camptothecin and HU caused a decrease in the number of detectable HR events".*

- The Reviewer makes an excellent point and one that has been discussed at length within our lab. We suggested the possibility of cell death in the original manuscript and have now further changed the wording to the more conservative statement suggested by the Reviewer.

- "We observed an increased frequency of pigmented eyespots in resultant litters following exposure … with a contrasting decrease in the frequency of detectable reversion events following camptothecin and hydroxyurea exposure."

- "In contrast, a marked decrease in the frequency of detectable reversion events was observed for the

ribonucleotide reductase inhibitor (hydroxyurea) and Top1 inhibitor (camptothecin) measured in our study."

6) *Only the major result and none of the more minor results appear in the abstract, making what is new not as clear as it could be.*

   - To this regard we only included the major results in the abstract as the minor results would need the necessary explanation of the p^{un} assay in order to understand the further subdivision of single- and multicell eyespot data as well as positioning of the eyespots on the RPE.

7) *In both the introduction and in the discussion, the agents are listed with their background/results, which makes for a long list of information that is not as obviously interconnected as it could be. It might be helpful to draw more attention to the bigger themes/mechanisms of action and the implications of those mechanisms in order to make the impact of the work more clear.*

   - We thank the Reviewer for this suggestion to make the manuscript easier to read. The introduction has been shortened to only include the salient points needed to set the scene for the work to be mentioned. The discussion includes more details of the mechanisms of action for each damaging agent and relevant *in vitro* studies that are now furthered by our *in vivo* approach.

8) *It would be helpful if the difference between the results of this study and those of previous studies were made more apparent - e.g., it is not obvious which of these agents had been studied using the pun assay previously. Clarifying what is new in the introduction would be helpful.*

   - This is a good point and we felt that the most appropriate place would be in the discussion section following the *in vitro* work done for each respective DNA damaging agent. This was done purposely in order to compare and contrast work previously done and that which is being put forth in this manuscript.

   In the Introduction:
   - "Aside from the alkylating agents and camptothecin, to our knowledge the remaining DNA damaging agents have not been assessed previously using an *in vivo model* such as the p^{un} system."

In the Discussion:

- "Using the *in vivo* p^{un} fur-spot assay, other studies have demonstrated that HR is induced by either EMS or MMS, which we now recapitulate in this paper using the more sensitive RPE-based p^{un} mouse model."

- "A similar phenomenon of robust induction of HR reversion events in more central regions of the RPE, and specifically in single-cell eyespots as seen in this study, was also reported in a paper by Bishop *et al.* using the p^{un} eyespot assay with X-ray damage." Similar in that Bleomycin is often considered a radiomimetic.

- With regards to Camptothecin- "Surprisingly, we did not have a robust induction of HR in our p^{un} eyespot assay, although our preliminary fur-spot results indicated an induction recapitulating an earlier report with the p^{un} fur-spot assay using this agent."

9) Line 197 - *it is not necessarily the case that chemotherapeutics eliminate cancer cells.*

- This statement has been eliminated from the manuscript.

10) Line 216 - *Issues of dose-response would be good to clarify. What is the anticipated result if the dose is too high? Dose is mentioned, but the implications are not spelled out.*

- In general we selected the highest dose that did not apparently reduce numbers of mice per litter, that is, little teratogenic effect. Our assumption was that more damage without reduced embryonic viability would result in the maximal induction of HR. This is further clarified in the discussion section for camptothecin and HU. However, there may be differential effects in different tissues; the dose selected may have been too high for the RPE in general or specifically at the time of exposure during development. In contrast we observed a robust induction of HR in the fur-spot assay indicating that the agent did impact the embryos, and induced HR, but surprisingly we obtained a lack of response in the normally more sensitive eyespot assay.

- "Further, we observed an induction of reversion events following camptothecin exposure using the p^{un} fur-spot assay (similar to that reported by others), but a decrease in the p^{un} eyespot assay for the same animals. This suggests a tissue-specific difference in response, perhaps with RPE cells being more sensitive to camptothecin, resulting in greater cell death, permanent cell cycle arrest, or repair by other pathways without induction of HR events."

- "It is interesting that these latter data contrast with the clear induction observed using the fur-spot assay, which indicated that the selected doses should induce p^{un} reversion, albeit with possible cytotoxic effects in the RPE (Table 1). The resultant litters from pregnant dams exposed to EMS, showed a clear induction of p^{un} reversion in the RPE (compared with no induction in the fur), which indicates an increased sensitivity of the eyespot assay to detect damage-induced HR events."

11) Line 229 to 234. As HR is specific to S and G2, single cells are almost certainly the result of an HR event in a cell that did not divide again (as it is stated). As such, stating that HR is more likely to be tied to replication for the multicell spots implies that HR is happening in non-dividing cells.

- We apologize for the misleading implication. The very fact that we observe multicell events suggests that these events are occurring in cells that are actively dividing (or continue to divide following the p^{un} reversion events). The p^{un} reversions that result in single cell eyespots could either arise from a replicating cell that is about to undergo its terminal division, or it may result from cells that are in G1, but perhaps resulting from a single strand annealing type event. However, since we observe that the induced events occur in specific regions of the RPE (and not in regions that are postmitotic at the time of exposure) suggests that whether single cell or multicell, p^{un} reversions arise in cells that are actively dividing at the time of exposure.

- "Thus, according to our criteria, we would score a clonally expanded multicell eyespot as a single reversion event. In contrast, a single-cell eyespot might have been derived from an event that was not necessarily tied to

replication or in a cell that was in its terminal division and did not continue to divide once the revertant *p* gene segregated into one daughter cell. However, the p^{un} reversions that result in single-cell eyespots may result from cells that are in G1 through a single strand annealing type event. Since we observe that the induced events occur in specific regions of the RPE (and not in regions that are post mitotic at the time of exposure) suggests that whether single-cell or multicell, p^{un} reversions arise in cells that are actively dividing at the time of exposure."

12) *The reference to cancer during pregnancy is somewhat confusing. Perhaps a reference could be added as well as a bit more information about how often chemotherapy is given to pregnant women. As this is likely to be a rarity, perhaps alluding to other aspects of the impact of this work would be stronger - e.g., a statement about DNA damaging agents in general and their potential impact during development (which shows up later in the discussion).*

- We are in agreement that this concept takes away from the more general characterization of DNA damaging agents and their potential impact on somatic changes that may be of consequence later in life. The statement about cancer during pregnancy has been removed.

13) *The discussion might be stronger if shortened. There does not need to be a paragraph about camptothecin (line 425) and then another one about camptothecin and HU. Perhaps these can be condensed.*

- The Reviewer makes a great point and we initially did combine our discussion points about these two agents but given that the observed eyespot frequency result was different than expected and different from the p^{un} fur-spot assay we expanded this section to better discuss these findings and possibilities that may have occurred regarding other repair mechanisms. Also discussed further in Response #15 below.

14) *Line 436 - The word "contender" is colloquial.*

- The word "contender" has been replaced with "strong possibility"

15) *Lines 465 to 475. The conjecture here seems to be a bit of a stretch away from the actual data.*

- We understand the Reviewer's point and we perhaps have provided too much conjecture on this point. Given that we saw an overall decrease in the frequency of detectable HR events by the p^{un} assay the idea of cytotoxicity does not completely explain the decrease seen below that of spontaneous levels. We have only observed decreased p^{un} frequency in our lab using BRCA1 or BRCA2 deficient mice, which have a deficiency in homologous recombination. The idea that we are specifically losing cells that undergo HR at the p^{un} locus due to lesions in the p^{un} locus seems an unlikely explanation for a decreased frequency of p^{un} reversion. It is for this reason that we suggest an alternative mechanism(s) might be intervening and causing the observed phenomenon, such as transcription coupled repair resulting in the decrease detected by our assay. We suggest this possibility since the p gene is actively transcribed at this time during development in the RPE but not in melanoblasts that give rise to furspots. There are other possibilities too, such as activation of BLM-mediated processes to dissolve HR intermediates, amongst others, but, as the Reviewer points out, these points are conjecture. However, we raise the possibility as the loss of cell specifically undergoing HR induced by lesions in this specific region seems a very unsatisfying explanation for the observed results. We therefore have worked to reduce this section, though we believe it is important to raise the possibility other repair activities are compensating in the RPE specifically, while HR is the dominant repair pathway to repair lesions in the p^{un} locus of melanoblasts.

Reviewer #2

1) *How were the doses selected for the exposures and how do the doses influence the outcome in this case? How do the empirically derived doses compare to the findings in Table A1?*

- The doses were empirically selected based on published LD50, or fetotoxic doses (detailed below). We then chose

doses for our experiment based on litter survival, litter size and percent fur spotting frequency. Details are outlined below for each agent:

- Cisplatin- the LD50 (mouse, intraperitoneal injection (ip) is 6.6 mg/kg. Cisplatin was found to be teratogenic and fetotoxic when administered as an ip dose of 3 mg/kg. We therefore chose 2.5 mg/kg in a volume of 0.2 mL of saline for the experimental dose. We hypothesized that this dose would result in survival of embryos and still give a robust spotting frequency.

- MMS and EMS were previously used in the p^{un} fur assay as stated in reference [10] (100 mg/kg). A lower dose of MMS was chosen as it resulted in larger litter sizes and still elicited a 22% spot frequency (similar to 25% in reported in the abovementioned publication). The same dose of 100 mg/kg in the abovementioned publication was also used in our study for EMS, however we observed a 0% spot frequency, possibly due to a small sample size. We moved forward with this dose since it did not seem to compromise litter sizes, and gave a robust response in the previous publication.

- Bleomycin- the reported LD50 is 210 mg/kg. We chose a dose much lower to minimize toxicity.

- 3AB-the oral LD50 for mouse is 300 mg/kg. We thus chose a dose above seeing that no toxicity was witnessed to the pregnant dam or in terms of litter size.

- Etoposide is fetotoxic in the range of 2 mg/kg. We chose this dose because we were still able to achieve good litter sizes and robust fur spot induction.

- Camptothecin- oral LD50 is 50 mg/kg; another studied found the LD50 for human epithelial cells to be in the range of 12.5-25 mg/kg. We tested a broad range of doses and ultimately used the lowest dose to maximize HR induction and minimize toxicity.

- HU- oral LD50 is 7330 mg/kg we chose doses far lower and again picked the dose that maximized HR induction and minimized toxicity in the fur spot assay.

2) *Figure 2 data are not clear, axis need to be present in the figures themselves, the text says "where 0.0 corresponds to the region near the optic nerve and 1.0 represents the edge of the RPE"*

- One axis title is denoted for all figures to maintain readability. The axis tick marks are denoted in every figure and explained in the figure caption.

3) *Figure 1: what is the difference between asterisks and diamonds, the number of both of those is clear where it is stated that significance is denoted by asterisks (*P <.05, **P < .01, ***P < .001, ****P < .0001) or diamonds (??P < .01,.but what do the shapes convey-were there different comparisons?-this need to be made clear*

- This has been clarified in the caption for figure 1. The asterisks denote a significant increase, while the diamonds denote a significant decrease

4) *Table 1 is a list of chemicals used-this would be better to include as a supplementary table: Table A1 is much more important to the findings of the study, these should be swapped*

-This change has been made

We have carefully considered the requests of the reviewers and once again thank them for their insightful comments. Their suggestions have clarified and strengthened our manuscript. We have made extensive revisions to the manuscript but are more than willing to perform additional changes if it is deemed to be necessary by the Reviewers and Editor. Please do not hesitate to contact me if there are any further questions.

Sincerely,

Alexander J.R. Bishop

Induction of Homologous Recombination Following

in utero Exposure to DNA-Damaging Agents

Bijal Karia[1,2], Jo Ann Martinez[1], and Alexander J. R. Bishop[1,2,3]

[1]Greehey Children's Cancer Research Institute, The University of Texas Health Science Center at San Antonio, 8403 Floyd Curl Drive, San Antonio, Texas 78229, USA

[2]Department of Cellular and Structural Biology, The University of Texas Health Science Center at San Antonio, 7703 Floyd Curl Drive, San Antonio, Texas 78229, USA

[3]Cancer Therapy and Research Center, University of Texas Health Science Center at San Antonio, San Antonio, Texas 78229, USA

Correspondence should be addressed to A.J.R.B., email: bishopa@uthscsa.edu, phone: (210) 562-9000

Abstract

Much of our understanding of homologous recombination, as well as the development of the working models for these processes, has been derived from extensive work in model organisms, such as yeast and fruit flies, and mammalian systems by studying the repair of induced double strand breaks or repair following exposure to genotoxic agents *in vitro.* We therefore set out to expand this *in vitro* work to ask whether DNA-damaging agents with varying modes of action could induce somatic change in an *in vivo* mouse model of homologous recombination. We exposed pregnant dams to DNA-damaging agents, conferring a variety of lesions at a specific time in embryo development. To monitor homologous recombination frequency, we used the well-established retinal pigment epithelium pink-eyed unstable assay. Homologous recombination resulting in the deletion of a duplicated 70 kb fragment in the coding region of the Oca2 gene renders this gene functional and can be visualized as a pigmented eyespot in the retinal pigment epithelium. We observed an increased frequency of pigmented eyespots in resultant litters following exposure to cisplatin, methyl methanesulfonate, ethyl methanesulfonate, 3-aminobenzamide, bleomycin, and etoposide with a contrasting decrease in the frequency of detectable reversion events following camptothecin and hydroxyurea exposure. The somatic genomic rearrangements that result from such a wide variety of differently acting damaging agents implies long-term potential effects from even short-term *in utero* exposures.

Key Words: Homologous recombination, DNA damaging agents, mouse, pink-eyed unstable*, in utero* exposure, *in vivo*

1. Introduction

Environmental exposures include many potential genotoxic agents, many of which are known carcinogens. Considering the variety of these agents, they are generally classified by their mode of action [1]. Irrespective of how they react with DNA, a DNA lesion that impacts DNA replication, inhibiting its normal progression, might potentially instigate genomic instability via aberrant repair processes, including homologous recombination (HR). HR is usually considered to be a high-fidelity DNA-repair process, because it uses a homologous template of DNA to repair damaged DNA. Therefore, it is not surprising that HR is most prevalent during or just after DNA synthesis, when the sister chromatid is present to act as the template and facilitate this type of repair and restoration of normal DNA replication [2]. However, there is also the potential that an HR event will be mediated by an alternate homologous sequence at some ectopic site, for example between simple repeats present in the genome (SINES or LINEs, segmental duplications, copy number variants, or even genes that share significant homology) [3]. Considering that copy number variations are now understood to constitute approximately 12% [4] of the mammalian genome, increasing the frequency of HR by exposure to DNA-damaging agents might be expected to significantly impact genome stability in a proliferating somatic cell. For instance, unlike genetic diseases (e.g., sickle-cell anemia or Tay-Sachs disease) which are often associated with mutation in a single gene and prevalent in certain populations, recombination-based genomic disorders (e.g. DiGeorge syndrome or Prader-Willi syndrome) result from frequent rearrangements of the genome in certain disease loci [5]. To better understand the impact of such recurrent change, we asked what the consequence would be on genomic stability following exposure to several differently acting DNA-damaging agents when many cells are actively dividing during development. To assess genome rearrangement we used a

well-established segmental duplication/deletion pigmentation assay, the pink-eyed unstable mouse model, with *in utero* exposures to several different agents.

The pink-eyed unstable (p^{un}) mutation in the mouse is a head-to-tail duplication of a 70 kb region of DNA—effectively a segmental duplication that disrupts the function of the *p* gene (also known as *Oca2*). The *p* gene encodes for an integral membrane protein that is required for the proper assembly of melanin in melanosomes and confers dark brown-black pigmentation [6]. The p^{un} mutation causes a dilution of this color in 2 pigmented cells of the mouse: melanocytes confer coat color to fur and to the retinal pigment epithelium (RPE) of the eye. Spontaneous reversion of the 70 kb duplication via deletion of one copy of the duplicated sequence renders a functional *p* gene, thus allowing for proper melanin packing in cells. These reversion events can be scored as black spots on an otherwise dilute fur coat or as pigmented cells in the RPE of the mouse eye [7]. Proliferation of these tissues occurs mainly during embryonic development; thus, we were able to expose pregnant dams to various agents during development and determine the impact on somatic HR using this simple pigment-based assay system [8, 9, 10, 11]. For this study we examined the effect of 8 different agents that can be categorized into 6 different classes of action; cisplatin, methyl methanesulfonate, ethyl methanesulfonate, bleomycin, 3-aminobenzamide, etoposide, camptothecin, and hydroxyurea.

Cisplatin works by aquating a chloride ligand, which results in the formation of a DNA adduct and, usually produces intrastrand DNA cross-links, which in turn impedes replication and transcription [12]. In contrast, alkylating agents such as methyl methanesulfonate (MMS) and ethyl methanesulfonate (EMS) are not used as frequently in clinical settings as chemotherapeutic agents, but they are considered cytotoxic, mutagenic and carcinogenic, and prototypical of other clinically relevant or environmentally present alkylating agents [13]. Recent findings have shed

light on the powerful potential of poly (ADP-ribose) polymerase (PARP) inhibitors to act as anticancer drugs. A first generation PARP inhibitor, 3-aminobenzamide (3AB), acts by attacking the catalytic site of the PARP family of enzymes, thereby competing with NAD^+ and resulting in the inhibition of the activity of PARP [14]. Bleomycin has been classified as an "antitumor antibiotic" by forming complexes with iron, which reduces molecular oxygen to superoxide and hydroxyl radicals, thereby causing single- and double-strand breaks in DNA. Etoposide, sometimes more appropriately termed a topoisomerase poison, acts by disrupting the normal functionality of the ubiquitous topoisomerase II (Top2) enzyme, which plays a role in cutting DNA strands to relieve tangles and supercoiling. Rather than binding or intercalating with DNA directly, etoposide stabilizes a ternary complex of Top2 that is covalently linked to DNA at a strand break [15]. The target of camptothecin is topoisomerase I (TOP I), an enzyme that relaxes DNA supercoiling. Camptothecin is a cell-cycle-specific agent that causes DNA replication-fork collapse in dividing cells, resulting in cell death [16]. Hydroxyurea (HU) works by inactivating the ribonucleotide reductase enzyme, thus reducing the availability of free nucleotides. As a consequence, HU inhibits the entire replicase complex, blocking DNA synthesis and resulting in the arrest of cells in the S phase of the cell cycle [17].

In this paper we sought to determine if *in utero* exposure to different classes of DNA-damaging agents caused the type of lesions that could increase the frequency of HR in our pink-eyed unstable mouse model. We observed a robust induction of HR following cisplatin and alkylating-agent exposure as well as a significant induction of HR following exposure to etoposide, bleomycin, and a PARP inhibitor used in our study, 3AB. In contrast, a marked decrease in the frequency of detectable reversion events was observed for the ribonucleotide reductase inhibitor (hydroxyurea) and Top1 inhibitor (camptothecin) measured in our study.

Aside from the alkylating agents and camptothecin, to our knowledge the remaining DNA damaging agents have not been assessed previously using an *in vivo model* such as the p^{un} system.

2. Materials and Methods

2.1 Mouse cohort and breeding

C57BL/6J $p^{un/un}$ mice were obtained from the Jackson Laboratory (Bar Harbor, ME). Experimental cohorts were maintained by breeding homozygous $p^{un/un}$ mice to generate sufficient numbers of animals for exposure experiments. All animal studies were conducted in accordance with University and Institute IACUC policies, as outlined in protocol 07005-34-02-A,B1,C.

2.2 Timing of pregnancy and exposure to agents

Mice homozygous for $p^{un/un}$ were bred with successful copulation, which was indicated by a vaginal plug and timed as 0.5 days *post coitum*. Pregnant dams were then exposed to various DNA-damaging agents (Table A.1) on embryonic day 12.5.

The DNA-damaging agents were prepared in 0.9% normal saline (also used as a control) and injected intraperitoneally to pregnant dams. The dose of each agent was calculated based on the weight of the pregnant dam (per 30 g) and prepared in a 0.2 mL solution.

2.3 Eye dissection and p^{un} reversion (homologous recombination) assay

Eyes from 30-day-old pups derived from exposed pregnant dams were harvested and dissected as previously described [8]. RPE whole mounts were prepared and imaged using a Zeiss Lumar version 12 stereomicroscope, Zeiss AxioVision MRm camera, and Zeiss AxioVision 4.6 software (Thornwood, NY). For each RPE, the total number of pigmented eyespots was scored along with the number of cells that comprised each eyespot as detailed in Claybon *et al.* [18]. The position of each pigmented eyespot was also recorded to confirm the correlation between the time of exposure and the location of any induced reversion events, as

previously described [9]. The criterion for scoring a p^{un} reversion event as well as the analysis of its position on the RPE was also previously outlined in Bishop *et al.* [8]. Briefly, an eyespot was scored as one or more reverted cell (indicated by black pigmentation in an otherwise transparent cell layer), separated by no more than one unpigmented cell.

2.4 Statistics

Statistical analysis was performed using GraphPad Prism 6.0 (La Jolla, CA) software. We first performed a normality test and determined that our data did not follow a normal Gaussian distribution. We therefore chose nonparametric tests that compare distributions of 2 unpaired groups. A Mann-Whitney test was used to analyze p^{un} reversion frequency between DNA-damaging agents and control. We used a Kolmogorov-Smirnov test to analyze distribution differences in eyespot position data between control and differing DNA-damaging agents.

3. Results

3.1 Survival analysis of pregnant dams' postexposure to varying doses of DNA-damaging agents

Dosing for each agent was empirically derived based on a combination of reported LD_{50} (lethal dose 50%) levels, published fetotoxicity data, and previous work done with the p^{un} fur-spot assay [10]. We performed a survival analysis study to determine which doses maximized dam survival, litter size, and p^{un} fur-spot induction (Table 1). The fur-spot assay was used merely as an indicator to confirm that the chosen dose for each agent was capable of inducing HR by our assay, but it generally requires many more mice to establish statistical significance compared to the eyespot assay. For cisplatin and MMS, a dose of 2.5 mg/kg and 0.2 mg/kg, respectively, resulted in robust litter sizes and p^{un} fur-spot induction. The 100 mg/kg dose for EMS did not result in spotted pups; however, given that the eyespot assay is more sensitive (one-cell resolution) compared with the clonal expansion of revertant cells needed to visualize a fur-spot,

we went forward with this dose for our study. Bleomycin proved to be quite toxic to the pregnant dams; therefore, we selected a dose of 5 mg/kg, which gave larger litter sizes and an 18% fur-spot frequency. In contrast, we selected the highest dose tested for 3AB because it did not appear to harm the dams. The topoisomerase inhibitors, etoposide and camptothecin, resulted in very few litters at high doses; however, lower doses of these agents still elicited a robust 36% fur-spot frequency. A midrange dose of the replication inhibitor, HU, resulted in a 27% fur-spot frequency and 100% survival (Table 1).

3.2 Exposure to DNA-damaging agents with different modes of action induces homologous recombination

Either naturally or by design, chemotherapeutic agents with differing modes of action lead to a variety of lesions, such as strand breaks, DNA adducts, and DNA cross-links, among others. These lesions are detected by surveillance machinery that operates by triggering a robust DNA-damage signal cascade, thereby prompting appropriate DNA-repair pathways. HR is one such pathway; however, much of our understanding of this pathway stems from either lower organisms or tissue-culture studies on the repair of induced double-strand breaks. Therefore, we set out to ask whether differing types of DNA lesions could induce somatic HR *in vivo*. We exposed pregnant dams at a specific time in embryo development (12.5 dpc) to DNA-damaging agents that have differing modes of action. The simplest assessment of these agents is to determine the frequency of reversion events in each RPE for each agent exposure compared to the saline control. Upon examining the frequency of eyespots (p^{un} reversions) per RPE, we found that all agents, except camptothecin and HU, significantly induced HR compared to the control (Fig. 1a and Table 2). The cross-linking agent, cisplatin, and both alkylating agents, MMS and EMS, showed a twofold induction of eyespots per RPE ($P < 0.0001$; Mann-Whitney test).

Though not as robust, PARP inhibition ($P < .001$; Mann-Whitney test), bleomycin, and the Top2 poison, etoposide ($P < .01$; Mann-Whitney test), also significantly induced HR in comparison to the control agent (Fig. 1a and Table 2). Whereas most of the agents resulted in a concomitant increase in the number of revertant cells (Table 2), camptothecin and HU showed a highly statistically significant decrease in the number of eyespots ($P < .0001$; Mann-Whitney test) and an overall fewer number of cells per RPE, possibly due to the dose selected for this study (Fig. 1a and Table 2). It is interesting that these latter data contrast with the clear induction observed using the fur-spot assay, which indicated that the selected doses should induce p^{un} reversion, albeit with possible cytotoxic effects in the RPE (Table 1). The resultant litters from pregnant dams exposed to EMS, showed a clear induction of p^{un} reversion in the RPE (compared with no induction in the fur), which indicates an increased sensitivity of the eyespot assay to detect damage-induced HR events. These results suggest that many forms of damage—not just strand breaks—are capable of inducing recombinogenic lesions.

3.3 *Induction of single-cell and multicell reversion events differ depending on the mode of action of DNA-damaging agents*

In addition to directly providing HR frequency information in a developing mouse RPE, the p^{un} RPE-based reversion assay allows for the further subdivision of eyespot frequency into those eyespots consisting of one cell (single-cell eyespots) and those with more than one cell (multicell eyespots). The idea is that events resulting in multicell eyespots are more likely to have been tied to replication, such that reversion in one cell that is actively replicating its DNA clonally expands into a group of daughter cells. Thus, according to our criteria, we would score a clonally expanded multicell eyespot as a single reversion event. In contrast, a single-cell eyespot might have been derived from an event that was not necessarily tied to replication or in a cell that

was in its terminal division and did not continue to divide once the revertant p gene segregated into one daughter cell. However, the p^{un} reversions that result in single-cell eyespots may result from cells that are in G1 through a single strand annealing type event. Since we observe that the induced events occur in specific regions of the RPE (and not in regions that are post mitotic at the time of exposure) suggests that whether single-cell or multicell, p^{un} reversions arise in cells that are actively dividing at the time of exposure.

Our data showed a significant increase in frequency of single-cell reversion events for cisplatin, EMS, and MMS ($P < .0001$; Mann-Whitney) with only a small increase in multicell events for MMS ($P < .05$; Mann-Whitney; Figs. 1b and 1c). 3AB and bleomycin also showed an increase in single-cell events ($P < .05$ and $P < .01$, respectively; Mann-Whitney) with no induction of multicell events (Figs. 1b and 1c). In contrast, HU exposure resulted in a significant decrease in single-cell events ($P < .01$; Mann-Whitney); in addition, both HU and camptothecin appeared to have a significant decrease in the frequency of multicell eyespots compared with the control agent ($P < .001$ and $P < .0001$, respectively; Mann-Whitney; Figs. 1b and 1c). An interesting finding was that, of the 17 RPE analyzed following camptothecin exposure, only 5 of 31 eyespots were scored as multicell reversion events, compared with 50% in the control group. Further, we observed an induction of reversion events following camptothecin exposure using the p^{un} fur-spot assay (similar to that reported by others; *eg*, [19]), but a decrease in the p^{un} eyespot assay for the same animals. This suggests a tissue-specific difference in response, perhaps with RPE cells being more sensitive to camptothecin, resulting in greater cell death, permanent cell cycle arrest, or repair by other pathways without induction of HR events.

3.4 Position frequency of reversion events following exposure to DNA-damaging agents

In addition to examining the frequency of events, another aspect of the p^{un} eyespot assay

is that the position of events found in the adult RPE can be related to the specific time during development when they occurred [8]. The RPE development results from an edge-biased pattern of proliferating cells that orient outward radially [20]. Previously, Bishop et al. demonstrated that the time of exposure to a DNA-damaging agent during development correlates strongly with the location of induced revertant events in the adult RPE [8]. Therefore, those eyespots that are near to the centrally located optic nerve occurred early in development, whereas those positioned toward the edge of the RPE (distal to the optic nerve head) most likely occurred later in embryo development. Considering that all of the exposures were conducted at embryo day 12.5, we expect this to correlate to an induction of p^{un} reversion events at approximately one third of the distance from the optic nerve head to the edge of the RPE (*ie*, "position 0.3").

To determine whether there was a positional effect of the observed increase in eyespots following exposure to DNA-damaging agents, we analyzed the distribution of p^{un} reversion events using a nonparametric Kolmogorov-Smirnov test to evaluate pattern shifts of eyespots between the control RPE and those exposed to DNA-damaging agents (Fig. 2a). Cisplatin ($P < .01$; Kolmogorov-Smirnov), MMS and EMS ($P < .05$; Kolmogorov-Smirnov) showed a significant shift in distribution of total reversion events compared to control (Fig. 2a). We further compared and contrasted the pattern of eyespot distribution for single- and multicell events separately. An examination of RPE for single-cell eyespots (Fig. 2b) revealed an induction pattern similar to that observed for total eyespots but positioned more toward the proximal region of the RPE for these agents ($P < .01$, $P < .05$, $P < .01$, respectively; Kolmogorov-Smirnov), with no significant distribution difference in multicell reversion events compared to the control agent (Fig. 2c).

Bleomycin did not have a significant pattern change in total eyespots but there was a

significance in single-cell eyespots ($P < .05$; Kolmogorov-Smirnov) with an apparent spike of reversion events in regions following induction suggesting a quick mode of action for this agent compared to the control agent (Figs. 2a and 2b). PARP inhibition and etoposide exposure also resulted in a robust distribution change in total eyespots ($P < .01$; Kolmogorov-Smirnov) and a shift to more proximal regions for single-cell eyespots ($P < .05$, $P < .01$, respectively; Kolmogorov-Smirnov), which was more substantial following 3AB induction compared to the control agent (Fig. 2b). Again no significance was indicated in multicell reversion events (Fig. 2c). The differences in position and pattern shifting between single and multicell events have been reported for various genetic backgrounds [21] and following DNA-damage exposure [8, 9].

It is interesting that the significant decrease seen in the total frequency of eyespots ($P < .05$, $P < .01$, respectively; Kolmogorov-Smirnov) was also recapitulated in the distribution pattern of these eyespots following camptothecin and HU exposure (Fig. 2a). For HU, the distribution difference is significant amongst single-cell reversion events ($P < .05$; Kolmogorov-Smirnov), with an apparent lack of eyespots directly following exposure, possibly due to cell death (Fig. 2b). Although not significant, the patterning of eyespots following camptothecin exposure indicates a loss in multicell eyespots in the more distal regions of the RPE, suggesting cytotoxicity in proliferating cells or an alternative pathway to repair the damage (Fig. 2c).

Previous work by Bishop *et al.* correlated an induction of damage-induced HR (using benzo[a]pyrene) to a particular time in fetal development [8]. Based on these calculations, we performed our inductions at embryo day 12.5 to maximize exposure to proliferating cells. However, the lack of significance in multicell reversion events following most of the DNA-damaging agents suggests that we might have missed the optimal "signal-to-noise" ratio for the agents used. Still, the results reported here suggest a significant difference in the repair of

different types of lesions resulting from exposure to different types of agents.

4. Discussion

Exposure to environmental genotoxins or endogenous byproducts of normal cellular

processes represents a peril to genomic integrity. Given this, many species have adapted a robust

set of DNA-repair processes that can remove DNA lesions and hopefully maintain the integrity

of the genetic material. Each repair process has a preferred substrate, although the significant

redundancy that exists between these processes creates overlap in the substrates. For example, it

has been shown that base excision repair, nucleotide excision repair, and recombination can all

repair the alkylation damage associated with MMS exposure [22]. Actually, HR is a process that

should be capable of repairing any genotoxic DNA lesion given the appropriate homologous

template. However, the fact that HR must be kept in delicate balance to maintain genomic

integrity and curb tumorigenesis is evidenced by mouse models deficient in key HR proteins. For

instance, previous work using the p^{un} eyespot assay with mice deficient in BRCA1 (breast cancer,

1 early onset) resulted in a decreased frequency of HR compared to wild-type mice, In contrast, a

hyperrecombination HR phenotype was seen in mice lacking RecQ helicase, BLM, the gene

associated with Bloom syndrome [23]. BRCA1 and BLM deficiency yield a polarized HR

phenotype, yet both lead to a higher incidence of cancer, most likely because of increased

chromosomal instability due to an imbalance of HR repair. In this study, we sought to determine

whether previously established DNA-damaging agents, either naturally occurring or

manufactured, were able to elicit deletion events at a particular locus by using the *in vivo p^{un}*

mouse model. By determining the frequency of pigmented cell spots in the RPE, we

demonstrated that *in utero* exposure to these agents at an established time in embryo

development resulted in an increased frequency of reversion events in our system compared to a

saline control. This increased frequency of HR in the RPE following exposure to DNA-damaging agents is likely to be representative of the somatic mutation and genetic alterations that may be induced in other highly proliferative cells during embryo development. Any such somatic change in development has the potential to be clonally expanded, altering the genetic makeup of subsets of cells in the adult body with long-term consequences on the genetic integrity of cells.

The cytoplasm of a wild-type RPE cell is packed with melanosomes (specialized organelles filled with melanin granules), which give these light-sensitive cells their dark guise. The murine pink-eyed dilution gene, p (also called the $Oca2$ gene) encodes for the P protein, which is involved in maintaining the pH balance necessary for melanin production [24]. When the p gene is nonfunctional (as in the $p^{un/un}$ genotype), melanin production is compromised, resulting in a dilute color compared to the normal, robust, black-brown pigmentation in the RPE and other pigmented tissues, such as the fur. In the event of an HR reversion of the disrupting 70 kb duplication segment in the p^{un} mutation, a pigmented eyespot can be visualized among a clear background. This readout allows us to determine baseline frequencies of HR, which we suggest is normal maintenance to ensure genomic integrity as well as any deviations—either hypo- or hyperrecombination—as evidenced by the aforementioned work done with mouse models deficient in HR proteins [23], as well as others [18, 25].

Studies that offer information about the developmental timing in which drugs might act can provide insight into consequences of clonal expansion of these somatic mutations. Due to its modes of action (adduction and cross-linking of DNA), cisplatin results in DNA damage. Once this damage is detected, DNA-repair machinery (such as HR) is initiated, or else the damage elicits an apoptotic response. Exposure to cisplatin has been shown to increase sister chromatid exchanges (SCEs) [26], a crossover event between 2 sister chromatids that is most likely a result

of HR [27]. In agreement with the findings of this *in vitro* study, cisplatin was also a strong

inducer of HR in our assay for the dose that was used. We saw a robust increase in total and

single-cell eyespots and a nonsignificant increase in multicell eyespots in the RPE of embryos

harvested from pregnant dams exposed to a single dose of 2.5 mg/kg of cisplatin. This dose

would be considered relatively low by clinic standards, which are often higher and given in

multiple regimens; nonetheless, the dose was able to elicit a response in our system, suggesting

that HR is instigated in response to lesions involving DNA adducts and cross-linking damage.

Alkylating chemotherapy drugs, such as temozolomide, ifosfamide, and

cyclophosphamide, have their effect in every phase of the cell cycle and are thus desirable for

use on a wide range of cancers. They have been shown to be very effective in the treatment of

slow-growing cancers, solid tumors, and leukemia but are also used to treat lung cancer, ovarian

cancer, breast cancer, and others. Both MMS and EMS are S(N)2 agents involved in base N-

methylation that can lead to the formation of apurinic sites that block replication [28]. Point

mutations are a common and typical consequence of alkylation damage due to guanine alkylation,

as are DNA strand breaks and DNA fragmentation. That these agents induce HR has been

indicated by an increase in SCEs in various murine tissues (including bone marrow, liver, and

kidney tissues) following intraperitoneal injection of MMS [29]. The frequency of HR was also

examined using recombination between 2 tandemly arranged neomycin gene fragments in the

ovary cells of Chinese hamsters (CHO:5) and was found to be increased by MMS treatment [30].

Using the *in vivo p^{un}* fur-spot assay, other studies have demonstrated that HR is induced by either

EMS or MMS [10], which we now recapitulate in this paper using the more sensitive RPE-based

p^{un} mouse model. We observed a significant increase in total and single-cell eyespots and a less

robust increase in eyespots consisting of more than one cell later in development (distal regions

of RPE) following MMS exposure. The latter results contrast our initial finding with the p^{un} fur-spot assay, which is reliant on clonal expansion of p^{un} reversion events to produce observable fur spots, indicating that we were able to detect multicell events in this tissue. We interpret this result to mean that the induction of multicell events was too weak for the dose used to observe an increase above the background frequency of spontaneous events in the RPE. Alternatively, if we had performed our exposures at an earlier time in fetal development (for example at E10.5 similar to previous studies with other agents [9]), then perhaps we could have observed a clearer induction as the background spontaneous frequency of multicell events is considerably less in the proximal region of the RPE. This may explain the general lack of significant induction of multicell events for all our exposures in this study.

Seminal work showing that PARP1 is involved in DNA repair [31] and activated by ionizing radiation and alkylation damage paved the way for PARP inhibitors to be used in a "synthetic lethality" approach with chemotherapeutic agents [32]. Much work has been done in the form of mouse models of PARP and in *in vitro* work that reveals its role as an early responder to DNA damage and facilitator of HR [33, 34]. PARP inhibition by 3AB is a potent inducer of SCEs in CHO cells [35, 36]. A hyperrecombination phenotype was also observed in work done by Claybon *et al*. using Parp1 nullizygous mice [18]. In the present study, we also show that pharmacological inhibition of PARP1 activity can induce HR in the *in vivo* p^{un} eyespot assay. We saw a significant increase in total and single-cell eyespots, and although not significant, a spike in multicell events closely following 3AB exposure. In the Parp1 nullizygous study, the greatest increase was in multicell events, which is to be expected considering that PARP1 preferentially binds to single-strand breaks, which is a critical step in base-excision repair. In the absence or inhibition of PARP1, a situation occurs where single-strand breaks are

not repaired correctly, resulting in a collapsed replication fork due to recombinogenic-associated double-strand break lesions in replicating cells [37, 38]. The weaker response in multicell events observed in the present study might reflect either the transient nature of the inhibitor exposure or the aforementioned issue with high background in spontaneous multicell events for our selected time of exposure.

Several studies involving radiation influence have reported an increased occurrence of cancer following *in utero* exposure [39, 40]. Bleomycin is generally considered to be radiomimetic and a potent source of oxidative stress [41]. Bleomycin and the other enediyne antibiotics achieve site-specific free radical attacks on sugar moieties in both strands of DNA that can result in double-strand breaks [41]. These breaks have been shown to induce HR following bleomycin exposure, as measured by SCEs in CHO cells [42]. A similar phenomenon of robust induction of HR reversion events in more central regions of the RPE, and specifically in single-cell eyespots as seen in this study, was also reported in a paper by Bishop *et al*. using the p^{un} eyespot assay with X-ray damage [9]. Further, the single-cell reversion events appear to have occurred quickly and for a limited duration, following bleomycin exposure, similar to the inductions observed with ionizing radiation reported previously [43].

Etoposide belongs to one of 2 classes of agents involved in enzyme-mediated anticancer properties through the stabilization of TOP2-DNA complexes and halting processes, such as transcription or replication. Although effective in clinical therapy, etoposide often results in secondary malignancies; indeed, it is thought that chemotherapy drugs targeting the TOP2β isoform may be the source. Etoposide has been shown to induce recombination in several studies. For instance, etoposide induces SCEs in both CHO cells [44] and cultured human lymphocytes [45]. Furthermore, this potent TOP2 inhibitor has been shown to induce somatic

intrachromosomal recombination in a whole mouse transgenic (pKZI) mutagenesis model in which a lacZ transgene is only expressed after a DNA inversion [46, 47]. In our study we were able to directly demonstrate that etoposide is capable of strongly inducing HR, specifically resulting in an increase of single-cell eyespots.

Camptothecin binds the TOP1-DNA complex selectively and efficiently, making it a potent chemotherapeutic. This agent has been shown to be involved in recombination in many tissue culture studies involving the induction of SCEs in CHO and human lymphoid cell lines [45, 48, 49, 50, 51, 52]. Enhanced frequency of reversion was seen in an *Hprt*-gene-based reversion-mutation assay in a CHO V79 plasmid system measuring intrachromosomal recombination following camptothecin exposure [53]. Surprisingly, we did not have a robust induction of HR in our p^{un} eyespot assay, although our preliminary fur-spot results indicated an induction recapitulating an earlier report with the p^{un} fur-spot assay using this agent [19]. Again, we observed a clear difference between our RPE and the fur-spot assay, suggesting tissue-specific differences. A developmental requirement for functional TOPI has also been evidenced by the death of *Top1* knockout mice early in embryogenesis [54].

Nucleotide pool disequilibrium is now a strong possibility in explaining many phenomena, such as replication stress associated with aberrant activation of the RB-E2F pathway in early stages of cancer [55] and slowed replication speed in Bloom syndrome [56]. HU inhibits ribonucleotide reductase, an enzyme crucial in the conversion of ribonucleotides into deoxyribonucleotides essential for DNA synthesis. A tight balance of intracellular deoxyribonucleoside triphosphate (dNTP) pools must be kept to maintain genomic integrity in yeast and at sites of damage in mammalian cells. In fact, many studies have shown that alterations in dNTP pools are coupled with genomic instability, mutagenesis, and tumorigenesis

[57]. Insufficient nucleotides will cause DNA replication stress and perhaps replication fork collapse, situations known to induce HR. In this respect HU treatment has been shown to be a positive inducer of SCEs in CHO cells [58, 59]. However, we did not observe an induction of HR in the eyespot assay following HU exposure, but did observe a significant decrease, similar to camptothecin.

Both camptothecin and HU exposure produced a surprising result in that, for the doses chosen, there was an apparent induction of fur-spots but a very significant decrease in eyespots. It is possible that, at the time during development that we performed our exposures, E12.5— melanocyte precursors (dormant migrating melanoblasts) that pigment the fur—are more robust or refractory to DNA damage, while the rapidly dividing RPE cells are either more sensitive or utilize an alternative pathway to repair the DNA lesions produced by camptothecin and HU. Cultured human RPE cells appear to be very sensitive to camptothecin [60], and camptothecin cytotoxicity has been shown to be dependent on DNA synthesis, as the DNA polymerase inhibitor aphidicolin completely blocks camptothecin cytotoxicity [61]. Although a tissue specific cytotoxicity in the developing RPE is a plausible explanation, it does not explain why we observed a decrease in HR events in the RPE below that of spontaneous levels. We have only ever observed a decreased frequency of eyespots when there was a genetic deficiency impairing the homologous recombination process, such as BRCA1 or BRCA2 deficiency ([23] and unpublished data). An alternative explanation is that the camptothecin-induced damage in the p^{un} gene is repaired differently in RPE cells compared to melanoblasts. It is interesting to not that the *Oca2* gene within the RPE is expressed at this time of development but not in melanoblasts [62]. Camptothecin will interrupt both RNA and DNA polymerase progression; thus; it is possible that any damage within the p^{un} gene could be repaired by another mechanism, possibly a

transcription-coupled repair mechanism, obviating the need for HR repair. Similarly, the lack of recombination following HU exposure might be due to a higher order response that results in a replication restart (thus avoiding frequent double-strand breaks caused by fork collapse) rather than recombination-mediated gene conversions that would be visualized by the p^{un} assay (see model in [23]). For instance, DNA fiber analysis revealed a defect in replication-fork recovery following HU-mediated imbalance of dNTP pools and a subsequent replication block in BLM-deficient cells [63]. This suggests that BLM may be involved in recovering a stalled fork before a collapse can occur (presumably induced by HU). If a low level of exposure to HU stimulates BLM activity, then converse to the hyperrecombination phenotype in the p^{un} eyespot assay we reported in the absence of BLM [23], activated BLM would be expected to reduce the frequency of p^{un} reversion events and may provide a reasonable explanation for the decreased frequency of eyespots we observed. It is interesting that both camptothecin and HU are known to result in BLM phosphorylation and presumably its activation [64].

According to the American Cancer Society, in 2013 about 580,350 Americans are expected to die of cancer. Cancer is the second most common cause of death in the United States, and cancer in children has an annual incidence of about 150 new cases per 1 million U.S. children. All cancers involve the malfunction of genes and the other contributions may be additive over a lifetime of internal and external risk factors. Given the number of cell divisions during *in utero* development, it is likely that there is a higher sensitivity during this time to carcinogen exposure [66, 67, 68, 69]. In addition, this might be due to less efficient DNA repair or defective apoptotic mechanisms that facilitate DNA damage into subsequent cell divisions [70]. Further, in mice, about one third of mutations arise before birth [71]. Animal and human epidemiologic studies show a causal relationship for *in utero* exposures (*ie*, diagnostic

radiographs [72]) and cancer incidence in children [73, 74, 75]. Given this, *in utero* exposure during critical times in development to DNA-damaging agents or other sources of damage may cause a clonal expansion of somatic mutations. The present study showed that a relatively low single exposure to a wide variety of differently acting agents resulted in an increase of genomic rearrangement (a DNA deletion) at one site in the genome. Notably, this one genomic site can be considered to be representative of up to 12% of the genome with similar structures. This would seem to suggest that a significant amount of somatic genomic rearrangements might be occurring as a consequence of environmental fetal exposures, which likely has a significant impact on the genetic diversity present in somatic tissues. This may explain some of the higher incidences of cancer associated with prenatal exposures.

References

[1]   D.J. Kirkland, M. Aardema, N. Banduhn, P. Carmichael, R. Fautz, J.-R. Meunier, et al.,

        In vitro approaches to develop weight of evidence (WoE) and mode of action (MoA)

        discussions with positive in vitro genotoxicity results, Mutagenesis. 22 (2007) 161–175.

        http://www.ncbi.nlm.nih.gov/pubmed/17369606

[2]   R.L. Maher, A.M. Branagan, S.W. Morrical, Coordination of DNA replication and

        recombination activities in the maintenance of genome stability, J. Cell. Biochem. 112

        (2011) 2672–2682. http://www.ncbi.nlm.nih.gov/pubmed/21647941

[3]   G. McVean, What drives recombination hotspots to repeat DNA in humans?, Philos.

        Trans. R. Soc. Lond., B, Biol. Sci. 365 (2010) 1213–1218.

        http://dx.doi.org/10.1098/rstb.2009.0299

[4]   R. Redon, S. Ishikawa, K.R. Fitch, L. Feuk, G.H. Perry, T.D. Andrews, et al., Global

        variation in copy number in the human genome, Nature. 444 (2006) 444–454.

        http://dx.doi.org/10.1038/nature05329

[5]   P. Stankiewicz, J.R. Lupski, Genome architecture, rearrangements and genomic disorders,

        Trends Genet. 18 (2002) 74–82. http://www.ncbi.nlm.nih.gov/pubmed/11818139

[6]   S. Rosemblat, D. Durham-Pierre, J.M. Gardner, Y. Nakatsu, M.H. Brilliant, S.J. Orlow,

        Identification of a melanosomal membrane protein encoded by the pink-eyed dilution

        (type II oculocutaneous albinism) gene, Proc. Natl. Acad. Sci. U.S.A. 91 (1994) 12071–

        12075. http://www.ncbi.nlm.nih.gov/pmc/articles/PMC45378/

[7]   R. Reliene, A.J.R. Bishop, J. Aubrecht, R.H. Schiestl, In vivo DNA deletion assay to

        detect environmental and genetic predisposition to cancer, Methods Mol. Biol. 262

        (2004) 125–139. http://www.ncbi.nlm.nih.gov/pubmed/14769959

[8]   A.J. Bishop, B. Kosaras, N. Carls, R.L. Sidman, R.H. Schiestl, Susceptibility of
        proliferating cells to benzo[a]pyrene-induced homologous recombination in mice,
        Carcinogenesis. 22 (2001) 641–649. http://www.ncbi.nlm.nih.gov/pubmed/11285201

[9]   A.J. Bishop, B. Kosaras, R.L. Sidman, R.H. Schiestl, Benzo(a)pyrene and X-rays induce
        reversions of the pink-eyed unstable mutation in the retinal pigment epithelium of mice,
        Mutat. Res. 457 (2000) 31–40. http://www.ncbi.nlm.nih.gov/pubmed/11106796

[10]   R.H. Schiestl, J. Aubrecht, F. Khogali, N. Carls, Carcinogens induce reversion of the
        mouse pink-eyed unstable mutation, Proc. Natl. Acad. Sci. U.S.A. 94 (1997) 4576–4581.
        http://www.ncbi.nlm.nih.gov/pubmed/9114032

[11]   R.H. Schiestl, F. Khogali, N. Carls, Reversion of the mouse pink-eyed unstable mutation
        induced by low doses of x-rays, Science. 266 (1994) 1573–1576.
        http://www.ncbi.nlm.nih.gov/pubmed/7985029

[12]   B. Rosenberg, Possible mechanisms for the antitumor activity of platinum coordination
        complexes, Cancer Chemother Rep. 59 (1975) 589–598.
        http://www.ncbi.nlm.nih.gov/pubmed/54213

[13]   L.S. Gold, N.B. Manley, T.H. Slone, G.B. Garfinkel, L. Rohrbach, B.N. Ames, The fifth
        plot of the Carcinogenic Potency Database: results of animal bioassays published in the
        general literature through 1988 and by the National Toxicology Program through 1989,
        Environ. Health Perspect. 100 (1993) 65–168.
        http://www.ncbi.nlm.nih.gov/pubmed/8354183

[14]   M.R. Purnell, W.J. Whish, Novel inhibitors of poly(ADP-ribose) synthetase, Biochem. J.
        185 (1980) 775–777. http://www.ncbi.nlm.nih.gov/pubmed/9703762

[15]   D.A. Burden, N. Osheroff, Mechanism of action of eukaryotic topoisomerase II and

drugs targeted to the enzyme, Biochim. Biophys. Acta. 1400 (1998) 139–154.
http://dx.doi.org/10.1016/S0167-4781(98)00132-8

[16]   Y.H. Hsiang, M.G. Lihou, L.F. Liu, Arrest of replication forks by drug-stabilized topoisomerase I-DNA cleavable complexes as a mechanism of cell killing by camptothecin, Cancer Res. 49 (1989) 5077–5082.
http://www.ncbi.nlm.nih.gov/pubmed/2548710

[17]   J.W. Yarbro, Mechanism of action of hydroxyurea, Semin. Oncol. 19 (1992) 1–10.
http://www.ncbi.nlm.nih.gov/pubmed/1641648

[18]   A. Claybon, B. Karia, C. Bruce, A.J.R. Bishop, PARP1 suppresses homologous recombination events in mice in vivo, Nucleic Acids Res. 38 (2010) 7538–7545.
http://dx.doi.org/10.1093/nar/gkq624

[19]   M. Lebel, Increased frequency of DNA deletions in pink-eyed unstable mice carrying a mutation in the Werner syndrome gene homologue, Carcinogenesis. 23 (2002) 213–216.
http://www.ncbi.nlm.nih.gov/pubmed/11756244

[20]   L. Bodenstein, R.L. Sidman, Growth and development of the mouse retinal pigment epithelium. I. Cell and tissue morphometrics and topography of mitotic activity, Dev. Biol. 121 (1987) 192–204. http://dx.doi.org/10.1016/0012-1606(87)90152-7

[21]   A.J.R. Bishop, M.C. Hollander, B. Kosaras, R.L. Sidman, A.J. Fornace Jr, R.H. Schiestl, Atm-, p53-, and Gadd45a-deficient mice show an increased frequency of homologous recombination at different stages during development, Cancer Res. 63 (2003) 5335–5343.
http://www.ncbi.nlm.nih.gov/pubmed/14500365

[22]   A. Memisoglu, L. Samson, Contribution of base excision repair, nucleotide excision repair, and DNA recombination to alkylation resistance of the fission yeast

Schizosaccharomyces pombe, J. Bacteriol. 182 (2000) 2104–2112.

http://www.ncbi.nlm.nih.gov/pubmed/10735851

[23]   A.D. Brown, A.B. Claybon, A.J.R. Bishop, A conditional mouse model for measuring the

frequency of homologous recombination events in vivo in the absence of essential genes,

Mol. Cell. Biol. 31 (2011) 3593–3602. http://www.ncbi.nlm.nih.gov/pubmed/21709021

[24]   M.H. Brilliant, The mouse p (pink-eyed dilution) and human P genes, oculocutaneous

albinism type 2 (OCA2), and melanosomal pH, Pigment Cell Res. 14 (2001) 86–93.

http://www.ncbi.nlm.nih.gov/pubmed/11310796

[25]   A.D. Brown, A.B. Claybon, A.J.R. Bishop, Mouse WRN Helicase Domain Is Not

Required for Spontaneous Homologous Recombination-Mediated DNA Deletion, J

Nucleic Acids. 2010 (2010). http://www.ncbi.nlm.nih.gov/pmc/articles/PMC2933912/

[26]   K. Trenz, S. Lugowski, U. Jahrsdörfer, S. Jainta, W. Vogel, G. Speit, Enhanced

sensitivity of peripheral blood lymphocytes from women carrying a BRCA1 mutation

towards the mutagenic effects of various cytostatics, Mutat. Res. 544 (2003) 279–288.

http://dx.doi.org/10.1016/j.mrrev.2003.06.011

[27]   E. Sonoda, M.S. Sasaki, C. Morrison, Y. Yamaguchi-Iwai, M. Takata, S. Takeda, Sister

chromatid exchanges are mediated by homologous recombination in vertebrate cells, Mol.

Cell. Biol. 19 (1999) 5166–5169. http://www.ncbi.nlm.nih.gov/pmc/articles/PMC84359/

[28]   B. Kaina, Mechanisms and consequences of methylating agent-induced SCEs and

chromosomal aberrations: a long road traveled and still a far way to go, Cytogenet.

Genome Res. 104 (2004) 77–86. http://www.ncbi.nlm.nih.gov/pubmed/15162018

[29]   R.E. Neft, M.K. Conner, Induction of sister chromatid exchange in multiple murine

tissues in vivo by various methylating agents, Teratog., Carcinog. Mutagen. 9 (1989)

219–237. http://www.ncbi.nlm.nih.gov/pubmed/2572066

[30]   D. Hellgren, S. Sahlén, B. Lambert, Mutagen-induced recombination between stably

        integrated neo gene fragments in CHO and EM9 cells, Mutat. Res. 226 (1989) 1–8.

        http://dx.doi.org/10.1016/0165-7992(89)90085-7

[31]   B.W. Durkacz, O. Omidiji, D.A. Gray, S. Shall, (ADP-ribose)n participates in DNA

        excision repair, Nature. 283 (1980) 593–596. http://dx.doi.org/10.1038/283593a0

[32]   T. Zaremba, N.J. Curtin, PARP inhibitor development for systemic cancer targeting,

        Anticancer Agents Med Chem. 7 (2007) 515–523.

        http://www.ncbi.nlm.nih.gov/pubmed/17896912

[33]   J.-F. Haince, D. McDonald, A. Rodrigue, U. Déry, J.-Y. Masson, M.J. Hendzel, et al.,

        PARP1-dependent kinetics of recruitment of MRE11 and NBS1 proteins to multiple

        DNA damage sites, J. Biol. Chem. 283 (2008) 1197–1208.

        http://www.ncbi.nlm.nih.gov/pubmed/18025084

[34]   J.-F. Haince, S. Kozlov, V.L. Dawson, T.M. Dawson, M.J. Hendzel, M.F. Lavin, et al.,

        Ataxia telangiectasia mutated (ATM) signaling network is modulated by a novel

        poly(ADP-ribose)-dependent pathway in the early response to DNA-damaging agents, J.

        Biol. Chem. 282 (2007) 16441–16453. http://www.ncbi.nlm.nih.gov/pubmed/17428792

[35]   J.L. Schwartz, W.F. Morgan, L.N. Kapp, S. Wolff, Effects of 3-aminobenzamide on

        DNA synthesis and cell cycle progression in Chinese hamster ovary cells, Exp. Cell Res.

        143 (1983) 377–382. http://dx.doi.org/10.1016/0014-4827(83)90064-2

[36]   A.T. Natarajan, I. Csukás, A.A. van Zeeland, Contribution of incorporated 5-

        bromodeoxyuridine in DNA to the frequencies of sister-chromatid exchanges induced by

        inhibitors of poly-(ADP-ribose)-polymerase, Mutat. Res. 84 (1981) 125–132.

http://www.ncbi.nlm.nih.gov/pubmed/7199115

[37]   G. Noël, N. Giocanti, M. Fernet, F. Mégnin-Chanet, V. Favaudon, Poly(ADP-ribose) polymerase (PARP-1) is not involved in DNA double-strand break recovery, BMC Cell Biol. 4 (2003) 7. http://www.ncbi.nlm.nih.gov/pubmed/12866953

[38]   J.E. Haber, DNA recombination: the replication connection, Trends Biochem. Sci. 24 (1999) 271–275. http://www.ncbi.nlm.nih.gov/pubmed/10390616

[39]   B. Modan, Low-dose radiation carcinogenesis, Eur. J. Cancer. 28A (1992) 1010–1012. http://www.ncbi.nlm.nih.gov/pubmed/22641644

[40]   Y. Yoshimoto, H. Kato, W.J. Schull, Risk of cancer among children exposed in utero to A-bomb radiations, 1950-84, Lancet. 2 (1988) 665–669. http://dx.doi.org/10.1016/S0140-6736(88)90477-1

[41]   L.F. Povirk, DNA damage and mutagenesis by radiomimetic DNA-cleaving agents: bleomycin, neocarzinostatin and other enediynes, Mutat. Res. 355 (1996) 71–89. http://dx.doi.org/10.1016/0027-5107(96)00023-1

[42]   G. Obe, C. Schunck, C. Johannes, Induction of sister-chromatid exchanges by AluI, DNase I, benzon nuclease and bleomycin in Chinese hamster ovary (CHO) cells, Mutat. Res. 307 (1994) 315–321. http://www.ncbi.nlm.nih.gov/pubmed/7513811

[43]   E.P. Rogakou, D.R. Pilch, A.H. Orr, V.S. Ivanova, W.M. Bonner, DNA double-stranded breaks induce histone H2AX phosphorylation on serine 139, J. Biol. Chem. 273 (1998) 5858–5868. http://www.ncbi.nlm.nih.gov/pubmed/9488723

[44]   H. Hashimoto, S. Chatterjee, N.A. Berger, Inhibition of etoposide (VP-16)-induced DNA recombination and mutant frequency by Bcl-2 protein overexpression, Cancer Res. 55 (1995) 4029–4035. http://www.ncbi.nlm.nih.gov/pubmed/7664276

[45] G. Ribas, N. Xamena, A. Creus, R. Marcos, Sister-chromatid exchanges (SCE) induction by inhibitors of DNA topoisomerases in cultured human lymphocytes, Mutat. Res. 368 (1996) 205–211. http://www.ncbi.nlm.nih.gov/pubmed/8692226

[46] P.J. Sykes, A.M. Hooker, A.A. Morley, Inversion due to intrachromosomal recombination produced by carcinogens in a transgenic mouse model, Mutat. Res. 427 (1999) 1–9. http://dx.doi.org/10.1016/S0027-5107(99)00084-6

[47] M. Matsuoka, F. Nagawa, K. Okazaki, L. Kingsbury, K. Yoshida, U. Müller, et al., Detection of somatic DNA recombination in the transgenic mouse brain, Science. 254 (1991) 81–86. http://dx.doi.org/10.1126/science.1925563

[48] C.C. Huang, C.S. Han, X.F. Yue, C.M. Shen, S.W. Wang, F.G. Wu, et al., Cytotoxicity and sister chromatid exchanges induced in vitro by six anticancer drugs developed in the People's Republic of China, J. Natl. Cancer Inst. 71 (1983) 841–847. http://www.ncbi.nlm.nih.gov/pubmed/6413744

[49] M. Lim, L.F. Liu, D. Jacobson-Kram, J.R. Williams, Induction of sister chromatid exchanges by inhibitors of topoisomerases, Cell Biol. Toxicol. 2 (1986) 485–494. http://www.ncbi.nlm.nih.gov/pubmed/2855799

[50] F. Degrassi, R. De Salvia, C. Tanzarella, F. Palitti, Induction of chromosomal aberrations and SCE by camptothecin, an inhibitor of mammalian topoisomerase I, Mutat. Res. 211 (1989) 125–130. http://dx.doi.org/10.1016/0027-5107(89)90112-7

[51] J.H. Zhao, H. Tohda, A. Oikawa, Camptothecin-induced sister-chromatid exchange dependent on the presence of bromodeoxyuridine and the phase of the cell cycle, Mutat. Res. 282 (1992) 49–54. http://dx.doi.org/10.1016/0165-7992(92)90073-Q

[52] J. Piñero, M. López Baena, T. Ortiz, F. Cortés, Sister chromatid exchange induced by

DNA topoisomerases poisons in late replicating heterochromatin: influence of inhibition

of replication and transcription, Mutat. Res. 354 (1996) 195–201.

http://www.ncbi.nlm.nih.gov/pubmed/8764948

[53]   L.H. Zhang, D. Jenssen, Studies on intrachromosomal recombination in SP5/V79

Chinese hamster cells upon exposure to different agents related to carcinogenesis,

Carcinogenesis. 15 (1994) 2303–2310. http://www.ncbi.nlm.nih.gov/pubmed/7955071

[54]   S.G. Morham, K.D. Kluckman, N. Voulomanos, O. Smithies, Targeted disruption of the

mouse topoisomerase I gene by camptothecin selection, Mol. Cell. Biol. 16 (1996) 6804–

6809. http://www.ncbi.nlm.nih.gov/pmc/articles/PMC231683/

[55]   A.C. Bester, M. Roniger, Y.S. Oren, M.M. Im, D. Sarni, M. Chaoat, et al., Nucleotide

deficiency promotes genomic instability in early stages of cancer development, Cell. 145

(2011) 435–446. http://dx.doi.org/10.1016/j.cell.2011.03.044

[56]   P. Chabosseau, G. Buhagiar-Labarchède, R. Onclercq-Delic, S. Lambert, M. Debatisse, O.

Brison, et al., Pyrimidine pool imbalance induced by BLM helicase deficiency

contributes to genetic instability in Bloom syndrome, Nat Commun. 2 (2011) 368.

http://dx.doi.org/10.1038/ncomms1363

[57]   C.K. Mathews, DNA precursor metabolism and genomic stability, FASEB J. 20 (2006)

1300–1314. http://www.ncbi.nlm.nih.gov/pubmed/16816105

[58]   A. Matsuoka, C. Lundin, F. Johansson, M. Sahlin, K. Fukuhara, B.-M. Sjöberg, et al.,

Correlation of sister chromatid exchange formation through homologous recombination

with ribonucleotide reductase inhibition, Mutat. Res. 547 (2004) 101–107.

http://dx.doi.org/10.1016/j.mrfmmm.2003.12.002

[59]   C. Lundin, K. Erixon, C. Arnaudeau, N. Schultz, D. Jenssen, M. Meuth, et al., Different

roles for nonhomologous end joining and homologous recombination following replication arrest in mammalian cells, Mol. Cell. Biol. 22 (2002) 5869–5878. http://www.ncbi.nlm.nih.gov/pubmed/12138197

[60]   A. Hueber, P. Esser, K. Heimann, N. Kociok, S. Winter, M. Weller, The topoisomerase I inhibitors, camptothecin and beta-lapachone, induce apoptosis of human retinal pigment epithelial cells, Exp. Eye Res. 67 (1998) 525–530. http://dx.doi.org/10.1006/exer.1998.0544

[61]   C. Holm, J.M. Covey, D. Kerrigan, Y. Pommier, Differential requirement of DNA replication for the cytotoxicity of DNA topoisomerase I and II inhibitors in Chinese hamster DC3F cells, Cancer Res. 49 (1989) 6365–6368. http://www.ncbi.nlm.nih.gov/pubmed/2553254

[62]   M.A. Mackenzie, S.A. Jordan, P.S. Budd, I.J. Jackson, Activation of the receptor tyrosine kinase Kit is required for the proliferation of melanoblasts in the mouse embryo, Dev. Biol. 192 (1997) 99–107. http://www.ncbi.nlm.nih.gov/pubmed/9405100

[63]   J.M. Sidorova, K. Kehrli, F. Mao, R. Monnat Jr, Distinct functions of human RECQ helicases WRN and BLM in replication fork recovery and progression after hydroxyurea-induced stalling, DNA Repair (Amst.). 12 (2013) 128–139. http://dx.doi.org/10.1016/j.dnarep.2012.11.005

[64]   S.L. Davies, P.S. North, I.D. Hickson, Role for BLM in replication-fork restart and suppression of origin firing after replicative stress, Nat. Struct. Mol. Biol. 14 (2007) 677–679. http://dx.doi.org/10.1038/nsmb1267

[65]   V.A. Rao, A.M. Fan, L. Meng, C.F. Doe, P.S. North, I.D. Hickson, et al., Phosphorylation of BLM, dissociation from topoisomerase IIIalpha, and colocalization

with gamma-H2AX after topoisomerase I-induced replication damage, Mol. Cell. Biol. 25 (2005) 8925–8937. http://www.ncbi.nlm.nih.gov/pubmed/16199871

[66]   L. Tomatis, Overview of perinatal and multigeneration carcinogenesis, IARC Sci. Publ. (1989) 1–15. http://www.ncbi.nlm.nih.gov/pubmed/2680943

[67]   L.M. Anderson, B.A. Diwan, N.T. Fear, E. Roman, Critical windows of exposure for children's health: cancer in human epidemiological studies and neoplasms in experimental animal models, Environ. Health Perspect. 108 Suppl 3 (2000) 573–594. http://www.ncbi.nlm.nih.gov/pmc/articles/PMC1637809/

[68]   F. Perera, K. Hemminki, W. Jedrychowski, R. Whyatt, U. Campbell, Y. Hsu, et al., In utero DNA damage from environmental pollution is associated with somatic gene mutation in newborns, Cancer Epidemiol. Biomarkers Prev. 11 (2002) 1134–1137. http://www.ncbi.nlm.nih.gov/pubmed/12376523

[69]   K.A. Bocskay, D. Tang, M.A. Orjuela, X. Liu, D.P. Warburton, F.P. Perera, Chromosomal aberrations in cord blood are associated with prenatal exposure to carcinogenic polycyclic aromatic hydrocarbons, Cancer Epidemiol. Biomarkers Prev. 14 (2005) 506–511. http://www.ncbi.nlm.nih.gov/pubmed/15734979

[70]   S.C. Edwards, W. Jedrychowski, M. Butscher, D. Camann, A. Kieltyka, E. Mroz, et al., Prenatal exposure to airborne polycyclic aromatic hydrocarbons and children's intelligence at 5 years of age in a prospective cohort study in Poland, Environ. Health Perspect. 118 (2010) 1326–1331. http://www.ncbi.nlm.nih.gov/pubmed/20406721

[71]   Y.R. Paashuis-Lew, J.A. Heddle, Spontaneous mutation during fetal development and post-natal growth, Mutagenesis. 13 (1998) 613–617. http://www.ncbi.nlm.nih.gov/pubmed/9862193

[72]   R. Doll, R. Wakeford, Risk of childhood cancer from fetal irradiation, Br J Radiol. 70

        (1997) 130–139. http://www.ncbi.nlm.nih.gov/pubmed/9135438

[73]   S.G. Selevan, C.A. Kimmel, P. Mendola, Identifying critical windows of exposure for

        children's health, Environ. Health Perspect. 108 Suppl 3 (2000) 451–455.

        http://www.ncbi.nlm.nih.gov/pmc/articles/PMC1637810/

[74]   A.F. Olshan, L. Anderson, E. Roman, N. Fear, M. Wolff, R. Whyatt, et al., Workshop to

        identify critical windows of exposure for children's health: cancer work group summary,

        Environ. Health Perspect. 108 Suppl 3 (2000) 595–597.

        http://www.ncbi.nlm.nih.gov/pmc/articles/PMC1637823/

[75]   L.S. Birnbaum, S.E. Fenton, Cancer and developmental exposure to endocrine disruptors,

        Environ. Health Perspect. 111 (2003) 389–394.

        http://www.ncbi.nlm.nih.gov/pmc/articles/PMC1241417/

Table 1

INDUCTION OF HOMOLOGOUS RECOMBINATION

Table 1: p^{un} Fur-spot assay results following exposure to varying DNA-damaging agents and a saline control

| agent	dose (mg/k)	number of dams injected	litters	number of pups								total pups	spotted pups	% spotted
Control	0.9% normal saline	8	8	8	8	8	6	6	5	5	4	50	9	18
Cisplatin	2.5	7	4	9	8	5	3					25	8	32
MMS	100.0	6	4	7	6	6	4					23	23	100
	0.2	6	6	9	8	8	8	7	5			45	10	22
EMS	100.0	4	3	7	6	5						18	0	0
Bleomycin	10.0	5	2	3	1							4	3	75
	5.0	4	3	11	8	3						22	4	18
	2.5	8	5	8	7	6	6	5				32	5	16
	1.0	3	1	3								3	0	0
3AB	400.0	4	3	8	6	6						20	0	0
	300.0	4	3	9	8	7						24	0	0
	200.0	4	3	7	6	4						17	0	0
	100.0	4	3	11	10	6						27	0	0
Etoposide	60.0	3	0											
	40.0	3	0											
	20.0	7	2	6	8							14	3	21
	10.0	7	0											
	5.0	6	1	4								4	3	75
	2.5	3	3	7	5	2						14	5	36
	1.0	3	3	7	5	4						16	3	19
Camptothecin	40.0	4	0											
	20.0	4	0											
	10.0	4	0											
	5.0	3	0											
	2.0	9	2	2	4							6	1	17
	1.0	5	5	8	5	6	5	4				28	10	36
Hydroxyurea	5000.0	4	0											
	3000.0	4	1	8								8	2	
	1000.0	4	0											
	300.0	3	3	8	6	8						22	6	27
	200.0	2	1	3								3	1	33
	100.0	2	2	6	2							8	0	0

Table 2

INDUCTION OF HOMOLOGOUS RECOMBINATION

Table 2: Summary of p^{un} reversion events and RPE examined following a saline control and various DNA-damaging agents

Agent	Dose (mg/kg)	Total			Average		
		RPE	Eyespots	Cells	Eyespots per RPE	Cells per RPE	Cells per eyespot
Control	Saline	26	104	203	4.0 ± 1.1	7.8 ± 4.0	2.0 ± 1.3
Cisplatin	2.5	16	140	404	8.8 ± 3.2	25.3 ± 22.5	2.9 ± 4.4
MMS	0.2	15	123	290	8.2 ± 3.6	19.3 ± 14.2	2.4 ± 2.9
EMS	100.0	17	133	281	7.8 ± 2.6	16.5 ± 9.6	2.1 ± 2.2
3AB	400.0	17	104	215	6.1 ± 2.6	12.6 ± 9.6	2.1 ± 2.0
Bleomycin	5.0	17	106	274	6.2 ± 3.0	16.1 ± 15.7	2.6 ± 3.4
Etoposide	2.5	16	97	255	6.1 ± 2.4	15.9 ± 10.5	2.6 ± 3.5
Camptothecin	1.0	17	31	45	1.8 ± 1.9	2.6 ± 3.3	1.5 ± 1.7
Hydroxyurea	300.0	17	29	78	1.7 ± 2.4	6.5 ± 14.4	3.0 ± 3.5

Figure 1

INDUCTION OF HOMOLOGOUS RECOMBINATION

Figure 1
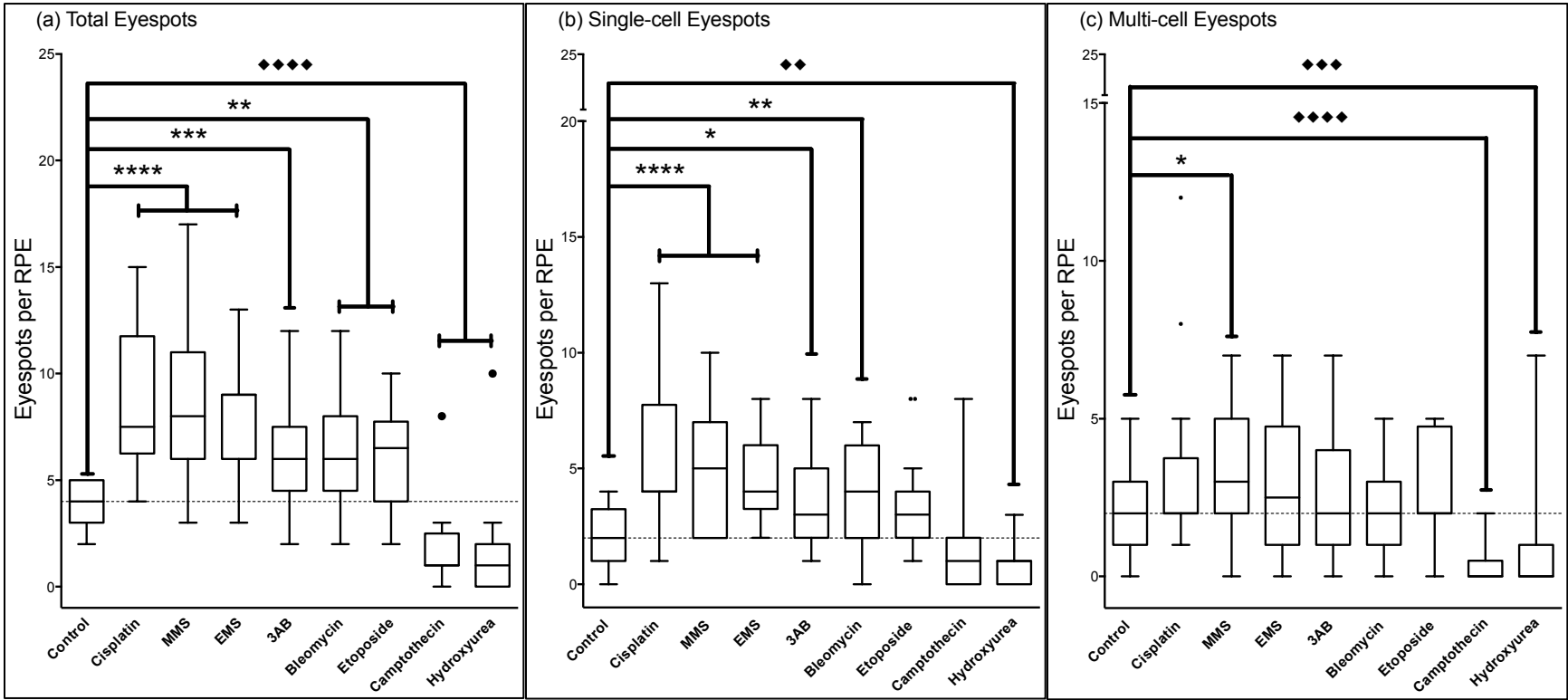
(a) Total Eyespots
(b) Single-cell Eyespots
(c) Multi-cell Eyespots

Figure 2

INDUCTION OF HOMOLOGOUS RECOMBINATION

Figure 2

(A) Total Eyespots   (B) Single-cell Eyespots   (C) Multi-cell Eyespots
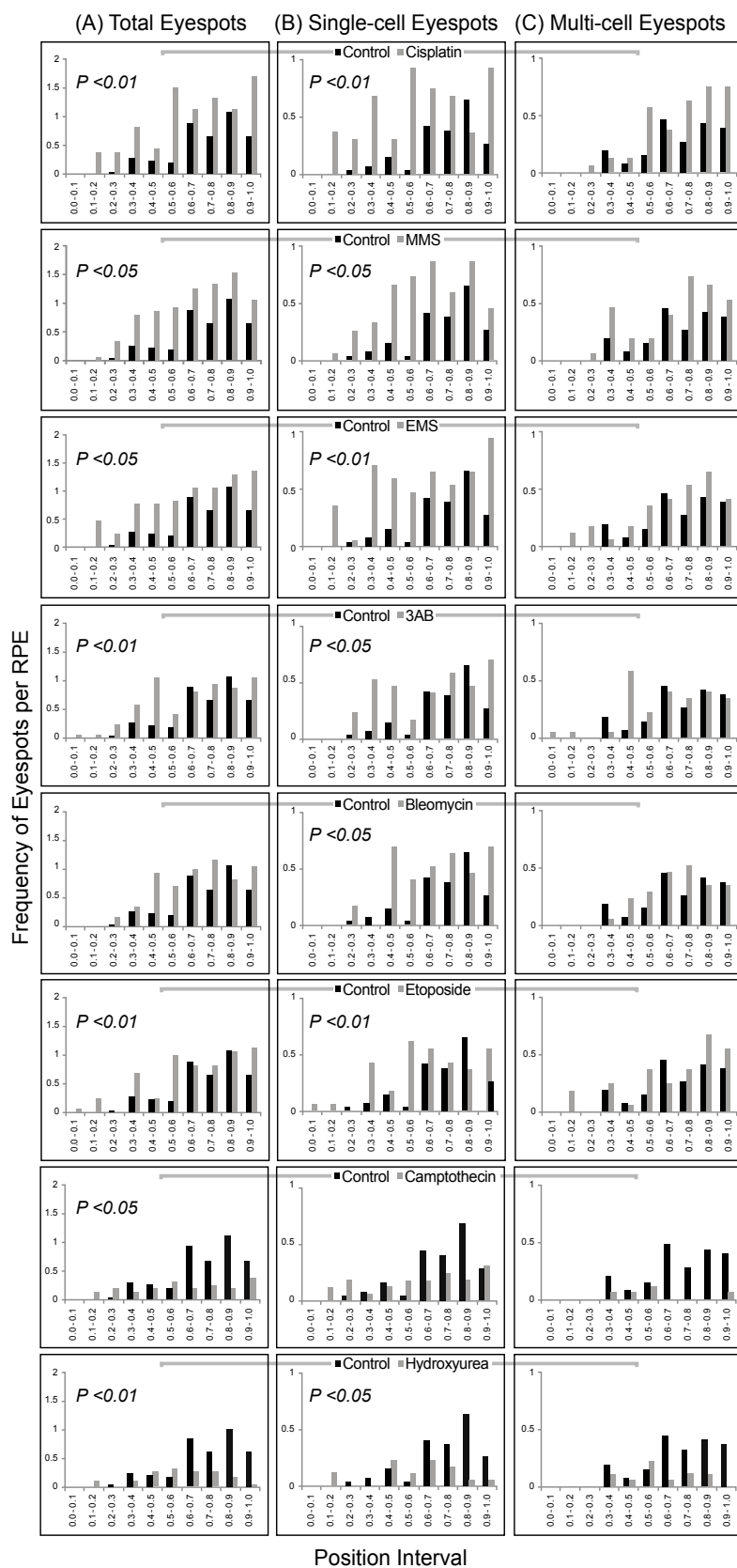
INDUCTION OF HOMOLOGOUS RECOMBINATION

Figure Captions

Figure 1: Tukey box and whiskers plot of the frequency of p^{un} reversion events for (a) total (b) single-cell and (c) multicell eyespots per RPE following saline control and DNA-damaging agents. The dashed line indicates the control frequency for comparison. A nonparametric Mann-Whitney test was used to analyze the frequency data; increased significance is denoted by asterisks ($*P < .05$, $**P < .01$, $***P < .001$, $****P < .0001$) and a significant decrease is denoted by diamonds ($\blacklozenge\blacklozenge P < .01$, $\blacklozenge\blacklozenge\blacklozenge P < .001$, $\blacklozenge\blacklozenge\blacklozenge\blacklozenge P < .0001$).

Figure 2: Position analysis of reversion events per RPE. Position intervals are indicated on the x-axis, where the 0.0 position interval corresponds to the central region of the RPE near the optic nerve and the position interval 1.0 represents the edge of the RPE. A Kolmogorov-Smirnov test was used to analyze position distributions with individual significance denoted in each figure.

Table A.1

Specific Aim 1: Determine whether DNA-damaging agents with varying modes of action can induce somatic change in an in vivo mouse model of homologous recombination

Time frame: 1 year

- Breed $p^{un/un}$ mice (months 1-3)
- Expose pregnant dams to DNA-damaging agent (chemotherapeutics), conferring a variety of lesions at a specific time in embryo development (E12.5) (month 4-6)
- Assess the frequency of spontaneous p^{un} HR deletion on resultant pups from exposed dams (months 7-12)

o Milestone: publication of different DNA damaging agents (chemotherapeutics) administered in vivo and their role in homologous recombination.

Specific Aim 2: Determine whether p53 mutants R172P and R172H suppress spontaneous levels of homologous recombination the same as wild-type p53.

o Time frame: 1 year

- Continue to expand R172P, R172H and neo cohorts (months 1-12)
- Continue to intercross heterozygous mice in each cohort (months 1-12)
  - $p53^{R172P/+} \, p^{un/un}$, $p53^{R172H/+} \, p^{un/un}$ and $p53^{neo/+} \, p^{un/un}$
- Assess the frequency of spontaneous p^{un} HR deletion for each $p53$ genotype (months 5-12)
- Set up timed matings for primary MEFs of each $p53$ genotype (months 5-12)
  - Intercross heterozygous mice: $p53^{R172P/+} \, p^{un/un}$, $p53^{R172H/+} \, p^{un/un}$ and $p53^{neo/+} \, p^{un/un}$
- Rad51, Rad52, 53bp1 Foci using primary MEFs (months 5-12)
- Co-immunoprecipitation experiments to determine differential binding of wildtype and mutant p53 to proteins in the HR pathway
- *In vitro* DR-GFP, SSA assay to determine the mechanism of HR being utilized by p53
- Microarray analysis of differential p53 target genes in wildtype and p53 mutant genotypes

o Milestone: publication comparison of spontaneous HR frequency data between p53 mutants, wild type and nullizygous mice. Include *in vitro* data showing the mechanism by which p53 is suppressing HR – transcriptional transactivation/repression or protein: protein interaction with HR machinery.

Specific Aim 3. Determine the global impact of p53 by measuring copy number variation in p53 mutant mouse models.

- <u>Time frame: 1 year</u>
  - Set up timed matings for primary MEFs of each *p53* genotype (months 5-12)
    - Intercross heterozygous mice: $p53^{R172P/+} p^{un/un}$, $p53^{R172H/+} p^{un/un}$
    - Culture MEFs and harvest DNA using Qiagen kit
    - Harvest respective tumor tissue and extract DNA
    - Perform an aCGH on samples using JAX standard DNA as reference genome

- <u>Milestone:</u> additional data for publication in specific aim 2. Global genomic component of p53 mutation on genetic variation.